Baseline 1999-2000

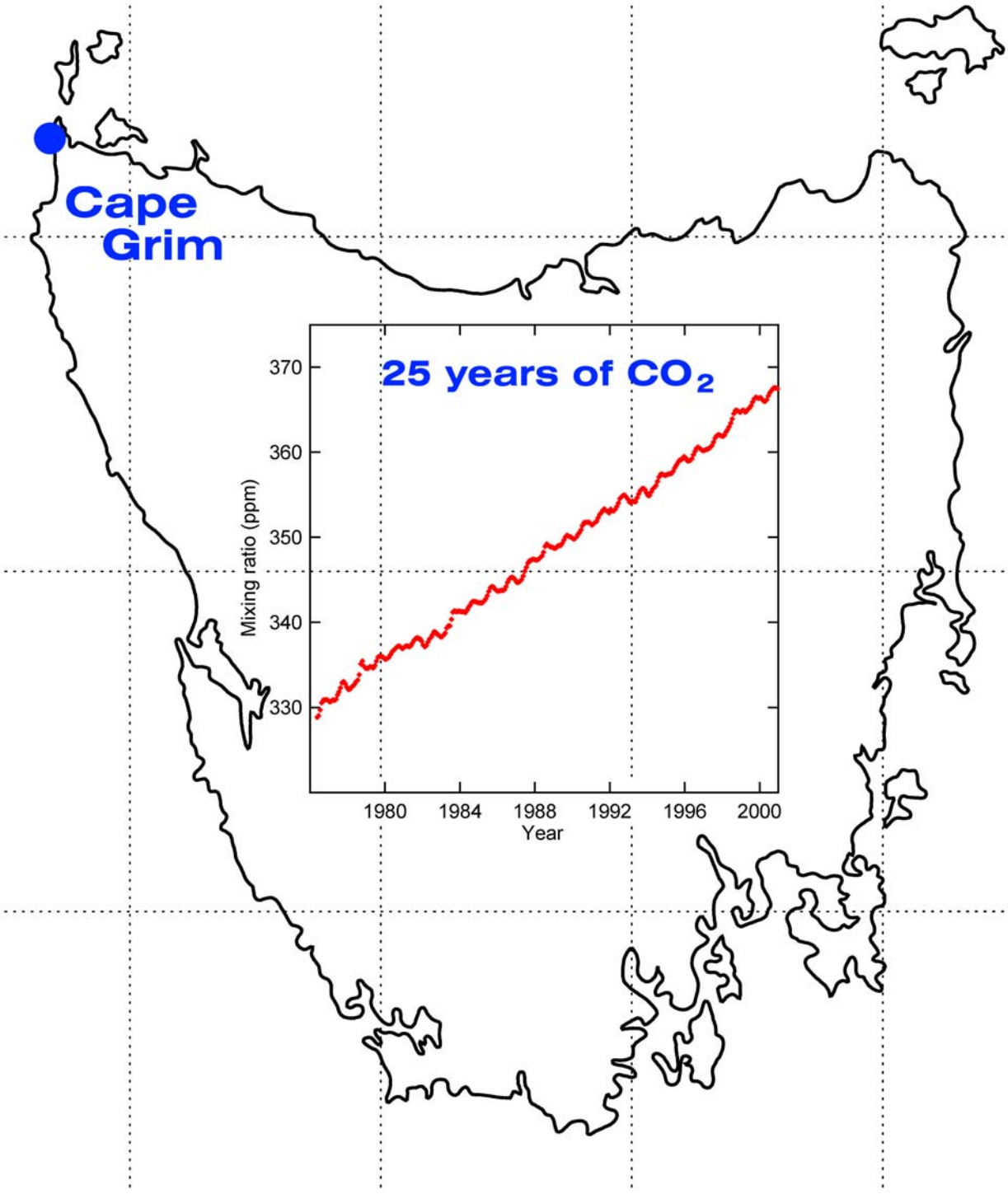

Bureau of Meteorology
and
CSIRO Atmospheric Research

Baseline Atmospheric Program Australia 1999-2000

Edited by N W Tindale, N Derek and P J Fraser

2003

Published for the Bureau of Meteorology and
CSIRO Atmospheric Research, Melbourne

ISBN 0 643 06882 1

FOREWORD

It is a great honour to be asked to write a preface to this 25th Anniversary report of Cape Grim. The Cape Grim project has truly been an enormously successful undertaking in terms of both its contribution to the science of global atmospheric change and the relevance of that science to key environmental issues of regional and global importance. At the outset, the founding scientists recognised the potential for human impact on the composition of the atmosphere to influence climate and thus almost everything humans and our non-human co-inhabitants do. But they could never have fully appreciated at the time, the true magnitude of the issues and how, 25 years later, the world would face the need to come to grips with managing these issues.

During the several years in the lead up to the establishment of the Cape Grim observatory, several commitments were made. First to the length of engagement; all players saw this as a 50-year program. Second, a commitment was made to excellence in attention to precision observations and calibration/inter-calibration, and in the application of the data to the solution of important questions of knowledge. Third a commitment was made to continuous improvement, the balance between continuity and inter-decadal consistency of data and recognizing the need for constant update of the suite of components to be measured and the instrumentation and technologies to be applied.

Such ambitious goals would create a challenge for the most capable modern managerial guru; a sensitive balance of individual freedom for scientists and the objectives of continuity; an element of acceptable ambiguity of purpose and shared commitment to the underpinning purpose. These have been achieved through, often controversial, but proven hands-on control of the program by the scientists themselves.

As with most endeavourers, success derives primarily from the quality of the people and their commitment to the task. It is here that Cape Grim has found its greatest strength. The most committed and talented people have served it and have seen the station through a revolution of technology particularly with respect to data handling and storage, chemical measurement, and brilliant application of data to problem solving. This does not just happen, but reflects the provision of the right equipment and operating environment, personal commitment to the world's scientific community and its very frontiers and the wise definition of important but soluble problems. These successes also derive from a level of collaboration between scientists, students, technician and administrative staff, between partner institutions and with international colleagues. All of these have been ongoing features of Cape Grim.

A major, but by no means only, institutional collaboration has been between the Bureau of Meteorology and CSIRO. This is reflected in the Bureau's unwavering support for the Station and the CSIRO's ongoing support for Cape Grim science, underpinned by the complementary laboratory facilities developed at CSIRO in Melbourne.

I wish to pay tribute to the Cape Grim Station staff, who working in an isolated location, have offered sterling service to maintain a 24-hour, 365 days a year, scientific operation. The partnership between researchers and Station staff has been another critical element in its success.

Cape Grim was established with the purpose of observing the changes taking place in the composition of the background atmosphere and to understand the role in atmospheric dynamics in transporting these gases around the world.

In the broad, these objectives remain relevant today, but how much the rationale has changed. In the early 1970s, the fact that the greenhouse gas, carbon dioxide, was rising in the atmosphere was based on a single set of observations carried out by C D Keeling. It was necessary to check the integrity of this finding, important as it was. Simple things such as how quickly gases released into one hemisphere mix into the other hemisphere, were poorly understood, as was the importance of the stratification of the atmosphere in predicting spatial distributions of gases.

The setting up of Cape Grim was also extremely timely to investigate a second global atmospheric challenge. Rowland and Molina had only just posed the question about the impact of chlorofluorocarbons (CFCs) on stratospheric ozone, yet very little was known about the behaviour of these gases in the global atmosphere.

Today, thanks to observations such as those made at Cape Grim and the sister observatories operated by other nations, these questions have by and large been answered. Observational data have been integrated into studies of the chemical transport and transformations and land-sea and air sea exchange for many gases, including carbon dioxide. This has developed our understanding sufficiently to underpin the relationships between compositional changes and the observed climate changes; to underpin the United Nations Framework Convention on Climate Change and the Montreal Protocol on Ozone Depleting Substances.

Cape Grim's contribution has truly evolved from pioneering science and academic curiosity to one that is a mixture of continued knowledge development (e.g. how will the current global cycles of carbon dioxide be changed by the warming and the dynamics of the Southern Ocean?) and applications (e.g. how has the Montreal Protocol for Ozone Depleting Substances impacted on the growth of these substances in the atmosphere?).

But what of the future? We are entering a new century and a new age in which a massive transition will take place as we navigate our way from where we are with all our unsustainable technologies and behaviours to where we need to be, balancing the economic, social and environmental aspect in all we do and considering our actions in terms of their constraints on further generations. A transition to sustainability. Cape Grim is more relevant and necessary today than ever before. The list of components to be measured is longer, the techniques are improved and more sophisticated but the need for courageous and strategic planning of new observational programs remains whilst maintaining the integrity of the others.

We have only relatively recently come to discover the significant value of the 'non-baseline' observatories of the station that are revealing information concerning the exchanges of materials between the Australian continent and the atmosphere. In a similar way, the observations are contributing to air quality studies as the plumes of cities such as Melbourne occasionally make their way to Cape Grim.

The world needs Cape Grim. It is just one of a wide range of institutions that we will need for the development of the knowledge to underpin decisions made in this global transition, and to monitor their success.

Twenty-five years ago Cape Grim offered vision and appropriateness for the future. We need right now to recommit to the next decades. For who can say that all is known or that there is not another 'ozone hole' already happening about which we are currently ignorant? Indeed, the new emphasis on the role of aerosols in climate reinforces the vision of establishing aerosol monitoring at the very beginning of the program as these measurements underpin the new studies.

These are serious and difficult challenges. Indeed one wonders if such a project as Cape Grim, with its long-term nature, its monitoring components, its public good focus and its exploratory nature was proposed today, could it find the commitment and support to become established? I am not sure. On the one hand, concerns about the integrity and future of our environment have never been more widespread. On the other hand, we now live in a world dominated by the short term, the immediate pay off and the constant challenge of 'who pays?' What I do know is, if we could not, for whatever reason, find the commitments of scientists or administrators/politicians to another 'Cape Grim', then we have lost an essential ingredient: the opportunity for our own curiosity to lead us to where no strategic plan will be wise enough to envisage. For this is what our Cape Grim has done.

It has been my pleasure to have been a part of this success story, one that all who have contributed should feel justly proud. Like previous authors of 'Forewords' to Baseline, your endeavours and devotion is recognised by too few. Well done, and happy anniversary Cape Grim

Graeme Pearman
Co-Manager Cape Grim Program
Chief CSIRO Atmospheric Research

October, 2002

PREFACE

Baseline 1999-2000 reports on the activities and scientific program at the Cape Grim Baseline Air Pollution Station in North West Tasmania, Australia, for the two calendar years of 1999 and 2000. Included are scientific papers, based on research at Cape Grim, as well as operational reports on the various experiments and monitoring conducted at the station over the two year period.

For this edition of *Baseline*, we are fortunate to have a *'Foreword'* supplied by Dr Graeme Pearman, the former Chief of the CSIRO-Atmospheric Research division. Graeme has had a long connection with the Cape Grim program both as a Lead Scientist, member of the CGBAPS Working Group, and later as one of the members of the Cape Grim Management Group. Graeme was one of the leading advocates for a baseline station in Australia and his input and guidance helped create the Cape Grim program and station. Through his various roles in Cape Grim, he has been a major factor in the success of Cape Grim.

Following the style of recent issues of *Baseline*, the layout of this edition includes both research papers and reports from the various scientific programs in operation at the CGBAPS station. Program Reports contain the status of the research programs for only the two year period. The Research Papers are stand-alone scientific articles that may present research results and data up to the time of final submission. While the Program Papers and Research Reports look similar, the important distinction between the two is that the Research Papers are stand-alone, scientific articles that are scientifically peer-reviewed by at least two independent referees before being considered acceptable for publication.

The Research Papers follow the American Geophysical Union (AGU) publications formatting and referencing styles. Limited numbers of reprints of these papers are available and should be requested directly from the lead authors of each report.

N W Tindale, N Derek and P J Fraser

February 2003

CONTENTS

1. STATION SPECIFICATION

2. OFFICER-IN-CHARGE'S REPORT

3. RESEARCH PAPERS

4. PROGRAM REPORTS (calendar years 1999-2000)

APPENDICES

1. STATION SPECIFICATION

1.1 GENERAL

Name	Cape Grim Baseline Air Pollution Station	
Latitude	40° 40' 56" S	
Longitude	144° 41' 18" E	
Roofdeck elevation	94 metres	
Air intake elevations	104 metres 164 metres	(10-m intake) (70-m intake)
WMO station classification	Baseline (global)	
Status	Fully operational	
Station ID indices	WMO station code 94954 WMO index number A2000 101 WMO turbidity code number 03 050 WMO ozone code number 230 AWS station code 94954	
Time zone	Australian Eastern Standard Time (AEST) (AEST = UTC + 10 hours; the station operates on AEST year-round)	
Office hours	0845-1700 local time (AEST plus 1 hour in summer)	
Telephone	Smithton office International dialling Station Facsimile Smithton Facsimile Station	(03) 6452 1629 61 3 6452 1629 (03) 6452 2181 (03) 6452 2600 (03) 6452 2582
E-mail	capegrim@bom.gov.au	
Postal address	P.O. Box 346, Smithton, Tasmania 7330, Australia	
Freight address	159 Nelson Street, Smithton, Tasmania 7330, Australia	

1.2 SITE PLAN

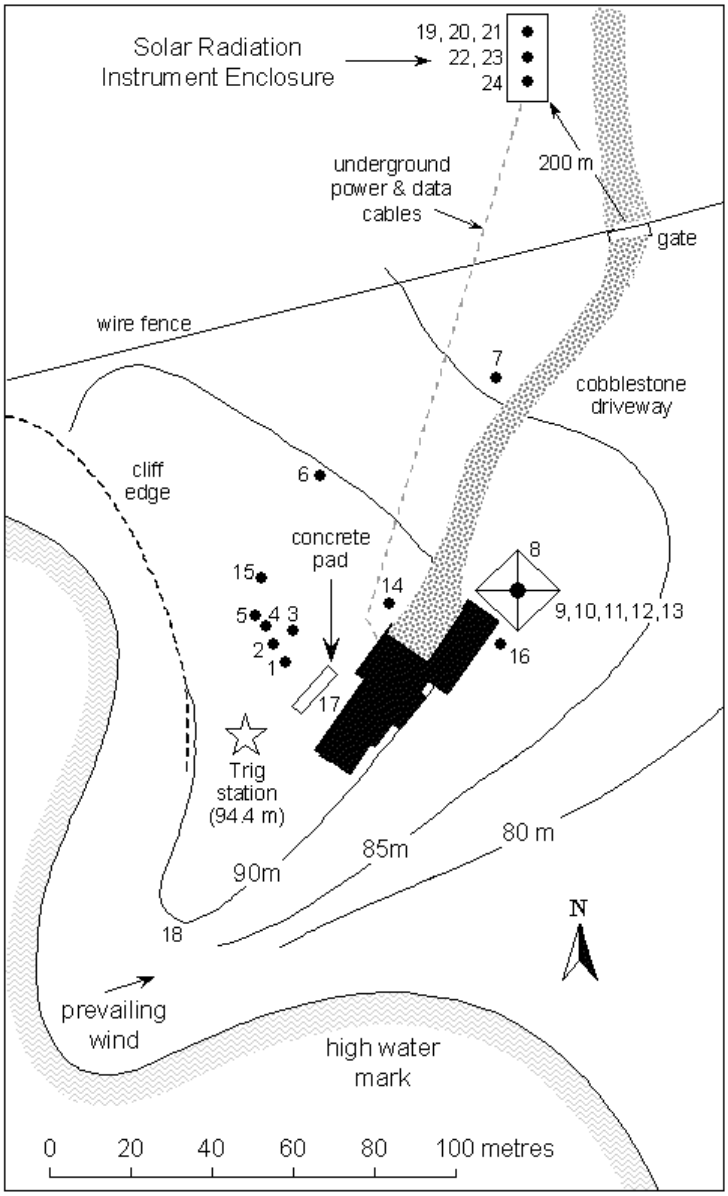

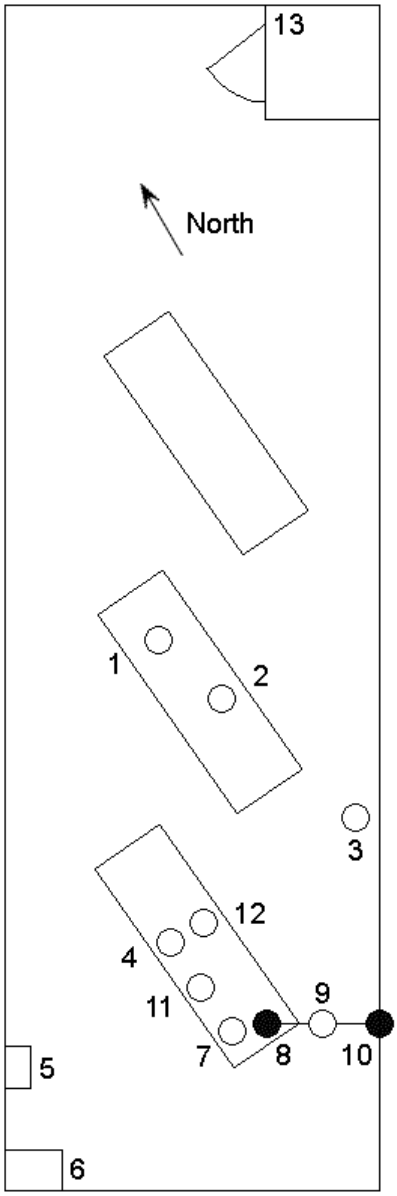

Site Plan

1. Baseline ERNI
2. Continuous ERNI
3. Raindrop sensor
4. Tipping-bucket rain gauge
5. Standard 203 mm rain gauge
6. Stevenson screen
7. Station exhausts
8. Telstra tower (74 m)
9. 70-m intake
10. Wind vane and anemometer (50 m)
11. 50-m Temp and humidity
12. Wind vane and anemometer (30 m)
13. Pb isotopes sampler (70 m)
14. Liquid water radiometer
15. 'Auslig' GPS antenna
16. Radon detector (HURD2)
17. Concrete slab & power box for containers
18. NIES flask sampling

Solar Radiation Instruments

19. Sunphotometer
20. Direct pyrheliometer
21. Diffuse pyranometer
22. Global pyranometer
23. Long wave radiometer (Pyrgeometer)
24. Spectral radiometer (SRAD)

Roof deck plan

1. UV-B radiometer
2. UV pyranometer
3. Barometer static head and DOE transmitter
4. Elemental carbon LVS
5. DOE HVS
6. CSIRO 'Goldtop' HVS
7. 'Particulate' rain gauge
8. 10-m anemometer and wind vane
9. 10-m air intake
10. 10-m anemometer
11. LVS for sulfate MSA, NH_4^+, SO_2
12. ANSTO ASP sampler
13. LIDAR

1.3 PROGRAM SUMMARY

This section summarises programs in operation at Cape Grim during the calendar years 1999 and 2000.

(a) Automated measurements

Species	*Instrument*
CO_2	Siemens Ultramat 5E
CO_2	CAR 'LO-FLO' (started May 2000)
CCl_3F, CCl_2F_2, CCl_2FCClF_2,	AGAGE GC-Multi Detector (GC-MD) system:
$CHCl_3$, CH_3CCl_3, CCl_4, N_2O	(HP5890 GC (two electron capture detectors);
CH_4	Carle (flame ionisation detector);
CO, H_2	Trace Analytical RGA-2/RGD-2 (mercuric oxide reduction detector)}
HCFCs, HFCs & methylhalides	AGAGE GC-Mass Spectrometry (GC-MS) system
Formaldehyde & peroxides	LC-wet chemistry (ceased July 1999)
Surface O_3	Thermoelectron (UV) / Monitor Labs (UV)
Surface NO_x	CAR-chemiluminescent (started February 1999)
Rn	alpha detector / delay tank (x2)
Irradiance	
Solar Aureole Direct	(500 nm)
Direct	Eppley pyrheliometer; WMO (368,500,778,862 nm)
Global	Kipp & Zonen CM11; CGBAPS 500 nm
	Eppley long- and short-wave radiometers
Diffuse	Kipp & Zonen CM11
UV-A	Eppley (290-385 nm)
UV-B	Optronics OL-752
	Biometer - Solar Light 501A
Atmospheric H_2O	Liquid Water Radiometer – Hughes (ceased October 2000)
Condensation Nuclei (CN)	TSI 3020 / TSI 3760 (TSI 3025 from January 1999)
Aerosol size distribution	auto-Pollak and diffusion battery
Particulate Carbon	Magee Scientific Aethalometer
Temperature (wet & dry)	Rosemount (Pt) / Vaisala DTS12 (50 m)
Wind speed	Synchrotac 3-cup (10 m) / Vaisala WAA-15 (10 m, 30 m, 50 m)
Wind direction	Vaisala WAV-15 (10 m, 30 m, 50 m)
Pressure	Rosemount / static head
Rainfall	Rauchfuss (0.2, 0.1 mm)
Radionuclides	Gamma detector
Clouds and Aerosols	LIDAR (ceased October 2000)

(b) Component collections

Component	*Method*	*Nominal number per month*	*Species analysed*	*Analysing Agency^*
CO_2	cryo	4	$\delta^{13}C$, $\delta^{18}O$	CAR
CO_2	Raschig tubes	2	$\Delta^{14}C$	UH
Soluble Aerosol	LVS filters*	4	inorganic ions	CAR (ceased June 1999)
SPM	HVS*	4	inorganic ions	CAR
SPM	HVS	4	radionuclides	DOE
SPM	LVS*	4	elemental carbon	U Stockholm
Aerosol	LVS	8	metals	ANSTO
Aerosol	LVS**	16	meatls	ANSTO (started September 1998)
Rain	ERNI*	4	pH, conductivity, inorganic ions	CAR
	ERNI	1	tritium, δD, $\delta^{18}O$	ANSTO; CSIRO-Adelaide
	Standard gauge	20	oxygen isotopes	U Tasmania
	Funnel & bottle	20	oxygen isotopes	ANU (started September 2000)
Aerosol	LVS filters	2	Pb isotopes	Curtin University (ceased April 2000)
Soil emissions	Flux chamber	2	methyl halides, halocarbons	CGBAPS/CAR (started September 2000)
Marine gases	Sea water sampling	2	methyl halides & alkyl nitrate	CGBAPS/UEA (started April 2000)
Marine biology	Sea water sampling	1	phytoplankton, salinity, temperature, etc.	U Tasmania (started November 2000)

* operated on baseline events switch (BEVS); ^ - Appendix C (p. 110)
** operated on conditional events switch (baseline, aged baseline, mainland, Tasmanian sectors).

(c) Whole air collections – episodes[+]

Flask type (litre)	*Pressure (kPa)*	*Drying*	*Nominal number per month**	*Species analysed*	*Analysing Laboratory^*
G (0.5)	100 p	Dehydrite	4	CO_2, CO, CH_4, H_2, N_2O	
				$\delta^{13}C$ and $\delta^{18}O$ of CO_2	CAR
	50 p	Dehydrite	4	O_2/N_2, CO_2, CO, CH_4, H_2, N_2O	
				$\delta^{13}C$ and $\delta^{18}O$ of CO_2	CAR
G (2.5)	100 p	-	4	CO_2, CO, CH_4, H_2	
				$\delta^{13}C$ and $\delta^{18}O$ of CO_2	CMDL
	0 p	cryo	4	O_2/N_2, CO_2	URI
	0 p	cryo	2	O_2/N_2, CO_2	CAR
G (5)	0 p	cryo	2	O_2/N_2, CO_2	SIO
G (5)	0 p	cryo	2	O_2/N_2, CO_2	CAR
SS (0.8/2.5/3.0)	280 p	-	4	N_2O, halocompounds	CMDL
SS (35)	3000 c	-	(6)	archive / AGAGE standards	CAR/CGBAPS
SS (3.2)	500 c	-	(2)	halocarbons by GC-MS	UEA
SS (1.6)	100 p	Dehydrite	1	SF_6 [also G (0.5) CAR species]	CAR/UH
SS (6.0)	100 p	-	8	VOCs	CAR (ceased March 2000))
SS (6.0)	150 p	-	2	Methyl halides, SF_6, Halocarbons, N_2O	SIO
G (2.0)	100 p	Dehydrite	1	CO_2	CFR
SS (1.0)	100 p	Dehydrite	1	CO_2	U. of Tohoku
SS (6.0)	100 p	-	2	Methyl halides	NIES (started February 2000)
SS (35)	3000 c	-	2	O and N isotopes of N_2O	UC-San Diego (started September 2000)
SS (3.2)	150 p	-	2	methyl halides and alkyl nitrates	GCBAPS/UEA

p - pump; c - cryogenic trap; * () indicates per year,[+]each episode may include multiple flask traps; ^ - Appendix C (p. 110)

(d) Discrete sampling

Parameter	*Method*	*Occasion*
Temperature (wet & dry)	Mercury-in-glass	1/day
Temperature (max & min)	Mercury-in-glass	1/day
Condensation Nuclei (CN)	Manual Pollak	4/day
Cloud Condensation Nuclei (CCN)	Thermal Diffusion (5 Supersaturations)	3/day
Rainfall	Standard 203 mm rain gauge	1/day

2. OFFICER-IN-CHARGE'S REPORT

2.1. INTRODUCTION

The highlight of 1999-2000 was the successful staging of the second Southern Ocean Atmospheric Photochemistry Experiment (SOAPEX-2). Expanding on from the first SOAPEX held at Cape Grim in January/February 1995, the aim of the second experiment was to conduct the definitive study of tropospheric photochemistry in the clean and slightly polluted air encountered at the Cape Grim station. The five groups of scientists from the UK and Australia had the capability to measure all of the necessary parameters including hydroxyl and hydroperoxyl radicals, total (hydro and organic) peroxy radicals, photolysis rate coefficients for ozone and NO_2, ozone, nitrogen oxides, per-oxides, formaldehyde, carbon monoxide, nonmethane hydrocarbons, etc. So in early January 1999, the SOAPEX-2 researchers and students descended on Cape Grim and the Circular Head region for the summer. All the additional instrumentation and people strained resources at Cape Grim, particularly laboratory space and electric power. Demands for electricity often exceeded the 'rated' capacity at the station but, with some careful redistribution and balancing of power loads (and crossing of fingers) we were able to keep operating without too many problems. Cape Grim staff were busy accommodating requests from SOAPEX researchers, and supporting the experiment, as well as maintaining normal day-to-day operations.

As part of SOAPEX-2, a newly developed research plane, the Aerosonde was used. With development partially supported by the Bureau, the Aerosonde is a small pilotless aircraft that can fly up to three kilometres in altitude, collecting data on atmospheric pressure, temperature, relative humidity and wind speed. In the six flights it made, the aerosonde flew for a total of 64 hours, making repeated vertical soundings in the vicinity of, and upwind of, Cape Grim in support of the chemistry observations in SOAPEX2.

Unfortunately, as in many field experiments, 'Murphy's Law' applied and easterly winds dominated for much of the time, resulting in a record low percentage of baseline conditions during the experiment! While conditions were less than optimal for the science objectives, it appeared that all of the visiting researchers enjoyed their experience at Cape Grim. The entire experiment went very smoothly with only minor problems encountered and which were quickly dealt with. In all, about 50 extra people worked at, or visited, the station as part of SOAPEX-2. There was considerable press coverage with film crews and reporters interviewing researchers and staff. Local and national newspapers also covered the experiment.

Staff were busy in late 1999 undertaking a complete stocktake of all the scientific and computing equipment at the station and office so as to value the scientific equipment 'assets' of the program. Due to the Bureau moving to an accrual budget system, funds for asset replacement would, in theory, be derived from the depreciation of the existing assets and so it was critical to know the existing asset base. As many of the scientific instruments purchased as part of the Cape Grim program are at other locations such as CSIRO in Aspendale, off-site assets were also included in the stocktake.

The other significant (or insignificant as the case may be...) event during 1999-2000 was the end of century, 'Y2K' change. Given all the publicity and dire warnings associated with Y2K, and our reliance on automated instruments, computers and internet communications, it was with some trepidation that we awaited the passing of 31 December. Even though we had spent considerable time and effort testing our equipment for Y2K compliance, and installing software patches to our older, more vulnerable computers, there was still the possibility that some unforeseen mishap would occur with serious implications to our operations and data collection. In all, the event passed as a bit of an anticlimax with only a few minor glitches, due mainly to old legacy software on some of the program computers, all easily fixed. All of the Cape Grim system software and hardware functioned smoothly, a compliment to the preparation and efforts of the Cape Grim staff. The benefit of Y2K was that it did force us to reevaluate longer-term plans for our computer network and system and to address other potential problems in our network and data flow.

After numerous rumours of plans to build a wind farm in the vicinity of Cape Grim, meetings with staff of the Tasmanian Hydro Electric Commission confirmed the decision to build a wind farm on Woolnorth. As part of the preplanning, a number of Hydro and Tasmanian state officials visited the station at different times during 2000 to discuss potential issues associated with the construction of a wind farm, and possible impacts on the monitoring and operations at the station. The location chosen for the proposed wind farm was on the west coast, starting from the headland across from the station, on the other side of Valley Bay and extending further south along the coastline.

New measurements at Cape Grim that started in 1999-2000 included flask sampling for methyl halides for Dr Yoko Yokouchi of the Japanese National Institute of Environmental Studies, starting in February 2000. In April 2000, the collection of seawater samples from off Cape Grim and the NW coast began as part of a collaborative BoM-CSIRO-UEA-Univ. of Tasmania project on marine biogenic gas production. The aim was to relate the production and emission of biogenic marine gases, including methyl bromide and alkyl nitrates, with primary productivity, phytoplankton speciation and seawater conditions in coastal surface waters. Additional flask collections of air commenced in September 2000, this time for Martin Wahlen at the University of San Diego, California, for stable-N isotopic measurement. Rainwater sampling was also initiated in September as part of a study on oxygen isotope ratios in rain for comparison with the corresponding signal in cave calcite deposits at Mole Creek and Hastings cave sites. This work was part of Pauline Treble's Ph.D. studies at ANU in Canberra.

A major upgrade to the station scientific equipment was the installation in May 2000 of the new 'Lo-Flow' CO_2 analyser. The new instrument had been under

development at CSIRO-AR for several years and we had been waiting for some time for the installation and testing at Cape Grim. One of the key features of the new instrument is the very low flow rates of air required for a measurement (hence 'Lo-Flow') which allows a dramatic reduction in the consumption of standard and reference gases. A number of minor improvements and upgrades were also carried out on the AGAGE instruments, although problems with batches of contaminated carrier gas caused numerous, persistent problems with failure of the clean-up traps and decreasing precision.

Of interest in November of 2000, was the celebration of the VDL company 175-year anniversary. A lunch and function were held out at Woolnorth in honour of the occasion. Many ex-Woolnorth staff attended and, as befitting the longest serving staff member, Laurie Porter represented Cape Grim.

2.2. BUILDINGS AND MAINTENANCE

Other than the usual minor repairs around the station there were several notable mishaps during 1999-2000. Probably the most potentially serious occurred in May 1999. The main UPS at the station had been experiencing several minor faults and during heavy fog one evening, a short circuit within the UPS caused a small fire, triggering a smoke detector and the fire alarm. After a relatively slow drive to the station due to the fog and poor visibility, closely followed by the local fire engine, we were greeted by the acrid smell of burnt plastic and wiring. Luckily damage was limited to the UPS, which was a write off.

April 2000 brought a major power failure to the station. After several weeks of intermittent power cuts, the mains power failed completely. Rainwater had entered the cable where it joined the overhead wires in the paddock, causing major damage on the power pole and shorting out the cable where the water had penetrated under ground. To restore power and repair the cable, several metres of cable had to be dug out of the ground, the damaged portion cut off, the power pole moved closer to the station and the cable re-attached to the overhead lines. Not to mention that additional short lengths of overhead lines had to be spliced in so that they could still reach the relocated power pole. After some confusion in sorting out details of who had installed the original cable and connection to the station, it turned out that the underground cable 'belonged' to Cape Grim, so it was our responsibility to organize the repair and get the power back on. Thankfully the generator functioned flawlessly during the week and there were no major disruptions to the station operations.

In late 1999, following protracted deliberations the office building in Nelson Street, Smithton was sold into private ownership. It was surprising how time consuming the whole process was as it affected everything including the cleaning contract, maintenance contracts, fire alarm monitoring etc. Building inspections and repair work were required before the building could be sold, creating further disruptions.

In January 2000, following a break in to the office in Smithton and the theft of one of our vehicles, a monitored alarm system was installed and security plates fitted over doorlocks etc. The extra security proved its worth several months later during another attempted break in when glass in the office front door was smashed. A similar alarm system was fitted at the station in May 2000, in conjunction with the man-down alarm. All alarms are monitored continuously, improving safety conditions for staff and visiting researchers and students at the station.

In addition to security of the buildings, working conditions and OH&S were a priority during 1999-2000. With assistance and advice from Bureau Head Office and CSIRO-AR technical staff, regular OH&S inspections were initiated. All electrical equipment at the station and office now has to be regularly tested. This particularly applies to equipment being newly installed at the station. Inspections found several pieces of equipment with potentially dangerous faults. Improvements to freight handling, liquid nitrogen use, and the inventory of chemicals on site were also implemented.

To improve communications and planning, regular monthly staff meetings were held during both years and issues related to operations and research, OH&S etc. were discussed as well as staffing issues, trips, leave relief etc. Ongoing planning for upgrades, replacements and repair were a priority. Improvements to our IT operations during this period include upgrades to the station computer network and servers, with new network storage using RAID hard-disk array and new, faster LAN hubs. Development on our internal web page and data processing and delivery system continued. Both raw and hourly average data are now available from our internal web page. Instrument logbooks have been digitised and many improvements suggested by Cape Grim staff and visiting researchers, have been implemented to make the Cape Grim computer system more useful and data access easier. The network upgrade included additional Internet connections and improved email and Internet access for visitors to Cape Grim.

In mid-2000, the CGBAPS Management Group visited the station in conjunction with the government's Office of Asset Sales and IT Outsourcing (OASITO) fact-finding visit. The aim of the visit was to research the issues associated with outsourcing of Cape Grim IT resources and support. It was clear that outsourcing of a complex computing environment like Cape Grim would be difficult, particularly given the remoteness of the location the wide range of hardware and software in use, including operating systems. Following the visit, even the OASITO staff admitted that standard models of outsourcing might not apply at Cape Grim or other similar sites.

During routine training for ANARE Antarctic expeditioners in October, there was a somewhat annoyed, unexpected, local visitor to the station. A large tiger snake, which we believe may have been hibernating in cable ducting beneath the station, joined the training session in the main laboratory. After much tap dancing and climbing on furniture, and a protracted

find and remove operation, the snake was escorted outside, to the great relief of all involved!

The CGBAPS Annual Science meetings for 1999 and 2000 were both held in Aspendale, Victoria at CSIRO Atmospheric Research. Over 40 talks and posters were presented each year by the 50+ participants to each meeting. Jill Cainey (NIWA, NZ) and Ed Dlugokencky (NOAA-CMDL, USA) attended the 1999 meeting from overseas. The 2000 meeting had a larger than usual number of visitors, including Leong Chow Peng and Irene Eu Swee Neo from the Malaysian GAW program, Dominic Ferretti from the Univ. of Colorado, USA, Masayuki Katsumoto and Hitoshi Mukai from the Center for Global Environmental Research, NIES, Japan, and John Barnes from the Mauna Loa GAW observatory in Hawaii, USA.

2.3. STAFF AND STUDENTS

There were several changes to the lineup of staff at Cape Grim during 1999 - 2000. In March 1999, Dr Georgina Sturrock, after two years in residence at Cape Grim as a CSIRO researcher, moved to the CSIRO-AR laboratory in Aspendale to continue her Cape Grim related work. March also saw the loss of Alan Gough, the station ITO2 for several years. Alan transferred to the Bureau of Statistics in Hobart and his last official act, as ITO2 before leaving, was to switch off the old Grimco-1 system! Randall Wheaton, from the Bureau's Rockhampton office, was chosen as Alan's replacement and commenced work at Cape Grim in early August. Craig McCulloch, working at the station as a Technical Officer contractor for CSIRO-AR, and his wife Lisa celebrated 2000 with their first child, Cameron, born on 31 January. Bob Parr, a local farmer and a retired technical officer from the agricultural research laboratories in New Zealand, joined the staff at Cape Grim as a temporary CSIRO-AR employee. Bob is responsible for managing the alkyl nitrate/methyl halide sampling, and last but not least for staff news, after a brief 26-year courtship, Brian Weymouth (SITO-C) quietly stole away from Cape Grim to a remote Pacific Island beach in order to marry Joyce!

2.4. INTERNATIONAL ACTIVITIES AND VISITORS

During SOAPEX2, there was a flood of visitors to Cape Grim, with researchers from the Universities of East Anglia, Leeds and Leicester formed the core of foreign participants. As part of our support for the Indonesian GAW station at Bukit Koto Tabang, two of the Indonesian GAW staff, Budi Suhardi and Ully Nasrullah, visited Cape Grim for a week of training especially of the ozone instrumentation as part of their visit to CGBAP and CSIRO-AR at Aspendale. Similarly, as part of the Memorandum-Of-Understanding (MOU) between the Bureau and the Hydrometerological Service of Vietnam, Pham Thi Thuy Hoan and Nguyen Dinh Huong visited Cape Grim as part of a background, fact-finding visit to gather ideas and input for their newly proposed monitoring station in northern Vietnam. Leong Chow Peng and Irene Eu Swee Neo from Malaysia also visited the station as part of their visit to the Bureau and CSIRO-AR and attendance at the CGBAPS science meeting.

Other visitors from overseas during 1999 included Richard Turco from the University of California, Jim Elkins from NOAA-CMDL in Boulder, and Jin Ju from the Chinese Ministry for Science and Technology, and scientific attaché at the Chinese Embassy in Canberra. Kimberly Mace, a Ph.D. student from Texas A&M University stayed and worked at Cape Grim from October to December 2000 to study organics in rainwater. In a déja-vu repeat of the SOAPEX experiment, sampling conditions during the period were marginal at best, with only a couple of brief periods when rain samples could be collected under baseline conditions.

In a prelude to the Sydney Olympics, we were contacted by the NBC 'Today' film crew and producer to shoot footage of the station and surrounding area for their USA morning television show. They were in Tasmania to find background material for their coverage of the Olympic games. While they were at the station, we were blessed with a generally fine day with passing clouds and the odd light shower, apparently excellent filming conditions. While the film crew were outside, filming the vista around the station, an adult sea eagle, as if on cue, soared up over Cape Grim and obligingly flew back and forth several times over the station, right out in front of the camera, to the great delight of the 'Today Show' crew!

Cape Grim staff overseas travel included trips by the OiC to the annual CMDL meeting in Boulder and the Fall AGU meeting in San Francisco. The Senior Technical Officer, Laurie Porter, attended AGAGE meetings in Barbados and Hawaii. The trip to Barbados included a visit to the Scripps Institute of Oceanography on the return leg.

2.5. OPERATIONAL BUDGET

The Cape Grim program expenditure allocations for financial years 1998/1999, 1999/2000 and 2000/2001 are indicated below. Staff salaries, and road and building maintenance are not included as they are covered by other parts of the Bureau of Meteorology budget. Salaries of the technical officers employed at DAR to assist in Cape Grim related research are included in the 'Research' allocation.

	1998/1999 $	1999/2000 $	2000/2001 $
Station operation	194,800 *	179,730 *	177,690*
Research	507,200	522,270	524,310
Equipment	50,000 **	200,000 **	200,000**
Total	752,000	902,000	902,000

* Station Operation allocation includes additional computer link funding of $17,000, which had previously been paid from BoM-Head Office funds.

** Additional equipment funding from new minor capital/asset replacement funds.

Compiled by N. W. Tindale.

BACK TRAJECTORIES TO CAPE GRIM: INVESTIGATING SOURCES OF ERROR

M Tully and A Downey
Bureau of Meteorology, Melbourne, Victoria 3001, Australia.

Abstract

Ninety-six hour back trajectories terminating at Cape Grim are calculated and archived daily. They are currently computed using data from the Bureau of Meteorology's Limited Area Prediction System (LAPS) using the HYSPLIT-4 model. In this paper we investigate the accuracy of the trajectories using radon as a tracer. We consider the effect of selecting different vertical motion schemes, and study the accuracy of trajectories sorted by the mean sea level pressure on arrival at Cape Grim, giving a first approximation to the effect of synoptic complexity of the flow on reliability. It is found that large discrepancies in calculated radon content are associated with large values of vertical wind shear and complex and rapidly changing flow regimes.

1. Introduction

Knowledge of air mass origin is clearly of great importance in the interpretation of measurements of trace atmospheric constituents, and back trajectories are widely used for this purpose in atmospheric chemistry. A longstanding problem with their use, however, is that it is difficult to make any very precise quantitative statement about their reliability [Kahl 1993].

Here, we investigate the extent to which the routine radon observations made at Cape Grim can be accounted for using back trajectories generated using the HYSPLIT-4 trajectory model and a simple model of radon emission from land. The study period is from 1 May to 31 December 2000. Thirteen of the 245 days are missing due to the unavailability of archived meteorological data. While this time period of eight months is too short for climatological study it is long enough that interseasonal variation might well be evident. Previous related studies of radon transport to Cape Grim include Whittlestone *et al*. [1985], Downey *et al*. [1990], Whittlestone *et al*. [1998], Siems *et al*. [2000] and Kowalczyk and McGregor [2000], the first four of these also using back trajectories.

2. Trajectories

Ninety-six hour back trajectories terminating at Cape Grim at 10.00 am and 10.00 pm local time, are routinely generated and archived, using the HYSPLIT-4 code [Draxler 1998] and meteorological fields from the Bureau of Meteorology's Limited Area Prediction System (LAPS) [Puri *et al*. 1998]. The model domain is from 65°S to 15°N, and 65°E to 185°E, with horizontal resolution of 0.375° and twenty-nine vertical sigma levels, ranging from approximately 10 m to 20 km in altitude.

A total of five different methods are available for calculating the vertical motion of the air parcel and these will be discussed in section 5 below.

The accuracy of calculated air trajectories has previously been investigated using a variety of methods as reviewed by Stohl [1998]. These include comparison with the path of constant-density tetroons or manned balloons, conserved meteorological quantities, data from dedicated tracer experiments or so-called 'tracers of opportunity' such as dust, sand, smoke and pollen. All such methods present difficulties of some kind, however, and these studies have not to date been particularly conclusive. Figures such as 200 km per day or 20% of travel distance are typical of the errors that have been given in the literature, however these numbers represent mean values and the accuracy of individual trajectories may vary considerably.

Errors in trajectories result primarily from interpolation of meteorological variables in both time and space, and inaccuracies in the wind fields supplied by the underlying meteorological model. If one assumes a randomly distributed error in the horizontal wind fields of the order of 1 m s^{-1}, then in conditions of static, uniform flow the final error in position after ninety-six hours will typically be some 44 km. However, if conditions are changing rapidly or large wind shears are present, small differences in position are amplified, leading to exponential growth in the error and a much greater final error.

3. Radon

Radon has often been used in the study of atmospheric transport processes [Dentener *et al*. 1998] due to its relatively uncomplicated behaviour. It is emitted almost exclusively from land and has no further sources or sinks other than mixing and radioactive decay with a convenient half-life of 3.8 days. While the release rate over the Australian continent is known to be variable to some extent [Schery *et al*. 1989], a typical rate may be taken to be about 1 atom cm^{-2} s^{-1}. If we assume a well-mixed boundary layer of about 2km, then ignoring any net horizontal transport we would expect continental air to have a radon concentration of some 5000 mBq m^{-3}.

Measurements of radon at Cape Grim show periods of low concentration punctuated by periodic bursts of elevated concentration, presumably due to the arriving air having at least some continental influence [Whittlestone 1985]. A figure of 100 mBq m^{-3} has previously been used [Whittlestone *et al*. 1998] as a limit of what may be considered 'baseline' levels. During the study period, thirty-five episodes of radon levels above this limit took place, of which ten contained peak readings greater than 4000 mBq m^{-3}. The maximum reading was 6990 mBq m^{-3} and the median 110 mBq m^{-3}.

The model of radon uptake used here is elementary, consisting only of a linear increase in radon concentration for every hour an air parcel spends over land, followed by exponential decay once the parcel is no longer over land. More complicated models than this were considered in an effort for greater physical realism but were found not to produce any better correlation with the radon data set.

In Downey *et al*. [1990] a similar model was used and was able to produce good correlations (with a maximum correlation coefficient of 0.64) between their calculations and measured radon values at Cape Grim.

Trajectories were computed with finishing heights of 100 m, 300 m, 500 m, 1000 m, 3000 m and 5000 m for each day in the study period. We then determined the correlation of the time series of the radon calculated for each trajectory using the uptake model with the radon actually measured for each day at ten o'clock. We also repeated the calculation using radon measurements up to several hours both before and after the nominal finishing time of the trajectory, so that the correlation coefficient could be plotted as a function of lag.

Figure 1 shows hourly radon measurements over a sample two week period together with calculated radon based on the corresponding daily back trajectories over that time.

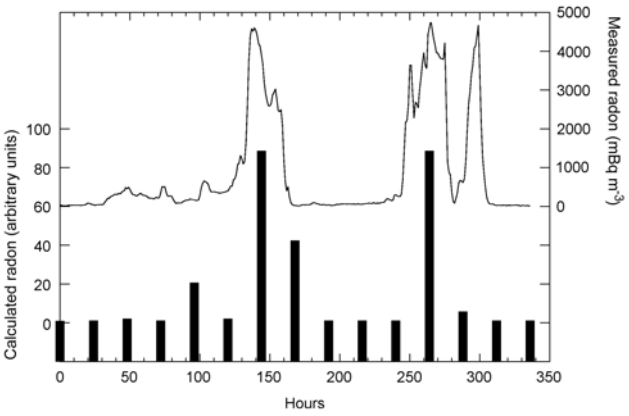

Figure 1. A time series showing measured radon values for a two-week period beginning 9 June 2000 (line), together with calculated radon values based on the daily back trajectories (solid bars).

4. Results

Figure 2 shows the correlation of measured radon to calculated radon values as a function of lagged time for trajectories with different finishing heights. For clarity only three of the six curves are plotted. Maximum correlation factors for the six heights listed above were 0.74, 0.76, 0.76, 0.74, 0.68 and 0.55 respectively. Note that the lag for maximum correlation increased with trajectory finishing height, that is to say, the actual radon transport became further ahead of the calculated radon transport as height increased. As might be expected, the correlation decreased with height, but only above 1000 m. Figure 3 shows a scatter plot for trajectories finishing at 500 m.

It is evident that in general the predictions based on the trajectories are in good agreement with the measured results. Baseline levels were predicted on 123 occasions, of these, 96 had radon readings of less than 100 mBq m^{-3}, and non-baseline levels predicted the remaining 110 times, of which 98 had radon readings greater than 100 mBq m^{-3}.

Inspection of individual trajectories gives some indication of the possible causes of erroneous results, and three factors were identified, one or more of which was associated with almost every sizeable discrepancy.

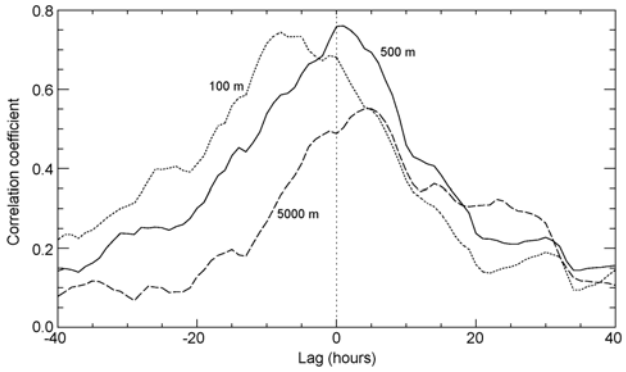

Figure 2. Lagged correlation of measured radon with calculated values based on land contact time for trajectories ending at 100 m (dot), 500 m (solid) and 5000 m (dash).

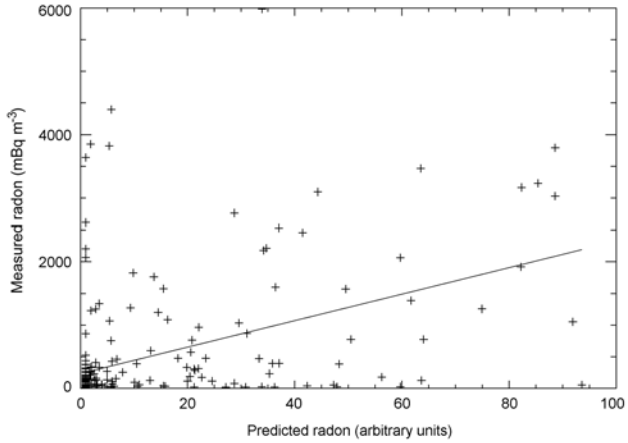

Figure 3. Scatter plot of measured radon against calculated values based on land contact time for trajectories finishing at 500 m (no lag). The ninety-five percent confidence interval for the correlation is 0.70 – 0.81.

Firstly, most of the inaccurate trajectories indicate abrupt changes in wind direction resulting in kinks or loops in the path (an example is shown in Figure 4). As HYSPLIT is linearly interpolating between six-hourly data, rapid changes, such as would occur with the passage of a front, are not well resolved [Whittlestone *et al*. 1998]. It should also be borne in mind that numerical weather prediction models such as LAPS have difficulty in accurately resolving frontal passages themselves.

Secondly, in some cases the four lowest-level trajectories followed very different paths, suggesting the presence of significant wind shear (an example is shown in Figure 5). In this situation using a single trajectory would not in general be expected to be accurate.

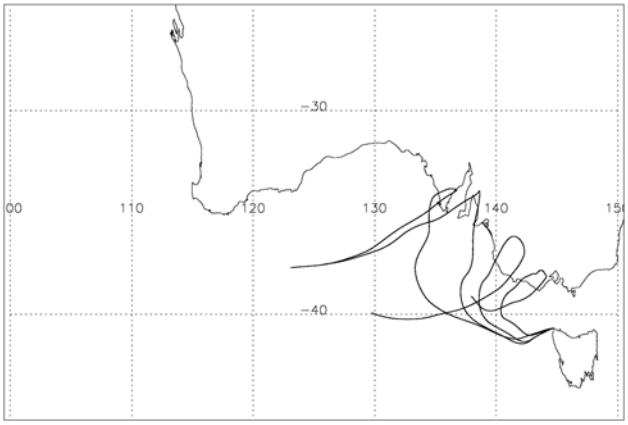

Figure 4. The four lowest level trajectories for 11 December, 2000, showing looping and kinking in the paths.

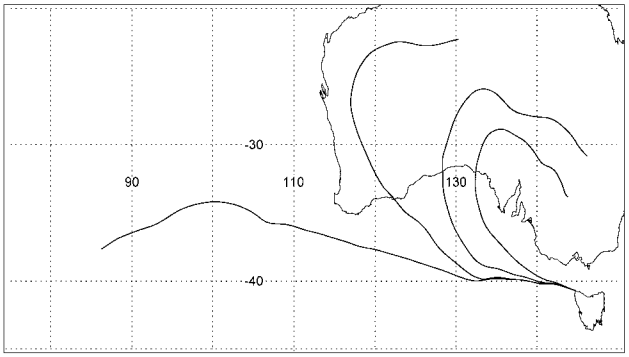

Figure 5. The four lowest level trajectories for 16 June 2000, showing divergence in the paths for different finishing heights.

To further consider this question of spreading in the trajectories of different heights, averages of various combinations of the four lowest level trajectories were also tested and found to yield slightly improved results. The highest correlation was found for the average of all four levels combined (i.e. 100 m, 300 m, 500 m and 1000 m), as shown in Figure 6. This is in line with previous work [Stohl and Wotawa 1995] suggesting that some form of averaging over the boundary layer gives more accurate results than any single trajectory. Further, the total difference in radon predictions of the four trajectories was found to correlate well with the discrepancy between the predicted and measured values, and this suggests a possible path towards developing some measure of the reliability of a given individual trajectory [Kahl 1996].

The third factor associated with inaccurate radon predictions is nearness of the trajectory to a coastline, obviously a situation in which relatively minor errors in displacement lead to large discrepancies in radon uptake, and thus the radon tracer method for estimating errors in back trajectories does not work very well. This was found to be a particular problem in cases where the air parcel was calculated to have passed overland shortly before arrival at Cape Grim, and trajectories that crossed Tasmania generally did not accurately predict the measured radon value.

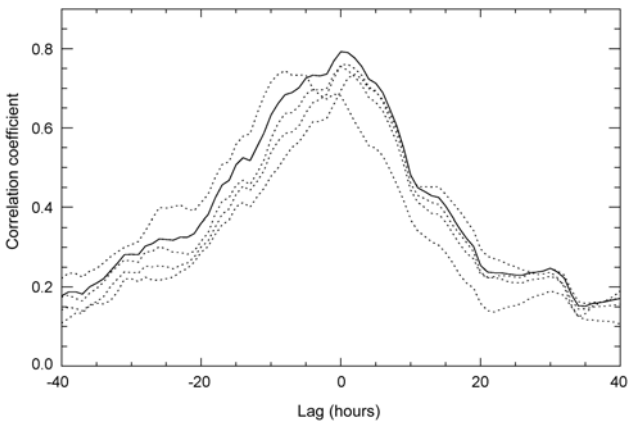

Figure 6. Lagged correlations for the four lowest level trajectories (dotted lines) and the correlation obtained by averaging all four (solid line).

It would be expected that the reliability of an individual trajectory could well depend on the particular weather system prevailing at the time. It was therefore decided to separate the data set into five divisions depending on the sea-level pressure recorded at Cape Grim at the time of arrival, as a crude means of characterising the prevailing system. As shown in Figure 7, the correlation obtained for trajectories terminating in the lowest quintile of sea-level pressure (below 997 hPa) was markedly better than for higher pressures.

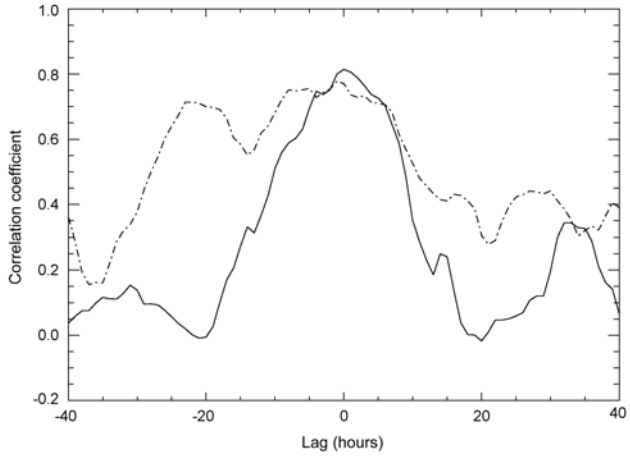

Figure 7. Lagged correlation of measured radon with calculated values for trajectories finishing at 500 m, grouped by sea-level pressure at arrival time at Cape Grim. The solid line is the correlation for trajectories in the lowest quintile of pressure, the dotted line for all other trajectories.

This result would seem to be due to the fact that the lower pressure at Cape Grim is indicative of relatively simple and well-determined flow regimes. Inspection of the data shows that the lowest pressure quintile contains the highest proportion of baseline winds but has also a relatively high mean radon content, due to the presence of strong northerly winds coming from the Australian continent. The lowest quintile also has the highest mean wind speed, in line with previous work [Heffter *et al*. 1990; Haagenson *et al*. 1990; Stunder 1996] suggesting trajectory error was inversely proportional to wind speed.

5. Vertical motion

As mentioned earlier, the HYSPLIT program offers five choices for determining the vertical motion of the air parcel. These are:

1. *isobaric*, where a parcel is constrained to move along a surface of equal pressure;
2. *isosigma*, where a parcel is constrained to move along a surface of equal sigma (these are simply defined as the atmospheric pressure divided by the surface pressure);
3. *isopycnic*, where a parcel is constrained to move along a surface of equal density;
4. *isentropic*, where a parcel is constrained to move along a surface of equal equivalent potential temperature; and
5. where the vertical motion is taken directly from the analysis fields (referred to henceforth as 'data').

The different methods generally give somewhat different results. Table 1 gives the mean horizontal and vertical separation after twenty-four hours of trajectories calculated using the data fields with those calculated using the other methods[1]. Figure 8 shows a sample cross-section of trajectories calculated using the five different schemes.

Table 1. Mean vertical and horizontal separation of the air parcel position calculated using four of the vertical motion schemes from the position obtained using the data fields after twenty-four hours.

	100 m		*3000 m*		*5000 m*	
Scheme	*Horiz. (km)*	*Vert. (m)*	*Horiz. (km)*	*Vert. (m)*	*Horiz. (km)*	*Vert. (m)*
Isobaric	74	102	83	556	94	658
Isentropic	192	945	185	1245	203	1520
Density	83	199	91	617	100	724
Sigma	46	95	91	602	102	723

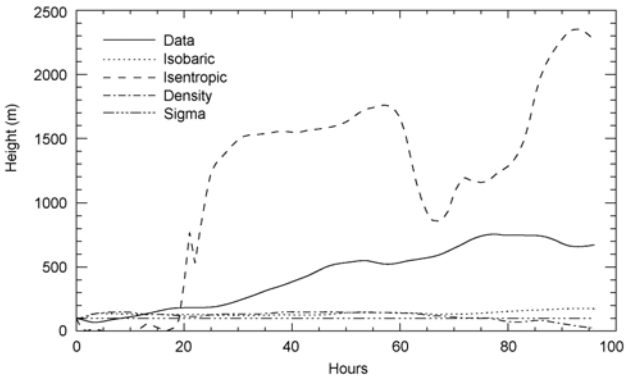

Figure 8. Cross-section of trajectories for 7 June 2000, calculated using the five different schemes for vertical motion.

The sigma, isobaric and density schemes, offer little in the way of vertical motion (as one would expect). The isentropic unrealistically intersects the surface but there is some degree of agreement between the data and the isentropic schemes.

It is generally thought [Stohl 1998] that the most accurate method is to use vertical motion based directly on numerical weather prediction models.

For each day in our study period, trajectories were calculated using all five schemes for finishing heights of 100 m, 3000 m and 5000 m and again the expected radon calculated based on hours of land contact. The results are shown in Figure 9 (for clarity, only data, isentropic and isosigma are shown). However, we were unable to obtain any significant differences in correlations of predicted with measured radon values. We conclude that this method is too coarse to be able to distinguish between the accuracy of the vertical motion schemes.

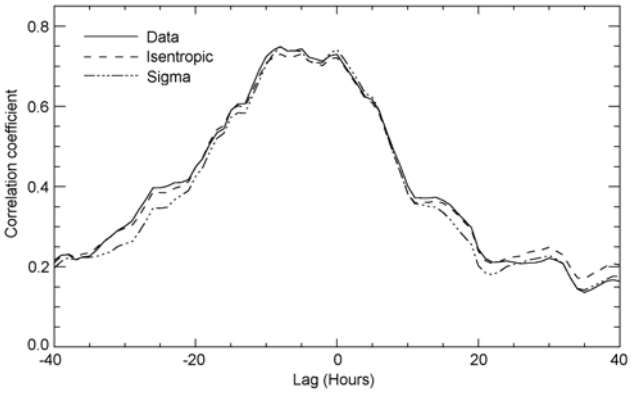

Figure 9. Lagged correlation of measured radon with calculated values based on land contact time for trajectories finishing at 100m, using three different methods for computing vertical motion.

6. Conclusion

Using a simple model of radon uptake over land, good correlations (up to 0.76) were able to be obtained between measured radon values at Cape Grim over an eight month period and those calculated using the HYSPLIT trajectory model and the Bureau of Meteorology's LAPS data fields. Particularly good correlation was found for the trajectories terminating in conditions of very low sea-level pressure. Factors associated with inaccurate trajectories were abrupt changes in direction, and large separation between trajectories calculated for different finishing heights. The single most important factor affecting reliability appears to be the passage of a front.

No significant difference in correlation was found when different schemes for computing vertical motion were used, despite the often, large discrepancies in horizontal position. Given that large divergences in the lower level trajectories were found to be a major indicator of poor radon correlation, the importance of accurate vertical motion seems clear and thus these large discrepancies are a cause for concern.

The goal of giving an indication of uncertainty for individual trajectories remains an ongoing subject of investigation.

[1] Separation did not generally increase with time in a linear fashion, but rather, the rate of increase either itself increased or decreased with time depending on the particular case.

Acknowledgements

The authors would like to thank S. Whittlestone (University of Wollongong) and W. Zahorowski (ANSTO) for the Cape Grim radon data.

References

Dentener, F., J. Feichter, and A. Jeuken, Simulation of the Transport of Rn^{222} using on-line and off-line global models at different horizontal resolutions: a detailed comparison with measurements, *Tellus*, 51B, 573-602, 1998.

Downey, A., J. D. Jasper, J. L. Gras, and S. Whittlestone, Lower tropospheric transport over the Southern Ocean, *J. Atmos. Chem.*, 11, 43-86, 1990.

Draxler, R. R. and G. D. Hess, An overview of the HYSPLIT_4 modelling system for trajectories, dispersion and deposition, *Aust. Met. Mag.*, 47, 295-308, 1998.

Haagenson, P. L., K. Gao, and Y-H. Kuo, Evaluation of meteorological analyses, simulations, and long-range transport calculations using ANATEX surface tracer data, *J. Appl. Met.*, 29, 1268-1283, 1990.

Heffter, J. L., B. J. B. Stunder, and G. D. Rolph, Long-range forecast trajectories of volcanic ash from redoubt volcano eruptions, *Bull. Amer. Met. Soc.*, 71, 1731-1738, 1990.

Kahl, J. D., A cautionary note on the use of air trajectories in interpreting atmospheric chemistry measurements, *Atmos. Env*. 27A, 3037-3038, 1993.

Kahl, J. D. W., On the prediction of trajectory model error, *Atmos. Env*., 30, 2945-2957, 1996.

Kowalczyk, E. A., and J. L. McGregor, Modelling Trace Gas Concentrations at Cape Grim using the CSIRO Division of Atmospheric Research Limited Area Model (DARLAM), *J. Geophys. Res*., 105, 22,167-22,183, 2000.

Puri, K., G. S. Dietachmayer, G. A. Mills, N. E. Davidson, R. Bowen, and L. W. Logan, The new BMRC Limited Area Prediction System, LAPS, *Aust. Met. Mag*., 47, 203-223, 1998.

Schery, S. C., S. Whittlestone, K. P. Hart, and S. E. Hill, The flux of radon and thoron from Australian soils, *J. Geophys. Res*., 94, 8567-8576, 1989.

Siems, S. T., G. D. Hess, K. Suhre, S. Businger, and R.R. Draxler, The impact of wind shear on observed and simulated trajectories during the ACE-1 Lagrangian experiments, *Aust. Met. Mag*., 49, 109-120, 2000.

Stohl, A., Computation, accuracy and application of tracjectories – A review and bibliography, *Atmos. Environ*., 32, 947-966, 1998.

Stohl, A., and G. Wotawa, A method for computing single trajectories representing boundary layer transport, *Atmos. Env*., 29, 3235-3238, 1995.

Stunder, B. J. B., An Assessment of the quality of forecast trajectories, *J. Appl. Met*., 35, 1319-1331, 1996.

Whittlestone, S., Radon measurements as an aid to the interpretation of atmospheric monitoring, *J. Atmos. Chem*., 3, 187-201, 1985.

Whittlestone, S., J. L. Gras, and S.T. Siems, Surface air mass origins during the first Aerosol Characterisation Experiment (ACE-1), *J. Geophys. Res*., 103, 16,341-16,350, 1998.

AIR FLOW OVER CAPE GRIM – A LABORATORY MODELLING STUDY FOR OPTIMUM OBSERVATION SITES

P G Baines and D L Murray
CSIRO Atmospheric Research, Aspendale, Victoria 3195 Australia

1. Introduction

This study is in response to a request from the Cape Grim Baseline Air Pollution Station to examine characteristics of the flow past the observational site at Cape Grim. The specific objective was to carry out a laboratory experimental study to identify the minimum height above the ground that instruments could be placed, in order that air passing them would not have had prior contact with the local ground. This height was required for a range of wind directions from 180° to 315°, at two specific locations, namely the Telstra tower, and another site designated site B, closer to the cliff face (see Figure 1). In other words, for these wind directions air received by the instruments at these locations above these heights would be from the Southern Ocean to the west, without contamination by local sources on land in Tasmania.

The study was carried out in the Geophysical Fluid Dynamics laboratory at CSIRO Atmospheric Research, Aspendale. A similar study for Cape Grim, with slightly different objectives, was carried out several years ago, and is described in Baines and Murray [1994]. The techniques and equipment used here are generally the same. However, in the present study the model was larger, and considerable effort was made to make it as accurate a representation of the real topography of the Cape as possible.

The problem in question is an example of bluff-body aerodynamics, in which the pattern of flow past the obstacle is largely determined by the obstacle shape. Water is used as the working fluid in place of air, which is possible because air is effectively incompressible (like water) at wind speeds much less than the speed of sound, which is the case at Cape Grim.

2. The Experiment

Constructing an accurate model of a three-dimensional shape as large and complex as the Cape Grim terrain is not an easy task. For the purposes of this study, it was felt that the model used for the previous study was too small. Since this would be a wholly new model, considerable effort was made to get an accurate description of the topography by making a fresh assessment of it. The authors had access to incomplete contour maps dating from the construction of the station in the 1980s, a range of photographs taken at various times, and opinions from various personnel who had worked at CGBAPS. To substantiate this information and fill gaps in it, we visited the site for two days in March 2001, when we took a large number of additional photographs, from all angles and elevations, and made additional measurements of heights and distances. From this information, a model of the terrain was made in plasticene with the scale 10 m (actual) = 12.5 mm (model). This was checked with all available data, including contour maps and photographs, and was consistent with them when viewed from all angles. This process is still somewhat subjective, but we are confident that it is as accurate as one can reasonably attain by this process.

As there was a request for more than one model, this initial model was not used in the experiments, but was instead used to make a latex rubber mould which could then be used to create others using fibre glass. The model actually used in the experiments is shown in Figure 1.

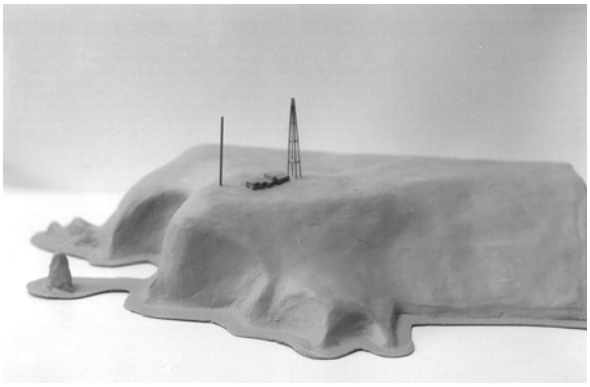

Figure 1. The model of Cape Grim used in the experiments, viewed from a southerly aspect. The vertical pole (scaled height 58 m) near the cliff face denotes the location of site 'B'. The heights above sea level of these sites are 89 m (Telstra tower) and 94 m (site B).

The experiments were carried out in an open tank of length 4 m, width 1.5 m and depth 0.4 m. This tank was filled to a depth of 0.38 m, which was effectively the maximum depth. The model was placed on a flat tray (thickness 1.5 mm) that could be towed along the tank by wires connected to an external motor. In all runs this tray was towed at a uniform speed of 43.2 mm per second, giving a towing time of about 90 seconds. This time is sufficiently long for the flow over the Cape to reach an approximately steady state, and the observations of this steady state were used to generate the conclusions of this study. Runs were carried out with a variety of different orientations of the obstacle, representing wind directions from 180° to 315°.

The question of dynamical similitude of experiments of this nature was discussed in Baines and Murray [1994]. We assume that the air flowing over the region is effectively potentially isothermal to heights greater than twice the topographic height. Over this range of depths, there are two main considerations. Firstly, the effect of viscous and frictional forces is primarily confined to drag and vorticity production at the solid and air-sea boundaries. These effects are characterised by the Reynolds number

$$\mathrm{Re} = UH/\nu \qquad (1)$$

where U is the undisturbed wind (in reality) or towing speed (in the tank), H is the topographic height, and ν is the kinematic viscosity of the fluid. In the atmosphere, the value of Re is very large for Cape Grim (6×10^7). Such values are not realisable in the laboratory, and instead we appeal to the principle of large Reynolds number similarity. This principle states that the flows in two situations that are dynamically similar, except that the Reynolds numbers differ, should be independent of the Reynolds number provided that its value is large (>> 100) in each case. For these experiments Re = 5400, so that the laboratory and atmosphere meet this criterion.

The other main factor concerns the nature of the upstream wind profile $U(z)$, where z is the height above the sea. In the atmosphere, this is well known to have the logarithmic form [e.g. Garratt 1992]

$$U(z) = \frac{u_*}{k} \ln\left(\frac{z}{z_0}\right) \qquad (2)$$

where u_* is the friction velocity, defined by $\tau = \rho u_*^2$, where ρ is the density of the air and τ is the surface stress. k is the von Kármán constant, having a value of 0.4, and z_0 is the roughness length of the underlying surface. In the laboratory, on the other hand, the fluid is initially stationary, implying a uniform velocity with height as seen in the frame of reference of the Cape Grim model. Since this model rests on a moving tray, the no-slip condition on the lower boundary implies that this uniform flow is disturbed by a Blasius boundary layer that grows in thickness from the leading edge of this tray. The thickness δ of this layer (to the height at which the velocity reaches $0.95U$) is approximately [Jones and Watson 1963]

$$\delta = 3(\nu x/U)^{1/2}$$

where x is the downstream distance from this leading edge. This provides some similarity to the atmospheric profile at low levels. Above this level there are differences between the logarithmic and the uniform profiles, as shown in Baines and Murray [1994], but these are not large, and are assumed to be insignificant in promoting differences between the modelled and actual flows around as large and bluff an obstacle as Cape Grim.

A third factor concerns the finite depth of the tank. This has the effect of reducing the vertical displacements of the streamlines, but from theoretical considerations of potential flow [e.g. Batchelor 1967] the effect should be small for the flow close to the obstacle, which is the focus here. Moreover, the overlying stratification higher in the atmosphere (which varies from day to day and hence is effectively unknown) will tend to have the same effect.

As a result of these considerations we believe, as in Baines and Murray [1994], that this experiment provides a sufficiently realistic simulation of the air flow over the upstream face and summit of Cape Grim to provide useful data for the purposes required.

Seven different wind directions were studied (see Table 1), and these were realised by varying the orientation of the obstacle. For some runs, small nearly neutrally buoyant beads were suspended in the fluid as tracers, and were made visible by illuminating a vertical cross section of the flow with an oscillating laser beam. This technique gave an overall picture of the character of the flow in a vertical plane. However, for most data-gathering runs, the flow was visualised by releasing dye from a vertical rake that was situated upstream on the moving tray. This rake had five outlets with scaled heights of 10, 30, 55, 85 and 110 metres above sea level. Since we are interested in two sites at Cape Grim (the Telstra tower, and site B), the position of this rake was adjusted between runs until the released dye passed over the site in question, and data from this run were then used to obtain results. In principle, this implies two productive runs for each wind direction (i.e. one for each site). The dye was forced through the rake by a peristaltic pump. This resulted in a somewhat lumpy dye trace. This is readily allowed for in interpreting photographs of the experiments, where the flow is mostly smooth and laminar, and the lumpiness is due to the nature of the source of dye rather than the fluid motion. Where turbulence and mixing occur due to topographic effects, the dye in the affected fluid becomes elongated and diffuse, and this is readily discerned in the photographs shown in the next section. The dye traces were recorded on videotape using a camera situated to best observe the dye lines, and record their character. A photograph of the experimental set-up is shown in Figure 2.

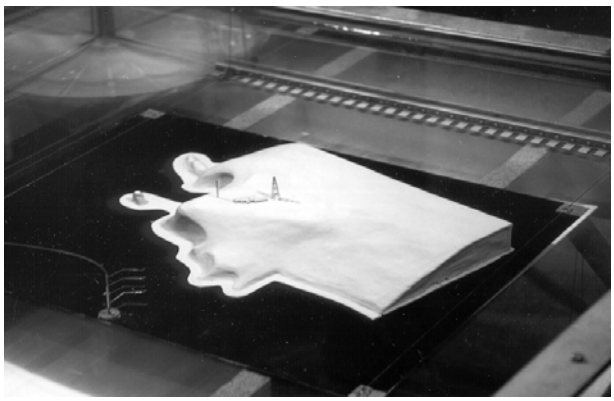

Figure 2. Photograph of part of the towing tank and experimental set-up. The model is situated on the towing tray (dark in colour) near the 'upstream' end of the tank, prior to a towing run. The tray is towed from top right to bottom left, and the rake that releases dye is visible upstream of the model.

3. Results

The main results are summarised in Table 1, which gives the minimum height above the ground at each of the two sites for instruments to be free of air that has had direct contact with the local terrain. These heights were inferred from observing the videotapes of the runs in which the dye traces passed over the site under study (i.e. the tower, or site B). Prudence would dictate that a margin for error of 5 metres should be added to these figures, for use in practice.

Table 1. The minimum height above ground for which the flow is not affected by turbulence generated by the topography, for a range of wind directions for each site.

Wind Direction from (°)	*Compass Point*	*Minimum height above ground for non-turbulent flow* (m)	
θ		*Telstra Tower Site*	*Site B near Cliff Top*
180°	S	25	15
203°	SSW	25	15
225°	SW	30	10
248°	WSW	30	25
270°	W	45	35
293°	WNW	> 70	35
315°	NW	> 70	40

Representative photographs for each wind direction, and for each site, are provided in Figures 3 and 4. In these pictures, the uppermost dye line emanates from the outlet at (scaled) height 110 m, the next down from the 85 m outlet, and so on. Dye from the lowest two outlets is generally not visible in these pictures because it has been deflected laterally at lower levels.

Videos of these flows, taken from cameras showing plan views and vertical sections, may be viewed at CSIRO Atmospheric Research.

One question examined in this study was the possible presence of a 'separation bubble' at the cliff top. In flow over steep obstacles, particularly with sharp corners, the flow may separate from the surface at the corner and then subsequently re-attach (e.g. Baines [1995], Figures 6.22 and 6.23). If they occur, such flow patterns tend to be turbulent and highly variable. However, no evidence of a 'separation bubble' at the cliff top near site B was seen in any of the videos and photographs, probably because the topographic nose is well rounded, and not too abrupt.

In the flow from direction 225° (south-west), the incoming flow is relatively undisturbed, except that when approaching the Telstra tower the low-level flow encounters the buildings of the Baseline Station. Accordingly, the lower region of the tower is affected by the wake of the Station, making the minimum usable height there higher than for 203°, for example. The entries in Table 1 show that the minimum usable height increases as the wind direction tends northerly. This is mainly because the flow near the observation point becomes progressively more affected by bursts of air from the large 'gulch' on the northwest side of the station. As described by Baines and Murray [1994], low level air in this 'gulch' circulates and slowly rises to rejoin and mix with the prevailing wind at the top. This is an unsteady process, and as indicated in Figures 3f and 3g, these bursts may pass the tower in the form of eddies that extend over the whole 70 metres of it. Site B at the cliff top is less affected by this process for the directions studied, and usable heights for these directions at site B were discerned from our observations. Most runs were carried out with steady wind conditions. However, a small number of runs were also carried out in which the wind speed was varied, being reduced from a 'large' value to small values and even zero, before being increased again. As expected, these variations had little or no effect on the pattern of motion of the fluid in the irrotational (non-vortical) region away from the boundary and mixing region. Here, the flow pattern was unchanged, with fluid speeds varying in proportion to the towing speed. The only significant effect of the speed variation was that, at near-zero speeds, the mixing region tended to expand upward slightly, above the ground. However, this disturbance was small, and is effectively covered by the values given in Table 1, provided that the time of near-zero velocity is very short. Hence these results are also valid for varying winds provided that it does not approach zero, and in particular does not become negative. In the latter case, vortical motions caused by the topographic features may be expected to carry boundary-mixed fluid to heights in excess of the values given in Table 1. If the criterion for acceptable air intake is based on a time average (of an hour, say), it is possible that some wind from the north and east, with consequent ground contamination, may enter the intakes even though the overall mean is within the acceptable sector. If it is very important to exclude ground-contaminated air, this air could be monitored on a continuous basis, but the effort involved would probably render this practice impractical. A reasonable alternative may be to compile statistics of the reliability of the wind source for given mean wind speed within the acceptable sector, and then select a minimum mean wind speed for each sector as the simplest reasonable practical criterion.

4. Conclusions

The main results of this study are contained in Table 1. This gives heights at the two sites (Telstra tower, Site B near the cliff top) above which instruments may be placed to receive air that has not been contaminated by contact with the local ground, for winds from a range of specified directions. These winds may vary in speed and direction, provided they do not become too small, or vary outside the acceptable sector. A principle conclusion is that Site B is to be preferred over the Telstra Tower, since (i) the minimum required heights are lower, and (ii) the site is less susceptible to contamination from wind that strays outside the acceptable sector. This applies particularly to the effects of bursts from the northwest 'gulch'.

References

Baines, P.G., *Topographic Effects in Stratified Flows,* Cambridge University Press, Cambridge, UK, 482 pp., 1995.

Baines, P. G., and D. Murray, Modelling of the airflow over Cape Grim, in *Baseline Atmospheric Program (Australia) 1991*, edited by A. L. Dick and J. L. Gras, Bureau of Meteorology and CSIRO, Division of Atmospheric Research, Melbourne, Australia, 20-24, 1994.

Batchelor, G.K., *An Introduction to Fluid Dynamics*, Cambridge University Press, 615 pp., 1967.

Garratt, J. R., *The Atmospheric Boundary Layer,* Cambridge University Press, 316 pp., Cambridge, UK, 1992

Jones, C. W. and E. J. Watson, Two-dimensional boundary layers, in *Laminar Boundary Layers*, edited by L. Rosenhead, Oxford University Press, Oxford, UK, 198-257, 1963.

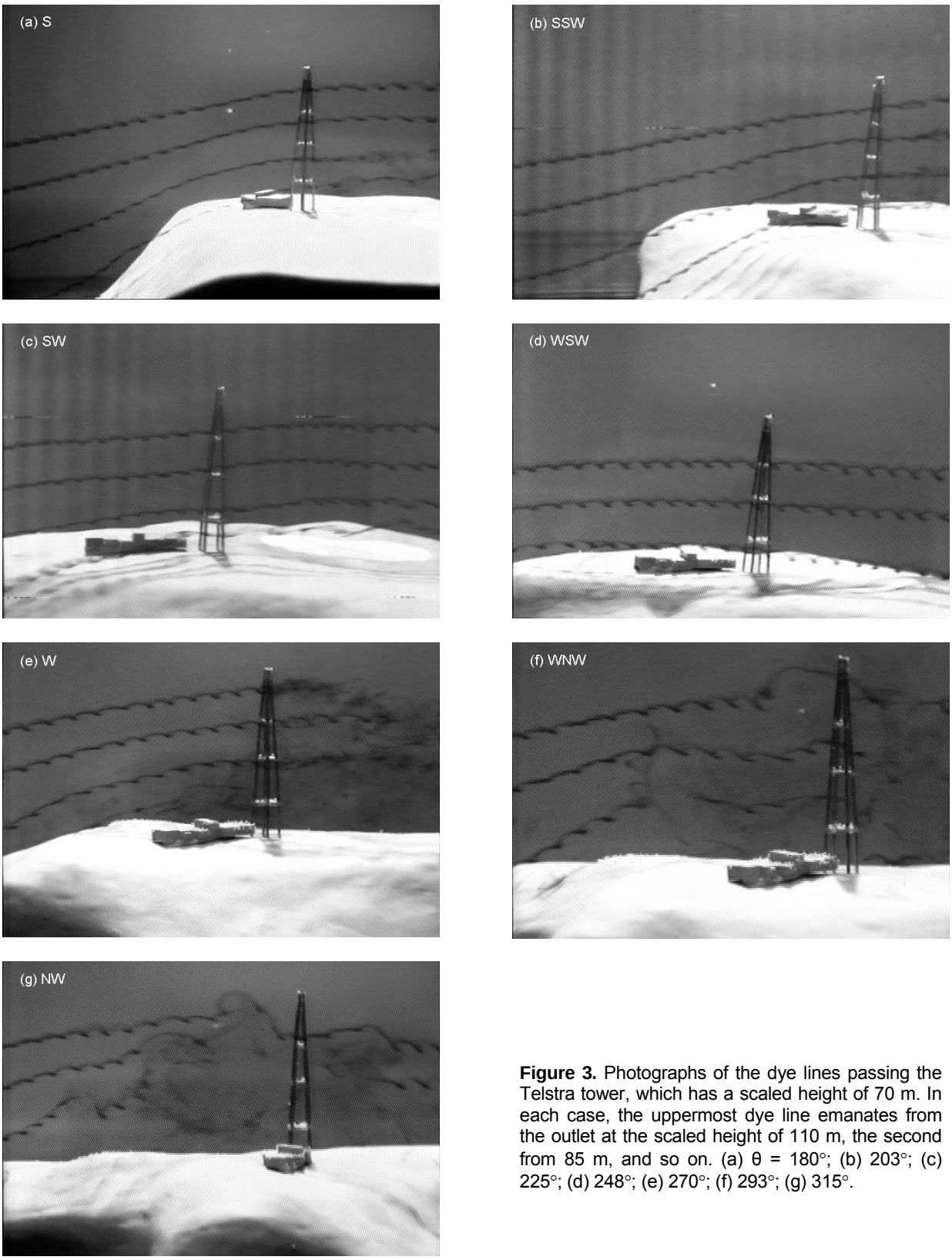

Figure 3. Photographs of the dye lines passing the Telstra tower, which has a scaled height of 70 m. In each case, the uppermost dye line emanates from the outlet at the scaled height of 110 m, the second from 85 m, and so on. (a) θ = 180°; (b) 203°; (c) 225°; (d) 248°; (e) 270°; (f) 293°; (g) 315°.

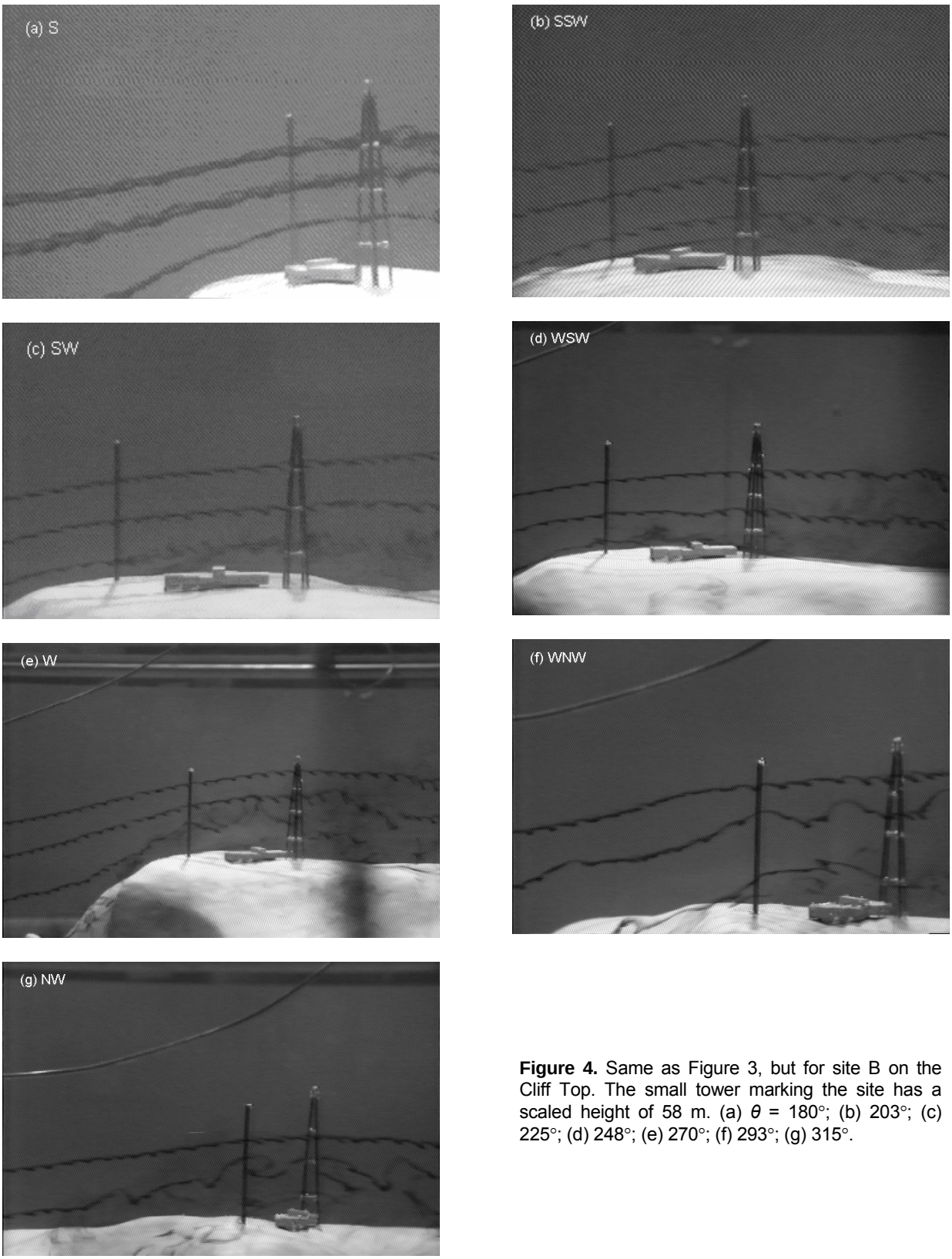

Figure 4. Same as Figure 3, but for site B on the Cliff Top. The small tower marking the site has a scaled height of 58 m. (a) θ = 180°; (b) 203°; (c) 225°; (d) 248°; (e) 270°; (f) 293°; (g) 315°.

PARTICLE TRANSMISSION EFFICIENCY OF THE CAPE GRIM 10-m SAMPLING INLET

H Granek[1], J Gras[1] and D Paterson[2]

[1]CSIRO Atmospheric Research, Aspendale, Victoria, Australia 3195
[2]CSIRO Building Construction And Engineering, Victoria, Australia 3190

Abstract

The particle transmission efficiency of the 10-m inlet is modelled using finite volume techniques based on CFX software. Particles examined fall in the range 1-20 μm aerodynamic diameter to simulating aerosol. Dependence on wind speeds and angle of attack is also examined. Computed average transmission efficiencies are close to 100 percent for the smaller particles in this range but fall to below 25% above about 20 μm. When the incident flow is at small inclined angles, some enhancement or depletion is observed in the calculated particle concentration in the sampling region.

1. Introduction and aims

At Cape Grim aerosol studies have been made since 1976 as part of the Australian Background Air Pollution Program. This program is Australia's major contribution to the World Meteorological Organisation (WMO) Global Atmosphere Watch (GAW), a project that aims to provide high-quality climate data and atmospheric composition data relevant to air quality, over multi-decadal timescales and across the globe.

Aerosol measurements require some form of physical inlet for sampling ambient air, unless the measurements are based on in-situ or remote sensing principles. These inlets interface between various measurement instruments and the atmosphere and have stringent performance requirements placed on their operation. The instruments are required to:

i. operate over a wide range of wind speeds and directions,
ii. have low losses for particles ranging in size from nanometres to several tens of micrometres,
iii. operate at some point or height above ground where relatively undisturbed air flow can be sampled,
iv. minimally influence the parameter being measured via aerodynamic flow effects,
v. exclude rain, insects and birds.

A practical inlet is generally a compromise based on these various demands.

Since 1980 the community 10-m (shared across various projects) inlet system at Cape Grim has comprised an aspirated 0.15 m diameter stainless-steel stack, sampling 10 m above ground level or 104 m above mean sea level. Most aerosol microphysical instruments have sub-sampled from this stack, which services both gas and aerosol samplers. The inlet has a protective rain hood, and the lower section has various sub-sampling manifolds, which, for aerosol sampling are generally operated isokinetically. The inlet is cylindrical and samples the oncoming air stream.

To date the inlet has mainly been sampling sub-micrometre diameter particles relevant to cloud nucleating activity, integrated particle number, photochemically produced particle size distribution and some composition analyses such as elemental carbon determination by light absorption. Further applications may require an ability to determine particle concentrations for particles larger than 1 μm. *In situ* tests have confirmed suitability of the inlet system for sub-micrometre diameter particles however determination of the transmission efficiency for micrometre diameter and larger particles has not been possible because a detailed behaviour of the particle flow needs to be known, and this becomes increasingly different from the airflow at increasingly large particle sizes.

Air inlets employed for sampling aerosol or dust particles for environmental studies around the world come in a very wide range of designs. Numerous studies have quantified transmission through the inlets and other structures. These studies vary between analytical approaches to simple geometries and complex geometries, which use numerical techniques. Examples of such work can be found in Vincent, Hutson and Mark [1982]; Chung and Dunn-Rankin [1992]; Tsai and Vincent [1993] and Dunnett [1999]. Other studies, Mercer and Stafford [1969]; Marple *et al*. [1974a,b] and Marple and Willeke [1976], are examples of an impactor, which is a related device. Wen and Ingham [2000] present theoretical work for a simplified inlet. Other methods of determining aspiration efficiency involve experiments in wind tunnels [e.g. Ramachandran *et al*. 1998].

This article summarises the work that has been done to address the question of the transmission efficiency for particles in the range 1-20 μm entering the Cape Grim station's 10-m inlet, and provides some additional information relating to the averaged (over angle of attack) behaviour of the incident flow omitted from a more detailed article by Granek *et al*. [2003]. The work was done using a computational fluid dynamics approach, where we numerically study the airflow and aerosol transport around and inside the head of the inlet and down the inlet tubing. The task was carried out using CFX computational fluid dynamics software, developed by AEA Technology in the UK [AEA Technology 1999].

The first stage of a realistic modelling exercise is constructing a grid that accurately represents the structure to be modelled. The difficulty of this task depends on the required detail and complexity of the design, which could be very demanding and time consuming.

The modelled inlet comprises a 0.15 mm diameter, 10 m high vertical stainless steel tube, capped with a domed rain hood (held in place by a thin collar and three radial supports which were not modelled). In addition, there is a coarse mesh of fine wire between the hood and the tube to prevent birds from entering the inlet. The vertical stack also has an external skin in two sections with drilled holes to reduce vortex-shedding and suppress oscillation of the stack during strong winds. For this initial investigation, these effects are not included in the numerical model. This does not affect the model results since the steel stack is assumed to be perfectly rigid. The domain for the numerical realisation of the stack extends approximately 1 m down the inlet tube. The flow varies little once the initial velocity profile inside the vertical stack tube has been established. Figure 1 shows a full view of the inlet, and Figure 2 shows a schematic view of the modelled region.

Figure 1. *In situ* view of the 10-m Cape Grim air inlet

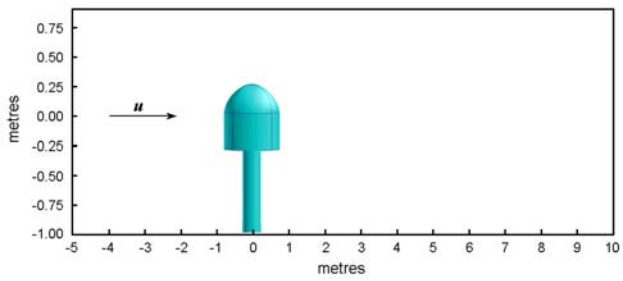

Figure 2. Schematic view of the modelled region, showing the direction of the incident air flow.

2. Model properties and limitations

Summary of the model conditions and parameters is as follows. The model is:

- designed for uniform steady incident flow, which is a parameter in the range of 7-20 m s^{-1};
- the angle of incidence varies up to 20º from (above or below) the horizontal flow;
- the flow down the stack was fixed at 293 l min^{-1}, (mean inlet speed of about 0.28 m s^{-1});
- the air phase was modelled for ambient temperature (288 K) and 1 atmosphere mean pressure;
- in the incident flow, where the velocity is about 20 m/s and the distance is 10 m, Reynold's number, $Re = 1.4\times10^{7}$;
- in the flow around the inlet tube, with 20 m s^{-1} and 0.15 m, $Re \sim 2\times10^{5}$;
- in the flow inside the inlet tube, with 0.28 m s^{-1} and 0.15 m, Re = 2,900.

At Reynolds numbers above 2000 [see Gibson 1991] the turbulent flow applies. We have chosen to use the Wilcox low Reynolds number k-ω model of turbulence [Wilcox 1998; Granek *et al*. 2003].

The mean flow determined is a quasi-stationary type of flow where the *statistically averaged* fields are determined, rather than a time-dependent flow, which gives the development of fields as a function of time. The solution is obtained from the final iteration when the iterations are considered to have converged.

2.1. Grid properties

The model is based on a finite volume mesh in Cartesian three-dimensional space.

The grid for the simulation is a block-structured body-fitted grid. The whole flow domain is split into blocks in an unstructured way as shown in Figure 3. Each of these blocks is split into hexahedral volume elements in a structured way. This allows CFX to use the preconditioned gradient solver for pressure and Stone's strongly implicit [Stone 1968] solver variables. Granek *et al*. [2003] provide more detail on the numerical techniques used by CFX.

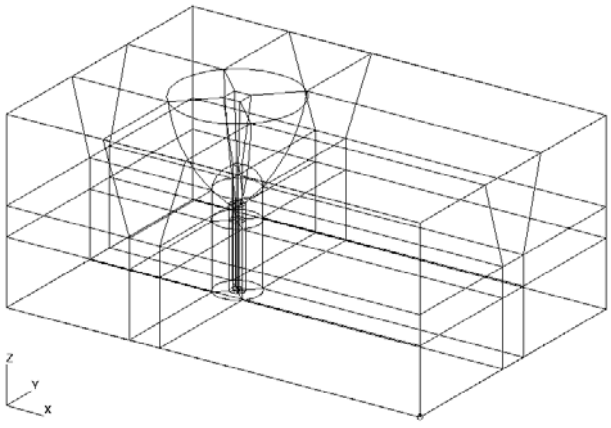

Figure 3. A view of the modelled domain split into coarse grid blocks.

2.2. Summary of fluid modelling

The partial differential equations for momentum and turbulence are formulated using primitive variables [Patankar 1983], Simplec [Van Doormaal and Raithby 1984], cell-centres [Rhie and Chow 1983] and SUPERBEE [Hirsch 1990].

The motion of atmospheric particles is driven by wind. There are always three possible approaches to model the particles; the Lagrangian approach, the drift-flux approach and the multiphase approach each with their respective advantages and disadvantages. In this study, we have chosen the multiphase approach, in which each particle category adds extra 6 partial differential equations for conservation of mass and momentum. This is a good method to model particles moving across fluid streamlines and their interactions with the turbulent flow [AEA Technology plc, 1999].

The boundary conditions in the particle phase need to be fixed for the sticky aerosol particles because in the default state it is assumed that particles bounce off with coefficient of restitution of one (i.e. by default full elasticity is assumed). In our implementation, only one particle size was modelled at a time so the equations are reduced to a two-phase flow. The multiphase approach also has the advantage of being fully coupled, that is, the particles drag air along with them and this affects the air because the free airflow is obstructed by these particles. Drag is handled with a drag coefficient C_D. The time derivative of momentum is force (Newton's law) so the drag force is simply added in to the momentum equations. The force added is the product of the drag force on a single particle and the number of particles per unit volume.

The viscosity of the particle phase was set to that of the surrounding air (1.789×10^{-5} Pa s), as small aerosols considered in this paper are diffused by turbulence in the air nearly the same way as the air molecules. The density of individual particles in the particulate phase was set to the density of water (1000 kg m^{-3}). This affects the momentum – which is important because it controls deposition and gravitational settling rate, and the settling rate is small enough so it can be neglected.

In the two-phase fluid modelled here, the first phase (continuous) consists of air and the second phase (dispersed) consists of the aerosol particles. The particles in the flow are subjected to both inertial and viscous effects, which are accounted for by allowing slip between the two phases. Setting the concentration of the aerosol phase to zero wherever that phase comes into contact with, or very close to, a physical wall incorporates particle loss. This assumes negligible particle bounce, which is a reasonable assumption given the maritime location of Cape Grim. The density (ρ) of the particles in the dispersed phase is set to 1000 kg m^{-3} allowing particle description in terms of aerodynamic size. In practice, a series of fixed aerodynamic particle sizes was used for the calculating a range of flow patterns as a function of *d*, the aerodynamic size. Conversion to other aerodynamic particle sizes and densities can be achieved simply by using the Stokes' parameter [Mercer and Stafford 1969]. For a given flow this yields a relationship of $\rho \sim d^{-2}$. Paterson and Cole [2003] found that this relationship holds even in the case when turbulent diffusion is included, provided the 10-100 μm diameter transition regime is avoided. For smaller particle sizes (below about 10 μm), Paterson and Cole [2001] show that turbulent diffusion loss is relatively small and independent of particle size and at much larger sizes its effect can be neglected entirely. They also show that the transition regime is dependent on the size of the structure (or the upstream distance reached by the disturbance), with larger structures extending the regime dominated by turbulent diffusion to larger particle sizes. The implication is that at larger Reynolds numbers turbulence is sufficiently intense to affect larger particles in the same way as the small ones. In other words, the transitional particle size is expected to increase with Reynolds number.

2.3. Boundary conditions

There are two general types of boundary conditions for the model; air-air and wall interfaces. The former includes those at the outer limits of the domain being modelled as well as the outlet of the inlet tube. The latter occurs on the outside and inside metal faces of the air inlet. The external surfaces of blocks of grids are body-fitted to the shape of the metal (see Figure 3).

Air-air interfaces: The air inflow is always either horizontal or inclined at a relatively small angle, so the grid does not need to extend very far above the dome. The horizontal dimensions of the grid are significantly larger outside the structure than the inside so detail of the flow pattern can be better modelled and viewed. The walls facing the incident flow as well as the top and bottom boundaries of the domain allow for inflow and outflow from the domain. The boundary conditions at the bottom of the inlet were set to a uniform velocity flow and constrained to an outflow of 293 l min^{-1}. Some more details, including the turbulence parameters can be found in Granek *et al*. [2003].

Wall boundary conditions: CFX has default wall boundary conditions where a log-law velocity profile with transition to an inner linear sublayer is implemented. These could not be used because CFX does not allow flow through walls. Therefore the walls were modelled as inlets with zero air velocity, which is satisfactory for a fine grid for the momentum and pressure corrections. The particle deposition was calculated from the velocity component perpendicular to metal surfaces in the near wall control volumes. If particles are not being deposited then the volume fraction of air at the wall is set to one, otherwise the volume fraction gradient is set to zero. The grid was made fine enough to resolve the log-linear layer. The treatment of these boundary conditions is described in more detail in Granek *et al*. [2003].

2.4. Other properties of the model

The steady-state condition placed on the model means that the solution is formed when further iterations do not lead to significantly altered fields such as *u, v* and *w* velocity, pressure, volume fraction and the turbu-

lence parameters *k* and ω. We are solving a Cauchy-type problem, where the interior solution is fully determined by the boundary conditions. Although the Navier-Stokes' equations are non-linear and it is possible to get non-unique multiple solutions this rarely happens. Care needs to be taken in selecting initial conditions because initial conditions that are too far from the final solution can lead to non-converged unrealistic solution.

3. Results

One of the main objectives of this work is to determine aerosol transmission efficiency inside the 10-m Cape Grim air inlet. This is calculated as the ratio of the mass fraction of aerosol (phase 2) in the detection region and the value at the inflow boundary. During normal inlet operation, aerosol is sub-sampled using a series of secondary inlets arranged annularly inside the lower section of the stack. Thus it is desirable to understand the physical distribution of particles within the stack as well as the mean cross-sectional average concentrations.

The model has a number of parameters that affect the flow pattern and the efficiency of particle detection at the outlet. Of all the parameters investigated, we consider the particle size, incident flow speed and inclination to the horizontal to be most important. The effects of these parameters on the efficiency of detection are described in the sections below.

3.1. Air phase properties of the flow

Modelled average air flow around the inlet conforms to laminar behaviour, with a high pressure region developing on the upwind side of the structure as the flow impinges on and diverges around the structure. The main complications in the flow occur inside the domed rain hood, where various eddies form depending on the external boundary conditions of the flow. For example, the eddy structure (see e.g. Figure 4) varies with the vertical angle of attack of the flow and the mean upwind speed.

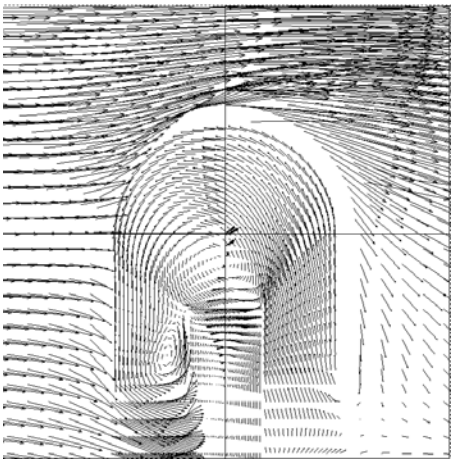

Figure 4. An example of the air flow pattern along the x-axis through the vertical cross-section of the inlet (vector size and orientation proportional to the wind speed and direction, incident wind speed 11 m s^{-1}).

3.2. Aerosol phase

3.2.1. Variation down inlet stack

The flow pattern down the inlet is found to change very little or not at all once the distance to the top of the cylindrical tube exceeds the tube diameter. Therefore, it is enough to examine the flow at the bottom of the modelled region. This flow pattern is largely dependent on the pattern established in the hood, which then extends all the way down the stack. Figure 5 shows a flow pattern for angle of attack, $\alpha = 0^o$, incident wind speed u = 11 m s^{-1} and aerosol particle size d = 1 μm. The aerosol is collected at the bottom, so we examine this region in more detail.

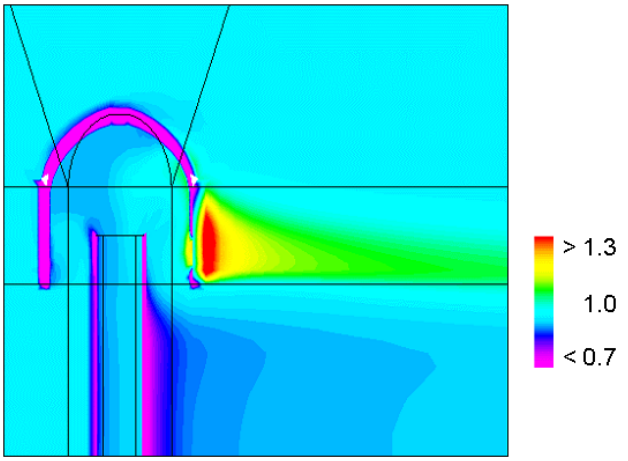

Figure 5. Aerosol mass fraction cross-section through the air inlet along the direction of air flow (x-axis) for angle of attack $\alpha = 0^o$, incident air speed u = 11 m s^{-1} and aerodynamic particle diameter d = 1 μm. Concentrations are in parts per 10^3 by volume.

3.2.2. Effects due to varying particle size

The model is run for several different particle sizes in the range 1-20 μm. For increasing particle size we expect greater slip and greater difficulty in 'going down the stack'. This effect is much more pronounced as particle size increases from 1 μm to 10 μm, and at around 20 μm very little aerosol is expected to propagate down the stack. This is clear when looking at the results in Table 1, where we give percentage efficiencies at a horizontal angle of attack ($\alpha = 0^o$) for different particle sizes. These data are graphed in Figure 6. The results show a drop in detection efficiency as the particle size increases. The reductions become more rapid as the particle size reaches the upper level of the size range investigated. Note also that the mean efficiency curve is closer to the maximum efficiency at smaller particle sizes but at larger particle sizes it is closer to the minimum curve indicating that the reduced concentration region is initially small and gradually expands to fill the entire cross section of the stack. This is actually observed in the modelling results [see Granek *et al*. 2003].

Table 1. Maximum, average and minimum percentage particle efficiencies at the bottom of the inlet tube for various particle aerodynamic diameters and an incident wind speed of 7 m s^{-1}.

	1 μm	*2 μm*	*4 μm*	*10 μm*	*20 μm*
maximum	101	98	97	83	48
average	100	92	89	69	25
minimum	96	70	62	47	13

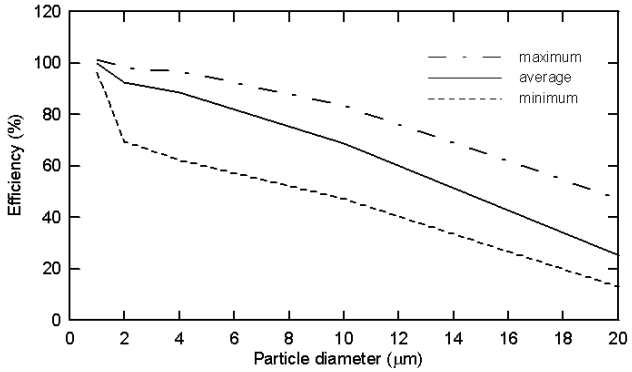

Figure 6. Maximum, average and minimum percentage particle efficiencies at the bottom of the inlet tube with horizontal angle of attack, $\alpha = 0^{o}$, air speed u = 7 m s^{-1}.

3.2.3. Effects due to varying incident wind speed and direction

The angle of attack is an interesting parameter as it affects the flow patterns and under certain circumstances, outlined below, can cause enhancement to the particle concentrations above the concentrations in the incident flow. In general for a horizontal flow the greatest aerosol concentration occurs directly behind the dome collar (see Figure 5). For a slightly upward inclined flow, the pattern inside the dome and the inlet pipe changes in such a way that an axial enhancement in aerosol intensity forms (see Figure 7). This enhancement is also dependent on external flow speed and attains a maximum somewhere in the wind speed range of 7-20 m s^{-1}. As the particle size increases, the enhancement region reverses and becomes a depletion region with aerosol concentration lower than that of the surrounding region. This kind of behaviour has been demonstrated in the design of a concentrator, where an increase in particle concentration is required [Clark *et al*. 1997].

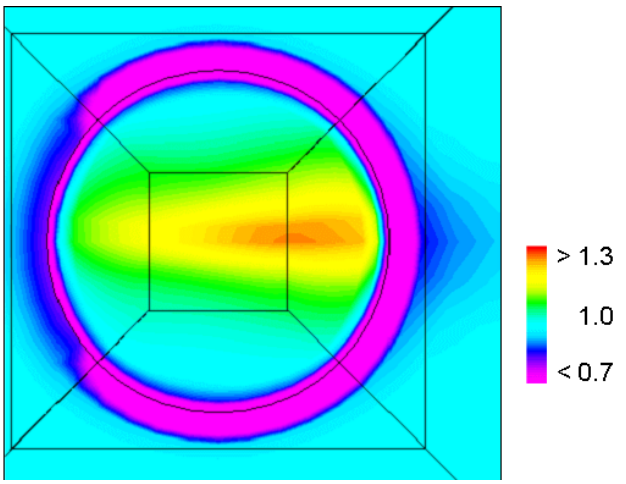

Figure 7. Aerosol mass fraction cross-section through the air inlet at the base of the stack for angle of attack α=10^{o}, incident air speed u = 11 m s^{-1} and aerodynamic particle diameter d = 1 μm. Concentrations are in parts per 10^{3} by volume.

The model was tested for 3 different wind speeds: 7 m s^{-1}, 11 m s^{-1} and 20 m s^{-1}, where the lower limit is determined by the cut-off wind speed criterion used for baseline atmospheric conditions. Our expectation is that the concentration of particles in the inlet becomes depleted as the wind speed increases, because the faster particles will find it harder to 'turn the corner' and go 'down the stack'. This is in fact what is sometimes found. The effect is sensitive to the angle of attack, which affects the flow pattern under the hood, and for angles investigated the greatest enhancement occurs at an upward inclination of around 10°-15°. Consequently, the effect of wind speed on particle concentrations is less important than the effect of particle aerodynamic size.

Table 2 gives a summary of the results discussed above. The selected cases are run for 1-μm particles. We consider cross-sectional average concentrations over the bottom of the inlet region as well as the minimum and maximum cases when the angle of attack and incident speed are varied. Note that the strong enhancement in efficiency at about 10° at the lower end of the incident speed range, but closer to 15° at the higher end of the wind speed range. There are also other slight variations in efficiency over the range of angles investigated. These effects are most likely due to air circulation patterns established inside the dome, which then control the pattern established in the downpipe.

Table 2. Maximum, average and minimum percentage particle efficiencies for the cross-section at the bottom of the inlet tube for d = 1 μm aerodynamic particle diameter and three wind speeds.

	Percentage efficiency								
	maximum			*average*			*minimum*		
	7 m s^{-1}	*11 m s^{-1}*	*20 m s^{-1}*	*7 m s^{-1}*	*11 m s^{-1}*	*20 m s^{-1}*	*7 m s^{-1}*	*11 m s^{-1}*	*20 m s^{-1}*
-20°	94	95	94	89	90	88	64	62	57
-10°	91	94	96	87	89	90	63	63	60
0°	101	99	97	100	94	92	96	73	65
5°	97	95	101	92	90	93	65	61	60
10°	112	137	108	107	109	96	77	69	60
15°	97	97	122	93	93	100	67	64	61
20°	98	99	114	93	94	97	66	63	60

In Table 3 we give a weighted average over the angle range for the results in Table 2, and these results are plotted in Figure 8. The results in Table 3 show that the angle-averaged minimum and maximum concentrations diverge from the mean angle-averaged concentrations. The angle-averaged mean does not change very much over the range of particle speeds, which confirms the efficiency at a given speed and location in the cross-section is very sensitive to the flow pattern established under the hood. This in turn is highly dependent on the angle of attack α.

Table 3. Maximum, average and minimum percentage particle efficiencies at the bottom of the inlet tube for d = 1 μm aerodynamic particle diameter averaged over the available angle of attack range for three wind speeds.

	Percentage efficiency		
	7 m s^{-1}	*11 m s^{-1}*	*20 m s^{-1}*
maximum	97	99	102
average	94	93	93
minimum	72	66	61

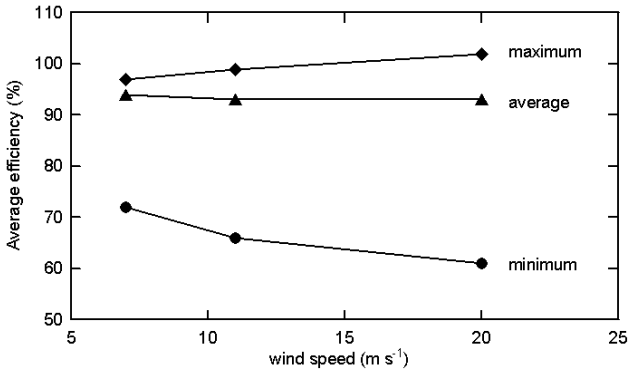

Figure 8. Angle of attack averaged percentage efficiencies of Table 3.

3.2.4. Variation across the inlet

It is found that cross-sectional pattern varies a lot depending on parameters such as the incident wind speed *u*, wind inclination α and the aerodynamic particle diameter *d*. In particular, the pattern along the x-axis (flow direction in the horizontal plane) can change from peak concentrations (Figure 7) to the lowest concentrations (see Figure 9). In addition, a ring of reduced concentration forms close to the cylindrical wall as a result of aerosol deposition, but this region has the highest concentrations when the interior is strongly depleted of particles. Occasionally, higher concentration lobes appear when the concentrations are lower along the x-axis and near the walls.

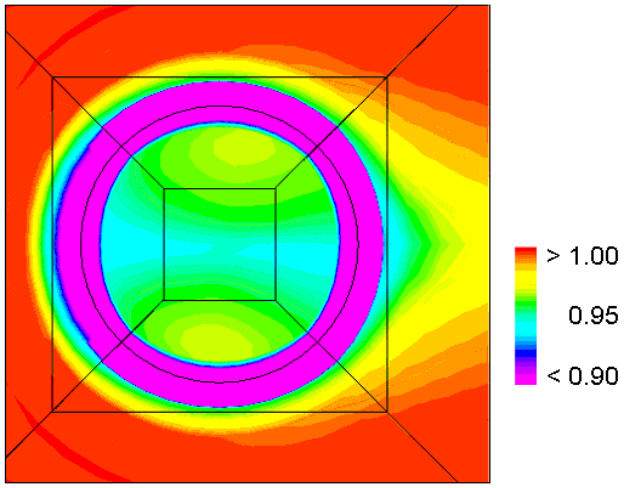

Figure 9. Aerosol mass fraction cross-section through the air inlet at the base of the stack for angle of attack α = 15^{o}, incident air speed u = 7 m s^{-1} and aerodynamic particle diameter d = 1 μm. Concentrations are in parts per 10^{3} by volume.

When the results for various angles of attack are averaged, as in Table 3, we note that as the incident flow speed increases to 20 m s^{-1} the average concentrations of particles along the axis increase and those in the side lobes decrease (see Figures 10, 11 and 12). This is responsible for the averages remaining almost unchanged. Furthermore, there are configurations where a strong enhancement occurs along the x-axis and this contributes to the spreading out of angle-averaged cross-sectional minimum and maximum values of the particle concentrations (see Table 3). The conclusion here is that, at least for 1 μm diameter particles, wind speeds in the baseline sector do not affect the average flow of particles in the inlet, but they influence where the particles mostly turn up in the sub-sampling region.

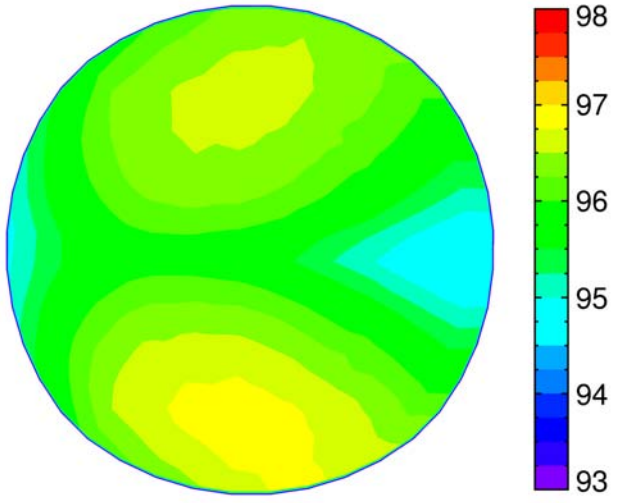

Figure 10. Air inlet percentage detection efficiency at the base of the stack averaged over the angles of attack (–20^{o} to 20^{o}), incident air speed u = 7 m s^{-1} and aerodynamic particle diameter d = 1 μm. Maximum, average and minimum values for this figure are given in Table 3.

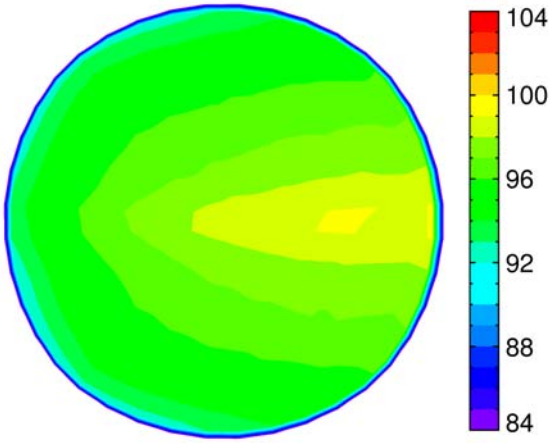

Figure 11. Air inlet percentage detection efficiency at the base of the stack averaged over the angles of attack (–20° to 20°), incident air speed u = 11 m s^{-1} and aerodynamic particle diameter d = 1 μm. Maximum, average and minimum values for this figure are given in Table 3.

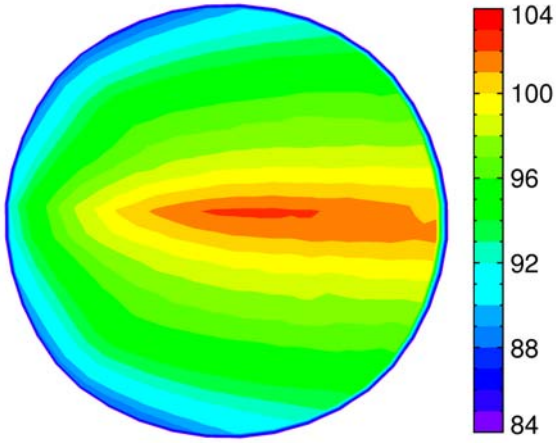

Figure 12. Air inlet percentage detection efficiency at the base of the stack averaged over the angles of attack (–20 ° to 20°), incident air speed u = 20 m s^{-1} and aerodynamic particle diameter d = 1 μm. Maximum, average and minimum values for this figure are given in Table 3.

4. Conclusions

In this article we have demonstrated the ability of CFD software (CFX in this case) to solve numerically the problem of aerosol flow into a detection apparatus (blunt air inlet). The results still need to be verified for the physical apparatus. The sensitivity of the flow to the different boundary conditions, such as incident wind speed, wind inclination and particle size was examined. We note the following behaviour of the model:

- rapid loss of detection efficiency for particles above ~ 5–10 μm diameter range;
- a general variation of the order of about 10% in detection efficiency from the mean value depending on the angle of inclination. In some cases, deviations were significantly large;
- some variability due to incident wind speed, but detection efficiency depends on the convection pattern established under the dome. Generally decreasing efficiency, but occasional increases observed particularly for the positive angle of inclination;
- very little change in flow pattern observed as the flow moves down the tube;
- a large sensitivity of the efficiency pattern across the tube depending on different boundary conditions and particle size. The pattern was least variable for the smallest particles moving at low speeds.

References

AEA Technology plc, CFX-4 Documentation, CFX-4.2 Solver User's Manual, 1999.

Clark, J. M., E. V. J. Foot, S. R. Preston, D. Shakeshaft, and B. D. Short, The design, modelling and experimental investigation of a new high volume high ratio aerosol concentrator for the collection of small particles, *J. Aerosol Sci*., 28, 332, 1997.

Chung, I.P., and D. Dunn-Rankin, Numerical simulation of two-dimensional blunt body sampling in viscous flow, *J. Aerosol Sci*., 23, 217-232, 1992.

Dunnett, S. J., An analytical investigation into the nature of the airflow near a spherical bluff body with suction, *J. Aerosol Sci*., 30, 163-171, 1999.

Gibson, C. H., Turbulence, in *Encyclopaedia of Physics*, edited by R. G. Lerner and G. L., Trigg, VCH Publishers Inc., New York, 1310-1314, 1991.

Granek, H., J. L. Gras, and D. Paterson, The aerosol transmission efficiency of the Cape Grim Baseline Air Pollution Station 10-m sampling inlet, in preparation, 2003.

Hirsch, C., Numerical computation of internal and external flows, Volume 2, John Wiley & Sons, Chichester, England, New York USA, 714 p., 1990.

Laitone, J. A., Erosion prediction near a stagnation point resulting from aerodynamically entrained solid particles, *J. Aircraft*, 16, 809-814, 1979.

Marple, V. A., Y. H. Liu, and K. T. Whitby, Fluid mechanics of the laminar flow aerosol impactor, *Aerosol Sci.* , 5, 1-16, 1974a.

Marple, V. A., Y. H. Liu, and K. T. Whitby, On the flow fields of inertial impactors, *J. of Fluids Engineering - Transactions of the ASME*, 96, 394-400, 1974b.

Marple, V. A. and K. Willeke, Impactor design, *Atmos. Environ*., 10, 891-896, 1976.

Mercer, T. T., and R. G. Stafford, Impaction from round Jets, *Annals of Occupational Hygene*, 12, 41-48, 1969.

Patankar, S. V., Numerical heat transfer and fluid flow, *Hemisphere*, 1983.

Paterson, D., and I. Cole, Aerosol deposition on and pollutant removal from structures, CSIRO DBCE Doc. 01/438, in press, 2003.

Ramachandran, G., A. S. Sreenath, and J. H., Vincent, Towards a new method for experimental determination of aerosol sampler aspiration efficiency in small wind tunnels, *J. Aerosol Sci*., 29, 875-891, 1998.

Rhie, C. M., and W. L. Chow, Numerical study of the turbulent flow past an airfoil with trailing edge separation, AIAA J1, 21, 1527-1532, 1983.

Tsai, P.-J., and J. H. Vincent, Impaction model for the aspiration efficiencies of aerosol samplers at large angles with respect to the wind, *J. Aerosol Sci*., 24, 919-928, 1993.

Van Doormaal, J. P., and G. D. Raithby, Enhancements of the SIMPLE method for predicting incompressible fluid flows, *Numer. Heat Transfer*, 7, 147-163, 1984.

Vincent, J. H., D. Hutson, and D. Mark, The nature of air flow near the inlets of blunt dust sampling probes, *Atmos. Environ*., 16, 1243-1245, 1982.

Wen, X. and D.B. Ingham, Aspiration efficiency of a thin-walled cylindrical aerosol sampler at yaw orientations with respect to the wind, *J. Aerosol*, 31, 1355-1365, 2000.

Wilcox, D. C., Turbulence modelling for CFD, 1998, DCW Industries, 1998.

TAPM MODELLING STUDIES OF AGAGE DICHLOROMETHANE OBSERVATIONS AT CAPE GRIM

M Cox[1], S Siems[2], P Fraser[3], P Hurley[3] and G Sturrock[4]

[1]Centre for Atmospheric Chemistry, York University, Toronto, Ontario M3J 1P3, Canada
formerly at School of Mathematical Sciences, Monash University, Australia
[2]School of Mathematical Sciences, Monash University, Clayton, Victoria 3800, Australia
[3]CSIRO Atmospheric Research, Aspendale, Victoria 3195, Australia
[4]School of Environmental Sciences, University of East Anglia, Norwich NR4 7TJ, UK
formerly at CSIRO Atmospheric Research, Aspendale, Victoria 3195, Australia

Abstract

AGAGE *in situ* observations of dichloromethane (CH_2Cl_2) at the Cape Grim Baseline Air Pollution Station are compared with simulations from a regional transport model (The Air Pollution Model, TAPM), incorporating emissions of CH_2Cl_2 from the Port Phillip region (PPR, largely Melbourne) as estimated in the Victorian Environmental Protection Authority source inventory. Observations and simulations were compared over an 18-month period. TAPM showed a high degree of skill in predicting the arrival of large pollution events from Melbourne, but overall model concentrations were, on average, a factor of five to six lower than the AGAGE observations.

Various potential sources of error in the model simulations were considered. A major source of error could be that the EPA inventory is a factor of three too low for CH_2Cl_2 based on considerations of the net imports of CH_2Cl_2 into Victoria compared to the EPA source inventory for the PPR. Another source of error could be a systematic bias in the model meteorology. These high pollution events are almost always found in the boundary layer of pre-frontal air masses, whose dynamics may be difficult to simulate.

Key words: dichloromethane, back-trajectories, air pollution modelling, Cape Grim Baseline Air Pollution Station.

1. Introduction

Dichloromethane (CH_2Cl_2) is a short-lived atmospheric species that contributes small amounts of chlorine to the stratosphere and thus plays a minor role in depletion of stratospheric ozone. The lifetime of CH_2Cl_2 in the troposphere is approximately 6 months [Kurlyo *et al*. 1999], which allows for the species to be transported into the stratosphere by deep convection in the tropics. The primary source of CH_2Cl_2 is its use as an industrial and commercial solvent and in domestic consumer products. Global observations of CH_2Cl_2 show an inter-hemispheric ratio of 1.7, with higher concentrations in the Northern Hemisphere where most of the emissions occur [Khalil 1999]. Minor natural sources of CH_2Cl_2 originating from the ocean and biomass burning have been reported (Keene *et al*., 1999), but their magnitudes are very uncertain. The main sink for CH_2Cl_2 is destruction by the hydroxyl radical, largely in the troposphere.

Since early 1998, the Advanced Global Atmospheric Gases Experiment (AGAGE) has collected high-frequency, *in situ* measurements of short-lived chlorine species in the boundary layer. Identical GC-MS (gas chromatography-mass spectrometry) instrumentation and calibration procedures have been employed at Mace Head, Ireland (52°N) and Cape Grim, Tasmania (41°S), to contribute to an understanding of their global and regional sources and sinks [Prinn *et al*. 2000; Sturrock *et al*. 2001; Cox *et al.* 2002].

The Victorian Environment Protection Authority (EPA) has estimated that CH_2Cl_2 emissions for the Port Phillip Region (PPR, which includes Melbourne) were 500 tonnes yr^{-1} for the years 1995/1996 [Environmental Protection Authority 1998], based on industry surveys. Melbourne industry is the dominant source of CH_2Cl_2 within the Port Phillip region, and trace gas emissions from Melbourne have been observed at Cape Grim [Cox *et al*. 2000]. It should be possible to use the CH_2Cl_2 observations from Cape Grim to verify the EPA regional inventory. Similar efforts have been undertaken for the AGAGE observations at Mace Head [Ryall *et al*. 2001]. Transport of emissions from the Port Phillip region to Cape Grim usually takes less than 24 hours, which allows CH_2Cl_2 to be treated as a passive tracer in a chemical transport/air pollution model. In this paper, The Air Pollution Model [TAPM; Hurley 1999], developed at CSIRO Atmospheric Research, has been used with the EPA CH_2Cl_2 emissions inventory to simulate CH_2Cl_2 observations at Cape Grim. Comparison of model results and observations is a test of both TAPM's ability to represent transported pollution at Cape Grim and the accuracy of the EPA CH_2Cl_2 emissions inventory.

2. AGAGE CH_2Cl_2 observations at Cape Grim

In situ GC-MS CH_2Cl_2 measurements (6 per day) began in March 1998 as part of the AGAGE program [Prinn *et al*. 2000; Sturrock *et al*. 2001]. The AGAGE instrumentation consists of a Carboxen-filled micro-trap (20 µl) in an adsorption (-55°C) – desorption (240°C) system for air-sampling (Nafion dried, 2 litres per measurement, 40 minutes trapping time), coupled to an HP 6890/5973 GC-MS using analysis techniques developed at the University of Bristol (UB) [Simmonds *et al*. 1995; Sturrock *et al*. 1998; Prinn *et al*. 2000]. In the 25-month period (March 1998 – March 2000) approximately 3500 calibrated measurements of CH_2Cl_2

were made at Cape Grim. Minor data gaps are due to instrument servicing and down time. The monthly mean precision (% standard deviation) achieved in 1998 for about 150 standard measurements per month was 0.9%, while the variability in background ambient air measurements was 3%. The CH_2Cl_2 standards employed at Cape Grim and resulting data are discussed in Prinn *et al*. [2000], Sturrock *et al*. [2001] and Cox *et al*. [2002].

Cape Grim CH_2Cl_2 observations show a seasonally varying background concentration (7-11 ppt, late summer minimum, spring maximum), with a number of episodic events of up to 100 ppt, largely in winter. Figure 1 shows the CH_2Cl_2 observations, with the annual background cycle subtracted, for the 18-month period of June 1998 to November 1999, inclusive. The identification and specification of background data used CO_2 variability and wind direction selection criteria, followed by a Fourier filter and curve fit [Thoning *et al.* 1989; Cox 2002].

3. Air Mass Origin and Meteorology

High pollution events were simply defined as those CH_2Cl_2 observations that fell within the upper 20% of all observations (above background). By assigning each high pollution event to the nearest back-trajectory in time, the air mass origin of the high pollution events could be examined. The back-trajectories were initialised to have a 100-m final elevation at Cape Grim and follow isobaric surfaces. Back-trajectories were obtained by using data from the Bureau of Meteorology regional transport model [Limited Area Prediction System – LAPS; Puri *et al*. 1998] as input to the Hy-SPLIT trajectory code [Draxler 1992]. These back-trajectories were limited to 24 hours in duration at 1-hour intervals. Back-trajectories were calculated for March to mid-September 1998 at 0600 UTC and at 0000, 0600 and 1200 UTC for mid-September 1998 to March 2000.

Figure 2 is a trajectory frequency distribution of the air mass position over the specified time periods, which illustrates the air mass origin for the high pollution events before reaching Cape Grim. The geographic location of an air mass was recorded hourly along its 24-hour back-trajectory. These 24 latitude/longitude readings were then placed into $1° \times 1°$ bins and sorted by time before arrival at Cape Grim. The bin count was then normalised by the most populated bin. Figure 2a shows the air mass in the interval of 7-12 hours before reaching Cape Grim. The most populated bin for this air mass is just south of Melbourne, essentially due north of Cape Grim. In Figure 2b the 13-18 hour trajectory frequency distribution shows the air mass origin north of Melbourne. As expected, the variability of the air mass origin location widens, both latitudinally and longitudinally with time.

Figure 2 clearly indicates that the source region for the high pollution events observed at Cape Grim was Melbourne. Moreover, these high pollution events came directly from Melbourne in about 12 hours. Their transit velocity is approximately 6-7 m s^{-1}. While the air mass origin data for other short-lived chlorinated methanes, such as methyl chloride (CH_3Cl) and chloroform ($CHCl_3$), suggested Victorian and Tasmanian coastal sources, CH_2Cl_2 pollution appeared to originate mainly from Melbourne [Cox *et al*. 2002]. The uniform transport time further suggests that high pollution events at Cape Grim happen under approximately the same meteorological conditions. A study of Cape Grim climatology reveals that this is common in the period (several hours) before a frontal passage at the station.

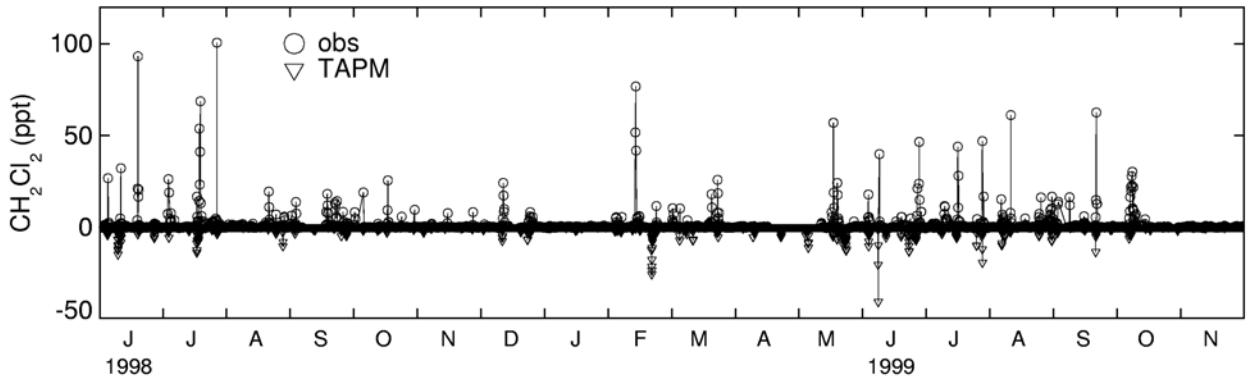

Figure 1. AGAGE observations and TAPM simulations of CH_2Cl_2 for the period of June 1998 to November 1999; the TAPM simulations are presented as negative values.

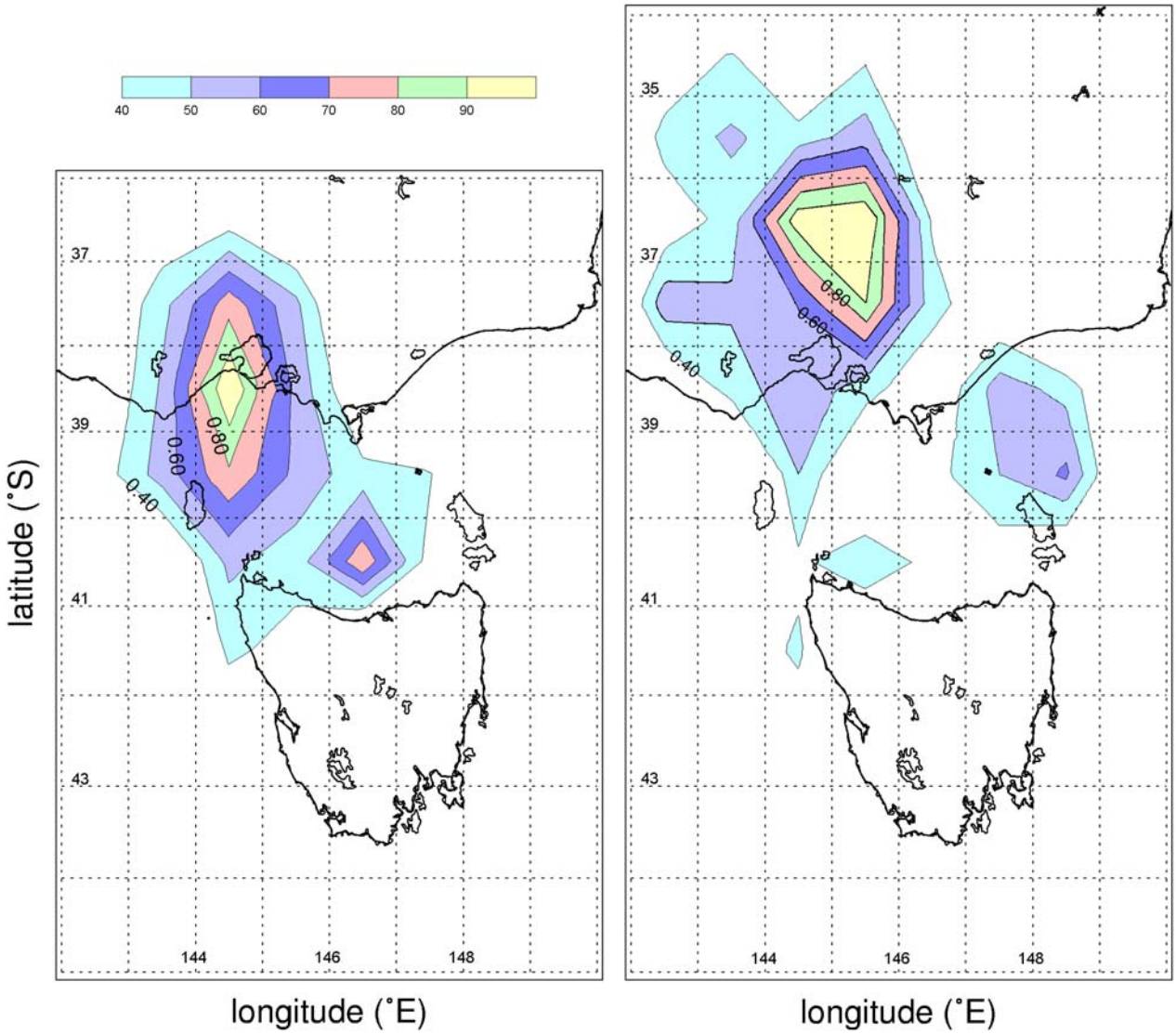

Figure 2. The trajectory frequency distribution for high CH_2Cl_2 pollution events observed at Cape Grim for (a) 7-12 hours and (b) 13-18 hours before arrival at Cape Grim. Each bin is 1° x 1° and is normalised by the maximum count at that time.

4. TAPM modelling

4.1. Model configuration

A PC-based three-dimensional prognostic model [TAPM; Hurley 1999] has been used to investigate the fate of CH_2Cl_2 released in the Port Phillip Region. The TAPM domain is nested within an archive of analyses from the LAPS model [Puri *et al*. 1998], which provides the initial meteorological conditions. The TAPM simulation is 'nudged' towards the LAPS analyses at subsequent time steps through a standard relaxation technique. TAPM predicts the mesoscale flows important to local and regional air pollution studies, as well as the concentration of pollutants at ground level.

The meteorological component of the model solves the incompressible, non-hydrostatic, primitive equations with a terrain-following vertical coordinate. The model solves the momentum equations for horizontal wind components, the incompressible continuity equation for vertical velocity, and scalar equations for potential virtual temperature and specific humidity of water vapour, cloud water and rain-water. Terrain height data are from a United States Geological Survey 30-second resolution data set (approximately 0.9 km). A vegetative canopy and soil scheme is used at the surface, while radiation both at the surface and at upper levels is also included. CSIRO Wildlife and Ecology provided vegetation and soil-type data on a longitude/latitude grid at 3-minute spacing (approximately 5 km). TAPM was configured with a 100×100 point 10-km resolution outer grid extending over Victoria and Tasmania and a 100×100 point 5-km nested inner grid centred north of Cape Grim. The version of TAPM used in this study employed 20 vertical levels between 10 m and 8 km.

An analysis of the temporal and spatial performance of the modelled Melbourne plume in relation to observed pollution episodes at Cape Grim has been carried out. In making these comparisons, the spatial constraint of the position of Cape Grim within the TAPM grid was relaxed by $\pm$ 40 km, the effective lateral crosswind width of the plume at Cape Grim [Cox *et al*. 2000, based on Carras and Williams 1988].

4.2. Source inventory

The EPA has estimated an emissions inventory for CH_2Cl_2 for the Port Phillip control region [Environment Protection Authority 1998; Figure 3]. The methodology used to derive this inventory is described in detail in Boyle *et al*. [1996]. The emissions inventory was based mainly on the response to an industrial survey. As industrial production of CH_2Cl_2 is believed to account for 93% of the total anthropogenic source emissions, the EPA inventory should capture the most significant sources. The EPA provided the source inventory in a 3 km^2 grid over the PPR with a high resolution 1 km^2 grid over Melbourne. The CH_2Cl_2 emissions inventory was then used as input to TAPM to model the Melbourne pollution episodes.

5. Discussion

Figure 1 shows the ground level concentration of CH_2Cl_2 calculated at the TAPM grid point that includes Cape Grim. Qualitatively the modelled and observed readings show a high degree of correlation. This is primarily a reflection on the ability of the TAPM/LAPS to model the pre-frontal transport time from Melbourne to Cape Grim. Quantitatively, however, the simulated readings are a factor of 5-6 lower than the AGAGE observations. This is a significant difference that must reflect problems with the emissions inventory and/or the transport model.

There are several possible sources of error that may account for the difference between the TAPM simulations and the AGAGE observations. The EPA source inventory for CH_2Cl_2 in the Port Phillip region may not be accurate. The EPA inventory estimates the source to be approximately 500 tonnes per year for 1995/1996, and this is the value of the emissions used in these model runs. ABS (Australian Bureau of Statistics) data records the import and export of CH_2Cl_2 into and out of Victoria. Net imports averaged 1900 ± 100 in 1994-1995 and 2000 ± 400 tonnes per year for the period of 1994 through 2000. The average for 1998-1999 was 1800 ± 250 tonnes [ABS 2001]. Assuming all CH_2Cl_2 imported into Victoria (less exports) was emitted in the Port Phillip region or within Victoria on a population basis gives a range of CH_2Cl_2 emissions for the Port Phillip region in 1998-1999 of 1250-1800 tonnes, 2.5 to 3.6 times the EPA estimate during this period. Scaling the EPA source inventory by this amount would bring the TAPM simulations to within a factor of 2 of the AGAGE CH_2Cl_2 observations. This is similar to the level of agreement that has been achieved using TAPM, the EPA carbon monoxide (CO) inventory and AGAGE Cape Grim CO pollution episodes observations [Cox *et al*. 2000, 2002; B. Dunse, U. Wollongong, personal communication, 2002]. Another potential source for error is the chemical removal of the CH_2Cl_2 in the atmosphere by reaction with OH during the time it takes for CH_2Cl_2 emissions from Melbourne to reach Cape Grim (typically 12 hours). As CH_2Cl_2 has a lifetime of approximately 6 months, it was handled as a passive tracer within TAPM. The error associated with such an assumption is minimal (less than 1%). Another potential source of error that proves to be negligible pertains to the temporal period of the AGAGE observation versus the TAPM readings. The 40 minutes trapping time for the GC-MS is quite close to the hourly averaging employed by TAPM. Another possible source of error within TAPM pertains to the effective dispersion, i.e. the rate at which the pollution is diluted. The parameter within TAPM was set to 0.5 based on empirical observations. An error in the dispersion leads to error in the variability of the simulated readings, but not in the integrated total. Figure 4 examines the cumulative probability distribution function of the AGAGE observations and TAPM simulations. Here again we see that the TAPM simulations are roughly a factor of six less than the AGAGE observations.

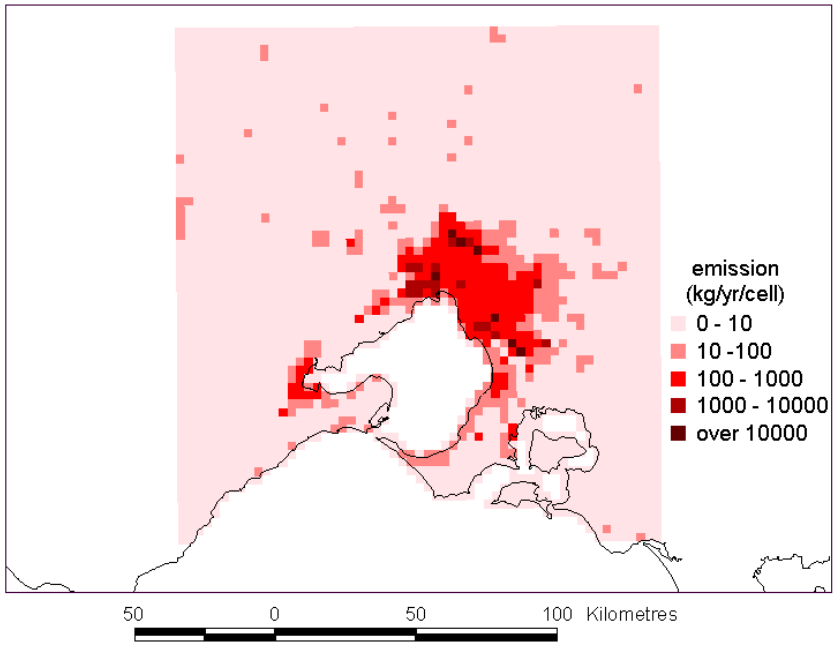

Figure 3. The EPA source inventory for CH_2Cl_2 in the Port Phillip Region (EPA, 1998).

Figure 4 also indicates that random errors in the meteorology cannot account for this error. Over the course of 18 months the number of 'false' pollution episodes observed in the model would approximately balance the number of missed high pollution events in the observations.

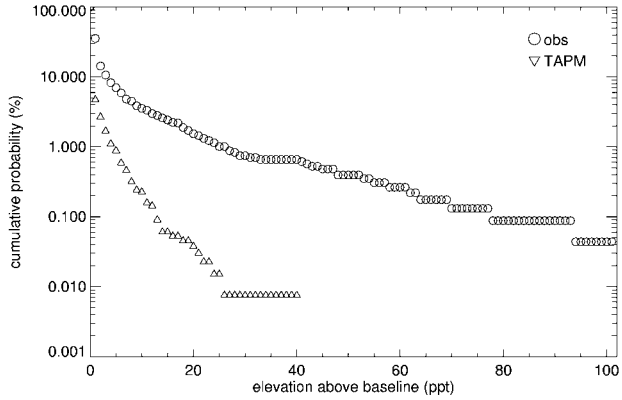

Figure 4. The cumulative probability density functions of the TAPM simulations and AGAGE observations of CH_2Cl_2 over the 18-month period, June 1998 - November 1999.

We are left with one last potential source of error: systematic errors in the meteorology. At first sight this might be dismissed based on the fact that TAPM has been used successfully a number of times under a wide variety of meteorological conditions. However, when the specific meteorology of these high pollution events is considered, errors in model transport may be possible. As discussed earlier, high pollution events are observed in the pre-frontal air masses that travel relatively quickly from Melbourne to Cape Grim. These fronts define the sharp separation of two air masses. TAPM, however, relaxes the simulated dynamics to the LAPS analysis. Under most meteorological conditions, this is fundamentally sound. Under a frontal passage, however, the LAPS analysis offers less resolution than TAPM. The front is effectively being weakened by this relaxation. The exact impact of this has not been investigated fully. However, an error in the depth of the boundary layer could possibly account for a significant fraction of the approximate factor of 2 underestimation of observations in the TAPM simulations.

Even without this relaxation, it should be noted that the pre-frontal boundary layer might be quite difficult to simulate. Air flowing from Melbourne to Cape Grim is classically defined as warm air advection. The air mass at Melbourne is warmer than that at Cape Grim or the water of Bass Strait. This leads to a stable boundary layer that mixes predominantly via wind shear rather than surface heating. In the winter, air over Bass Strait can be warmer than Melbourne air, so cold air advection might be occurring. Still, the pre-frontal air mass will be moving at high velocity and creating shear through the boundary layer. As noted in Siems *et al*. [2000], the boundary layer over the Southern Ocean can have numerous layers rather than being homogenous. This may be difficult to simulate given the limited vertical resolution in TAPM. Finally, the boundary layer may also be poorly defined in the pre-frontal air mass as there is little or no subsidence occurring. At this time, however, the magnitude of a possible error brought about by the limited ability to model the pre-frontal air mass remains an open question.

6. Summary

The regional transport model TAPM accurately simulates the timing of air masses that pass over Melbourne and are transported to Cape Grim in pre-frontal northerly airflows. Incorporation of the EPA PPR emissions inventory for CH_2Cl_2 into TAPM results in CH_2Cl_2 levels at Cape Grim during pollution episodes that are a factor of 5-6 lower than observations at Cape Grim. ABS import data suggest that about half of this discrepancy between model simulations and observations could be due to errors in the EPA emissions inventory for CH_2Cl_2. A significant component of the remaining discrepancy could be due to the inability of TAPM to accurately simulate boundary layer structure and dynamics in pre-frontal conditions between Melbourne and Cape Grim.

Acknowledgements

The authors gladly acknowledge the entire AGAGE team and the Cape Grim team for the AGAGE data. The authors are particularly grateful for the assistance of Nada Derek.

References

ABS: Australian Bureau of Statistics, Dichloromethane import/export data obtained from Australian Bureau of Statistics, International Trade Section, Belconnen, ACT, international.trade@abs.gov.au, 2001.

Boyle, R., P. Dewundege, J. Hazi, D. H. C. McIntosh, A. Morrell, Y. L. Ng and R. Serebryanikova, Technical Report on the Air Emissions Trials for the National Pollutant Inventory, Canberra, ACT, AGPS, Melbourne, Environment Protection Authority, Victoria, 1996.

Cox, M., P. J. Hurley, P. J. Fraser, and W. L. Physick, Investigation of Melbourne region pollution events using Cape Grim data, a regional transport model (TAPM) and the EPA Victoria carbon monoxide inventory, *Clean Air*, 34, 35-40, 2000.

Cox, M. L., G. A. Sturrock, P. J. Fraser, S. T. Siems, P. B. Krummel, and S. O'Doherty, Regional Sources of methyl chloride, chloroform and dichloromethane identified from AGAGE observations at Cape Grim, Tasmania, 1998-2000, *J. Atmos. Chem.*, in press, 2003.

Cox, M. L., A regional study of the natural and anthropogenic sources and sinks of the major halomethanes, *Ph.D. Thesis*, School of Mathematical Sciences, Monash University, Clayton, Australia, 188 pp., 2001.

Carras, J. N. and D. J. Williams, Measurements of relative σ_y up to 1800 km from a single source, *Atmos. Environ*., 22, 1061–1069, 1988.

Draxler, R. R., HYbrid Single-Particle Lagrangian Integrated Trajectories (HY-SPLIT): Version 3.0 - User's guide and model description, AA Technical Memorandum, ERL ARL-195, Air Resources Laboratory, Silver Spring, Maryland, USA, 26 p., 1992.

EPA: Environment Protection Authority, Air Emissions Inventory, Port Phillip Region, Publication No. 632, Melbourne, Victoria, Australia, 48 p., 1998.

Hurley, P., The Air Pollution Model (TAPM) Version 1: technical description and examples, CSIRO Atmospheric Research Technical Paper No. 43, 41 pp., 1999.

Keene, W. C., M. A. K. Khalil, D. J. Erickson, A. McCulloch, T. E. Graedel, J. M. Lobert, M. L. Aucott, S. L. Gong, D. B. Harper, G. Kleiman, P. Midgley, R. M. Moore, C. Seuzaret, W. T. Sturges, C. M. Benkovitz, V. Koropalov, L. A. Barrie, and Y. F. Li,

Composite global emissions of reactive chlorine from anthropogenic and natural sources, Reactive Chlorine Emissions Inventory, *J. Geophys. Res.*, 104, 8429-8440, 1999.

Khalil, M. A. K., Reactive chlorine compounds in the atmosphere, in *Reactive Halogen Compounds in the Atmosphere*, edited by P. Fabian, and O. N. Singh, Springer-Verlag, Berlin, Heidelberg, 45-79. 1999.

Kurylo, M. J., J. M. Rodriguez, M. O. Andreae, E. L. Atlas, D. R. Blake, J. H. Butler, S. Lal, D. J. Lary, P. M. Midgley, S. A. Montzka, P. C. Novelli, C. E. Reeves, P. G. Simmonds, L. P. Steele, W. T. Sturges, R. F. Weiss, and Y. Yokouchi, Short-lived ozone-related compounds, in *Scientific assessment of ozone depletion: 1998*, WMO Global Ozone Research and Monitoring Project – Report No. 44, NOAA/NASA/UNEP/WMO/EC, Geneva, Switzerland, 2.1-2.56, 1999.

Prinn, R. G., R. F. Weiss, P. J. Fraser, P. G. Simmonds, D. M. Cunnold, F. N. Alyea, S. O'Doherty, P. Salameh, B. R. Miller, J. Huang, R. H. J. Wang, D. E. Hartley, C. Harth, L. P. Steele, G. A. Sturrock, P. M. Midgley, and A. McCulloch, A history of chemically and radiatively important gases in air deduced from ALE/GAGE/AGAGE, *J. Geophys. Res*., 105, 17,751-17,792, 2000.

Puri, K., G. S. Dietachmayer, G. A. Mills, N. E. Davidson, R. A. Bowen, and L. W. Logan, The new BMRC Limited Area Prediction System, LAPS, *Aust. Met. Mag*., 47, 203-223, 1998.

Ryall, D. B., R. G. Derwent, J. J. Manning, P. G. Simmonds, and S. O'Doherty, Estimating source regions of European emissions of trace gases from observations at Mace Head, *Atmos. Environ.*, 35, 2507-2523, 2001.

Siems, S. T., G. D. Hess, K. Suhre, S. Businger, and R. R. Draxler, The impact of wind shear on observed and simulated trajectories during the ACE-1 Lagrangian experiments, *Aust. Met. Mag*., 49, 109-120, 2000.

Simmonds, P. G., S. O'Doherty, G. Nickless, G. A. Sturrock, R. Swaby, P. Knight, J. Ricketts, G. Woffendin, and R. Smith, Automated gas chromatograph/mass spectrometer for routine atmospheric field measurements of the CFC replacement compounds, the hydrofluorocarbons and hydrochlorofluorocarbons, *Anal. Chem.*, 67, 717-723, 1995.

Sturrock, G. A., S. Doherty, and P. Fraser, *In situ* measurements of CFC replacement chemicals at Cape Grim, Tasmania, The AGAGE GC-MS program, in Proceedings of the *14th International Clean Air and Environment Conference*, 18-22 October 1998, Melbourne Victoria, Clean Air Society of Australia and New Zealand, Mitcham, Victoria, 511-516, 1998.

Sturrock, G. A, L. W. Porter, and P. J. Fraser, *In situ* measurement of CFC replacement chemicals and halocarbons at Cape Grim: AGAGE GC-MS program, in *Baseline Atmospheric Program (Australia) 1997-98*, edited by N. W. Tindale, N. Derek, and R. J. Francey, Bureau of Meteorology and CSIRO Atmospheric Research, Melbourne, Victoria, 43-49, 2001.

Thoning, K. W., and P. P. Tans., Atmospheric carbon dioxide at Mauna Loa observatory, 2. Analysis of the NOAA-GMCC data, 1974-1985, *J. Geophys. Res.*, 94, 8549-8565, 1989.

AEROSOL CHEMISTRY AT CAPE GRIM

M Keywood
CSIRO Atmospheric Research, Aspendale, Victoria, Australia 3195

Abstract

The Aerosol Chemistry Program at Cape Grim has been alive in one form or another since the inception of the Cape Grim Baseline Station in 1976 and consequently a long-term record of soluble aerosol chemistry exists for Cape Grim. However, with numerous people having had some involvement in the program over the years and there being aerosol chemistry incorporated into a number of the intensive measurement programs at Cape Grim, there is a great deal of information and data scattered in many places. The aim of this report is to consolidate the aerosol chemistry data set for Cape Grim and to provide a record of the activities in aerosol chemistry that have occurred at Cape Grim since 1976. This report will also include a summary of the main features displayed by the aerosol chemistry up to December 2000.

1. History

For the purpose of this report, all investigations that have involved some sort of aerosol chemistry measurement that could be located are included. Programs at Cape Grim that included aerosol chemistry have had various titles. Initially, (1976-1984) aerosol chemistry measurements involved the operation of a high volume (Hi-Vol) sampler under the supervision of Helen Goodman. In 1984, the operation of the Hi-Vol sampler was transferred to John Ivey and Greg Ayers. In 1986, John Ivey became the sole lead scientist for the Precipitation Chemistry Program and a Sulfur Program lead by Greg Ayers was established. In 1989, the Hi-Vol was incorporated into the Sulfur program. The Sulfur Program ceased at the end of 1996. The Soluble Aerosols Program, under the leadership of Chad Dick, was established in 1993, with the aim of investigating inadequacies in the aerosol chemistry measurements at Cape Grim. Currently, work has been carried out under the Multi-phase Atmospheric Chemistry Program under the leadership of Greg Ayers. In 1999, a review of the Aerosol Chemistry Program at Cape Grim was initiated, resulting in the current report.

1.1. Hi-Vol

The backbone of aerosol chemistry measurements at Cape Grim has been the operation of a high volume aerosol sampler (Hi-Vol). A Hi-Vol without a size-selective inlet operated near the cliff edge between August and December 1976. Filters were exchanged manually in conjunction with major changes in wind direction. In 1978, the Hi-Vol was installed on the cliff edge and run under baseline conditions with automatic switching. Baseline was defined as winds between 190 and 280° (10-m winds) and particle counts (CN) below 600 cm^{-3}. Sampling was carried out until July 1980 and in March 1981 the sampler was overhauled and reinstalled at the southern end of the roof deck. In July 1983 a second Hi-Vol was installed in the south-west corner of the roof deck and run in parallel with the original sampler. Polystyrene filters were exposed for 300 hours under baseline conditions at 70 $m^3 hr^{-1}$. Gravimetric mass was determined by Australian Government Analytical Laboratories (AGAL), as were the concentrations of chemical species using Atomic Adsorption Spectroscopy (AAS), however, only minimal gravimetric mass data have been reported, for example, total suspended particles (TSP) averaging 18.6 µg m^{-3} was reported in *Baseline 78*. In February 1985 sampling times were changed to weekly. In 1988, trials began using the Goldtop Hi-Vol sampler with a PM10 size-selective inlet and pressure transducers regulating flow rate. In December 1988 the Goldtop was operated using Pallflex teflon filters. AGAL began performing anion analysis by Ion Chromatography (IC) in 1989. CSIRO began determining cation and anion concentrations using IC in 1996.

1.2. Soil Composition Measurements

The observatory buildings at Cape Grim are located 20 m back from the cliff edge. Coupled with the considerable mechanical turbulence of air passing over the cliff top and buildings, precipitation samples are contaminated by local soil eroded from the cliff. This problem was recognised by Ayers and Ivey [1988] who collected and analysed six soil samples from around the observatory building. They concluded that the soil extracts contained enhanced alkalinity, K^+ and Ca^{2+}, but decreased Cl^- compared with seawater. This had implications for estimations of Cl^- loss, thus compromising the data set's usefulness when addressing issues such as the influence of halogen loss from sea-salt on the marine ozone budget [Sander and Crutzen 1986; Vogt *et al*. 1996].

A further program of soil sampling was carried out during December 1997 (summer season) and June 1998 (winter). The aim was to determine a unique chemical source signature for the soil, in a similar way that sea-salt has a unique signature. Thus a soil dust correction can be made to all precipitation samples collected at Cape Grim. The results of this work were presented in *Baseline 97-98* [Ayers 2001, which outlines a procedure for correcting for soil dust based upon Mg^{2+}/Na^+ ratios. This method has been adopted in all subsequent analyses of Hi-Vol data.

1.3. Other Activities

1.3.1. Sulfur Program

A low volume sampler, known as the Quadrupod, was operated on the roof deck between November 1988 and August 1996. The Quadrupod sampled on two filters and operated during baseline conditions. Particles with diameters approximately greater than 2 µm were collected on a polycarbonate filter with 8-µm pore sizes (Nucleopore) and particles smaller than 2 µm in diameter were collected on a teflon filter with 1-µm pore sizes (Fluropore). The aim of this work was to assess the concentration of aerosol non-sea-salt SO_4^{2-} (NSSS), methanosulfonic acid (MSA) and NH_4^+, after removing high loadings of sea-salt SO_4^{2-} in the coarse particles.

In 1993 a cascade impactor sampler, the Micro-Orifice Uniform Deposit Impactor (MOUDI), was installed on the roof deck at Cape Grim. It sampled during baseline conditions, collecting 100 m^3 per sample and was operated with a heated inlet. Between 1993 and 1996 Jill Cainey operated the MOUDI and the study formed the basis of a PhD thesis. In addition the results have been included in a number of scientific papers on sulfur aerosol chemistry at Cape Grim.

A low volume sampler, known as the Octopod, was operated during December 1983 and during December 1984 as part of two three-week-long intensive sampling programs to monitor sulfur species at high frequency (SO_2, methane sulfonic acid (MSA), dimethyl sulfide (DMS) and non-sea-salt sulfide (NSSS)). The Octopod was made up of eight collection areas controlled by eight solenoid valves and each collection area had four areas: an impactor to remove sea-salt particles, a 1-µm teflon filter (Fluropore) for NSSS and MSA and finally two teflon filters for SO_2 and blanks.

Results from the Sulfur Program have been presented in a number of publications on DMS and its oxidation products, and are summarised in Ayers and Gillett [2000].

1.3.2. Soluble Aerosols Program

The Soluble Aerosols Program was set up in 1993 to investigate inadequacies in the aerosol chemistry measurements at Cape Grim. One issue was to experiment with sampling at the top of the telecommunications tower to prevent contamination from the cliff. Sampling was carried out during 1993, 1994 and 1995 (with some interruptions) using specially constructed filter packs with teflon filters on the roof deck and at the top of the tower. Sampling ceased in August 1996 when the Quadrupod was used instead on the deck. As part of this program a Hi-Vol sampler from the University of East Anglia was also operated for the collection of samples for sulfur isotope analysis.

Results from the Soluble Aerosols Program were largely inconclusive.

1.3.3. Australian Nuclear Science and Technology Organisation (ANSTO)

ANSTO has been operating a PM2.5 cyclone sampler at Cape Grim since 1993. The sampler has a flow rate of 22 l min^{-1}, samples are collected on stretched teflon filter media and two 24-hour (midnight to midnight) samples are collected per week. The sample collection is determined by baseline conditions. The concentration of elements such as H, C, N, O, F, Na, Al, Si, P, S, Cl, K, Ca, Ti, Cr, Mn, Fe, Co, Cu, Ni, Zn, and Pb are determined using ion beam analytical methods. Program reports are presented in *Baseline 96* and *Baseline 97-98*. In addition a source apportionment analysis of data collected between July 1992 and December 1998 is presented in Cohen *et al*. [2000]. Sea-salt and soil were found to contribute to 60% of the fine particle mass, with the remaining 40% of mass being influenced by anthropogenic sources (smoke and industry). The Cape Grim data are used by ANSTO to correct for sea-salt in samples collected at sites in New South Wales.

1.3.4. Collaborative Projects

There have been a number of collaborative projects, some which have continued for one year or more, involving for example:

- *Stockholm University (1981-present)* – Elemental Carbon (EC). This involves a Hi-Vol sampler on the roof deck operating during baseline with a cyclone-collecting aerosol < 4 µm in diameter on a 47-mm diameter latex fibre filter at 5 m^3 hr^{-1}. After 1000 m^3 of baseline air has been sampled filters are sent to Stockholm University where they are analysed for elemental carbon by light absorption. Heintzenberg [1985] described the composition of fine particles collected between December 1981 and December 1983 as part of this collaboration and the results presented are shown in Table 1. EC concentrations were found to be a factor of two lower than the lowest values found in the Northern Hemisphere Arctic summer. Heintzenberg and Bigg [1990] reported spring maximum and winter minimum EC concentrations for data collected between 1982 and 1990, which the authors attributed to peaks in combustion products from biomass burning at low latitudes, moving throughout the Southern Hemisphere. In 1990, black carbon measurements became an internal component of the Cape Grim program using a Magee Scientific Aethalometer. An initial climatology for black carbon (BC) based upon data collected between 1990 and 1997 is presented by Gras [2001]. For all wind directions, northern Tasmania and Victoria (including Melbourne) were found to be the main contributors to BC at Cape Grim. Under baseline conditions, a spring maximum was again observed, which could be linked with wind direction with a time scale of two years. Absolute BC concentrations were not presented, since a program to determine the specific absorption of BC has yet to be completed.

Table 1. Concentration of species measured by Stockholm University.

Species	*Concentration*
Na	1100 ng m^{-3}
SO_4	140 ng m^{-3}
NSSS	80 ng m^{-3}
EC	1.3 ng m^{-3}
Pb	75 pg m^{-3}
Mn	36 pg m^{-3}
Cd	43 pg m^{-3}

- *University of Miami (1981-1996)* – South Pacific Aerosol Network. Professor J. Prospero operated a Hi-Vol sampler on the roof deck sampling continuously for one week at 1 m^3 min^{-1}. The samples were analysed in Miami for NO_3^-, SO_4^{2-} and radionuclides. The data set produced has been used in sulfur model intercomparisons e.g. Barrie *et al*. [2001] and Rotstayn *et al*. [2001] and are available from Dennis Savoie (dsavoie@rsmas.miami.edu) at the University of Miami. These data are compared with Cape Grim baseline data in Section 4 of this report.
- *Max Plank Institute (1988-1990)* – Size dependent aerosol measurements were made using a multistage impactor to allow for particle size separation. Samples were collected during baseline conditions on a weekly basis (volumes greater than 1000 m^3). Results are reported in Andreae *et al*. [1999].

1.3.5. Intensive Campaigns

In February 1978, scientists from the Max Plank Institute measured n-alkenes in gas and aerosol phase and showed that n-alkenes and total organic matter in marine aerosols are of marine origin. The concentrations measured at Cape Grim were similar to those found at Loop Head in Ireland [Eichmann *et al*. 1981].

Between February 1978 and May 1980, G. P. Ayers and J. L. Gras carried out a number of two-week experiments investigating particle size distribution and chemistry at Cape Grim. The results are described in Bigg [1980] and Gras and Ayers [1983]. Samples were collected under baseline conditions. Particles with diameter between 0.05 and 1 µm were collected on electron microscope screens using a 0.2-mm reduced pressure jet at 0.22 l min^{-1} and a 1-mm jet at 5 l min^{-1}. Particles with diameters greater than 1 µm were collected on glass microscope slides using a 5-mm diameter jet at 200 l min^{-1}. The particles were examined by transmission electron microscopy, and three types of particles were identified: ammonium sulfate, cubic sea-salt crystals, and a rarer insoluble component. Ammonium sulfate was found to dominate the number distribution and sea-salt the volume (mass) distribution.

In September 1979, Florida State University operated a six-stage single orifice cascade impactor [Andreae and Bernard 1981]. Using PIXE, the concentrations of 18 elements were determined. Stacked filter samples were also collected and analysed by proton elastic scattering. During baseline conditions, no fine particle mode was observed in the sulfur distribution. Carbon concentrations were measured at 0.25 µg m^{-3} and during baseline conditions, no soot carbon was detected.

In 1981 as part of the Cape Grim Aerosol Program, particles were collected on electron microscope grids in size range 0.06 to 0.6 µm and 0.1-1 µm diameter for subsequent physical and chemical analysis. In addition, particles were collected on filters for selected wind directions for IC analyses of ions such as SO_4^{2-}, NO_3^-, Cl^- and NH_4^+.

In 1981 scientists from the University of Antwerp collected a small number of aerosol samples on electron microscope grids using a five-stage impactor. Individual particles were analysed by light microscopy, electron microprobe analysis and transmission electron microscopy.

In January 1984 Dr R. Ferek, from Florida State University, collected rainwater and aerosols with cascade impactors and filters for analysis of elemental composition, excess SO_4^{2-} and MSA at Florida State University. This was a small adjunct to a program of DMS measurements at Cape Grim, which in turn complemented measurements taken from the North and South Atlantic, Gulf of Mexico and equatorial Pacific Ocean regions.

In December 1986 scientists from Florida State University and CSIRO Atmospheric Research carried out a series of airborne measurements (including aerosol ions, DMS and SO_2) to the west and south of Tasmania. This experiment was aimed at understanding the biogenic sulfur cycle in the marine atmosphere [Berresheim *et al*. 1990].

The Southern Ocean Atmospheric Photochemistry Experiment (SOAPEX) was carried out at Cape Grim during the periods 1-20 August 1994, 3 August-8 September 1995, 16 January-26 February 1995. SOAPEX 2 was conducted during January and February 1999. The aerosol chemistry components of these campaigns were minimal.

The Aerosol Characterization Experiment (ACE-1) campaign took place at Cape Grim between 15 November and 14 December 1995. This experiment was designed to characterise aerosols in the Southern Hemisphere marine atmosphere. It incorporated measurements at Cape Grim as well as aircraft and shipboard measurements over the south-west Pacific Ocean, and included investigations of virtually all aspects of aerosol microphysics and chemistry. An overview of the experiment is given in Bates *et al*. [1998]. Of specific interest to this work were the size-resolved chemistry determinations carried out by Sievering *et al*. [1998] and Huebert *et al*. [1998] and the single particle chemistry determination reported in Middelbrook *et al*. [1998] and Murphy *et al*. [1998].

2. Chemistry of Aerosols at Cape Grim - published data

2.1. Size-resolved chemistry

As described above, there have been a number of campaigns to determine the size-resolved chemistry of aerosol at Cape Grim. The most long-term and comprehensive was that of Cainey [1998], in which a MOUDI was operated on the roof-deck of the observa-

tory between 1993 and 1996, collecting samples of 100 m^3 under baseline conditions. The size-resolved chemistry of samples collected was found to be dependent on the source of particles. Sea-salt species such as Cl^-, Br^-, Na^+, Mg^{2+} and Ca^{2+} displayed a unimodal distribution with a peak at 4-µm diameter. Species such as NSSS and MSA produced by the atmospheric oxidation of dimethylsulfide (DMS) showed trimodal distributions with peaks at diameters of 0.06, 0.3 and 4 µm.

Other investigations involved short-term and or intensive campaign measurements, as described above, including the early work of Bigg [1980] and Ayers and Gras [1983] in which three types of particles were identified; ammonium-sulfate, cubic sea-salt crystals, and a rarer insoluble component (possibly organic aerosol). Ammonium sulfate was found to dominate the number distribution and sea-salt the volume (mass) distribution.

Andreae *et al*. [1999] reported on the collection of weekly Hi-Vol cascade impactor samples under baseline conditions over 20 months between 1988 and 1990. The authors claim that the use of a cascade sampler enabled the collection of coarse particles (where they claim significant amounts of NSSS reside), while avoiding the problem of contamination by soil addressed by Ayers *et al*. [1991]. All contamination was restricted to the first stage of the impactor. This sampler was operated at ambient temperature and humidity. During ACE-1 Huebert *et al*. [1998] operated two MOUDIs within the Cape Grim laboratory using the 10-m Cape Grim Community Aerosol Inlet (which was warmed to 50% RH). Also during ACE-1 Sievering *et al*. [1999] deployed a six-stage Hi-Vol cascade impactor at the 50-m level of the Telstra Tower. Sievering et al. (1999) also reports the MOUDI results collected by Cainey for this period. The campaigns by Andreae, Huebert and Sievering were focused on the chemistry of non-sea-salt particles, particularly the components, NSSS, MSA, NH_4^+ and nitrate.

NSSS was found in the coarse particle range by all investigators. For example, Andreae *et al*. [1999] reported NSSS to have a significant coarse mode at > 1.2 µm in diameter, with the coarse fraction accounting for 58% of NSSS in winter and 35% in summer. MSA was also observed in the coarse fraction, making up 31% without evidence of a seasonal change. Huebert *et al*. [1998] reported that NSSS was bimodal, with 40% greater than 1 µm. MSA displayed a similar distribution. Sodium was observed in even the smallest size fractions of the MOUDI samples.

In samples collected by Sievering *et al*. [1999] the size distribution of NSSS was trimodal, with almost 50% of NSSS located in particles > 0.7 µm in diameter. Low sulfuric acid gas concentrations suggested that NSSS could not be due to H_2SO_4 scavenging of the coarse sea-salt particles. NH_4^+ was not associated with these particles, therefore cloud processing was a minor contributor. Instead, O_3 oxidation of SO_2 in sea-salt aerosol water buffered by biogenic carbonate (resulting from $CaCO_3$ in the ocean microlayer) was invoked to explain 70-90% of the concentration of NSSS in the coarse particles. Note that the buffering capacity of sea-salt aerosol water was enhanced over that of seawater. Normally the O_3 oxidation reaction is limited at pH 6 (normal pH of seawater). The rate is increased two-fold at pH 8, the pH of the sea-salt aerosol water.

In the work of Huebert *et al*. [1998] NH_4^+ was unimodal, with no NH_4^+ outside of the accumulation mode. Thus the NH_4/NSSS ratio was greater than one in the accumulation mode, dropping to zero at larger sizes. MSA/NSSS distribution reflected that MSA dissolves readily in liquid water, which is more prevalent on sea-salt aerosol than in submicron particles.

Cainey [1997] and Ayers *et al*. [1997a] showed that the chemistry of the gaseous precursor species such as NH_4^+, MSA, oxalic acid and NO_3^- were dependent on pH and the surface area of particles at a given size range. NH_4^+ showed a minimum concentration in the alkaline sea-salt region of 4-µm diameter, and condensed on strong acids in submicron particles since the large particles, comprised of sea-salt, were sufficiently alkaline to inhibit the ionization of the weakly alkaline gas. The acidic gases were distributed according to their strengths in comparison to sulfuric acid, with the weaker oxalic and nitric acids showing maximum concentrations in association with sea-salt particles. MSA condensed onto coarse mode particles because of the greater available surface area.

Sulfur was detected as sodium sulfate and was internally mixed with sea-salt in particles determined by a single-particle mass spectrometer during ACE-1 [Murphy *et al*. 1998]. Although sodium sulfate was identified in most particles, ammonium sulfate and sulfuric acid were rarely found under baseline conditions, maybe due to the aerosol size range sampled. Sodium sulfate was more concentrated in particles smaller than 0.4-µm diameter. MSA was only detected if its concentration was greater than NaCl (due to an interference in the spectra). This was seldom observed. About 3% of baseline spectra showed metal ions, possibly indicating their long-range transport to Cape Grim. Nitrate was detected on small particles, in sharp contrast to results at continental locations and other studies at Cape Grim [Cainey 1997].

2.2. Seasonal patterns

In 1986 Ayers, Ivey and Goodman published the first seven years of Hi-Vol data (1976 to 1985) and identified a distinct diurnal cycle in MSA, with minimum in winter and maximum in summer [Ayers *et al*. 1986]. They found no comparable cycle in NSSS, however this was due to the lack of size selection in the Hi-Vol sampler used.

Ayers and Gras [1991] published nine years of MSA and CCN data from Cape Grim (1981 to 1989) and showed a significant seasonal (but non-linear) relationship between CCN and MSA. These results were used to conclude that DMS strongly influences CCN concentrations but that there may be another source of CCN apart from DMS.

In 1991 Ayers, Ivey and Gillett published MSA and NSSS data from the Quadrupod and DMS concentrations from 1988 to 1990 [Ayers *et al*. 1991]. They showed a pronounced DMS cycle with mid-summer maxima and mid-winter minima. The similar time series

displayed by MSA suggested that DMS and MSA were coupled. Submicron NSSS displayed a seasonal cycle with a mid-winter minimum and a mid-summer maximum, however the amplitude of the variation was smaller than DMS or MSA. The non-linearity of the seasonal cycles of MSA and NSSS implied the existence of another source of aerosol sulfur in addition to DMS. These results highlighted the need for size-distributed aerosol composition and gas phase concentrations (for DMS and SO_2) over seasonal timescales.

As a follow-up to this work, Ayers *et al*. [1997b] published measurements of SO_2 between 1990 and 1994 using carbonate impregnated filter downstream of Quadrupod aerosol filters. The aim of this work was to investigate SO_2 as an intermediate product of the oxidation of DMS in the production of MSA and NSSS. Coherence between the SO_2 and DMS annual cycles suggested that DMS oxidation is the main source of SO_2 at Cape Grim. Comparison with other locations revealed that the SO_2/DMS ratio is latitudinal dependent since higher SO_2 was observed in tropical locations than in mid-latitude sites, suggesting that the DMS oxidation reaction by the hydroxyl radical is temperature dependent. This reaction starts with either OH abstraction of an H atom or addition of OH to an S atom. Hydrogen-abstraction is favoured at higher temperatures, and leads to SO_2. The OH addition to S atom leads to formation of MSA and SO_3 and is favoured at low temperatures.

However, the seasonal cycle in SO_2/DMS showed an increase in this ratio during winter, similar to the MSA/NSSS ratio maximum also observed in winter, suggesting that temperature dependence in reactions other than the initial hydroxyl attack may be significant. Ayers *et al*. [1996, 1997a] used the DMS decomposition pathway of Yin *et al*. [1990] with modifications for temperature dependent rates of key species to model SO_2, MSA and NSSS formation. While MSA/DMS ratio observations were simulated, the SO_2/DMS ratio was not approximated, with the modelled SO_2 concentrations being too low in absolute terms. This suggested the presence of another source of SO_2 (fairly minor, of about 3 ppt), either from the oxidation of other trace gas species (H_2S etc.) or entrainment of SO_2 from the lower free troposphere. Measurements are required to test this theory.

Cainey [1997] showed seasonal patterns in the size-distributed chemistry of several species. Sea-salt species showed winter maxima, consistent with the seasonal cycle in wind speed. MSA, NH_4 and NSSS showed summer maxima corresponding to increased biological activity in the warmer months. Gong *et al*. [1997] used 5 years of Na^+ data from Cape Grim (December 1988 to May 1993) in a global sea-salt model. While the model generated a seasonal cycle with maximum sea-salt during the winter months, this was not observed in the data, and was attributed to high wind speeds used in the climate model.

Andreae *et al*. [1999] also reported a pronounced seasonal and interannual variability for all non sea-salt constituents, with maximum concentrations in NSSS, MSA NH_4^+ and NO_3^- in summer. Sea-salt constituents however, displayed little seasonal variation and little dependence on wind speed. The seasonal pattern of sulfur species was again attributed to the oxidation of biogenic DMS being dominant in the production of NSSS during summer. However, during winter, a continental source of NSSS was invoked to explain the sulfur concentrations observed.

2.3. Diurnal patterns

During ACE-1, in addition to the MOUDI samples, Huebert *et al*. [1998] collected bulk filter aerosol samples on the 30-m level of the Telstra tower, exposing the filters on average for 3-hour intervals. This enabled an assessment of the diurnal patterns displayed by various chemical species. NSSS displayed no diurnal pattern (however this may have been due to sea-salt corrections), while MSA data showed a clear diurnal pattern, suggesting a production rate of 6 ppt day^{-1}.

2.4. Sea-salt

During ACE-1 a single-particle mass spectrometer was operated by NOAA. Under baseline conditions more than 90% of particles measured at Cape Grim (between 0.16 and 3 µm diameter dry) contained sea-salt [Murphy *et al*. 1998], with salt containing particles extended down to 0.16 µm in diameter. This was in agreement with the earlier measurements of Gras and Ayers [1983]. Other species were internally mixed with sea-salt. Bromine was found in association with sea-salt, while iodine was enriched with respect to seawater and was variable between particles. The lack of $(NH_4)_2SO_4$ particles measured was most likely due to the coarse nature of particles being collected.

Ayers *et al*. [1999] used data from the Hi-Vol record, size-resolved chemistry (collected using the MOUDI) and rainwater chemistry, to investigate multiphase autocatalytic halogen activation processes. Sea-salt is an important source of halogens to the atmosphere, and reactions involving chlorine and bromine are believed to affect the concentrations of ozone, hydrocarbons and cloud condensation nuclei [Sander and Crutzen 1996]. The loss of chloride from aerosols in polluted air has been observed in many studies [e.g. Hitchcock et al. 1980]. It has been attributed to acid displacement reactions whereby a strong acid such as sulfuric acid, derived from anthropogenic SO_2, might displace chloride atom in the form of more volatile HCl from sea-salt particles. Recent studies [Sander and Crutzen 1996] have suggested that a more efficient dehalogenation process for sea-salt aerosol may involve the acid-catalysis of bromide with the faster bromide reactions resulting in a greater loss of bromide than chloride. Ayers *et al*. [1999] and Vogt *et al*. [1996] showed that this reaction occurs in the remote marine atmosphere, where its clean nature means that there is little acidity present to provide the acid catalysts. These authors and Keene *et al*. [1998] also showed that the activation of sea-salt bromide is greater than chloride. Ayers *et al*. [1999] showed that chloride deficits in sea-salt aerosol at Cape Grim were low, while bromide deficits were large with a strong seasonal cycle (being

greater in summer). Chloride and bromide deficits were linked to the availability of sulfur acidity.

Fresh marine aerosols measured during ACE-1 by single-particle mass spectrometry [Middlebrook *et al*. 1999] were indicated by particles containing very little sodium sulfate. While these were uncommon, when present they also contained iodine. Thus, iodine was only present in particles that were fresh, suggesting that upon interaction with sulfate, iodine is liberated in much the same way as chloride and bromide, described above.

2.5. Organics

Huebert *et al*. [1998] showed that gravimetric mass and inorganic chemical masses in samples collected during ACE-1 were not equivalent. They interpreted this to indicate that under baseline conditions over the Southern Ocean, organic matter makes up between 10 and 47% of the gravimetrically determined mass. Middlebrook *et al*. [1998] report on observations of organic material in individual particles also measured during ACE-1. Organic matter was found to comprise up to 10% of particles on some occasions. The presence of organic material and sodium sulfate in particles was indicative of aged aerosol produced by coagulation of sea-salt aerosols with small sulfate aerosol, the latter produced by oxidation of DMS, and/or the gas-phase or heterogenous oxidation of sulfur compounds. The organic matter likely included gaseous species adsorbed and/or absorbed by the aerosol, as well as surface-active organic compounds present in the sea-surface microlayer that were incorporated into the aerosol during the bubble bursting process.

3. Chemistry of Aerosols at Cape Grim - Long-term Hi-Vol records

The following section describes features from the Cape Grim Hi-Vol record (1976 to 2000) collected under baseline conditions (BASELINE) and the Hi-Vol record collected by the University of Miami between 1983 and 1996 under all conditions (ALL). These records provide a means to compare baseline PM10 chemistry with all-conditions PM10 chemistry. As described in Section 2.2, the BASELINE data set was screened for soil contamination. Removing data with $Na^+_{soil}/Na^+_{sea\text{-}salt}$ greater than 20% decreased the data size from 550 records to 442 records. The remaining data were corrected for soil contamination.

The sea-salt species, Na^+ and Cl^-, make up most of the soluble ionic composition of the BASELINE and ALL data sets at Cape Grim. Comparison of the species presented in both data sets (Na^+, Cl^-, NSSS, SO_4^{2-}, NO_3^- and NH_4^+) reveals that the ALL samples have higher concentrations for all species than the BASELINE samples (Table 2). The sum of these species (an approximation of total mass) is higher by 25% in the ALL samples. In absolute terms, Cl^- has the largest difference between the two data sets; in relative terms, NO_3^- and NH_4 make a greater contribution in the ALL data set (360% and 690% increases).

Table 2. Monthly average concentrations of selected species sampled under all conditions [All] and under baseline conditions [Baseline] at Cape Grim. * Data from University of Miami.

Species	*ALL** $\mu g\ m^{-3}$	*BASELINE* $\mu g\ m^{-3}$
Cl^-	10.52	8.69
Na^+	6.09	4.81
SO_4^{2-}	1.83	1.41
$NSSS^{2-}$	0.30	0.19
NO_3^-	0.26	0.06
NH_4^+	0.07	0.01
SUM	19.07	15.17

The correlation coefficients (R) obtained from linear regression of the monthly-averaged concentrations of all species in the ALL data set against selected meteorological parameters (temperature, wind speed at 10 m and CN) are shown in Table 3. The sea-salt species, Cl^- and Na^+, show a high degree of correlation with each other, and the correlation of Na^+ with SO_4 is significantly different from zero. The sea-salt species also show a high degree of correlation with total mass (calculated from summing all analysed ionic components), which is expected since these species make up most of the total mass. The non-sea-salt species, NSSS and NH_4^+, display a high level of correlation with each other and are negatively correlated with the sea-salt species.

The sea-salt species are moderately correlated with wind speed and show an inverse correlation with temperature. They show a negative and moderate correlation with CN. The non-sea-salt species show a very strong positive correlation with temperature and CN and a moderate negative correlation with wind speed.

Nitrate is not well correlated with any other chemical species in the ALL data set.

The relationships with wind direction displayed by the sea-salt species (represented by Na^+), the non-sea-salt species (represented by NSSS), NO_3^- and CN are shown in Figure 1. The highest concentrations of NO_3^- and CN are associated with wind directions between north and north-west, i.e. from the Australian continent. Maximum concentrations in NSSS occur with wind from the mainland Australia and with winds from the south-east. Maximum Na^+ concentrations appear to be associated with winds from the west of Cape Grim.

Table 3. Correlation coefficients (R) between chemical species measured under all conditions and selected meteorological parameters (ALL data set).

	Na^+	Cl^-	SO_4^{2-}	NSSS	NH_4^+	NO_3^-	sum	temp	ws	CN
Na^+	1.00									
Cl^-	0.99	1.00								
SO_4^{2-}	0.68	0.60	1.00							
NSSS	-0.53	-0.63	0.21	1.00						
NH_4^+	-0.59	-0.70	0.09	0.96	1.00					
NO_3^-	-0.16	-0.20	-0.28	0.10	0.10	1.00				
sum	1.00	0.99	0.71	-0.51	-0.58	-0.16	1.00			
temp	-0.52	-0.63	0.22	0.96	0.96	0.02	-0.50	1.00		
WS	0.55	0.64	0.28	-0.48	-0.59	-0.47	0.57	-0.52	1.00	
CN	-0.48	-0.56	0.26	0.89	0.82	-0.07	-0.45	0.90	-0.41	1.00

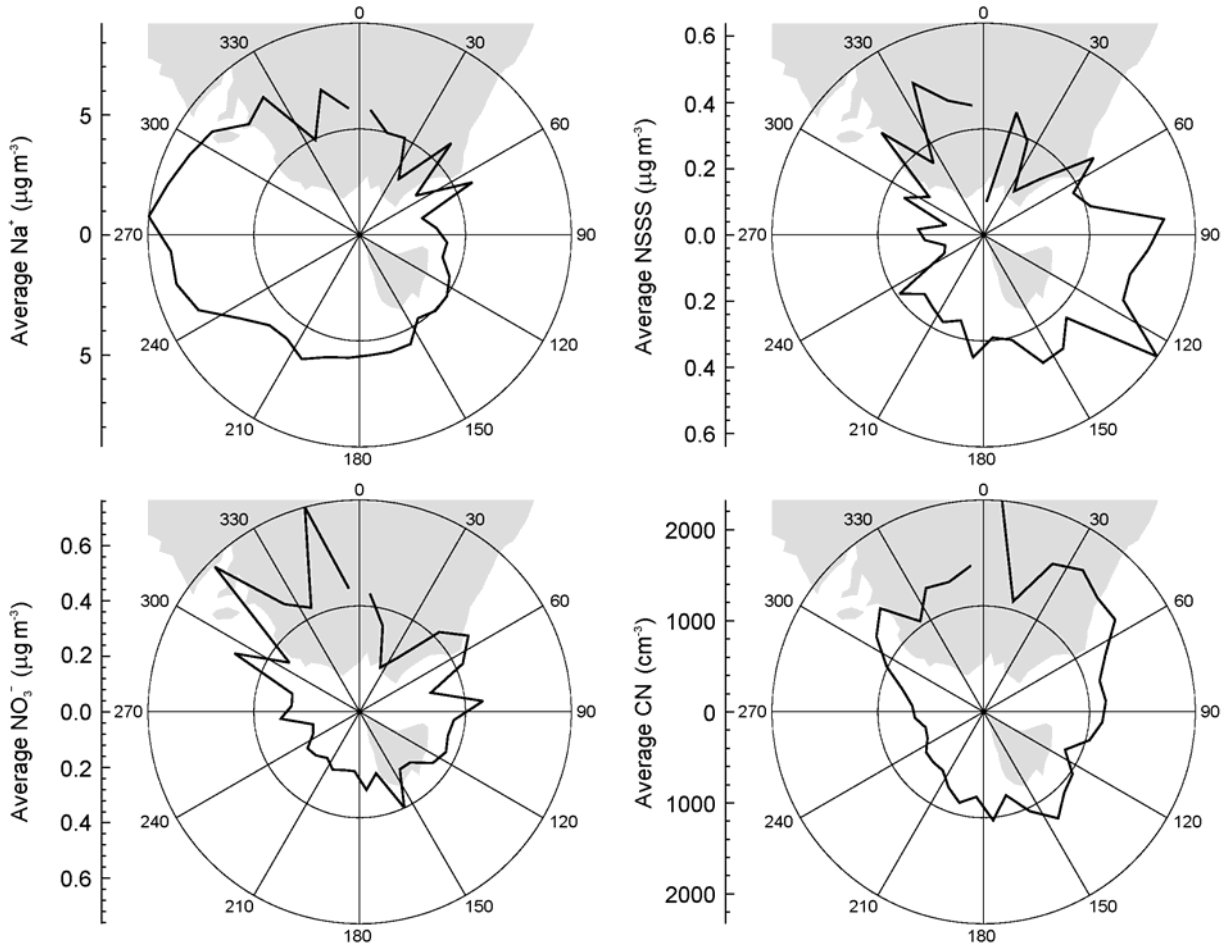

Figure 1. Concentrations of Na^+, NSSS, NO_3^- and CN as a function of wind direction for the ALL data set.

In the BASELINE dataset, the sea-salt species, Na^+, Cl^- and Mg^{2+}, show strong correlations (Table 4). The moderate correlation displayed between Br^- and the sea-salt species is probably due to the concentrations of Br^- being close to detection limits of the analytical system. The correlation between SO_4^{2-} and the sea-salt species is very poor. Again the sea-salt species display a high degree of correlation with total mass. K^+ and Ca^{2+} display weak correlations with the sea-salt species. The non-sea-salt species, NSSS, MSA, NH_4^+, display strong positive correlations with each other and are moderately negatively correlated with the sea-salt species.

The sea-salt species display a weakly negative correlation with temperature and CN and a positive correlation with wind speed. The non-sea-salt species show a strong positive correlation with temperature and CN. The correlation of NO_3^- with sea-salt species is weakly negative and with the non-sea-salt species is strong. NO_3^- displays a strong positive correlation with CN and temperature.

The concentrations of sea-salt species (represented by Na^+), non-sea-salt species (represented by NSSS), NO_3^- and CN as a function of wind direction are shown for the BASELINE data set in Figure 2. As expected the winds are restricted to between 190° and 280°, with maximum concentrations in Na^+ and NSSS associated with winds from the west. CN appears to be evenly concentrated in all baseline wind directions, and NO_3^- maxima is associated with winds from the SSW.

Table 4. Correlation coefficients (R) between all chemical species measured under baseline conditions and selected meteorological parameters (BASELINE data set).

	Na^+	Cl^-	Mg^{2+}	Br^-	K^+	Ca^{2+}	SO_4^{2-}	NSSS	MSA	NH_4^+	NO_3	sum	temp	WS	CN
Na^+	1.00														
Cl^-	0.92	1.00													
Mg^{2+}	0.92	0.77	1.00												
Br^-	0.55	0.30	0.76	1.00											
K^+	0.48	0.52	0.29	0.05	1.00										
Ca^{2+}	0.36	0.48	0.28	-0.18	0.29	1.00									
SO_4^{2-}	0.28	0.08	0.10	0.09	0.29	-0.24	1.00								
NSSS	-0.76	-0.81	-0.80	-0.47	-0.25	-0.48	0.42	1.00							
MSA	-0.70	-0.72	-0.79	-0.52	-0.20	-0.47	0.44	0.96	1.00						
NH_4	-0.61	-0.62	-0.69	-0.35	0.11	-0.62	0.39	0.84	0.84	1.00					
NO_3	-0.46	-0.54	-0.55	-0.23	-0.08	-0.74	0.49	0.77	0.73	0.78	1.00				
sum	0.97	0.97	0.82	0.39	0.56	0.40	0.29	-0.72	-0.63	-0.54	-0.44	1.00			
temp	-0.65	-0.78	-0.58	-0.07	-0.39	-0.73	0.32	0.82	0.79	0.77	0.81	-0.68	1.00		
WS	0.56	0.44	0.58	0.35	0.57	0.23	0.28	-0.34	-0.28	-0.20	-0.43	0.52	-0.49	1.00	
CN	-0.55	-0.59	-0.67	-0.46	0.08	-0.60	0.39	0.79	0.80	0.89	0.87	-0.51	0.70	-0.25	1.00

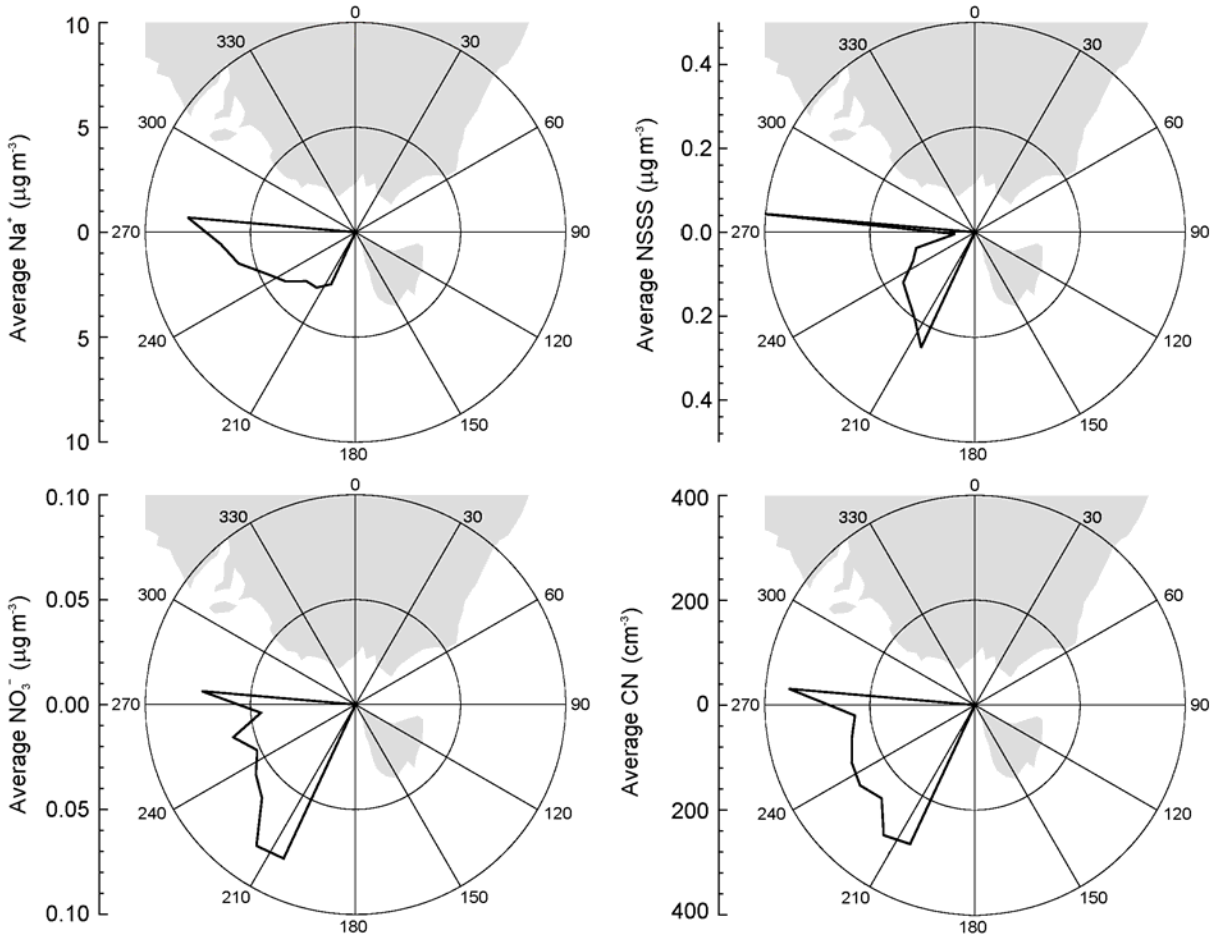

Figure 2. Concentration of Na^+, NSSS, NO_3^- and CN as a function of wind direction for the BASELINE data set.

The correlation between sea-salt species and wind speed in both data sets is due to the process of formation of sea-salt aerosol by sea-spray at the ocean surface, which is more efficient at high wind speeds. Sea-salt species do not show temperature dependence. The negative correlation between sea-salt species and CN arises because sea-spray formation is a mechanical process that produces predominately large particles.

The strong positive correlation between non-sea-salt species, temperature and CN in both data sets is the result of production of CN by oxidation of DMS. This is discussed in detail elsewhere (Section 3.2).

Nitrate under baseline conditions shows similar correlations with CN and meteorological parameters as the non-sea-salt species, suggesting that NO_3^- may also be produced in the fine particles in the marine atmosphere by gas-to-particle conversion. Under ALL conditions, the lack of correlation between NO_3^- and non-sea-salt species most likely results from the presence of urban-derived NO_2 masking the relationships, as suggested by the high NO_3^- concentrations associated with wind from the northwest.

Monthly means and seasonal means were calculated (summer = December, January and February; autumn = March, April and May; winter = June, July and August; spring = September, October and November) to determine the presence of an annual cycle. T-test statistics were used to determine significant differences (at 95% confidence) between monthly and seasonal averages.

The only species that show statistically significant seasonal cycles are the non-sea-salt species. Figure 3 displays these cycles for both the BASELINE and ALL data sets, with NSSS representing the species MSA and NH_4^+. The seasonal cycle of minimum concentrations during winter and maximum concentrations during summer has been extensively discussed elsewhere (see Section 3.2), and reflects a combination of the dependence of the source strength of DMS and its oxidation, on temperature.

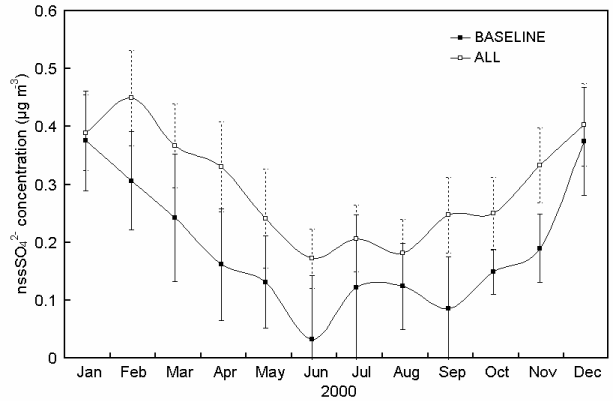

Figure 3. Monthly-averaged concentrations of NSSS (representing non-sea-salt species) for the BASELINE and ALL data sets. Error bars represent the standard error. The seasonal cycle of minimum concentrations during winter and maximum concentrations during summer is well documented elsewhere.

Figure 4 displays the monthly averages for the sea-salt components (represented by Na^+) for the BASELINE and ALL datasets. While there may appear to be a slight annual cycle with minimum concentrations in February and maximum concentrations in August, there is no significant difference between the monthly and seasonal averages of the sea-salt species data. This is also the case for the seasonal averages, except for Cl^- under baseline conditions, where summer averages are statistically lower than winter averages.

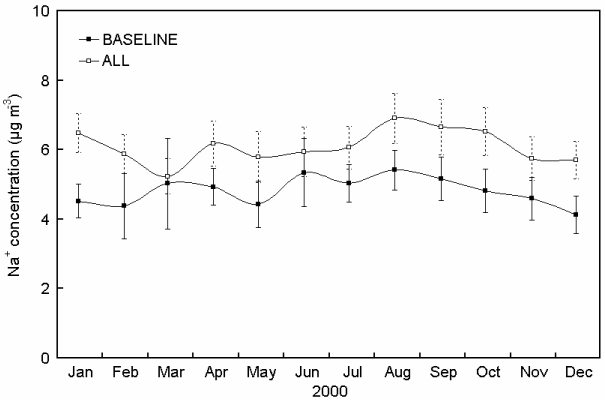

Figure 4. Monthly-averaged concentrations of Na^+ (representing sea-salt species) for the BASELINE and ALL data sets. Error bars represent the standard error.

The monthly-averaged concentrations for NO_3^- are shown in Figure 5. Again, the differences between monthly and seasonal averages are not statistically significant. As noted above, the NO_3^- concentrations during ALL conditions are greater than during BASELINE conditions. This is due to the influence of NO_2 during non-baseline periods when air is advected from mainland Australia to Cape Grim.

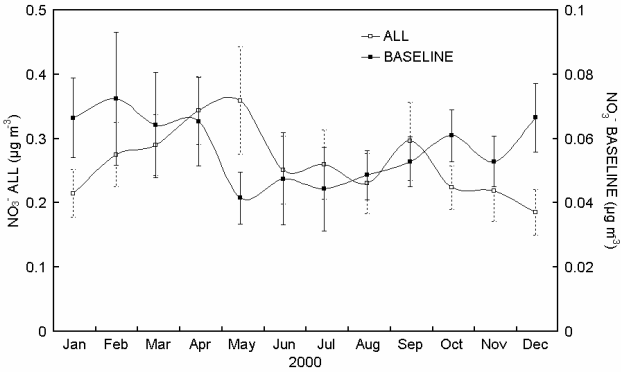

Figure 5. Monthly-averaged concentrations of NO_3^- (for the BASELINE and ALL data sets). Error bars represent the standard error.

The difference between monthly averages during ALL and BASELINE sampling for NO_3^- and NSSS are shown in Figure 6. Both species show a broadly similar pattern of variation with minimal differences between ALL and BASELINE concentrations during the summer months and maximum differences during the winter months. Because the differences in NSSS between data sets are small, error propagation suggests that this seasonal pattern may not be significant. The small differences are due to NSSS being predominately of marine origin. SO_2 of urban origin is less significant, and is expected to be low because of the low S content of fossil fuels used in Victoria. However, the difference in NO_3^- between the two data sets is large, and the seasonal cycle of minimum differences in summer and maximum during winter is significant. Thus NO_2 from urban areas appears to be most significant during the winter months.

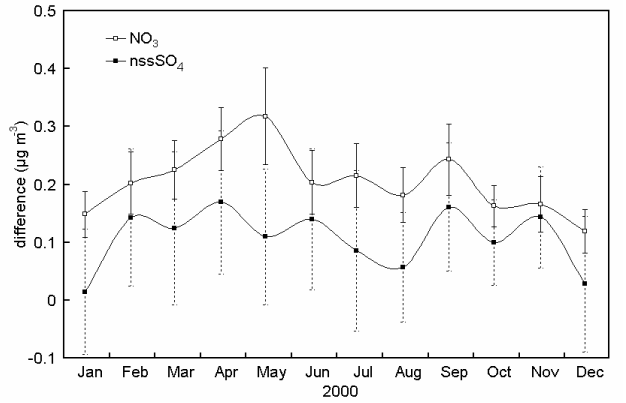

Figure 6. Differences between ALL and BASELINE monthly concentrations of NO_3^- and NSSS.

The monthly-averaged chloride-deficits for both BASELINE and ALL data sets are shown in Figure 7. As expected, the chloride-deficits for the ALL data set are greater than for the BASELINE data set due to acid displacement of Cl^- from sea-salt by weak HNO_3 present in air masses sourced from the Australian mainland. Ayers *et al*. [1999] investigated chloride- and bromide-deficits in Hi-Vol and MOUDI samples collected at Cape Grim (see section 3.4) and found chloride-deficits to be low and the presence of a seasonal cycle in the bromide-deficits. However, in this work, a bromide-deficit seasonal cycle was not significant.

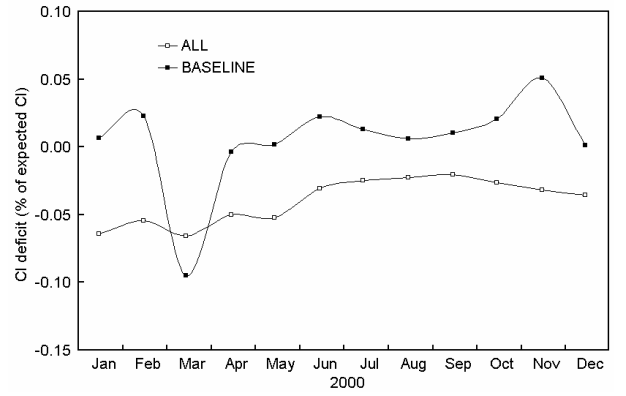

Figure 7. Chloride-deficit (as a function of expected Cl^-) for the BASELINE and ALL data sets. Chloride-deficits are calculated from the expected Cl^- concentration using the ratio of Na^+/Cl^- in seawater and assuming that all Na^+ is of sea-salt origin.

3.1. Summary

The composition of the high volume samples collected under BASELINE and ALL conditions at Cape Grim between 1976 and 2000 can be divided into sea-salt, non-sea-salt and NO_3^- components, with only non-sea-salt components displaying a significant seasonal cycle. The sea-salt components show a strong correlation with wind speed, reflecting the origin of these particles in sea-spray. Greater chloride-deficits and the presence of higher NO_3^- concentrations in samples from the ALL data set, indicate acid displacement of Cl^- by weak HNO_3 found in polluted air masses sourced from the Australian mainland during ALL conditions. This acid displacement takes place on the weakly alkaline coarse sea-salt particles, resulting in the lack of correlation observed between NO_3^- and CN under ALL conditions. The strong correlation observed between NO_3^- and CN under BASELINE conditions suggests that NO_3^- under baseline conditions is not strongly affected by NO_2 advected from mainland Australia. While a seasonal cycle in chloride-deficits was not observed in either data set, differences in NO_3^- between the ALL and BASELINE suggests that more NO_2 is advected from the Australian mainland during winter.

The seasonal cycle displayed by non-sea-salt species being minimum during winter and maximum during summer has been well documented. The correlation between the non-sea-salt species and CN and temperature in both data sets show that the concentration of these species are governed by the production of particles during oxidation of DMS and subsequent transformation reactions, such as neutralisation of SO_4^{2-} by NH_4^+.

4. Conclusions

This report provides a summary of aerosol chemistry at Cape Grim between 1976 and 2000, reviewing activities and results from the various Cape Grim aerosol chemistry research programs as well as long-term collaborative and intensive short-term programs. A large number of publications have resulted from these programs, particularly concerning the role of DMS oxidation on climate. In addition, the size-resolved chemistry of soluble species has been well characterised in a number of intensive campaigns.

Major gaps still exist. These include a long-term record of aerosol mass closure. While a program is currently underway determining the mass of PM10 collected by the Goldtop Hi-Vol under baseline conditions, this program is not without problems due to the sampling method. Soil contamination of PM10 samples will continue to be a problem so long as the sampler remains in its current location. Alleviation of this problem could involve the installation of a tower or utilisation of a PM2.5 size selective inlet. Finally, the determination of total and organic carbon is required to achieve mass closure. This is not possible using the current sampling system.

Recommendations are for the 'basic' aerosol chemistry program at Cape Grim to include upgrading the current Goldtop Hi-Vol and installing a PM2.5 sampler that can collect samples for the determination of mass, soluble ion chemistry, total carbon, elemental carbon and organic carbon. These measurements will provide the backbone for other more specialised programs.

The Aerosol Chemistry Program at Cape Grim is an invaluable resource. It plays a continuing and important role as a southern hemisphere oceanic site in the Global Atmospheric Watch aerosol program. In addition, the program can be used to answer some very important and outstanding questions in aerosol chemistry. These include the role of organic species in CN behaviour in the marine atmosphere and the importance of aerosol in the overall reactive chemistry of the atmosphere, as highlighted by the recent work on halogen species [Ayers *et al*. 1999].

Acknowledgements

I would like to thank John Gras, Rob Gillett and Laurie Porter for reading the manuscript, and Greg Ayers, Stephen Wilson and Jane Warne for useful discussions. Thanks to Paul Krummel for his help with data analysis and Nada Derek for her complete collection of *Baseline*. Thanks to Paul Selleck, Jenny Powell, Kate Boast and Tom Firestone from CSIRO Atmospheric Research. Finally thanks to all the staff who have worked at Cape Grim over the past 25 years or so.

References

Andreae, M. O. and W. R. Barnard, Light element composition of the atmospheric aerosol at Cape Grim (Tasmania) and Townsville (Queensland) by PIXE and PESA., *Nuclear Instrument Methods*, 181, 383-390, 1981.

Andreae, M. O., W. Elbert, Y. Cai, T. W. Andreae, and J. Gras, Non-sea-salt sulfate, methanesulfonate, and nitrate aerosol concentrations and size distributions at Cape Grim, Tasmania, *J. Geophys. Res.*, 104, 21,695-21,706, 1999.

Ayers, G., R. W. Gillett, J. M. Cainey, and A. L. Dick, Chloride and bromide loss from sea-salt particles in Southern Ocean air, *J. Atmos. Chem.*, 33, 299-319, 1999.

Ayers, G. P., Influence of local soil dust on composition of aerosol samples at Cape Grim, in *Baseline Atmospheric Program (Australia) 97-98*, edited by N. W. Tindale, N. Derek and R. J. Francey, Bureau of Meteorology and CSIRO Atmospheric Research, Melbourne, Australia, 50-56, 2001.

Ayers, G. P., J. M. Cainey, R. W. Gillett, and J. P. Ivey, Atmospheric sulphur and cloud condensation nuclei in marine air in the Southern Hemisphere, *Philo. Trans. Roy. Soc. of London. Series B*, 352, 203-211, 1997a.

Ayers, G. P., J. M. Cainey, R. W. Gillett, E. S. Saltzman, and M. A. Hooper, Sulfur dioxide and dimethyl sulfide in marine air at Cape Grim, Tasmania, *Tellus*, 49B, 292-299, 1997b.

Ayers, G. P., J. M. Cainey, H. Granek, and C. Leck, Dimethylsulfide oxidation and the ratio of methanesulfonate to non sea-salt sulfate in marine aerosol, *J. Atmos. Chem.*, 25, 307-325, 1996.

Ayers, G. P. and R. W. Gillett, DMS and its oxidation products in the remote marine atmosphere: implications for climate and atmospheric chemistry, *J. Sea Res*., 43(3-4), 275-286. 2000.

Ayers, G. P. and J. L. Gras, The concentration of ammonia in Southern Ocean air, *J. Geophys. Res.*, 88, 10,655-10,659, 1983.

Ayers, G. P. and J. L. Gras, Seasonal relationship between cloud condensation nuclei and aerosol methanesulphonate in marine air, *Nature*, 353, 834-835, 1991.

Ayers, G. P. and J. P. Ivey, Precipitation composition at Cape Grim, 1977-1985, *Tellus* , 40B, 297-307, 1988.

Ayers, G. P., J. P. Ivey, and R. W. Gillett, Coherence between seasonal cycles of dimethyl sulphide, methanesulphonate and sulphate in marine air, *Nature*, 349, 404-406, 1991.

Ayers, G. P., J. P. Ivey, and H. S. Goodman, Sulfate and methanesulfonate in the maritime aerosol at Cape Grim, Tasmania, *J. Atmos. Chem*., 4, 173-186, 1986.

Barrie, L., Y. Yi, U. Lohmann, W.-R. Leaitch, P. Kasibhatla, G.-J. Roelofs, J. Wilson, F. McGovern, C. Benkovitz, M.-A. Meliere, K. Law, J. Prospero, M. Kritz, D. Bergmann, C. Bridgeman, M. Chin, J. Christensen, R. Easter, J. Feichter, A. Jeuken, E. Kjellstrom, D. Koch, C. Land, and P. Rasch, A comparison of large scale atmospheric sulphate aerosol models {COSAM}: Overview and highlights, *Tellus*, 53, 615-645, 2001.

Bates, T. S., B. J. Huebert, J. L. Gras, F. B. Griffiths, and P. A. Durkee, International Global Atmospheric Chemistry (IGAC) projects First Aerosol Characterization Experiment (ACE 1): overview, *J. Geophys. Res.*, 103, 16,297-16,318, 1998.

Berresheim, H., M. O. Andreae, G. P. Ayers, R. W. Gilltett, J.T Merrill, V. J. Davis and W. L. Chameides, Airborne measurements of dimethylsulfide, sulfur dioxide, and aerosol ions over the Southern Ocean of South Australia, *J. Atmos. Chem.*, 10, 341-370, 1990.

Bigg, E. K., Comparison of aerosol at four baseline atmospheric monitoring stations, *J. Appl. Met.*, 19, 521-533, 1980.

Cainey, J. M., The atmospheric sulfur cycle in the remote southern ocean environment, *PhD Thesis*, Monash University, Melbourne, Australia, 320 pp., 1997.

Cohen, D. D., D., Garton, and E. Stelcer, Multi-elemental methods for fine particle source apportionment at the global baseline station at Cape Grim, Tasmania, *Nuclear Instrument Methods in Physics Research- Section B Beam Interactions with Materials and Atoms*, 161, 775-779. 2000.

Eichmann, R., G. Ketseridis, G. J. R. Schebeske, J. Hahn, P. Warneck, and C. Junge, Co-operative experiment with Max-Planck Institute, West Germany, in *Baseline Atmospheric Program (Australia) 1978*, Depart of Science and Technology, Australian Government Publishing Service, Canberra, Australia, 23-24, 1981.

Gong, S. L., L. A. Barrie, J. M. Prospero, D. L. Savoie, G. P. Ayers, J.-P. Blanchet and L. Spacek, Modeling of sea-salt aerosols in the atmosphere 2. Atmospheric concentrations and fluxes, *J. Geophys. Res.*, 102, 3819-3830, 1997.

Gras, J. L., Aerosol black carbon at Cape Grim by light absorption, in *Baseline Atmospheric Program (Australia) 97-98*, edited by N. W. Tindale, N. Derek and R. J. Francey, Bureau of Meteorology and CSIRO Atmospheric Research, Melbourne, Australia, 20-26, 2001.

Gras, J. L. and G. P. Ayers, Marine aerosol at southern mid-latitudes, *J. Geophys. Res.*, 88, 10661-10666, 1983.

Heintzenberg, J., Physical and chemical aerosol characteristics in clean air masses at Cape Grim, Tasmania, *J. Rech. Atmos.*, 125-129, 1985.

Heintzenberg, J. and E. K. Bigg, Tropospheric transport of trace substances in the southern hemisphere, *Tellus*, 42B, 1990.

Hitchcock, D. R., L. L. Spiller, and W. E. Wilson, Sulfuric acid aerosols and HCl release in coastal atmospheres: evidence of rapid formation of sulfuric acid particulates, *Atmos. Environ*., 14, 165-182, 1980.

Huebert, B. J., S. G. Howell, L. Zhuang, J. A. Heath, M. R. Litchy, D. J. Wylie, J. L. Kreidler-Moss. and S. Cöppicus, and J. E. Pfeiffer, Filter and impactor measurements of anions and cations during the First Aerosol Characterization Experiment (ACE 1), *J. Geophys. Res*., 103, 16,493-16,509, 1998.

Middlebrook, A. M., D. M. Murphy, and D. S. Thomson, Observations of organic material in individual marine particles at Cape Grim during the First Aerosol Characterization Experiment (ACE 1), *J. Geophys. Res*., 103, 16,475-16,483, 1998.

Murphy, D., D. S. Thomson, A. M. Middlebrook, and M. E. Schein, In situ single-particle characterization at Cape Grim, *J. Geophys. Res*., 103, 16,485-16,492, 1998.

Rotstayn, L. D. and U. Lohmann, Simulation of the tropospheric sulfur cycle in a global model with a physically based cloud scheme, *J. Geophys. Res*., 107, 4592, doi:10.1029/2002JD002128, 2002.

Sander, R. and P. J. Crutzen, Model study indicating halogen activation and ozone destruction in polluted air masses transported to the sea., *J. Geophys. Res*., 101, 9129-9138, 1996.

Sievering, H., B. Lerner, J. Slavich, J. Anderson, M. Posfai, and J. Cainey, O_3 oxidation of SO_2 in sea-salt aerosol water: Size distribution of non-sea-salt sulfate during the First Aerosol Characterization Experiment (ACE 1), *J. Geophys. Res*., 104, 21,707-21,717. 1999.

Vogt, R., P. J. Crutzen and R. Sander, A mechanism for halogen release from sea-salt in the remote marine boundary layer, *Nature*, 383, 327-330, 1996.

Yin, F., D. Grosjean, and J. Seinfeld, Photoxidation of dimethlysulfide and dimethlydisulfide: mechanisms development, *J. Atmos. Chem*., 11, 309-364, 1990.

THE CSIRO (AUSTRALIA) MEASUREMENT OF GREENHOUSE GASES IN THE GLOBAL ATMOSPHERE

R J Francey[1], L P Steele[1], D A Spencer[1], R L Langenfelds[1], R M Law[1], P B Krummel[1], P J Fraser[1], D M Etheridge[1], N Derek[1], S A Coram[1], L N Cooper[1], C E Allison[1], L. Porter[2] and S Baly[2]

[1]CSIRO Atmospheric Research, Aspendale, Victoria 3195, Australia
[2]Cape Grim BAPS, Bureau of Meteorology, Smithton, Tasmania 7330, Australia

1. Strategy

Within the general Global Atmosphere Watch (GAW) framework for greenhouse gas monitoring, the CSIRO focus is on improved monitoring methods that reduce uncertainties in regional fluxes derived from atmospheric composition measurement [Francey *et al*. 2001a]. Ongoing areas of special effort include:

- Closely coordinated sampling and analysis of the major atmospheric greenhouse gases (CO_2, CH_4, N_2O) and some related gas species (stable isotopes, O_2/N_2, CO, H_2) that provide information about the greenhouse gas source and sink processes, referred to here as a '*multi-species approach*';
- Development of '*small-sample size*' requirements for sampling and analysis with outcomes of: a) understanding systematic biases that influence measurements, b) improving links to archived air samples that are dependent on small sample techniques, and c) addressing logistic constraints that hinder adequate spatial coverage in global sampling networks;
- *Redundancy* in methods for quality assurance purposes;
- Improved ability to merge data from different measurement laboratories by a combination of improved *diagnostic tools* (e.g. flask-air sharing; CLASSIC Circulation of Laboratory Air Standards for Stable Isotope inter-Comparisons; the GLOBALHUBS strategy) and by improving the *links to primary standards* (e.g. the LOFLO CO_2 analyser system), and
- Close cooperation with modelling groups to assess and improve *measurement strategies*.

2. Measurement facilities

The Australian greenhouse gas monitoring program is built around two key facilities:

2.1. Global Atmospheric Sampling Laboratory (GASLAB)

Located in CSIRO Atmospheric Research, Aspendale, Victoria (near Melbourne), the main functions are:

- Gas chromatograph and mass spectrometer analysis of contemporary air from a global flask sampling network
- Gas chromatograph and mass spectrometer analysis of archived air, including samples prepared in the associated Ice Core Extraction Laboratory (ICELAB)
- Calibration of GASLAB and Cape Grim measurements
- Development of improved methods

2.2. Cape Grim Baseline Air Pollution Station

Located in northwest Tasmania (Australia's WMO GAW baseline site, managed by the Bureau of Meteorology in cooperation with CSIRO) provides:

- Continuous comprehensive monitoring of atmospheric composition and physical properties;
- A well-supported flask sampling site (serving several international laboratories);
- Field trials for new methods.

An additional facility, the Cape Schanck Clean Air Facility, is operated as a GASLAB adjunct and is used to prepare air standards for GASLAB, Cape Grim and customer laboratories based on clean dry air from the Southern Ocean atmospheric boundary layer.

3. Sampling network

The readily accessible Cape Grim facilities, with advanced technical support, provide the premier sampling facility for the CSIRO program, featuring precise, high frequency monitoring and/or sampling, and an unusual degree of redundancy in methods.

The GASLAB program provides a global extension of Cape Grim records by analysing air from a network of fixed surface sites, from moving platforms (ships and aircraft) and from sources of archived air (the Cape Grim Air Archive and Antarctic ice and firn). The bulk of GASLAB samples are collected in cylindrical 0.5 litre glass containers with Teflon or PFA O-ring valves at each end. Flasks are flushed with anhydrous magnesium perchlorate-dried, marine boundary layer air, then pressurized to 80 kPa above ambient pressure. Typical analyses consumes approximately 250 mL of the 900 mL sample, after which the flask is topped up with clean dry southern hemisphere air for return to the same sampling site to await refilling. A small number of other containers and filling methods are in use, as determined by scientific or logistic considerations [Francey *et al.*, 1996].

Flasks of air are currently collected weekly at 10 sites, and less frequently or intermittently at other fixed sites (see Figure 1 and Table 1). Flasks are also collected in campaigns, mostly in collaborative support of activities coordinated by Jon Lloyd, initially of Australian National University, now of Max Planck Institute for Biogeochemistry (see Figure 1 and Table 2). The samples collected routinely using aircraft and ships, and on two occasions using high altitude balloons, are listed in Table 3.

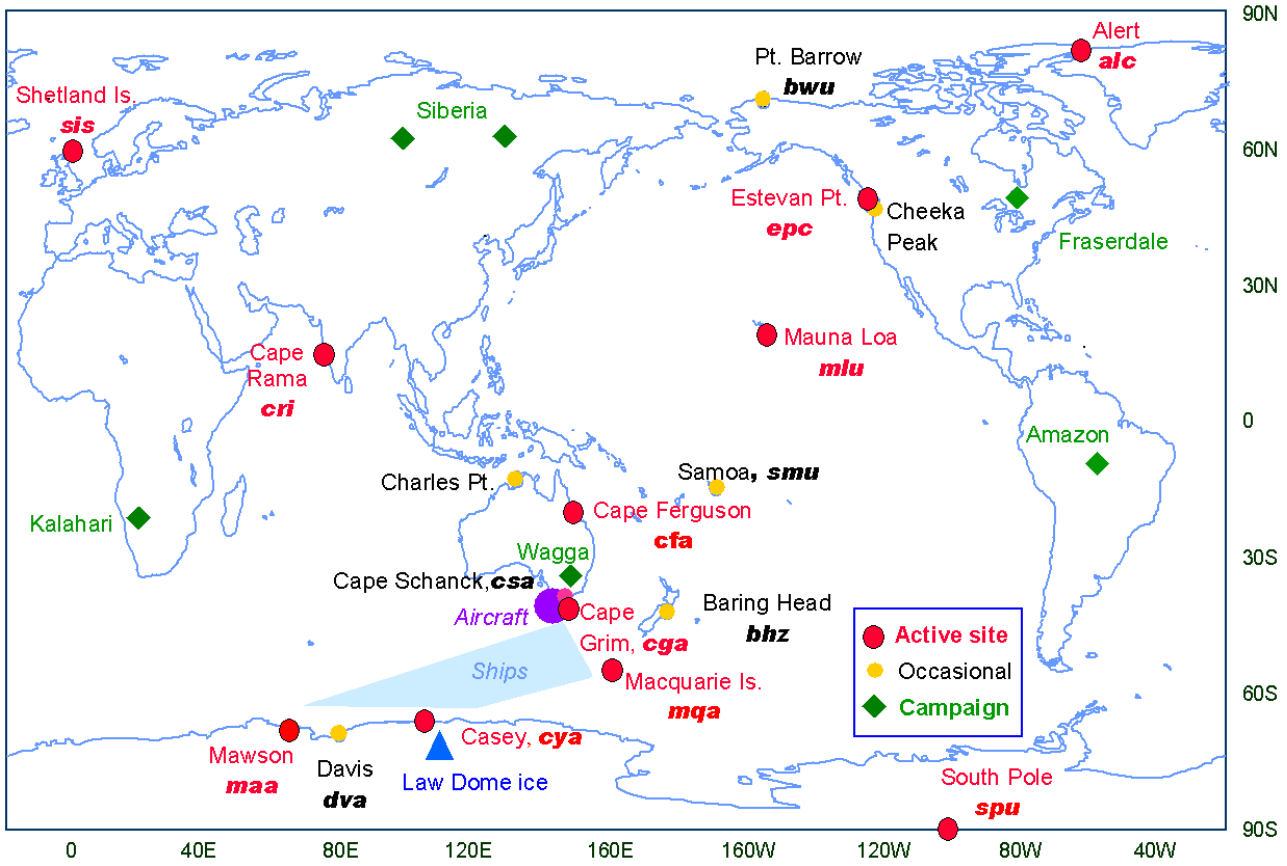

Figure 1. The CSIRO GASLAB global flask sampling network.

Table 1. Fixed sampling sites in the CSIRO flask network (see Figure 1 for locations of sites. Collaborator acronyms are listed at the end of this paper).

GASLAB ident.	*NOAA Ident.*	*Collaborator*	*Start*	*Interval*
alc	ALT	AES	1989	week
bhz	BHD	NIWA	1991	intermittent
cfa	CFA	AIMS	1989	week
cga	CGO	BoM	1977	week
csa		AMSA	1992[1]	intermittent
cya		AAD/BoM	1997	week
cri	CRI	PRL	1993	week
daa	DAA	UNT	1987[2]	
epc	ESP	AES	1993	3 weeks
maa	MAA	AAD/BoM	1993	week
mlu	MLO	NOAA	1984	week
mqa	MQA	AAD/BoM	1986	week
sis	SIS	NERC	1992	week
smu	SMO	NOAA	1984[3]	
spu	SPO	NOAA	1983	week

[1] high pressure cylinder; [2] ceased in 1998; [3] ceased in 1991

Table 2. Flask Sampling Campaigns

Site	*Sampled by ANU/MPI*	*Comment*
Brazil	May 93 - Dec 95	
Cameroon	Mar 1994	
Canada (Saskatchewan)	Jul 94	
Norway	Aug 94	
Australia (Wagga, OASIS)	Oct 94, Oct 95	
Siberia (Zotino)	Jul 96 – Jul 00	Aircraft
Botswana	Apr 99 – Jul 00	Aircraft
Scotland (Aberfeldy)	Jul 00	

Table 3. Sampling from Moving Platforms

Code	*Description*	*Collaborator*	*Start*	*Frequency*
aia	aircraft SE Australia	BoM	1991[1]	month
rva	ships Southern Ocean	CMR/AAD	1990[2]	intermittent
mis	balloon Kiruna Sweden	KFA	Jul 1990	2 ascents

[1] suspended in 2000; [2] 27 transects

Collection of ambient air (both dried and undried), in 35 litre electro-polished stainless steel containers typically 4 times per year, commenced in 1978. The samples are compressed to around 30 atmospheres above ambient. The Cape Grim Air Archive program is fully described in Langenfelds *et al.* [1996], with more recent results in Langenfelds *et al.* [1999], and Francey *et al.* [1999a, b].

Air has also been extracted from Antarctic ice and firn for trace gas analysis and results described in Etheridge *et al.* [1996, 1998], Francey *et al.* [1999a], Trudinger *et al.* [1999], and associated papers. Emphasis has been on ice cores with the age of trapped air spanning the last 1000 years. A feature of the ice core work is the availability of cores from sites with high accumulation rates, leading to high (decadal) time resolution compared to other work [Levchenko *et al.* 1996, 1997].

4. Analysis methods

4.1. Gas Chomatograph measurements of concentrations

An overview of methods is given in Francey *et al.* [1996] and a comprehensive technical document is in preparation [Langenfelds *et al.*, in preparation]. A Series 400 CARLE gas chromatograph with flame ionisation detector (FID) is used for the measurement of CH_4 and CO_2 (converted to CH_4 using a nickel catalyst at 400ºC). A Trace Analytical RGA3 gas chromatograph measures H_2 and CO with mercuric oxide reduction gas detector (RGD), which reduces HgO to Hg for detection by UV absorption. A Shimadzu GC-8A with electron capture detector (ECD) measures N_2O.

A HP6890 system is scheduled for deployment in 2001/2002 to measure all of the above gases: CO_2, CH_4, N_2O, CO, H_2, and add SF_6. It is anticipated that this system will replace the existing three gas chromatographs with improved precision and, overall, less sample requirement.

4.2. Non-dispersive infrared analysis of CO_2

A Siemens Ultramat 5E NDIR operates continuously at Cape Grim [Beardsmore *et al.*, in preparation]. Since May 2000 a prototype CSIRO LOFLO NDIR system [Da Costa and Steele 1997] has operated in parallel with the conventional analyser. The outstanding performance of this analyser, both with regard to a factor of 10 or more improvement in precision/stability and operating cost. The stable, precise operation, and the potential for a portable robust instrument that can operate for periods of many months largely unattended, represent technological breakthroughs with significant scientific implications. These are explored further below.

4.3. Mass Spectrometry

Routine analyses of the stable isotopes of CO_2 are carried out on GASLAB and other flasks using a Finnigan MAT 252 mass spectrometer with an automated MT-Box C cryogenic extraction system [Allison and Francey 1999; Allison *et al*., 2002, 2003; Francey *et al.* 1996]. The overall system is characterised by the unusually small sample requirements for routine analyses (30-50 standard mL of air).

5. Calibration

Particularly in the Southern Hemisphere, trace gas signals are small. The precision requirements to monitor biogeochemical processes of interest (e.g. small Southern Ocean fluxes over huge spatial extent, or small decadal changes in large-scale terrestrial ecosystem average fluxes) are often more demanding than can be achieved in calibrations that link to primary standards. This continues to make the effective merging of data from different laboratories a major challenge for the atmospheric composition measurement community.

A full description of the calibration status, precision and maintenance of GASLAB measurements is reproduced in the following sub-sections.

5.1. Gas Chromatography (prepared by R L Langenfelds, L P Steele, and R J Francey, April 2001)

There are numerous sources of experimental uncertainty in atmospheric trace gas measurements and various ways in which these uncertainties impinge on interpretation of data. A comprehensive calibration strategy consists of various parts that help to minimise and define errors/uncertainties and distinguish relative contributions from different sources. Here we provide a brief summary of CSIRO's calibration strategies, and assign realistic uncertainties to key experimental parameters. These parameters are defined in a way to be directly applicable to field data. Uncertainty estimates are derived from various sources of information such as long-term statistics of instrument performance, intercomparisons with other laboratories (eg. of CO_2 with NOAA/CMDL who are also the current WMO Central CO_2 Calibration Laboratory, with the responsibility of maintaining and propagating the WMO Mole Fraction Scale [Zhao *et al.* 1997]) and results from laboratory and field tests. Key laboratory tests include evaluation of non-linearity in instrument response, regulator performance, preparation and analysis of test flasks (multiple flasks, of the same type used for field sampling programs, simultaneously filled from a high pressure cylinder) for characterisation of trace gas modification due to 1) analytical procedures tailored for limited sample volumes and 2) storage of air in these flasks [Cooper *et al.* 1999]. Data in Table 4 represent experimental uncertainty only and make no allowance for atmospheric variability.

5.1.1. Carbon dioxide (CO_2)

CO_2 is analysed by gas chromatography (GC), involving conversion of the separated CO_2 to CH_4 on a heated nickel catalyst (400°C) followed by flame ionisation detection (FID). Data are reported in the WMO CO_2 Mole Fraction Scale. The link to this scale was established with 9 primary standards (of a suite of 10 synthetic mixtures of CO_2, CH_4 and CO in zero air) in high-pressure cylinders that were calibrated by NOAA/CMDL in 1992. They span a CO_2 range of 291-377 ppm. NOAA recalibrated a subset of four of these in 1994 (mean differences −0.01, −0.04, 0.00, +0.05 ppm at 362, 349, 339, 326 ppm respectively). The primary suite retains 75% of original pressure (2000 psig) after 9 years. The scale is monitored using two broad approaches. Relative stability is monitored using about 15 assorted secondary standards with lifetimes of 4-10+ years. Stability against absolute scales is monitored (but the scale is never adjusted) by independent comparisons, including 6 Nippon Sanso standards (volumetrically prepared, calibrated against a gravimetric scale at Tohoku University), WMO Round-Robin (three cylinders in 1994-97 and again in 1998-99), IAEA CLASSIC (five cylinders: 1996-98, 1999-00) and other high pressure cylinder comparisons, and flask air

sharing comparisons with several laboratories (including ~six per month with NOAA/CMDL since 1992 [Masarie *et al.* 2001]). The best measure of how closely CSIRO has remained aligned to the WMO scale is obtained from results of eight (most reliable) cylinder comparisons, but excluding the nine primary standards. They imply a mean scale factor of 0.99986 ± 0.00012 (CSIRO/NOAA), equivalent to a difference of -0.05 ± 0.04 ppm (CSIRO-NOAA) at current ambient atmospheric CO_2 levels. This difference reflects collective uncertainty from both laboratories. There is no significant drift in the difference, but there are insufficient statistics to resolve a constant offset from any drift.

Uncertainties due to unaccounted variations of non-linearity in our instrument response are within 0.2% of mole fraction difference (eg. within ±0.04 ppm for a CO_2 difference of 20 ppm) and apply to any measurement of concentration differences, for example seasonal cycle amplitudes. Additional uncertainties apply to measurements from flask samples due to experimental factors specific to flasks. This is exemplified by the Cape Grim flask intercomparison program involving CSIRO and NOAA/CMDL [Masarie *et al.* 2001] where systematic differences of between 0.0 and 0.2 ppm have been observed, despite a much closer level of agreement demonstrated for high pressure cylinders. Resolution of such discrepancies must remain a high priority if CO_2 records from flask sampling networks of different laboratories are to be merged into a self-consistent global database. Further details of analytical techniques and calibration for CO_2 and other species measured by GC will be provided elsewhere [Langenfelds *et al.* in preparation].

Table 4. Measurement uncertainties and related information applicable to data from CSIRO analyses of flask air.

	CO_2	$\delta^{13}C$	$\delta^{18}O$	CH_4	CO	H_2	N_2O
Raw measurement precision (1σ)[a]	±0.09 ppm	±0.01 ‰	±0.02 ‰	±2.3 ppb	±0.6 ppb	±1.5 ppb	±0.3 ppb
Long-term scale stability[b]	±0.007 ppm yr^{-1}			±0.03 ppb yr^{-1}	±0.2 ppb yr^{-1}	±0.3 ppb yr^{-1}	±0.02 ppb yr^{-1}
Alignment of CSIRO's internal scale with established, independent scales[c]	0.99986 ±0.00012			1.00021 ±0.00010	?	?	?
Random uncertainty on individual flask samples (1σ)[d]	±0.13 ppm	±0.02 ‰	±0.1 ‰	±1.7 ppb	±0.7 ppb	±1.5 ppb	±0.3 ppb
Uncertainty relative to other CSIRO network sites[e]	±0.1 ppm			±0.4 ppb	±0.4 ppb	±1 ppb	±0.1 ppb
Uncertainty due to non-linearity of instrument response, expressed as a percentage of mole fraction (or δ) difference[f]	±0.2 %			±0.2 %	±1 %	±2 %	±1 %
High-precision calibration range[g]	290-380 ppm	δ45: ±2‰	δ46: ±2‰	300-1850+ ppb	20-400 ppb	430-1000 ppb	260-340 ppb

[a] Based on the long-term, mean standard deviation of repeat aliquots from high-pressure cylinder working standards. Of the listed species, CO shows greatest variation of precision over the range of mole fraction measured in the background atmosphere. The value shown here relates to a CO mole fraction of 100 ppb.

[b] Based on drift rates implied by long-term standards in high-pressure cylinders, the degree of relative stability among many such standards, and for CO_2, also from results of intercomparisons with NOAA/CMDL.

[c] The CO_2 scale factor is with respect to the manometrically-defined WMO CO_2 mole fraction scale. The CH_4 scale factor is with respect to the CH_4 scale maintained by NOAA/CMDL. Scale factors represent CSIRO/NOAA values of exchanged cylinder air. Alignment of CO and H_2 scales cannot be easily quantified due to time and concentration-dependent differences between CSIRO and NOAA/CMDL. Preliminary estimates of the N_2O scale factor are given in the text but are not yet reliably quantified and may not be consistent for NOAA's HATS and CCG groups.

[d] Based on raw instrumental precision, results from test flasks showing noise associated with flask sample analysis and dependence on storage time, and flask pair differences from Cape Grim which also include a contribution from noise associated with flask sampling procedures. The values shown here relate to use of CSIRO's glass, 0.5 litre flasks with dual PFA O-ring valves and are representative of a typical network site, although values for specific sites differ according to mean storage times. Similar values apply to other flask types except where storage-related drifts are significantly higher (eg. CO in glass flasks with Viton O-rings and 1.6 litre, stainless steel 'Sirocans').

[e] Based on uncertainty due to possible systematic error in allowance for storage drift, gauged from laboratory tests and from overlapping 0.5 and 5.0 litre glass flask data at other CSIRO sampling sites (South Pole and Macquarie Island). The values shown here relate to use of CSIRO's glass, 0.5 litre flasks with dual PFA O-ring valves and are representative of a typical network site, although values for specific sites differ according to mean storage times. Similar values apply to other flask types except where storage-related drifts are significantly higher (eg. CO in glass flasks with Viton O-rings and 1.6 litre, stainless steel 'Sirocans').

[f] Based on recognised uncertainty in assignments to primary standards (specifically in the accuracy of relative mole fraction or δ), variability of measurements from these standards (after correction for non-linearity, where applicable) as a function of mole fraction (or δ) difference from the working standard, and for CH_4 also from analysis of 6 standards with gravimetrically-derived assignments provided by Tohoku University.

[g] The range for which instrument response is well constrained and routinely monitored with calibration standards. Higher uncertainties apply to values outside of this range.

5.1.2. Methane (CH_4)

CH_4 is analysed by GC (FID). Data are reported in the CSIRO94 CH_4 scale [Steele *et al.* 1996], which is derived from the CH_4 scale maintained at NOAA/CMDL. The link to this scale was established with two high pressure cylinders containing dry, natural air that were calibrated by NOAA/CMDL between 1987 and 1990. Results from later exchange (1992-1997) of 12 high-pressure cylinders indicate a small, but measurable difference. The ratio of CSIRO/NOAA values for these samples is 1.00021 ± 0.00010, implying a difference of $+0.36 \pm 0.17$ ppb (CSIRO-NOAA) at 1700 ppb. Stability of the CSIRO scale is monitored with about 25 assorted standards with lifetimes of 4-10+ years. Instrument response has been evaluated with a suite of six Nippon Sanso CH_4-in-air standards (volumetrically prepared, calibrated against a gravimetric scale at Tohoku University) spanning the range 310-1845 ppb. The results show the response to be linear within confidence limits. A deviation from linearity of 0.2% of mole fraction difference was measured but is of similar magnitude to uncertainty of the gravimetric preparation technique. We thus treat the response as linear and allow for uncertainty of 0.2% of mole fraction difference, equivalent to only 2 ppb in a difference of 1300 ppb.

5.1.3. Carbon monoxide (CO)

CO is analysed by GC with 'reduction gas detection' where the separated CO reduces heated (275°C) mercuric oxide to mercury vapour that is subsequently detected by UV absorption. Data are linked to the gravimetrically-derived scale of NOAA/CMDL [Novelli *et al.* 1991] using a single high-pressure cylinder standard with CO mole fraction of 196 ppb. This standard is one of five synthetic mixtures of CO_2, CH_4 and CO in zero air, in the range 30–196 ppb, that were calibrated at NOAA/CMDL between 1992 and 1994. The reason that only the highest concentration standard is used to link the CSIRO and NOAA scales is that large discrepancies exist in the respective laboratories' determination of relative mole fraction among these standards and other high pressure cylinders exchanged since. The highest concentration is likely to give the smallest proportional error in linking the scales. We have established the instrument response characteristics of the CSIRO instrument by diluting air containing above-atmospheric CO and CH_4 mole fraction with varying amounts of zero air. Precise dilution ratios are determined by analysis of CH_4 for which non-linearity in instrument response is negligible by comparison to CO. The results of five such experiments between 1993 and 1999 show the relative CO mole fraction among these standards to consistently differ from that indicated by the NOAA assignments. Using 196 ppb as the fixed reference point for linking to the NOAA scale, differences of up to 4 ppb are found at lower concentrations. These discrepancies are most likely due to different treatment of instrument non-linearity, despite the fact that both laboratories employ similar analytical techniques. NOAA has used either cubic or quadratic functions to describe their instrument response. At CSIRO, we have found it necessary to use a different function ($y = ax^2 + bx + cx^d$, where y is CO mole fraction, x is peak height counts and a, b, c, and d, are fitted parameters) that better captures sharper non-linearity in instrument response at low concentrations (especially below 100 ppb). Stability of the CSIRO scale and variations in instrument response are monitored with about 20 high-pressure cylinder standards, with lifetimes of 4-10+ years, spanning a CO range of 20-400 ppb.

From our experience of maintaining a CO measurement program and extensive laboratory tests, we have identified several specific effects that can adversely affect data quality. For example, instrument 'blanks' (i.e. appearance of CO peaks in chromatograms from air containing no CO) affect the shape of the instrument response function, especially at low CO concentrations, and are monitored by regular analysis of zero air (where necessary scrubbed of residual CO). It is common for CO to be produced by internal surfaces of regulators and/or cylinder valves of high-pressure cylinders. Avoiding significant errors requires careful selection of standards (especially working standards), and adherence to suitable gas handling procedures that limit the residence time of air inside the valves/regulators. We have also observed an instrumental memory effect that causes H_2 and CO measurements to be affected by the CO mole fraction of preceding analyses. Knowledge of the existence of these effects allows us to implement analytical and/or data processing procedures that limits resulting uncertainty to acceptable levels. Further details will be provided elsewhere [Langenfelds *et al*. in preparation].

5.1.4. Hydrogen (H_2)

H_2 is analysed by GC on the same instrument and with identical techniques to that described above for CO. Data are reported in the CSIRO94 H_2 scale which was defined by dilution of high purity H_2 and CH_4 (in a 1:3 ratio) with zero air to produce a mixture with H_2 mole fraction close to atmospheric levels, and 'bootstrapping' to a gravimetrically-derived, absolute CH_4 scale. The relationship of the CSIRO94 H_2 scale with the gravimetrically-derived H_2 scale of NOAA/CMDL [Novelli *et al.* 1999] is not well-defined due to both time and concentration-dependent variations in the difference. Results from the Cape Grim flask air-sharing intercomparison show systematic, time-dependent differences of between 0 and 20 ppb between 1992 and 1998 [Masarie *et al.* 2001]. CSIRO instrument response was determined by the same 'dilution experiments' described above for CO and was found to be significantly non-linear and of similar shape to that of CO. Unlike CO, however, a constant response function is assumed because 1) we have too few well-behaved standards with mole fraction significantly different from ambient atmospheric levels to adequately describe variation in the response function ($y = ax^2 + bx + cx^d$), although these standards do constrain the magnitude of any variations and 2) the proportional range of variation in the background atmosphere is much smaller for H_2 than for CO so that minor changes in instrument re-

sponse are less critical for atmospheric studies. Stability of the scale is monitored with ~20 high-pressure cylinder standards, with lifetimes of 4-10+ years, spanning a H_2 range of 430–1000 ppb. Most of these cylinders are of electropolished, stainless steel construction. In our experience, the aluminium cylinders successfully used for long-term calibration of other GASLAB species are generally not reliable for H_2. Apart from a single batch of five of these cylinders, all have been found to grow H_2 at varying rates of up to hundreds of ppb per year. The suite of ~15 stainless steel and 5 aluminium cylinders are all stable against each other to better than $\pm$1 ppb yr^{-1}.

5.1.5. Nitrous oxide (N_2O)

N_2O is analysed by GC with electron capture detection (ECD). The scale maintained at CSIRO was established using six high-pressure cylinder standards (of a high purity N_2O/CO_2 mixture diluted with varying amounts of zero air) that were gravimetrically prepared by NOAA/CMDL in 1993. Their N_2O mole fraction values were assigned on the basis of the gravimetric preparation with a nominal uncertainty of $\pm$1 ppb, and span a range of 264-344 ppb. In 1995, two high-pressure cylinders were exchanged with NOAA/CMDL's Halocarbons and other Atmospheric Trace Species (HATS) group. Comparison of GC measurements, which are of higher precision than the gravimetric assignments, indicated a scale factor of 1.0014 (CSIRO/NOAA) at this time, equivalent to a difference of 0.44 ppb (CSIRO-NOAA) at 315 ppb. However, further cylinder intercomparisons will be necessary to reliably quantify the scale difference and identify any time variation. A difference of similar magnitude is observed in early results from the Cape Grim flask intercomparison conducted with NOAA/CMDL's Carbon Cycle Group (CCG), but the precise relationship between HATS and CCG scales is not known at this stage. Stability of the CSIRO scale is monitored with about 30 high-pressure cylinder standards, with lifetimes of 4-9+ years.

5.2. Mass Spectrometry (prepared by C E Allison and R J Francey, April 2001)

The CO_2 $\delta^{13}C$ and $\delta^{18}O$ data are reported on the international VPDB-CO_2 scale. Samples are measured using a dual-inlet Finnigan MAT252 mass spectrometer with an MT Box-C cryogenic pre-treatment attachment for the extraction of CO_2 from air samples (normally dried at collection). First, δ45 and δ46 values of sample CO_2 are obtained with respect to a pure reference CO_2. The reference CO_2 is one of six sub-samples of an ultra-high purity high-pressure cylinder of CO_2 (HC453) maintained in large-volume glass containers. HC453 has been the sole source of reference CO_2 for use at CSIRO since 1977 and HC453 sub samples were measured against NBS-19 in the 1980s resulting in an assignment of VPDB-CO_2 values of $\delta^{13}C$ = -6.396‰, and $\delta^{18}O$ = -13.176‰ [Francey and Goodman 1988]. The link to VPDB-CO_2 has been maintained by comparisons between these sub-samples. Corrections to convert δ45 and δ46 values to preliminary $\delta^{13}C$ and $\delta^{18}O$ are applied using methods described by Allison *et al.* [1995]. This includes correction for the presence of nitrous oxide, co-trapped with the CO_2, using measured concentrations of N_2O and CO_2 in each sample [Francey *et al.* 1996].

Final $\delta^{13}C$ and $\delta^{18}O$ values on the VPDB-CO_2 scale are obtained after a correction based on comparison of measured and assigned values in air standards (high-pressure cylinders of air) that are processed every 4 samples. The initial assignment of VPDB-CO_2 isotopic values to air standards was referred to as CG92 [Allison and Francey 1999]. A revised assignment, CG99, was developed during 1999-2000, which takes into account recently identified and independently quantified systematic biases [e.g. *Francey and Allison* 1994; Meijer *et al.* 2000]. The CG99 assignment is used here.

CSIRO expressions of the VPDB-CO_2 scale are monitored using a number of high-purity CO_2 standards (GS-19, GS-20, OZTECH-3, OZTECH-30, OZTECH-40) and a number of surveillance standards (high-pressure cylinders of air). The very small sample requirements mean that all high-pressure cylinder air standards used since 1991 remain in the surveillance suite. (Note: Measurements made on all surveillance gases are used solely for diagnostic, not adjustment, purposes). CSIRO monitors its expression of the VPDB-CO_2 scale relative to those of other laboratories, using a range of samples that includes the NIST high-purity CO_2 SRMs [Verkouteren 1999], the IAEA CLASSIC cylinders [two four-laboratory circulations of five cylinders, Allison *et al.,* 2003], flask air sharing comparisons with several laboratories (for example, six flasks of air per month with NOAA/CMDL since 1992) and through participation in other comparison exercises.

5.3. Intercomparison activities

Developing methods to maintain an adequate level of precision has been a key part of calibration strategies at CSIRO. It involves an ongoing process of searching for, discovering, documenting and rectifying systematic bias. We participate in well-planned international intercomparison activities such as the WMO Round-Robins for CO_2 or the NIES NARCIS program [Mukai, 2003] for comparing stable isotope measurements of CO_2. We have also sought to play an expanded international role in the 'data-merging' challenge in two ways:

The immediate objective is to contribute to the detection and rectification of systematic error throughout global networks e.g.:

- The most successful development for monitoring relative precision and providing frequent diagnostic information for a range of trace gas species has been the flask-air sharing (or 'ICP') comparisons between CSIRO and NOAA [Masarie *et al.* 2001]. The program was originally catalysed by the very small GASLAB sample requirements, which permitted CSIRO sampling of a subset of NOAA flasks en route from Cape Grim to NOAA without detectable modification of sample integrity. (Similar comparisons with other laboratories have been useful but

not yet so effective, mainly as a result of lower sampling frequency, thus yielding inadequate statistics).

- For the measurement of stable carbon isotopes of CO_2, CSIRO has played an international role with the preparation and distribution of a subset of 10 high-pressure cylinders of air in the IAEA CLASSIC program, involving the four laboratories with substantial global networks [Allison *et al*., 2003]. Large, but apparently consistent, systematic differences are evident between laboratories that are not reflected in measurements of pure CO_2 standards. Under these circumstances, the IAEA CLASSIC cylinders remain a valuable international standard for CO_2-in-air isotope measurements, pending development of improved links to primary standards.
- The experience with CLASSIC and flask-air sharing programs (and the WMO Round-Robin program) led to the 'GLOBALHUBS' concept [Francey *et al.* 2001a, b]. Its aim is to place the powerful diagnostic elements of these experiments, and more, at the disposal of many more international laboratories. International coordination and prompt (preferably automated) reporting to a community web site are key ingredients.
- Most elements of the GLOBALHUBS concept are being evaluated in Europe (AEROCARB/TACOS programs of CARBOEUROPE) that has received sufficient funding to effectively establish a European HUB laboratory. CSIRO plays both an advisory and sub-contracting role to the AEROCARB program: [see *http://www.bgc-jena.mpg.de/public/carboeur/projects/index_p.html*].
- In a laboratory/diagnostic role, the LOFLO CO_2 analyser system has proven effective in detecting and quantifying previously undetectable systematic influences on CO_2 measurement due to regulators, valves, drying systems etc.

5.4. A contribution to the development of closer links to primary standards and/or constants.

For CO_2 concentration measurements, perhaps the most significant CSIRO contribution to calibration will result from the LOFLO development [Da Costa and Steele 1997]. The LOFLO system design includes seven high-pressure cylinders of air, with CO_2 values spanning 340-400 ppm, directly calibrated by the WMO Central CO_2 Laboratory. The system combines outstanding precision (a few ppb) with low sample consumption. Lifetime of the cylinders for continuous use (and assuming insignificant drifts in concentration) is expected to be decades. Thus the small sample techniques imply significant contraction of calibration hierarchies, and thus all of the error propagation and logistic overheads that accompany them (see Figure 2).

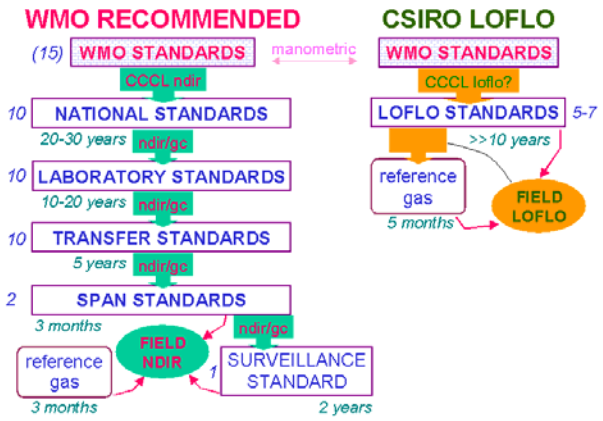

Figure 2. Proposed operational configuration of the LOFLO analyser with regard to reducing errors associated with propagation of the WMO CCL calibration scale. The 'WMO RECOMMENDED' hierarchy is adapted from WMO TD #980 [2000].

- For CO_2 stable isotopes, the European Commission TACOS program has provided an opportunity to improve links to primary standards by improving conventional approaches. Willi Brand, of MPI-Jena, working in collaboration with IAEA (primary carbonate reference material/scales) and CSIRO (CLASSIC cylinders; on-going flask-air sharing with several isotope laboratories) is to prepare CO_2-in-air standards using CO_2 evolved from a carbonate standard, for circulation to participating laboratories.
- Discussions with the Institute for Reference Materials and Methods (IRMM), Geel, Belgium, are exploring the possibility of using high precision mass comparators as a way of accurately determining the absolute ratio of ^{13}C to ^{12}C in CO_2 (effectively a link to the Avogadro constant).

6. Data availability

The calibration statements in sections 5.1 and 5.2 now provide a sufficiently robust foundation for more formal release of much of the CSIRO data. Until now, selected data have been released on request, for applications in which calibration uncertainty was not considered to be a limiting factor at the time. There still remain some data with site- or species-specific biases not yet fully accounted for; in the meantime, the majority of GASLAB data (post 1992) are submitted to the WMO GAW World Data Centre for Greenhouse Gases (WDCGG; http://gaw.kishou.go.jp/wdcgg.html), the CDIAC world data centre for atmospheric trace gases (http://cdiac.esd.ornl.gov/), the Cooperative Atmospheric Data Integration Project (http://www.cmdl.noaa.gov/ccgg/globalview/co2/) and other collaborator data repositories. Specific metadata including site, analysis and calibration details, as well as flagging anticipated upgrades/extensions.

A particular concern has been extra uncertainty associated with linking pre-GASLAB data (prior to 1991/92) to the more recent GASLAB records, with both the final 1-2 years of the older records and the initial 1-2 years of the new records experiencing extra difficulties (requiring non-standard processing). For a lim-

ited number of cases (see highlights below) this has been satisfactorily achieved. In subsequent regular releases of data the extended records will be progressively included.

A related significant challenge, currently being addressed, anticipates a requirement emerging from the development of inverse and multiple-constraint models. These models require a realistic uncertainty on individual measurements, a parameter with importance sometimes matching the actual value, particularly where uncertainty systematically varies with time within a record. The models also require specific sampling details (in particular actual sampling time) in order to optimise ever improving atmospheric transport representations (including nested boundary-layer/mesoscale models). Pending the accommodation of these extra parameters in international databases, this information will be developed within CSIRO archives alongside the composition data, and will be provided on request.

7. Recent milestones

The 6th International CO_2 Conference was held in Sendai, Japan, 1-5 October 2001. The international CO_2 conferences have been traditionally a watershed for release of CSIRO greenhouse gas results and this occasion is no exception. Appendix 1 lists publications representing significant milestones for the Australian global greenhouse gas measurement community (and modelling colleagues) and includes a high proportion of results described in more detail in the Extended Abstracts volumes of the Sendai conference.

Other significant publications of CSIRO data:

Pak, B. C-Y., Vertical structure of atmospheric trace gases over southeast Australia, *PhD thesis*, University of Melbourne, 2000.

8. New directions

With increasing efficiency and automation of basic monitoring activities, and completion of shorter-term contractual or development activities, there is the opportunity from time to time to undertake new initiatives. A number of such activities of potential interest to the wider measurement community are listed below:

8.1. LOFLO analysers

8.1.1. Commercialisation

The performance of the Cape Grim LOFLO CO_2 analyser system has led to a semi-commercial production of a further six units. A number of design changes were necessitated by evolution of software and by a requirement for portability. The design and construction of the MARK II LOFLO systems is being undertaken by the engineering sections of CSIRO Atmospheric Research, working in close collaboration with GASLAB (which provides input on optimum configurations for various applications, and for calibration, testing and commissioning). Depending on the success of the redevelopment and demand for the analysers, production of further MARK II units is under consideration. Motivated primarily by strategic scientific considerations (wider deployment of LOFLO systems is the best contribution we can make to reduce uncertainties in fluxes derived from inversion of atmospheric CO_2 measurements), plans for further improvement and a greater degree of commercialisation (a MARK III) are also under discussion.

8.1.2. Remote site operation

The French (LSCE) are preparing a MARK II analyser for deployment on Amsterdam Island in response to difficulties in maintaining skilled operators at the site. Greatly reduced operator requirements and greatly reduced provision and preparation of reference, span, and associated high-pressure cylinders [WMO 2000] are anticipated. The much lower cost of operation of a LOFLO analyser system compared to a conventional system is related to both factors. The day-to-day operation and diagnoses of the Cape Grim LOFLO system is conducted via telephone from Melbourne. The design envisages on-site operator intervention once every five months to change the reference tank and check the drying system; during the trial phase, minor adjustment, once per month, was also required. There is potential to lengthen the period between both the reference tank change and adjustment. At Cape Grim, consumables costs are reduced by about a factor of five compared to the conventional NDIR system. Production of LOFLO systems that will permit precision CO_2 monitoring in presently under-sampled global regions remains a strategic priority.

8.1.3. Continuous versus flask sampling

Prompted by the possible removal of logistic constraints that have restricted the wider deployment of continuous CO_2 analysers, Law *et al.* [2001] have attempted preliminary studies with a 3-dimensional atmospheric transport model to explore possible improvement in flux estimates from inversions of atmospheric CO_2 measurements, when flask-sampling at GLOBALVIEW-CO_2 sites is replaced with continuous LOFLO CO_2 analysers. Prior estimates of global emissions have been used to generate 'pseudo CO_2' data at 83 GLOBALVIEW sites. Using the same transport model, the psuedo-data at the 83 sites have been inverted to provide surface fluxes. In Figure 3, the mean level and uncertainty in these fluxes are compared to the prior estimates for different inversions using data averaged over one month (more typical of data available from flask sites), to every four hours (representing a continuous monitoring site). The influence of systematic calibration differences in the data is also explored.

A good inversion requires that the Root Mean Square Bias (RMSB; the estimated minus the prior source) be smaller than the Root Mean Square Uncertainty (RMSU, determined across 12 months), as observed in all 'clean' cases in Figure 3, and that the RMSU is small (which is particularly true for the more frequent and better calibrated data). There is support for wider deployment of continuous analysers in this plot.

(Note: More frequent sampling is an argument used in justifying the development of satellite sensors of

CO_2. Given other potential biases of satellite systems such as cloud, calibration and low precision, a parallel focus and effort in assessing wider deployment of high-precision, continuous, low-maintenance surface instruments, seems appropriate.)

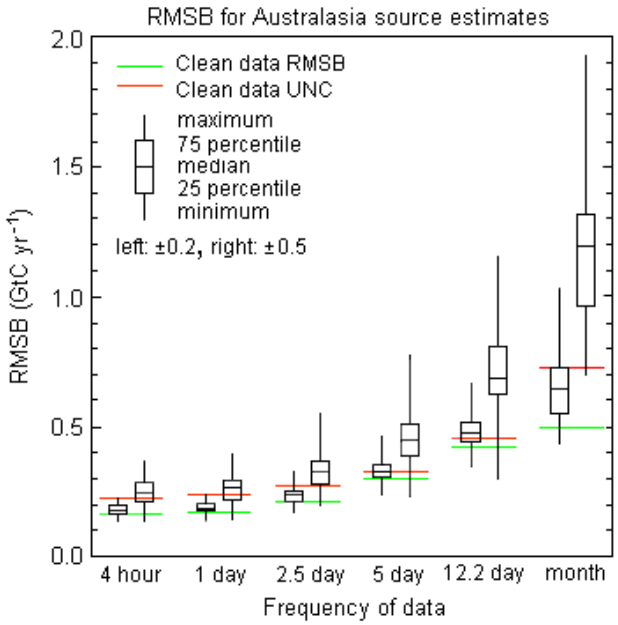

Figure 3. The Root Mean Square Bias (RMSB; the estimated minus the prior source; green line) and Root Mean Square Uncertainty across 12 months (UNC; red line) are given in the Australasian region, for clean data. The box and whiskers define the mean, 25 and 75 percentiles, maximum and minimum of the RMSB when up to ±0.2 ppm (left box) and up to ±0.5 ppm (right box) random offsets are applied to the data every two months. The offsets are intended to simulate likely errors in a conventional CO_2 monitoring system corresponding to span and reference gas changes, as suggested from the comparisons between the conventional and LOFLO system at Cape Grim, or intercalibration differences between laboratories [*Law et al.* 2001].

8.1.4. Regional (Continental) Inversions using a LOFLO system

Modelling studies using 'pseudo data' and 'perfect transport' have been applied to the deployment of a network of LOFLO systems across the Australian continent, with the target of better 'top-down' location and monitoring of regional flux changes. The results were similarly encouraging. Over the next two years, GASLAB hopes to deploy trial networks of continuous LOFLO CO_2 analysers, in close collaboration with flux tower measurements and intensive inventory/process studies of soils and plants, within a 'multiple-constraint' modelling framework.

In long-term continuous monitoring at continental sites, the LOFLO systems offers the opportunity to examine averaged selected data (on the basis of local transport and/or frequency domain filtering, etc.), at several sites, over decades, with precisions of a few tens of a ppb. There is a possibility that long-term, slow, but potentially serious, environmental change is first detected by such monitoring.

8.1.5. Ultra-High Precision Southern Ocean Monitoring

The potential for two LOFLO analysers to accurately monitor hourly CO_2 differences to a precision (≤10-20 ppb), an order of magnitude better than current instruments, similarly suggests new dimensions to global atmospheric CO_2 monitoring over the oceans. Ocean general circulation models [e.g. Matear *et al.* 1999] are suggesting that the Southern Ocean circulation is particularly sensitive to global warming and that changed efflux of CO_2 and other trace gases will result. There have also been suggestions of fertilisation of Southern Oceans to remove excess CO_2 from the atmosphere. An ultra-high-precision monitoring network for CO_2 over the Southern Oceans, possibly complemented by continuous O_2/N_2 monitoring to better characterise marine biota influences, is proposed as one way to best exploit the LOFLO analyser precision (see Figure 4).

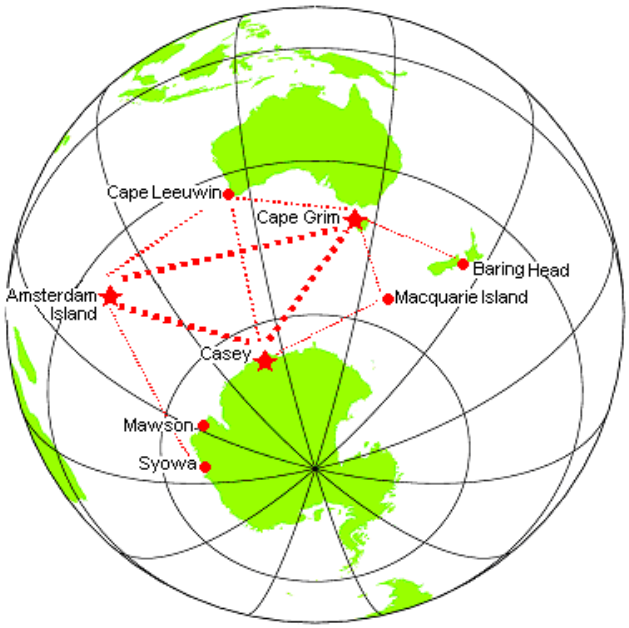

Figure 4. Possible configuration of an ultra-high precision Southern Ocean CO_2 and atmospheric monitoring network based on LOFLO CO_2 Analyser Systems. Complementary O_2/N_2 monitoring is also envisaged. (Thick dashes/stars envisaged by 2002/3).

With a LOFLO now operating at Cape Grim, the anticipated deployment of a second system at Amsterdam Island in 2002, and a third destined for use on the Antarctic supply ship *RV Aurora Australis* from 2002, the foundations of a Southern Ocean ultra-high precision monitoring are starting to emerge. Continuous O_2/N_2 monitoring at Baring Head, and anticipated monitoring from Cape Grim by NIES next year, further strengthen the vision. This will be reinforced as extra resources come to hand.

8.2. Intercomparison activities

GASLAB is steadily improving its capability of preparing high-pressure cylinders of air of specified composition for a range of long-lived trace gases, and of testing of components (especially high-pressure regulators),

containers etc., for systematic influence on atmospheric composition measurements. We have experienced a growing international demand for this expertise. Increasing automation and efficiency permits a continuing, possibly expanded role as a reliable provider of quality products whose widespread deployment significantly addresses our strategic objective of reducing uncertainty on global flux estimates from inversions of atmospheric composition data.

Acknowledgements

We thank the editors for inviting this report, which is closely based on a report submitted to the *11th WMO/IAEA Meeting of Experts on Carbon Dioxide Concentration and Related Tracer Measurement Techniques*, Tokyo, September 25-28 2001.

The CSIRO GASLAB establishment benefited substantially from Australian National Greenhouse Advisory Committee funding. GASLAB continues to enjoy the financial and technical field support of the Cape Grim Baseline Air Pollution Station. The scientific support of international collaborators is a crucial component of the global sampling and intercalibration activities.

References

Allison, C. E., R. J. Francey, and H. A. J. Meijer, Recommendations for the reporting of stable isotope measurements of carbon and oxygen in CO_2 gas. *Reference and Intercomparison Materials for Stable Isotopes of Light Elements, IAEA-TEDOC-825*, edited by K. Rozanski, Vienna, 155-162, 1995.

Allison, C. E. and R. J. Francey, $\delta^{13}C$ of atmospheric CO_2 at Cape Grim: The *in situ* record, the flask record, air standards and the CG92 calibration scale, in *Baseline Atmospheric Program (Australia) 1996*, edited by J. L. Gras, N. Derek, N. W. Tindale and A. L. Dick, Bureau of Meteorology and CSIRO Atmospheric Research, Melbourne, Australia, 45-56, 1999.

Allison, C. E., R. J. Francey, and L. P. Steele, The International Atomic Energy Agency Circulation of Laboratory Air Standards for Stable Isotope Comparisons: Aims, preparation and preliminary results, in *Isotope aided studies of atmospheric carbon dioxide and other greenhouse gases Phase II (IAEA-TECDOC-1269)*, edited by M. Groening and H. A. J. Meijer, International Atomic Energy Agency, Vienna, Austria, 5-23, 2002.

Allison, C. E., R. J. Francey, J. W. C. White, B. Vaughan, M. Wahlen, A. Ballenbacher, and T. Nakazawa, What have we learnt about stable isotope measurement from the IAEA CLASSIC, presented at the *11th WMO/IAEA Meeting of Experts on Carbon Dioxide Concentration and Related Tracer Measurement Techniques*, Tokyo, September 25-28 2001, in press, 2003.

Beardsmore, D. J., G. I. Pearman, L. P. Steele, and F. de Silva, The CSIRO (Australia) atmospheric carbon dioxide monitoring program by infra-red gas analysis: Post 1981 developments and data, *CSIRO Atmospheric Research Technical Report*, in preparation.

Cooper, L. N., L. P. Steele, R. L. Langenfelds, D. A. Spencer, and M. P. Lucarelli Atmospheric methane, carbon dioxide, hydrogen, carbon monoxide and nitrous oxide from Cape Grim flask air samples analysed by gas chromatography, in *Baseline Atmospheric Program (Australia) 1996*, edited by J. L. Gras, N. Derek, N. W. Tindale and A. L. Dick, Bureau of Meteorology and CSIRO Atmospheric Research, Melbourne, Australia, 98-102, 1999.

Da Costa, G. A., and L. P. Steele, A low-flow analyser system for making measurements of atmospheric CO_2, in *Report of the ninth WMO Meeting of Experts on Carbon Dioxide Concentration and Related Tracer Measurement Techniques*, Aspendale, Australia, edited by R. J. Francey, (Environmental Pollution Monitoring and Research Programme / Global Atmosphere Watch, 132; WMO/TD; no. 952), Secretariat of the World Meteorological Organization, Geneva, Austria, 16-20, 1999.

Etheridge, D. M., L. P. Steele, R. L. Langenfelds, R. J. Francey, J.-M. Barnola, and V. I. Morgan, Natural and anthropogenic changes in atmospheric CO_2 over the last 1000 years from air in Antarctic ice and firn. *J. Geophys. Res*., 101, 4115-4128, 1996.

Etheridge, D. M., L. P. Steele, R. J. Francey, and R. L. Langenfelds, Atmospheric methane between 1000 A.D. and present: evidence of anthropogenic emissions and climatic variability, *J. Geophys. Res.,* 103, 15,979-15,993, 1998.

Francey, R. J., and H. S. Goodman, The DAR stable isotope reference scale for CO_2, in *Baseline Atmospheric Program (Australia) 1986*, edited by B. W. Forgan and P. J. Fraser, Department of Science, Bureau of Meteorology with CSIRO Division of Atmospheric Research, Melbourne, Australia, 40-46, 1988.

Francey, R. J., and C. E. Allison, The trend in atmospheric $\delta^{13}CO_2$ over the last decade, in *Isotope variations of carbon dioxide and other trace gases in the atmosphere: final research coordination meeting*, coordinated research programme: final report, Vienna, Austria, edited by K. Rozanski, International Atomic Energy Agency, Vienna, Austria,. 7 p., 1994.

Francey, R. J., L. P. Steele, R. L. Langenfelds, M. Lucarelli, C. E. Allison, D. J. Beardsmore, S. A. Coram, N. Derek, F. de Silva, D. M. Etheridge, P. J. Fraser, R. J. Henry, B. Turner, and E. D. Welch, Global Atmospheric Sampling Laboratory (GASLAB): supporting and extending the Cape Grim trace gas programs, in *Baseline Atmospheric Program (Australia) 1993*, edited by R. J. Francey, A. L. Dick and N. Derek, Bureau of Meteorology and CSIRO Division of Atmospheric Research, Melbourne, Australia, 8-29, 1996.

Francey, R. J., C. E. Allison, D. M. Etheridge, C. M. Trudinger, I. G. Enting, M. L. Leuenberger, R. L. Langenfelds, E. Michel, and L. P. Steele, A 1000-year high precision record of $\delta^{13}C$ in atmospheric CO_2, *Tellus*, 51B, 170-193, 1999a.

Francey, R. J., M. R. Manning, C. E. Allison, S. A. Coram, D. M. Etheridge, R. L. Langenfelds, D. C. Lowe, and L. P. Steele, A history of $\delta^{13}C$ in atmospheric CH_4 from the Cape Grim Air Archive and Antarctic firn air, *J. Geophys. Res.*, 104, 23,631-23, 634, 1999b.

Francey, R.J., P. J. Rayner, and C. E. Allison, Constraining the global carbon budget from global to regional scales – the measurement challenge, in *Global Biogeochemical Cycles in the Climate System,* Academic Press, New York, 245-252, 2001a.

Francey, R., M. Groening, K. Holmen, K-R. Kim, J. Miller, P. Tans and N. Trivett Global quality control for long-lived trace gas measurements, *Mem. Natl. Inst. Polar Res*., *Spec. Issue*, 54, 81-90, 2001b.

Langenfelds, R. L., P. J. Fraser, R. J. Francey, L. P. Steele, L. W. Porter, and C. E. Allison, The Cape Grim Air Archive: the first seventeen years, 1978-1995 in *Baseline Atmospheric Program (Australia) 1994-95*, edited by R. J. Francey, A. L. Dick, and N. Derek, Bureau of Meteorology and CSIRO Division of Atmospheric Research, Melbourne, Australia, 53-70, 1996.

Langenfelds, R. L., R. J. Francey, L. P. Steele, M. Battle, R. F. Keeling, and W. F. Budd, Partitioning of the global fossil CO_2 sink using a 19-year trend in atmospheric O_2, *Geophys. Res. Letts.*, 26, 1897-1900, 1999.

Levchenko, V. A., R. J. Francey, D. M. Etheridge, C. Tuniz, J. Head, V. I. Morgan, and G. Jacobsen, The ^{14}C 'bomb spike' determines the age spread and age of CO_2 in Law Dome firm and ice, *Geophys. Res. Letts.*, 23, 3345-3348, 1996.

Levchenko, V. A., D. M. Etheridge, R. J. Francey, C. M. Trudinger, C. Tuniz, E. M. Lawson, A. M. Smith, G. E. Jacobsen, Q. Hua, M. A. C. Hotchkis, D. Fink, V. I. Morgan, and J. Head, Measurements of the $^{14}CO_2$ bomb pulse in firn and ice at Law Dome, Antarctica. *Nuclear Instruments and Methods in Physics. Research Section B*, 123 (1-4): 290-295, 1997.

Langenfelds, R. L., L. P. Steele, L. N. Cooper, D. A. Spencer, D. M. Etheridge, and M. P. Lucarelli, CSIRO GASLAB measurement of CO_2, CH_4, CO, H_2 and N_2O by gas chromatography, 1991-2001, *CSIRO Atmospheric Research Technical Report*, in preparation.

Law, R. M., P. J. Rayner, L. P. Steele, and I. G. Enting CO_2 inversions using high temporal frequency data. Extended Abstracts

of 6th International CO_2 Conference, Sendai, Japan, 2-5 October, 2001, paper MA20, 2001.

Masarie, K. A., R. L. Langenfelds, C. E. Allison, T. J. Conway, E. J. Dlugokencky, R. J. Francey, P. C. Novelli, L. P. Steele, P. P. Tans, B. Vaughn, J. W. C. White, and M. Trolier, The NOAA/CSIRO Flask-Air Intercomparison Program: A strategy for directly assessing consistency among atmospheric measurements derived from independent laboratories, *J. Geophys. Res.*, 106, 20,445–20,464, 2001.

Matear, R. J., and A. C. Hirst, Climate change feedback on the future oceanic CO_2 uptake, *Tellus*, 51B, 722-733, 1999.

Meijer, H. A. J., R. E. M. Neubert, and G. H. Visser, Cross contamination in dual inlet isotope ratio mass spectrometers, *Internat. J. Mass Spec.,* 198, 45-61, 2000.

Mukai, H., NIES pure CO_2 sample for inter-laboratory comparison of C and O isotope ratio analysis especially for atmospheric CO_2, presented at the *11th WMO/IAEA Meeting of Experts on Carbon Dioxide Concentration and Related Tracer Measurement Techniques*, Tokyo, September 25-28 2001, in press, 2003.

Novelli, P.C., J. W. Elkins, and L. P. Steele, The development and evaluation of a gravimetric reference scale for measurements of atmospheric carbon monoxide, *J. Geophys. Res.*, 96, 13,109-13,121, 1991.

Novelli, P. C., P. M. Lang, K. A. Masarie, D. F. Hurst, R. Myers, and J. W. Elkins, Molecular hydrogen in the troposphere: Global distribution and budget, *J. Geophys. Res.*, 104, 30,427-30,444, 1999.

Steele, L. P., R. L. Langenfelds, M. P. Lucarelli, P. J. Fraser, L. N. Cooper, D. A. Spencer, S. Chea, and K. Broadhurst, Atmospheric methane, carbon dioxide, carbon monoxide, hydrogen and nitrous oxide from Cape Grim flask samples analysed by gas chromatography, in *Baseline Atmospheric Program (Australia), 1994-95*, edited by R. J. Francey, A. L. Dick and N. Derek, Bureau of Meteorology and CSIRO Division of Atmospheric Research, Melbourne, Australia, 107-110, 1996.

Trudinger, C. M., I. G. Enting, R. J. Francey, D. M. Etheridge, and P. J. Rayner, Long-term variability in the global carbon cycle inferred from a high precision CO_2 and $\delta^{13}C$ ice core record. *Tellus*, 51B, 233-248, 1999.

Verkouteren, R. M., Preparation, Characterization, and value assignment of carbon dioxide isotopic reference materials: RMs 8562, 8563, and 8564. *Anal. Chem*., 71, 4740-4746, 1999.

WMO TD No. 980 Guide on sampling and analysis techniques for chemical constituents and physical properties in air and precipitation as applied at stations of the Global Atmosphere Watch. Part 1: Carbon Dioxide, (Prepared by N. Trivett and A. Kohler) *World Meteorological Organization Global Atmosphere Watch* No. 134, Geneva, Switzerland, 2000.

Zhao, C., P. Tans, and K. Thoning, A high precision manometric system for absolute calibrations of CO_2 in air, *J. Geophys. Res*., 102, 5885-5894, 1997.

Acronyms

AAD	Australian Antarctic Division
AEROCARB	Airborne European Regional Observations of the Carbon Balance
AES	Environment Canada
AIMS	Australian Institute of Marine Science
AMSA	Australian Maritime Safety Authority
BAPS	Baseline Air Pollution Station (Cape Grim)
BoM	Bureau of Meteorology (Australia)
CDIAC	Carbon Dioxide Information Analysis Centre
CLASSIC	Circulation of Laboratory Air Standards for Stable Isotope interComparisons
CMDL	Climate Monitoring and Diagnostics Laboratory, NOAA
CCG	Carbon Cycle Group (CMDL)
CMR	CSIRO Marine Research (Australia)
CSIRO	CSIRO Atmospheric Research, Australia
GASLAB	Global Atmospheric Sampling LABoratory
GAW	Global Atmosphere Watch (WMO)
HATS	Halocarbons and other Atmospheric Trace Species (CMDL)
IAEA	International Atomic Energy Agency
ICP	inter-comparison program
IRMM	Institute for Reference Materials and Methods (Belgium)
JMA	Japan Meteorological Agency
KFA	Forschungszentrum Julich, Germany
MPI	Max Planck Institute (Germany)
NERC	National Energy Research Council, UK
NIWA	National Institute of Water and Atmospheric Research, NZ
NDIR	non-dispersive infra red
NIES	National Institute for Environmental Studies (Japan)
NOAA	National Oceanographic and Atmospheric Administration
OASIS	Observations At Several Interacting Scales (Australia)
SRM	standard reference material
TACOS	Terrestrial and Atmospheric Carbon Observing System
WDCGG	World Data Centre for Greenhouse Gases (JMA)
WMO	World Meteorological Organization

Appendix 1

List of authors and conference papers presented at the 6th *International Carbon Dioxide Conference* [extended abstracts], 1-5 October 2001, Sendai, Japan, Organizing Committee of the 6th Conference, Sendai, Japan, 2001.

Allison, C. E., R. J. Francey, and P. J. Rayner, Stable isotopes of atmospheric carbon dioxide from the CSIRO Global Flask Sampling Network [AT07].

Langenfelds, R., R. Francey, B. Pak, P. Steele, J. Lloyd, C. Trudinger, and C. Allison, The use of multi-species measurements for interpreting interannual variability in the carbon cycle [AT44], (*also published in Glob. Biogeochem. Cycles*).

Steele, L. P., G. A. Da Costa, D. A. Spencer, P. B. Krummel, R. J. Francey, J. Bennett, B. Petraitis, R. Howden, C. Smith, S. Baly, and L. W. Porter, Future directions in atmospheric CO_2 measurement methods [AT45].

Francey, R. J., C. E. Allison, C. M. Trudinger, P. J. Rayner, I. G. Enting, and L. P. Steele, The interannual variation in global atmospheric $\delta^{13}C$ and Its link to net terrestrial exchange [AT55].

Francey, R. J., C. E. Allison, P. Ciais ,and G., Hoffmann, The interannual variation in the $\delta^{18}O$ of atmospheric CO_2 over the last 25 years [AT56].

Law, R. M., P. J. Rayner, L. P. Steele, and I. G. Enting, CO_2 inversions using high temporal frequency data [MA20].

Rayner, P. J., Inferring terrestrial biosphere carbon fluxes from combined inversions of atmospheric transport and process based terrestrial ecosystem models [MB17].

Wang, Y. P., and D. J. Barrett, Estimation of carbon exchange fluxes in southern Australia using multiple constraints [TE51].

Peylin, P., P. Ciais, P. P. Tans, and R. Francey, Monthly estimates of terrestrial photosynthesis and respiration from atmospheric measurements of $^{18}O/^{16}O$ ratio in CO_2 [MA18].

Trudinger, C. M., I. G. Enting, P. J. Rayner, and R. J. Francey, A Kalman filter bubble deconvolution of ice core CO_2 and $\delta^{13}C$ data [MC04].

LeQuere, C., O. Aumount, L. Bopp, P. Bousquet, P. Ciais, R. Francey, M. Heimann, R. F. Keeling, H. Kheshgi, P. Peylin, S. C. Piper, I. C. Prentice and P. J. Rayner, Two Decades of Ocean CO_2 Sink and Variability [MC07].

Roy, T., P. Rayner, R. Matear, and R. Francey, Comparison of Southern Hemisphere Ocean CO_2 flux estimates with atmospheric inversion results [MC22].

NANO-PARTICLES AT CAPE GRIM: A REGIONAL VIEW USING SOUTHERN OCEAN ATMOSPHERIC PHOTOCHEMISTRY EXPERIMENT (SOAPEX-2) AS A CASE STUDY

S I Jimi[1,2], J L Gras[1] and S T Siems[2]

[1]CSIRO Atmospheric Research, Aspendale Victoria 3195, Australia
[2]School of Mathematical Sciences, Monash University, Clayton Victoria 3800, Australia

Abstract

Factors influencing the concentration of particles with diameters between 3 and 12 nm, at Cape Grim, were investigated during the SOAPEX-2 study in January-February 1999. Diurnal variation was examined for three broad air mass origins, Tasmania, continental Australia and clean maritime. Substantial differences were found in the diurnal cycles between these sectors with a broad daytime enhancement in the Tasmanian sector, attributed to urban/industrial activities. The diurnal variation for the continental sector had the appearance of a typical urban daytime activity pattern (morning and evening peaks), delayed by around 10 to 12 hours. In the baseline sector there was little evidence of photochemical enhancement of concentrations during the day but some evidence of a nighttime enhancement.

The behaviour of nano-particle concentrations following the three frontal passages during SOAPEX-2 was also investigated; enhancements were observed following each of the fronts. These enhancements were similar to those reported from ACE 1 but were of greater magnitude. The prevailing conditions during the SOAPEX-2 enhancements were very clean maritime air, low radon concentration and typical baseline concentrations of methane and carbon monoxide. Water vapour mixing ratios were reduced during the enhancement periods, supporting the hypothesis that the particle enhancements are related to subsidence of free tropospheric air.

1. Introduction

This study reports on *in situ* measurements of nano-particles in the marine boundary layer near south-eastern Australia defined here as particles with diameter (D_p) in the range $3 \leq D_p \leq 12$ nm. The measurements were made during the second Southern Ocean Atmospheric Photochemistry Experiment (SOAPEX-2) field campaign at the Cape Grim Baseline Air Pollution Station from 17 January to 19 February 1999. This period was selected because photochemical processes are most active at this time of year. The main objective of SOAPEX-2 was to study gas phase chemistry in very clean air over the Southern Ocean. The study included aerosol measurements because of the importance of photochemistry in aerosol production and also because of the role of aerosol in heterogeneous reactions. There are various reasons for focusing on particles in the low nanometre size range. Nano-particles are short-lived, rapidly growing into accumulation mode size particles by coagulation and condensational growth. The presence of significant concentrations of nano-particles is a good indicator of relatively recent new particle formation [O'Dowd *et al*. 1998].

Since its inception in 1976, the Cape Grim program has included measurements of integrated particle number concentration, including nanometer sizes ($D_p > 3$ nm), determined using a manually operated Nolan-Pollak photoelectric condensation nucleus (CN) counter. Over that period, a series of automatically operated CSIRO replica Nolan-Pollak CN counters have also been deployed and continue to be used. In 1984, a TSI 3020 CN counter was added [Gras 1986] and a TSI 3760 CN counter has also been used continuously since mid-1996. The use of a diffusion battery since the early 1980s has allowed the observation of size distribution to nanometre sizes, although with relatively low temporal and spectral resolution. With the addition of the TSI3025 UCN counter during SOAPEX-2 it has become possible to directly determine the concentration of particles in the range 3-12 nm with high temporal resolution.

In this study we examine some general properties of nano-particle concentrations and other indicators of air masses to identify possible sources of the nano-particles. Enhanced nano-particle concentrations were reported by Bates *et al*. [1998] from ship-based measurements for the Southern Ocean region during post-frontal subsidence for the period of the first Aerosol Characterization Experiment (ACE 1) in 1995. In this work we examine post-frontal conditions during SOAPEX-2 to extend the study of Southern Ocean nano-particle enhancement to Cape Grim.

2. Experimental

2.1. Site Description

The Cape Grim atmospheric observatory is located at the north-west tip of Tasmania (40°41′S, 144°41′E). Situated on a cliff 94 m above sea level, it is well located for sampling air from several relatively distinct regions. These can be broadly classed as the Australian continent (wind direction 280° - 80°), the island of Tasmania (80° - 190°) and clean maritime air (190° - 280°) that has traversed long distances over the Southern Ocean. These latter conditions are highly variable but typically occur about 50% of the time for the Cape Grim 10-m wind. This percentage is based on 14 years of data from 1988-2001 inclusive [Paul Krummel, CSIRO Atmospheric Research, personal communication, 2002]. The baseline definition in this study is based on wind direction only. The location of Cape Grim is indicated in Figure 1 (at the centre of the wind rose).

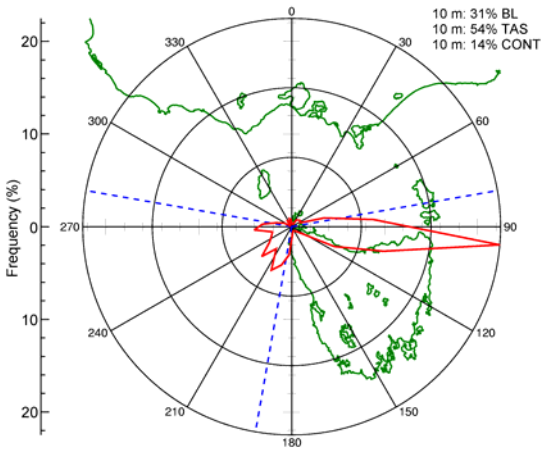

Figure 1. Wind direction frequency for SOAPEX-2 (17 January - 19 February 1999). The legend indicates wind direction frequencies, as percentages, for the baseline (BL), Tasmanian (TAS) and continental (CONT) sectors during the SOAPEX-2 period. The blue dotted lines indicate the borders between the three wind sectors.

2.2. Equipment

The concentrations of nano-particles, as reported here, were derived from the difference in concentration determined using a TSI 3025 UCN counter and a TSI 3760 CN counter. The lower detection limit (50% counting efficiency) for the Cape Grim TSI 3760 was determined by Wiedensohler *et al*. [1997] to be 12 nm. The Cape Grim TSI 3025 lower detection limit has not been individually established. A generic value of 2.5 nm, as determined for a group of seven TSI 3025 counters by Wiedensohler *et al*. [1997] is assumed. The spread at the cut-off detection limit (50% counting efficiency) for the seven counters tested ranged from 2.42 to 2.82 nm. The primary data for this work are one-minute averages of particle concentration from each of these counters.

One problem that was encountered during SOAPEX-2, and subsequent work with the TSI3025, is the adsorption of water in the butanol working fluid. The TSI3025 does not have a flush system and in humid conditions the butanol absorbs water. Subsequent correction involved regular automated flushing of the saturator. A similar problem occurs with continuous use of the TSI3760. In this case, the butanol reservoir is routinely manually replenished. The counting efficiency of both instruments is reduced as water is absorbed, and finally counting stops completely. For this study, any data suspected to be impacted by this problem were not included in the analyses.

2.3. Weather conditions during SOAPEX-2

The weather during SOAPEX-2 was marked by a relatively low frequency of conditions with clean maritime air of recent Southern Ocean origin (baseline conditions). The 10-m wind direction frequency for the SOAPEX-2 period is given in Figure 1. This wind rose plot shows that for the one-month period of the study, these conditions were observed for only about 31% of the time. The rest of the period was dominated by easterly flow (54%), which typically traversed the northern coast of Tasmania, or nearby Bass Strait. Back trajectory analyses show that continental airflow during SOAPEX-2 mainly traversed rural regions over New South Wales and eastern Victoria, before crossing Bass Strait and arriving at Cape Grim. Continental flow was infrequent (14%) during SOAPEX-2, as shown in Figure 1.

3. Results and Discussion

3.1. Nano-Particles – wind sector dependence

In order to establish the general behaviour of nano-particle concentrations from different source regions, air mass origins were categorised into three broad wind sectors: Tasmanian (80° - 190°), baseline (190° - 280°) and continental (280° - 80°). Figures 2a, b and c show median diurnal cycles of nano-particle concentrations for these three wind sectors. The plotted data are medians over the study period, of the hourly medians of minute data. As is evident from these figures, the three sectors have quite different diurnal patterns. Air arriving from the Tasmanian sector has a high probability of recently passing over regions that include urban and light industrial areas along the northern Tasmanian coast. For this sector, a broad increase can be seen during the day, commencing after about 0600 and reaching a maximum around mid afternoon. This overall pattern can reasonably be associated with relatively local, upwind urban/industrial activities. Figure 3, gives the corresponding diurnal pattern for radon concentration. This indicates less land contact during nighttime on average, a factor that will contribute to the very low nano-particle concentrations observed in this sector in the early morning.

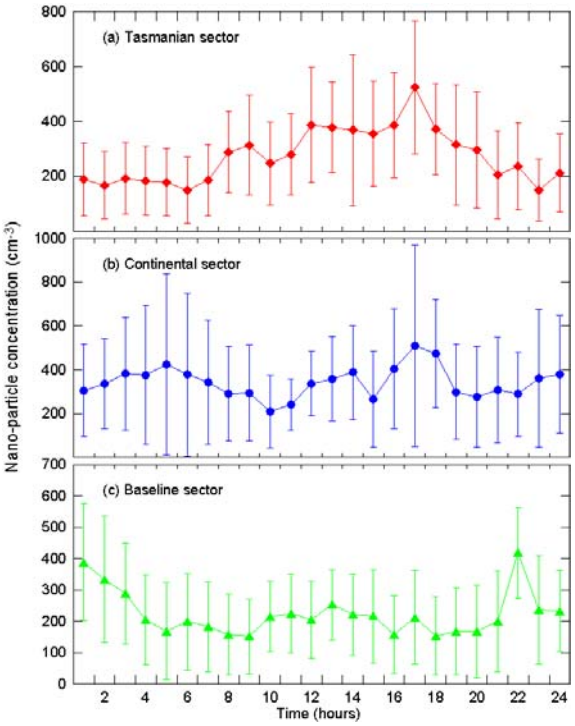

Figure 2. Median diurnal cycle of nano-particle concentrations for the (a) Tasmanian, (b) continental and (c) baseline sectors. The bars shown indicate the 25th and 75th percentiles.

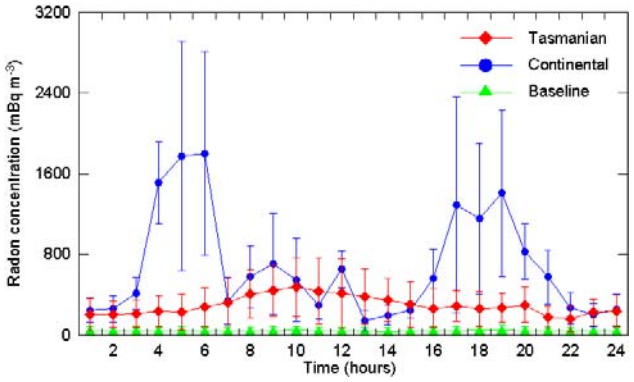

Figure 3. The diurnal cycle of radon concentrations for the three wind sectors: Tasmanian, baseline and continental. The bars shown are the 25th and 75th percentiles.

For the continental case two concentration peaks were observed, the first around 0400 and the second around 1600. Caution is needed in interpretation of these data due to the very limited number of cases available (typically this ranged from 2 to 8 cases per indicated hour). The general form of variation suggests a time-shifted daytime maximum, associated with urban/industrial activity on the Australian continent, for example comprising morning and late afternoon peaks. A lag of 10 to 12 hours would be required to shift the observed pattern in nano-particle concentrations into the previous day, and is consistent with the prevailing wind speed (30 km hr^{-1}) and the distance (300 km) to the nearer populated areas of south-eastern Australia. The diurnal pattern for radon, as shown in Figure 3, clearly shows a similar form suggesting that strong diurnal differences in surface coupling may have also played a role in the nano-particle concentration diurnal cycle in this sector. Very clearly, more data are required both to establish, and explain, the diurnal cycle in the continental sector.

In the baseline sector there is little evidence for daytime photochemical production of nano-particles over the study period, although there is some evidence for elevated concentrations overnight (2100 - 0300). The lack of diurnal variation in radon, and its low concentration for this sector (less than 100 mBq m^{-3}), indicate that the overnight nano-particle increase was not due to continental or island influences.

3.2. Nano-particle concentrations following frontal passages

Although the SOAPEX-2 primary objective related to clean post-frontal air, the frequency of frontal passages was relatively low. Three frontal passages over Cape Grim are considered. The periods encompassing the frontal passages, and containing both pre- and post-frontal conditions are 18 - 20 January and 14 - 19 February 1999. In the first case, a front passed over Cape Grim at 0130 on 19 January. The other two frontal passages occurred at 0415 on the 15 and at 0900 on 17 February. All times given are Australian Eastern Standard (UTC + 10 hours). The passage of these three fronts can be seen on the surface isobaric charts given in Figure 4, and their immediate effect at Cape Grim can also be seen in the strong wind direction shifts indicated by the dashed lines in Figures 5a and b, and the pressure minima in Figures 6a and b. The maximum uncertainty associated with determining the time of frontal passage is around 2 hours, which is mainly due to the time needed for the continental pre-frontal air stream to be completely replaced by the south-westerly post-frontal flow. This period is usually referred to as frontal transition time.

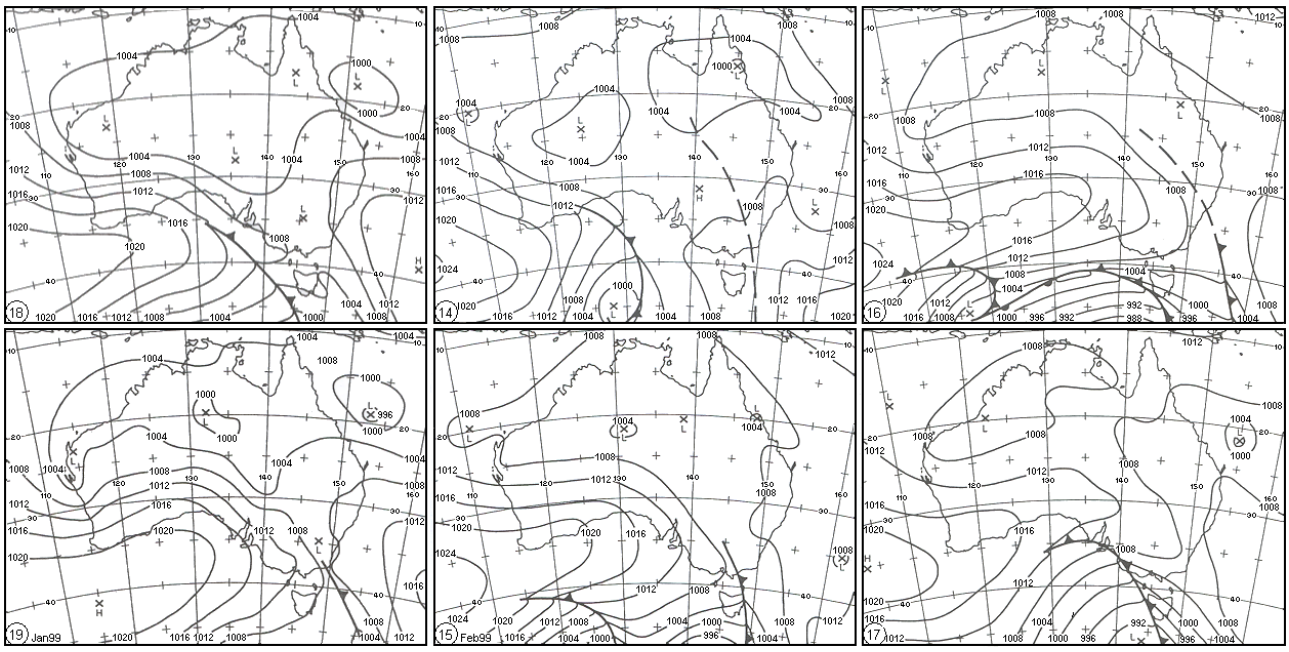

Figure 4. Surface isobaric maps for 0000 UTC 18 – 19 January 1999 (left), 14 – 15 February 1999 (middle) and 16 – 17 February 1999 (right).

The isobaric analysis charts suggest that the third front was the strongest. The pressure minimum for this front was also the lowest, further suggesting that this passage was the strongest. As shown in Table 1, the average wind speed also shows some differences during the three frontal passages. The wind direction shift and wind speed are determined from 3-hour pre- and post-frontal averages. The wind direction is the difference between the two and the wind speed is the average. As is evident in Figure 5a, the average pre-frontal wind flow for the first frontal passage was westerly, which is not typical for Cape Grim. However, wind direction shifts for the second and third frontal passages were continental to baseline, as is frequently observed at Cape Grim.

Table 1. Summary of frontal passages over Cape Grim during SOAPEX-2.

Front #	*Date 1999*	*Time (AEST)*	*Wind Direction Shift (degrees)*	*Wind Speed ($m\ s^{-1}$)*	*Pressure Minima (hPa)*
1	19 Jan	0130	271 - 211	7.4	996.2
2	15 Feb	0415	65 - 275	5.4	993.9
3	17 Feb	0900	328 - 287	11.4	986.6

Figure 5a and b also show that total number concentration of particles larger than 3 nm and 12 nm diameter both increased after the frontal passages.

After the first front, the nano-particle concentration progressively increased from a background level of ~100 cm^{-3} to a maximum of 547 cm^{-3} (for a 5-minute average), dropped to 300 cm^{-3} and then peaked again at 534 cm^{-3} (Figure 6a). For the second and third fronts, the maximum nano-particle peak concentrations observed were 982 cm^{-3} and 1312 cm^{-3} respectively (Figure 6b). Peaks did not occur immediately after the frontal passage, and the enhancement period ranged from a few hours to over a day.

The increase in nano-particle concentrations observed in this study exceeds those of the 13 events observed during ACE 1 [Bates *et al*. 1998], for which the maximum concentration observed was 450 cm^{-3}. The most significant difference between the two studies is probably the time of year. The observations of Bates *et al*. [1998] were made in late spring-early summer whereas the present study was undertaken closer to the summer maximum in photochemical activity. Another difference is latitude of the sampling sites. Cape Grim is located at 41°S whereas the ship track covered latitudes between Cape Grim and Macquarie Island (54.5°S). Some differences in solar radiation and sea-surface temperature would be expected although previous observations Bigg *et al*. [1984] do not show a strong latitude gradient in CN concentration.

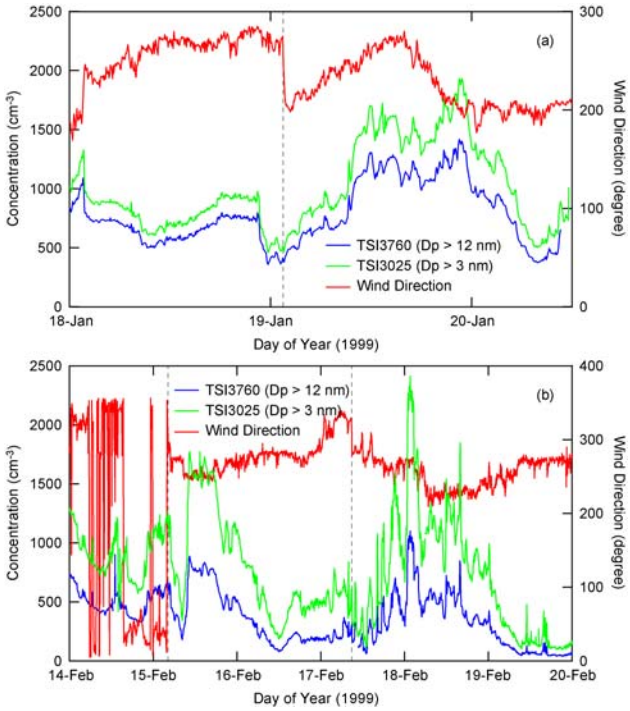

Figure 5. Five-minute mean particle concentrations and wind direction, showing enhancement in particle concentrations after the passage of a cold front for (a) 18 - 20 January 1999 and (b) 14 - 19 February 1999. The dashed lines indicate approximate time of frontal passage over Cape Grim.

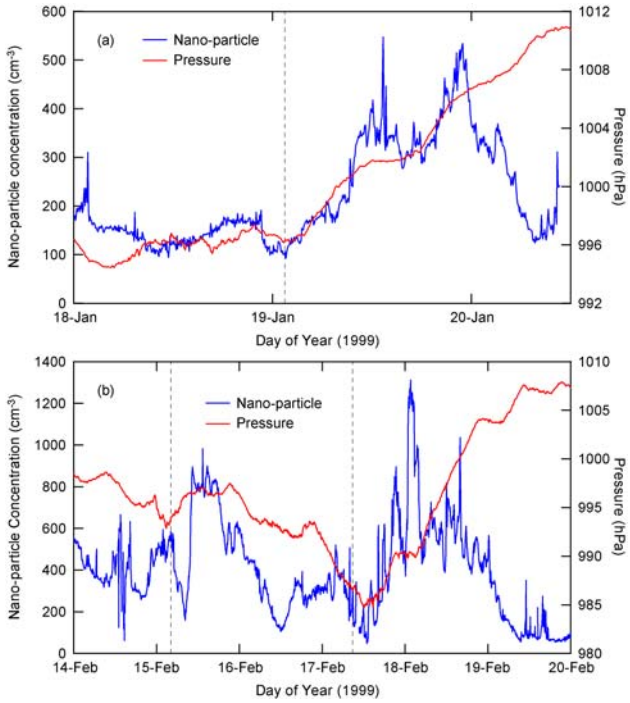

Figure 6. Five-minute mean nano-particle concentration and ambient pressure for (a) 18 - 20 January 1999 and (b) 14 - 19 February 1999. The dashed lines indicate approximate time of frontal passage over Cape Grim.

3.2.1. Further features of the SOAPEX-2 particle enhancement events

Bates *et al*. [1998] have attributed increases in nano-particle concentrations in this type of event to particle production in descending air masses that are typically associated with the high-pressure cell following cold fronts. Many aspects of the mechanisms that can give rise to such increases at ground level remain obscure, and detailed modelling of the three dimensional flow in the immediate post-frontal region in the Cape Grim region has not been undertaken. In this section we look briefly at a number of other parameters that give additional information relating to possible indicators of air mass during the SOAPEX-2 periods with enhanced particle concentrations. Back trajectories can be useful indicators of air mass origins. Trajectories were calculated using the Hybrid Single-Particle Lagrangian Integrated Trajectory model (HYSPLIT) [Draxler 1992] and Limited Area Prediction System (LAPS) [Puri *et al*. 1998] model, with analyses from the Australian Bureau of Meteorology [Tully and Downey 2003], for the periods with enhanced nano-particle concentrations. These trajectories are plotted in Figures 7-9, and show air mass location up to 96 hours prior to the indicated arrival time at Cape Grim, at approximately 100 m elevation. They confirm that the origin of the air arriving at Cape Grim was in the south-westerly stream well to the south of Australia for all three nano-particle events.

Radon concentrations during the three nano-particle enhancements also confirm a clean maritime origin, with concentrations around 50 mBq m^{-3} (Figures 10a and b). Methane and carbon monoxide concentrations during the enhancements were within the expected range for clean marine air being 1693 ppb and 45 ppb respectively. Subsidence of relatively dry, free tropospheric air into the marine boundary layer should be expected to result in some decrease in water vapour mixing ratio. In all three cases of nano-particle enhancement (Figures 11a and b) there was a clear association with air that was relatively drier than air sampled both before and after the period of enhancement. The decrease in water vapour mixing ratio was typically around 2-3 g kg^{-1} (Table 2), based on the difference between the immediate 3-hour post-frontal average and the average during the nano-particle enhancement period.

Although free tropospheric ozone concentrations are usually greater than at the surface, no consistent pattern is evident for ozone concentrations during the particle enhancements, as shown in Figures 11a and b. This is indicative of the complex chemical processes expected in mixing and descending air masses.

A summary of nano-particle peak characteristics, wind speed and decrease in water vapour mixing ratio during the maximum particle enhancement period is given in Table 2.

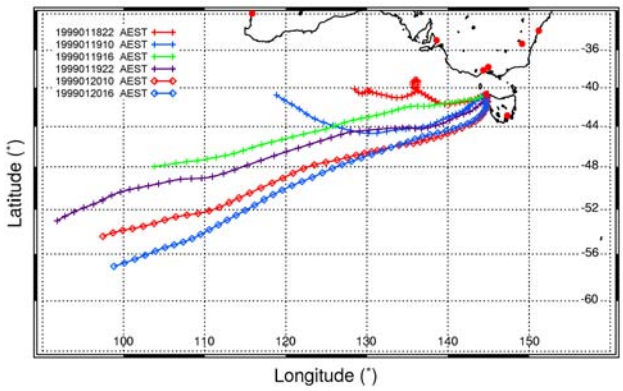

Figure 7. Back-trajectories for 18 - 21 January 1999, including pre- and post-frontal flows. The frontal passage occurred at about 0130 (AEST), 19 January. The legend shows arrival time for the trajectory at Cape Grim.

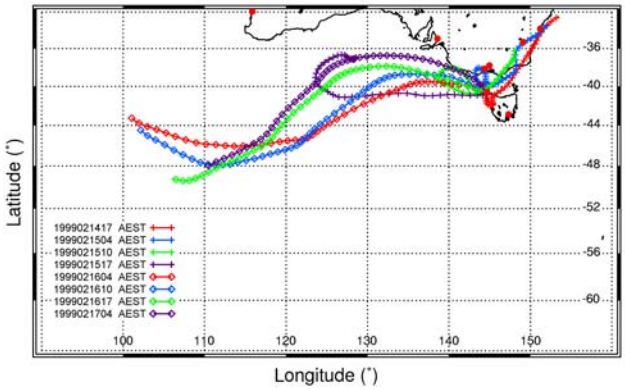

Figure 8. Back-trajectories for 14 - 16 February 1999, the frontal passage occurred at about 0415 (AEST) 15 February. The legend shows arrival time for the trajectory at Cape Grim.

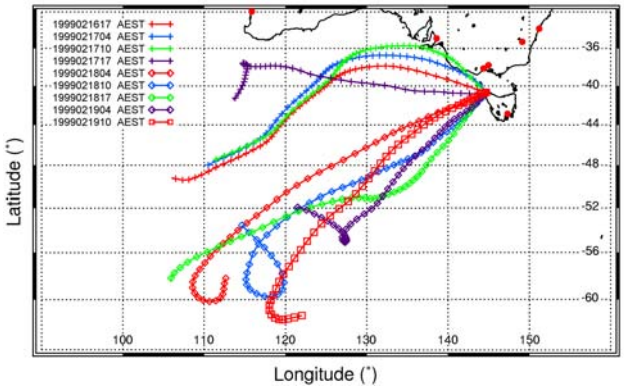

Figure 9. Back-trajectories for 16 - 19 February 1999, the frontal passage occurred at about 0900 (AEST) 17 February. The legend shows arrival time for the trajectory at Cape Grim.

Table 2. Summary of nano-particle peak characteristics showing concentration, duration of peak at the base and half-height, the time elapsed to reach peak concentration, wind speed at peak and decrease in water vapour mixing ratios following frontal passages.

Front #	*Concentration* (cm^{-3})	*Duration* Base (Hours)	Half	*Time Elapsed* (Hours)	*Wind Speed* ($m\ s^{-1}$)	*Water Vapour* ($g\ kg^{-1}$)
1	547	6	3	11.9	8.5	8.8-6.9
	534	8.3	4.2	21.5	11.1	8.8-6.2
2	982	24.8	12.4	9.2	11.0	11.4-8.1
3	1312	35.5	17.7	16.8	6.3	9.9-6.7

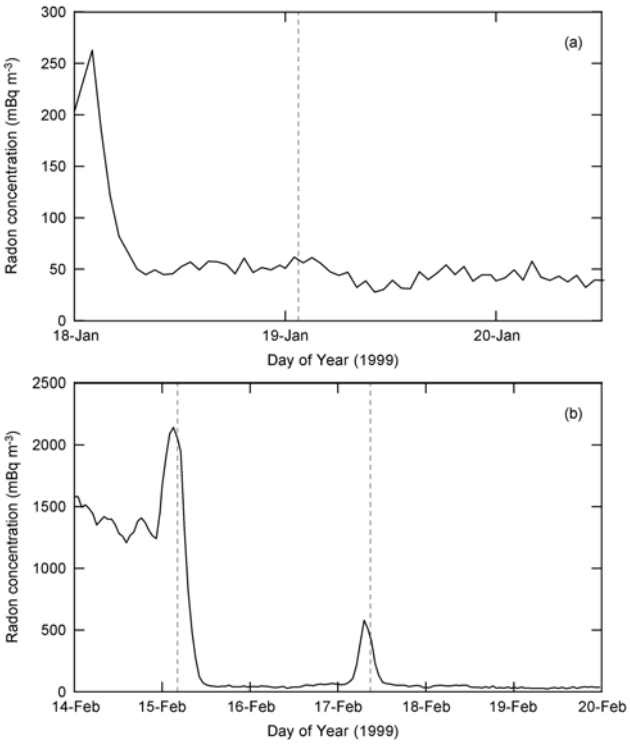

Figure 10. Radon concentration during pre- and post-frontal flows on (a) 18 - 20 January 1999 and (b) 14 - 20 February 1999, showing a baseline concentration well below 100 mBq m^{-3} for the post-frontal period during which elevation of nano-particle concentration was observed.

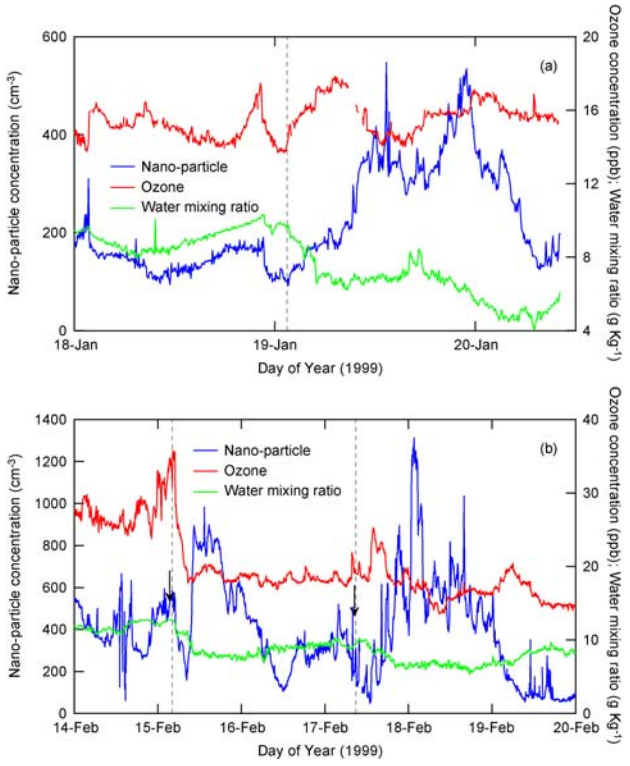

Figure 11. Nano-particle, ozone concentrations, and water vapour mixing ratio for pre- and post-frontal periods (a) 18 - 20 January 1999 and (b) 14 - 20 February 1999.

4. Discussion and summary

Nano-particle concentration at Cape Grim were examined, with a regional perspective, for the SOAPEX-2 study period of 17 January to 19 February 1999. Concentrations were determined for the size range of 3 – 12 nm (diameter) from the difference of concentrations measured with two CN counters, a TSI 3025 and a TSI 3760. Diurnal variation in nano-particle concentration was examined for three broad air mass origins, namely Tasmania, continental Australia and clean maritime (Baseline). Substantial differences were found in the diurnal pattern between these sectors with a clear daytime urban/industrial 'activity' in the Tasmanian sector. This had morning and afternoon concentration maxima as well as a less elevated increase throughout the daytime period. A diurnal pattern of weaker daytime contact with land was also suggested for this sector from the radon diurnal pattern and this may have influenced the nano-particle diurnal cycle. Land contact was less during the night. Unfortunately, during SOAPEX-2 there were very few occasions when a clearly continental airmass was observed. The diurnal pattern that was found for this sector had the appearance of an urban/industrial daytime activity pattern shifted by around 10 to 12 hours. Although this is consistent with the expected transit time of a continental airmass across Bass Strait, the diurnal cycle of radon concentrations shows an analogous form. This suggests that other explanations such as changes in atmospheric mixing or coupling to the surface are also likely to have been important in producing the particle diurnal pattern. Given the small number of samples for this sector these results must be considered as indicative only, and requiring further investigation. Within the clean maritime, or Baseline, sector a very weak diurnal pattern was evident and this showed a slight daytime enhancement of nano-particle concentration. This is consistent with some weak photochemical production.

The behaviour of nano-particle concentrations following frontal passages at Cape Grim was also investigated to extend the work of Bates *et al*. [1998]. Whilst the conditions during SOAPEX-2 were not highly favourable, with only three fronts and a much less than average frequency of clean maritime flow, nano-particle enhancements were observed following each of the three fronts in this period. Many of the properties of the enhancements were similar to those reported by Bates *et al*. [1998] although the magnitude in all cases was greater than those observed during ACE 1. During the periods of enhanced nano-particle concentration, which had a duration of up to 24 h the general picture was one of very clean maritime air with radon concentrations around 60 mBq m^{-3} and typical Baseline concentrations of methane (1693 ppb) and carbon monoxide (45 ppb). Water vapour mixing ratios were reduced during the periods when particle enhancement occurred, supporting the hypothesis that the enhancements are related to subsidence of free tropospheric air, whilst no clear relationship was evident with ozone concentration. The stronger enhancements in nano-particle concentrations during SOAPEX-2, compared with ACE 1 as reported by Bates *et al*. [1998], is con-

sistent with the relative seasonal photochemical activity. ACE 1 was conducted in late-spring early summer, whereas SOAPEX-2 was carried out in late summer when the overall photochemical sulfate production at this latitude is nearer its maximum.

Acknowledgements

The following investigators obtained trace species and meteorological data reported in this study as part of the Cape Grim Baseline Program. Their willingness to provide the data is highly appreciated. Carbon monoxide and methane: Paul Steele, Paul Krummel and Paul Fraser; Ozone: Ian Galbally and Mick Meyer; Radon: Stewart Whittlestone and Wlodek Zahorwski; Meteorological Data: Arthur Downey and Brian Weymouth; LAPS Backtrajectories: Arthur Downey. Special thanks to Paul Krummel who kindly provided IDL code for plotting the wind rose, and his useful comments and discussions on the manuscript.

References

Bates, T. S., V. N. Kapustin, P. K. Quinn, D. S. Covert, D. J. Coffman, C. Mari, P. A. Durkee, W. J. De Bruyn, and E.S. Saltzman, Processes controlling the distribution of aerosol particles in the lower marine boundary layer during the First Aerosol Characterisation Experiment, *J. Geophys. Res*., 103, 16,369-16,383, 1998.

Bigg E. K., J. L. Gras, and C. Evans, Origin of Aitken particles in remote regions of the Southern Hemisphere, *J. Atmos. Chem.*, 1, 203-214, 1984.

Draxler, R. R., 1992: Hybrid Single-particle lagrangian integrated trajectories (Hy-Split), Version 3.0 - User's guide and model description, NOAA Technical Memorandum, ERL ARL-195, Air Resources Laboratory, Silver Spring, Maryland, USA, 26 pp., 1992.

Gras, J. L., Calibration in the Cape Grim condensation nucleus particle program, in *Baseline Atmospheric Program (Australia) 1986*, edited by B. W. Forgan and P. J. Fraser, Department of Administrative Services, Bureau of Meteorology and CSIRO, Division of Atmospheric Research, Melbourne, Australia, 10-13, 1988

O' Dowd, C. D., M. Geever, M. K. Hill, M. H. Smith, and Gerard Jennings, S., New particle formation: Nucleation rates and spatial scales in the clean marine coastal environment, *Geophys. Res. Letts.*, 25, 1661-1664, 1998.

Puri, K., G. S. Dietachmayer, G. A. Mills, N. E. Davidson, R. A. Bowen, and L. W. Logan, The new BMRC Limited Area Prediction System, LAPS, *Aust. Met. Mag*., 47, 203-223, 1998.

Tully, M., and A., Downey, Back Trajectories to Cape Grim: investigating sources of error, in *Baseline Atmospheric Program (Australia) 1999-2000*, edited by N. W. Tindale, N. Derek, and P. J. Fraser, Bureau of Meteorology and CSIRO Atmospheric Research, Melbourne, Australia, 8-12, 2003.

Wiedensohler, A., D. Orsini, D. S. Covert, D. Coffmann, W. Cantrell, M. Havlicek, F.J. Brechtel, L.M. Russell, R. J. Weber, J. Gras, J. G. Hudson, and M. Litchy, Intercomparison study of size-dependent counting efficiency of 26 condensation particle counters, *Aerosol Sci. and Tech.*, 27, 224-242, 1997.

4. PROGRAM REPORTS

4.1. INTRODUCTION

The Program Reports section documents the status and preliminary results of the scientific experiments and measurements at Cape Grim during the years 1999 and 2000. There are essentially three types of measurement programs at Cape Grim.

The first and main group are the Cape Grim Programs which are long-term and provide the core measurements of compounds monitored in the atmosphere at Cape Grim. The Lead Scientists for these programs collectively form the Cape Grim 'Working Group', essentially the scientific steering committee, and are responsible for maintaining the continuity and quality of the core data from Cape Grim.

The second group of scientific programs are the short-term, more research orientated, studies labelled as 'Pilot Projects'. Generally these studies only last from one to three years and are designed to develop and test new sampling techniques and/or equipment, or for short-term intensive measurements of compounds that are difficult to measure routinely.

The final group of programs includes all the Collaborative Programs, primarily the longer-term international collaborations where samples and data are collected and shared with international colleagues. Some of these collaborative studies form part of global surveys and Cape Grim provides assistance and samples to outside researchers. Sometimes included in the collaborative program reports are the short-term intensive studies made by scientists and research students who are visiting Cape Grim to take advantage of the sampling facilities and support at the Cape Grim station.

Cape Grim reports

The Program, Pilot Project and Collaborative reports included in this edition of *Baseline* are categorised into four groupings:
General (including climatology and transport tracers, and the report on the Cape Grim database and data management)
Trace Gases (radiatively or chemically active gases)
Multi-phase (including precipitation, particles and multiphase studies and
Radiation (electromagnetic radiation monitoring).

Missing reports

A brief summary is included below of the Cape Grim and collaborative programs that have not submitted reports for 1999-2000, but were in operation during at least some of this period.

Isotopes in precipitation; Approximately 24 monthly 'continuous' samples were collected for analysis of oxygen isotopes, tritium and deuterium in rain water. The rain water samples are initially sent to ANSTO, with a subsample forwarded to the CSIRO-Division of Soils. The data ultimately end up archived at, and available from, the International Atomic Energy Agency (IAEA) in Vienna, Austria.

Other precipitation samples were collected from the manual rain gauge on a daily basis, and from the weekly ERNI 'Baseline' collector, for the University of Tasmania for isotope analysis.

Aerosol radionuclides; Weekly hi-volume aerosol filter samples are collected and counted for radionuclide radiation. Data are then directly transmitted by satellite to the Department of Energy (DOE), USA. Filters and data backups are sent approximately every month.

Elemental carbon; Weekly low-volume aerosol filters are collected and sent to the University of Stockholm, Sweden, for the analysis of particulate elemental carbon.

Lead Isotopes; Regular sampling for particulate Pb was conducted using a trace metal/particle clean sampler installed near the top of the Telstra tower. This work was part of a related program on regional Pb isotope ratios, based at Curtin University, Perth, WA and ceased in mid-2000.

4.2. DATA MANAGEMENT

R P Wheaton

Cape Grim Baseline Air Pollution Station, Bureau of Meteorology, Smithton, Tasmania 7330, Australia

Introduction

Data is collected at CGBAPS from 2 broad sources: the analog Data Acquisition System (DAS) and instrument control PC's. The DAS consists of a HP3497A 60-channel scanning DVM controlled over HP-IB interface by custom software on a HP9000/715 HP workstation ('Jacob'). The DAS samples voltages from each channel 10 times per minute and reduces these 10 raw readings to mean, max, min, standard deviation & first reading for each minute. The resulting data is stored in a daily binary-format file. All 60 channels are sampled although not all are in use at any given time.

Newer experiments at CGBAPS have tended to use a decentralised approach in which an instrument is controlled by a dedicated PC. The controlling PC typically accesses a central file server over the network to archive its data. Instrument control software and hardware are developed elsewhere by the responsible scientist. Due to the development being left to the individual a wide range of software and operating systems is in use at CGBAPS. Older instrument PC's communicate with the central server using PC-NFS or LANMAN network client software while newer machines use their built-in SMB clients to access our 'samba' service.

System Operation

The Data Acquisition System lost 1493 minutes in 1999 (a success rate of 99.71%) and 1261 minutes in 2000 (99.76%). Significant outages for the period were evenly divided between hardware and software issues. Grimco I (The HP1000's 'Alf' and 'Bet') suffered further hardware failures in January and was retired from active service. Grimco II ('Jacob') experienced a hard disk failure leading to loss of approximately 16 hours of data acquisition in January. A second disk drive showed signs of failure in May 1999 but was replaced with minimal loss of data. The disks were replaced un-

der maintenance agreement with the vendor. The failure of the station UPS with subsequent fire caused some loss of data during May 1999.

Due to persistent disk failures on Jacob, Grimco II was augmented with a new high-availability file server 'Mauka'. The new server is a Dell, PowerEdge 4300 with hot-swappable RAID-5 hard disk array and triple redundant power supply for enhanced reliability. This server entered service in September 1999 with various instrument PC's being redirected to it progressively throughout the remainder of the year. This server has fulfilled its promise of enhanced reliability having suffered no unscheduled downtime (apart from mains failures) despite the failure of a hard disk and power supply.

The CGBAPS ethernet network was expanded by the addition of 3 CISCO switches. These devices are capable of 100Mb/s operation as compared to the previous 10Mb/s HP Advancestack hubs.

Data collection for the particles program was enhanced by the installation of network connections to the Auto-Pollak PC 'Blizzard' and the auto-CCN PC 'Katabat'. Data from these PC's are now automatically archived nightly without staff intervention. All of the particles PC's were successfully migrated to the new file server ('Mauka') with only minor changes required to their operating software. Some problems with the UCN PC 'Eps' being unable to access its network drive were traced to network configuration issues. Because the operation of Eps is now vital to the baseline switch determination a scheme was devised to attempt to restart the software in the (rare) event of it stopping.

A CD writer was purchased and a program of regularly archiving data to CD-ROM was commenced. Raw program data for archive are, in the first instance, stored on MOD at the station before being mirrored to a server in Smithton overnight. When sufficient quantity of such data has accumulated, they are recorded onto a CD-ROM and removed from online storage. All files on CD are recorded in a searchable online database for future retrieval.

Extensive effort went into ensuring that all computer systems were ‘Year 2000 compliant’. This involved testing all systems, applying software upgrades as appropriate and reviewing all locally-produced code. Despite our best endeavours minor issues were experienced with the ‘Hurd1’, Liquid Water Radiometer & Pb sampling PCs. These were all fixed or had workarounds running within the first few days of the new year.

The Oracle RDBMS host 'Virazon' was upgraded with an additional 256Mb of main memory to increase performance as usage of the Cape Grim database increased. A new PC 'lambda' was integrated into the CGBAPS network as part of the LoFlo CO_2 analyser. This machine is largely administered remotely from CSIRO-AR in Aspendale, but some routines were developed locally to make data available on our website, archive it and forward it to Aspendale automatically. Grimco II was further expanded with the commissioning, in October 2000, of 'Pampero' (Intel-based PC) as our new webserver, assuming most of the functions performed previously by the HP workstation 'Wilhelm'. 'Wilhelm' is to be retained as a backup for the DAS host 'Jacob' as they are identical machines.

Data Processing

Software for hourly results processing was developed for Grimco II. The former, yearly, binary file format was discontinued in favour of a daily, human-readable structure at the beginning of 1999. Copies of the daily results file are routinely disseminated to CSIRO-AR which has reduced the number of data requests from CSIRO researchers having to be handled by CGBAPS staff. The hourly results are also automatically entered into the Cape Grim Database, currently held in an Oracle RDBMS on a server in Smithton.

The monthly processing of aethelometer data was ported to Grimco II in June 1999. Ad-hoc processing of the Hi-Vol data was also ported to Grimco II in June 1999. The ‘baseline switch’ determination was changed to use the 30-m wind direction whilst the 50-m sensor was unserviceable between 11 May 1999 and 7 June 1999. The source of particles data for baseline determination was changed from the TSI3020 counter (connected to DAS channels 19 and 20) to the TSI3025 counter (controlled by 'Eps') on the 28 January 1999. Some disruption of the flow of back-trajectory data occurred late in 2000 when the Bureau migrated to a new supercomputer. The missing data were subsequently replaced with the assistance of Mat Tully (BoM).

Software Development

The Cape Grim web pages were finally placed on the Bureau's external web server for public access on 20 January 2000 after many months of design and revision. At this stage the publicly-accessible pages only give a general overview of CGBAPS role and programs. The Cape Grim internal website (accessible from within the Bureau, and by external users who have permitted access) was considerably enhanced with additions of back trajectories, hourly results, raw minute data, additional flask forms and station logs etc.

The DAS raw minute extraction software was enhanced with an interface to the ‘bad channels’ database and improved usage of the channel voltage limits stored in ‘chanJ’ parameter files: this means that raw minute voltages are now correctly converted using the applicable conversion factors for the time rather than current values, and flagged as ‘bad’ or ‘out-of-range’ where appropriate.

4.3. RADON AND RADON DAUGHTERS

S Whittlestone[1,2]

[1]University of Wollongong, NSW 2522, Australia in 1999

[2]Australian Nuclear Science and Technology Organisation, Menai, NSW 2234, Australia in 2000

[Supported by CGBAPS research funds.]

Radon

The newer Huge Radon Detector (HURD-2) has been rigorously tested, and shown to be much more stable than the original HURD. Data in the Cape Grim database are now taken from HURD-2, except during maintenance periods, when HURD data are used. In 1999 and 2000 a total of 20 hours data were lost, a data recovery rate of 99.9%.

This good performance is largely due to having two instruments. With HURD becoming progressively harder to maintain, installation of a replacement has become a matter of urgency.

The standard deviation of calibrations of HURD-2 over 4 days was 2%, compared to 15% for HURD. The difference is attributed to the effect of sun and wind creating temperature gradients in the tanks, which lead to increased turbulence and loss of radon decay products to the walls.

The major error in low-level measurements with HURD-2 is from instrumental background. This was determined by techniques involving comparison with HURD, study of the decay of activity when the flow is stopped, and a new test initiated by W. Zahorowsky in which radon-free air was introduced into the instrument. The latter technique was technically demanding, but eventually a set of results was generated from which it was possible to evaluate the equivalent radon concentrations of five components of the background: Internal emissions of Rn-222 are less than 2 mBq m^{-3}; and Rn-220 (thoron) are 19.7 mBq m^{-3}; Thoron intake via the inlet mast is negligible; Pb-210 accumulation on the wire screen is about 10 mBq m^{-3} per year and a steady background from the scintillator and electronics is 15.4 mBq m^{-3}. The statistical error in the background is 3 mBq m^{-3}. More data are required to determine if this is a realistic total error.

The need for a new detector head was established in *Baseline 97-98*. A major re-design was spurred by the retirement of a skilled technician, without whom the design current in 1999 was impracticable. The result was simpler, cheaper, more efficient and serviceable in the field by a technician with good general mechanical skills by no specialist training. Components for four units to be run in parallel in HURD-2 were purchased and assembled in early 2000. Relatively minor technical effort is required for installation in HURD-2, although trials are needed to determine the optimum number of units.

Tests with the new head show that HURD-2 would achieve a sensitivity of 0.98, compared to its present value of 0.59 counts s^{-1} per Bq m^{-3}. In addition, the instrument would be much less sensitive to changes in the high voltage to the photomultiplier, with an anticipated improvement from 1.4% per volt to 0.21% per volt. These improvements would significantly improve the quality of data sets for study of the baseline atmosphere.

Tables 1 and 2 show monthly summaries of radon. The results are similar to those of previous years, although at 20%, the proportion of samples in the baseline wind sector close enough to land to acquire more than 100 mBq m^{-3} of radon was lower than the 30% seen previously.

Table 1. Monthly means (mBq m^{-3}) of radon concentration in 1999. The baseline criterion is wind speed > 2 m s^{-1}, wind direction between 190 and 280°. The wind was required to persist in the sector for at least two hours. Rn is the average radon concentration in mBq m^{-3}.

Month	*Non-baseline Rn*	*Baseline*					
		All CN			*CN<=600*		
		Rn	*hours*	*hours Rn>100*	*Rn*	*hours*	*hours Rn>100*
Jan	418	133	126	43	57	55	7
Feb	565	126	123	24	40	54	4
Mar	934	149	287	73	104	175	49
Apr	576	162	267	67	50	219	31
May	1575	81	87	14	71	68	8
Jun	1588	166	175	82	160	172	79
Jul	2064	130	224	36	87	220	32
Aug	1397	107	335	57	99	333	55
Sep	994	196	223	56	131	194	39
Oct	693	74	262	60	53	188	32
Nov	222	53	255	25	31	172	6
Dec	721	72	291	24	32	190	8

Table 2. Monthly means (mBq m^{-3}) of radon concentration in 2000. The baseline criterion is wind speed > 2 m s^{-1}, wind direction between 190 and 280°. The wind was required to persist in the sector for at least two hours. Rn is the average radon concentration in mBq m^{-3}.

Month	*Non-baseline Rn*	*Baseline*					
		All CN			*CN<=600*		
		Rn	*hours*	*hours Rn>100*	*Rn*	*hours*	*hours Rn>100*
Jan	298	107	200	40	93	134	22
Feb	907	312	201	87	201	51	28
Mar	761	177	278	49	57	177	15
Apr	1377	113	207	26	43	163	6
May	1094	183	288	29	42	285	26
Jun	1418	85	298	56	66	280	42
Jul	972	181	172	57	89	160	45
Aug	1028	352	245	83	61	196	35
Sep	409	60	259	27	57	167	15
Oct	878	96	349	38	54	180	21
Nov	400	151	145	47	172	58	22
Dec	444	42	478	30	19	65	8

Again, the CN 600 cm^{-3} baseline criterion was ineffective in winter, and too severe in summer when used to select samples influenced by land.

Radon and thoron daughter measurements

Radon and thoron daughter measurements, suspended in December 1997 because of filter transport problems, were not made in 1999-2000. It has been decided that a major re-design is needed, and progress will depend on availability of funds and technical effort.

4.4. METEOROLOGY/CLIMATOLOGY 1999/2000

A Downey and M Tully

Bureau of Meteorology
Melbourne, Victoria 3001, Australia

[Supported by CGBAPS research funds]

Introduction

Tables 1 to 11 present a summary of the Cape Grim meteorological conditions for 1999 and Tables 12 to 22 for 2000.

Tables 1 - 4 and 12 - 14 contain monthly mean values for 0000, 0300, 0600, 0900, 1200, 1500, 1800, 2100 (AEST). These are computed using, for example, the mean of hours 2, 3 and 4 to represent 0300.

In Tables 5 and 16, 'extreme max' is the highest of all of minute means for the month. 'Mean daily max' is the mean of the daily maxima for the month. Similarly for 'mean daily min' and 'extreme min'.

Tables 6 and 17 show the monthly and annual rainfall in millimetres.

Tables 7 and 18 are derived from month-to-date and year-to-date counts of the number of minutes during which the 'baseline switch' was on. Baseline conditions are said to exist if wind direction is between 190° and 280° and the count of condensation nuclei is less than 600 cm^{-3}.

Tables 8 - 11 and 19 - 22 are derived from the hourly mean vector wind speed and direction from the 10-m and 50-m levels.

Figures 1 to 12 are derived from (raw) minute data. The monthly means presented are the mean of every minute that month. The mean monthly maxima and minima are the means of the daily maxima and minima for that month.

Overview of 1999

In summer the circulation is typically dominated by a weak circulation pattern associated with the migration of high pressure systems from west to east along the subtropical ridge and so it was in January 1999. In February a high pressure system over the Tasman was directing a north-easterly flow over the state leading to both wetter and warmer conditions than normal. During March and April the subtropical ridge was still a major influence though increasing frontal passages led to more reliable rain and below normal temperatures. By June a trend of being under the continued influence of high pressure systems was leading to warmer than normal conditions. This continued in August with high pressure systems centred over southern Australia, bringing warmer and drier conditions to much of Tasmania. In September high pressure systems in the vicinity once again made things warmer and drier than normal. There were also reports in northern Tasmania, of dust falling in rain. This appears to have been caused by strong northerly winds and convection over Victoria. There was below average rainfall over much of the State with many places in the east reporting the lowest monthly rainfall totals on record. October was mild with above average temperatures caused by the slow passage of systems and consequent north-westerly winds. Reversing the trend of previous months, November was cooler due to the frequent passage of frontal systems embedded in a predominantly south- westerly flow. By December Tasmania was, as is seasonally usual, under the influence of high pressure systems.

Temperature: In February both Marrawah and Wynyard airport recorded their highest mean daily minimum temperatures (14.4°C and 13.6°C). In August, high temperature returned with record high mean daily maximum temperatures at Scottsdale (14.2°C), Wynyard (14.1°C) and highest daily maximum at Marrawah (18.3°C). In September Scottsdale recorded its highest mean daily temperature for the month (16.1°C). October saw a number of records in the northwest of the state. With a highest mean daily maximum of 17.7°C and a highest mean daily minimum of 9.2°C at Marrawah and highest daily minimum at Scottsdale (13.7°C) and Marrawah (15.0°C).

Humidity: Tables 2 and 3 show the mean relative and mean absolute humidity respectively in 1999. These show that, apart from May, June, July and August, which had elevated average humidity, the levels were close to normal.

Pressure: Table 4 and Figure 2 show monthly average pressures during 1999 and show that pressures during autumn were a little below normal and were a little above normal after June with July and August having the only significant departures.

Rainfall: Table 6 shows rainfall at the station during 1999. The 686.4 mm recorded is well below the 20 year 806.2 mm average and it is the third year in a row with a substantial rainfall deficit. This is in line with a rainfall deficit over much of south-eastern Australia.

Baseline time: Table 7 shows Baseline time during 1999. This peaked in August (a spring peak is more usual) and was, on average, below normal (the long term average is about 32%) and compares with an average Baseline time of 31.8% in 1998.

Wind: Tables 8 and 9 show the wind speed and direction at the 10-m level during 1999. They show a peak frequency in the winds from the south-westerly direction and a peak frequency of high speeds during December. There is also a smaller peak in the northeasterly to easterly quadrant. This can be seen in Figures 3 and 4, which show the frequency distribution at 10 and 50-m respectively for 1999. Figures 5 and 6 show the monthly means of daily maxima, means and minima one-minute wind speeds at both heights for 1999.

Table 1. Monthly mean dry bulb temperature (°C) for 1999

Hour	*Jan*	*Feb*	*Mar*	*Apr*	*May*	*Jun*	*Jul*	*Aug*	*Sep*	*Oct*	*Nov*	*Dec*	*1999*
0000	14.6	15.7	14.4	12.1	12.4	10.7	10.3	10.2	10.7	11.1	11.0	13.3	12.2
0300	14.3	15.9	14.3	12.0	12.3	10.4	10.1	10.2	10.4	11.0	10.9	13.0	12.0
0600	14.9	16.2	14.7	11.9	12.3	10.3	9.9	10.0	10.4	11.5	11.7	13.6	12.3
0900	17.1	17.8	16.0	13.4	12.9	11.0	10.6	11.0	11.9	13.2	13.6	15.3	13.6
1200	18.1	18.6	16.9	14.7	13.5	12.2	11.6	11.9	12.9	13.9	14.3	16.1	14.5
1500	17.7	18.5	16.5	14.2	13.2	11.7	11.4	11.4	12.4	13.5	13.7	15.8	14.1
1800	16.3	17.0	15.1	12.8	12.4	10.9	10.7	10.6	11.2	12.1	12.4	14.6	13.0
2100	15.2	16.1	14.6	12.3	12.4	10.8	10.4	10.3	10.8	11.5	11.4	13.4	12.4
Mean	16.0	17.0	15.3	12.9	12.7	11.0	10.6	10.7	11.4	12.2	12.4	14.4	13.0

Table 2. Monthly mean relative humidity (%) for 1999.

Hour	*Jan*	*Feb*	*Mar*	*Apr*	*May*	*Jun*	*Jul*	*Aug*	*Sep*	*Oct*	*Nov*	*Dec*	*1999*
0000	84.3	86.1	79.0	78.4	88.0	82.8	84.7	85.1	80.5	83.7	83.0	81.5	83.1
0300	84.5	87.2	79.4	77.3	88.4	85.8	85.1	87.1	82.7	86.2	81.8	81.7	83.9
0600	82.0	86.2	79.2	77.5	89.4	85.8	86.5	89.0	84.6	84.1	79.0	78.7	83.5
0900	75.6	80.1	74.4	73.9	86.7	82.5	83.7	84.1	79.7	77.7	72.2	72.8	78.6
1200	71.9	77.0	70.6	69.8	84.1	77.3	81.3	80.2	74.3	74.3	70.7	71.0	75.2
1500	73.2	76.4	71.1	72.1	83.3	79.2	81.9	82.4	75.1	74.1	71.7	72.6	76.1
1800	79.0	81.6	77.7	76.1	86.1	81.9	85.0	86.4	79.8	80.6	76.7	77.1	80.7
2100	83.2	84.4	78.8	78.1	86.6	81.9	85.7	86.0	81.0	81.9	82.2	81.5	82.6
Mean	79.2	82.4	76.3	75.4	86.5	82.1	84.2	85.0	79.7	80.3	77.2	77.1	80.4

Table 3. Monthly mean absolute humidity (g m^{-3}) for 1999.

Hour	*Jan*	*Feb*	*Mar*	*Apr*	*May*	*Jun*	*Jul*	*Aug*	*Sep*	*Oct*	*Nov*	*Dec*	*1999*
0000	10.7	11.8	10.0	8.5	9.7	8.2	8.1	8.2	8.0	8.5	8.4	9.5	9.1
0300	10.5	12.0	10.0	8.3	9.7	8.4	8.1	8.3	8.1	8.6	8.3	9.5	9.1
0600	10.6	12.1	10.2	8.3	9.7	8.3	8.1	8.4	8.3	8.8	8.4	9.4	9.2
0900	11.1	12.3	10.3	8.7	9.8	8.4	8.2	8.5	8.5	9.0	8.6	9.6	9.4
1200	11.2	12.4	10.3	8.9	9.9	8.4	8.5	8.6	8.5	9.0	8.8	9.8	9.5
1500	11.1	12.2	10.2	8.9	9.6	8.4	8.4	8.5	8.3	8.7	8.6	9.9	9.4
1800	11.1	12.0	10.3	8.6	9.5	8.2	8.4	8.5	8.1	8.6	8.5	9.7	9.3
2100	10.9	11.8	10.1	8.6	9.5	8.2	8.3	8.3	8.1	8.5	8.6	9.6	9.2
Mean	10.9	12.1	10.2	8.6	9.7	8.3	8.3	8.4	8.3	8.7	8.5	9.6	9.3

Table 4. Monthly mean barometric pressure (hPa) for 1999.

Hour	*Jan*	*Feb*	*Mar*	*Apr*	*May*	*Jun*	*Jul*	*Aug*	*Sep*	*Oct*	*Nov*	*Dec*	*1999*
0000	1003.1	1003.8	1004.9	1011.8	1006.2	1009.0	1009.4	1010.2	1006.8	1005.3	1005.7	1003.5	1006.6
0300	1002.2	1003.1	1004.1	1011.1	1005.8	1008.6	1008.8	1009.6	1006.3	1004.3	1005.1	1002.8	1006.0
0600	1003.0	1003.8	1004.8	1011.6	1006.1	1008.7	1009.2	1010.0	1005.9	1004.9	1005.9	1003.6	1006.5
0900	1003.6	1004.5	1005.7	1012.5	1007.0	1009.6	1010.0	1010.9	1006.8	1005.5	1006.5	1004.1	1007.2
1200	1003.5	1004.1	1005.4	1011.9	1006.2	1008.9	1009.1	1010.3	1006.2	1004.9	1006.0	1003.7	1006.7
1500	1002.9	1003.4	1004.6	1011.2	1005.8	1008.3	1008.5	1009.5	1005.7	1004.1	1005.4	1003.0	1006.0
1800	1002.9	1003.4	1004.8	1011.7	1006.1	1008.9	1009.1	1010.0	1006.3	1004.6	1005.7	1003.1	1006.4
2100	1003.6	1004.3	1005.6	1012.2	1006.5	1009.3	1009.8	1010.6	1006.8	1005.5	1006.3	1003.9	1007.0
Mean	1003.1	1003.8	1005.0	1011.7	1006.2	1008.9	1009.2	1010.1	1006.3	1004.9	1005.8	1003.5	1006.6

Table 5. Monthly temperature data (°C) 1999.

	Jan	*Feb*	*Mar*	*Apr*	*May*	*Jun*	*Jul*	*Aug*	*Sep*	*Oct*	*Nov*	*Dec*
Extreme max	23.0	24.0	22.4	26.5	26.8	22.6	14.9	26.1	18.6	19.4	19.8	25.6
Mean daily max	19.4	19.9	18.2	16.4	15.9	13.6	12.6	13.6	14.3	15.1	15.3	17.6
Mean daily min	12.9	14.0	12.7	10.5	10.9	8.1	8.6	8.8	8.8	9.5	9.5	11.5
Extreme min	10.8	9.9	8.5	5.0	4.1	-1.2	4.7	5.0	5.3	5.3	6.6	8.5

Table 6. Monthly rainfall (mm) 1999.

	Jan	*Feb*	*Mar*	*Apr*	*May*	*Jun*	*Jul*	*Aug*	*Sep*	*Oct*	*Nov*	*Dec*	*Total*
1999	13.8	86.2	50.6	18.0	117.6	61.8	63.0	84.6	35.2	68.6	45.8	41.2	686.4

Table 7. Monthly baseline time (%) 1999.

	Jan	*Feb*	*Mar*	*Apr*	*May*	*Jun*	*Jul*	*Aug*	*Sep*	*Oct*	*Nov*	*Dec*	*Mean*
1999	5.8	6.8	16.5	21.0	19.4	24.9	28.3	42.4	25.0	23.1	21.0	24.0	21.6

10-m vector wind summary for 1999 (%)

Table 8. Speed (km hr^{-1}), Range [a,b) meaning less than b and equal to or greater than a (%), 1999.

Range	*Jan*	*Feb*	*Mar*	*Apr*	*May*	*Jun*	*Jul*	*Aug*	*Sep*	*Oct*	*Nov*	*Dec*	*1999*
[0 - 10)	8.7	4.8	4.0	4.7	3.1	2.6	4.6	5.2	5.8	4.8	2.6	2.6	4.5
[10 - 20)	15.0	18.5	20.2	19.2	28.4	18.3	16.8	18.5	25.6	20.0	12.1	8.6	18.4
[20 - 30)	18.8	12.1	23.9	31.8	27.2	34.4	23.8	22.7	21.5	23.1	24.2	16.1	23.4
[30 - 40)	18.1	19.0	19.5	25.3	19.6	22.4	21.5	33.3	20.3	22.8	20.1	21.2	22.0
[40 - 50)	21.4	17.8	18.4	12.1	12.6	16.0	18.4	14.0	15.7	18.3	23.1	25.3	17.8
[50 - 60)	14.2	17.2	9.4	4.0	6.9	3.2	6.9	4.6	7.5	9.3	11.4	16.0	9.2
[60 - 70)	3.4	7.8	2.3	2.2	2.0	2.1	5.5	1.6	1.9	0.9	6.5	5.9	3.5
[70 -)	0.3	3.0	2.3	0.7	0.3	1.0	2.4	0.0	1.7	0.7	0.0	4.3	1.4

Table 9. Direction (°), Range [a,b) meaning less than b and equal to or greater than a (%), 1999.

Range	*Jan*	*Feb*	*Mar*	*Apr*	*May*	*Jun*	*Jul*	*Aug*	*Sep*	*Oct*	*Nov*	*Dec*	*1999*
[0 - 45)	0.7	3.7	7.5	4.6	14.5	21.1	11.5	14.1	17.5	7.1	1.7	2.0	8.9
[45 - 90)	21.0	14.5	13.3	10.1	12.0	11.1	11.6	10.3	15.8	23.9	22.4	11.0	14.8
[90 - 135)	28.9	34.3	8.9	7.1	4.0	6.0	19.8	4.0	7.6	8.5	15.3	16.4	13.2
[135 - 180)	5.7	2.5	6.6	9.9	0.5	7.6	3.1	2.4	2.6	2.4	5.8	4.6	4.5
[180 - 225)	32.9	16.1	20.8	30.3	3.4	12.6	8.0	22.3	15.6	16.9	22.4	33.7	19.6
[225 - 270)	8.9	15.4	25.5	25.6	19.1	16.5	20.2	25.7	18.2	18.4	16.7	23.4	19.5
[270 - 315)	1.6	8.2	11.6	8.9	23.8	13.3	16.2	12.9	12.2	20.0	14.7	7.9	12.7
[315 - 360)	0.3	5.2	5.8	3.6	22.7	11.7	9.6	8.2	10.4	2.7	1.1	0.9	6.9

50-m vector wind summary for 1999 (%)

Table 10. Wind speed (km hr^{-1}), Range [a,b) meaning less than b and equal to or greater than a (%), 1999.

Range	*Jan*	*Feb*	*Mar*	*Apr*	*May*	*Jun*	*Jul*	*Aug*	*Sep*	*Oct*	*Nov*	*Dec*	*1999*
[0 - 10)	7.8	5.1	3.0	4.9	2.8	3.8	4.6	5.2	5.0	4.1	2.5	2.0	4.3
[10 - 20)	21.7	27.5	19.7	20.0	26.6	15.3	21.3	14.5	22.9	15.6	13.0	15.3	19.0
[20 - 30)	29.5	23.3	17.0	30.8	30.2	24.4	16.4	25.0	20.4	24.1	27.7	20.0	24.6
[30 - 40)	19.9	21.8	23.0	27.3	17.1	22.3	22.2	34.1	23.6	26.1	23.9	19.1	23.8
[40 - 50)	12.3	10.3	15.9	11.3	19.4	18.7	15.7	11.0	14.0	20.3	19.7	23.7	15.9
[50 - 60)	7.3	7.2	7.4	4.2	2.8	12.3	10.0	7.3	8.0	7.3	11.3	12.2	8.4
[60 - 70)	1.5	3.3	2.9	1.4	1.2	3.3	7.9	2.4	3.4	2.0	2.0	5.6	3.2
[70)	0.0	1.5	1.1	0.1	0.0	0.0	1.9	0.4	2.7	0.4	0.0	2.0	0.9

Table 11. Wind direction (°), Range [a,b) meaning less than b and equal to or greater than a (%), 1999.

Range	*Jan*	*Feb*	*Mar*	*Apr*	*May*	*Jun*	*Jul*	*Aug*	*Sep*	*Oct*	*Nov*	*Dec*	*1999*
[0 - 45)	1.1	3.9	7.0	3.7	16.3	25.0	13.4	13.1	17.6	7.3	1.7	1.7	8.8
[45 - 90)	38.1	41.4	20.5	13.2	6.3	8.8	17.1	12.2	18.5	26.8	32.7	19.9	22.2
[90 - 135)	12.3	7.5	2.3	4.4	0.8	3.0	11.2	0.8	3.6	4.5	5.0	7.1	5.5
[135 - 180)	11.7	6.9	7.9	12.1	1.6	11.5	4.5	7.3	4.5	4.1	8.8	13.4	8.2
[180 - 225)	29.9	17.8	29.2	37.8	5.2	11.2	12.9	28.7	17.6	18.5	23.6	32.8	23.2
[225 - 270)	4.4	10.6	19.3	17.3	29.0	18.2	17.6	20.7	16.4	21.1	17.2	17.3	16.8
[270 - 315)	1.9	6.9	7.5	7.0	22.6	7.7	12.5	7.3	10.3	14.8	9.9	6.2	8.8
[315 - 360)	0.5	5.1	6.2	4.5	18.3	14.6	10.8	10.0	11.5	2.9	1.1	1.5	6.5

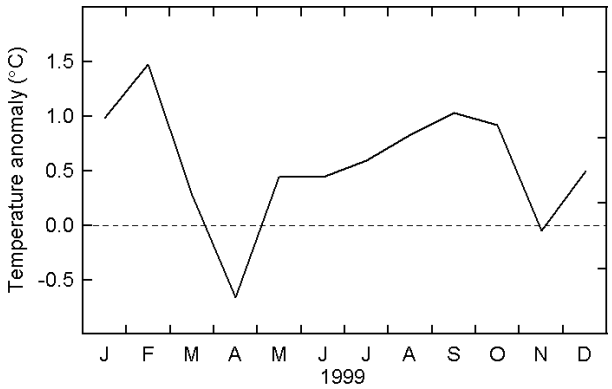

Figure 1. Monthly mean temperature anomaly during 1999 (1999 temperatures – long term [1987-98] means).

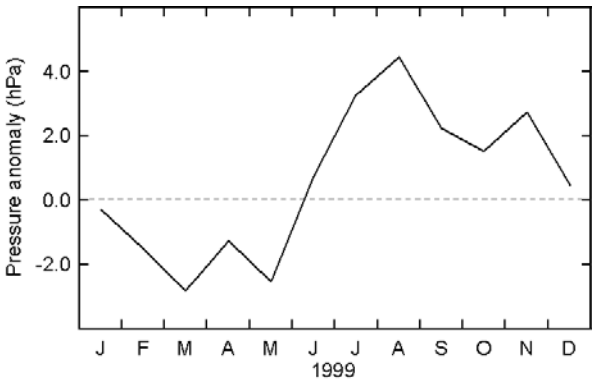

Figure 2. Mean monthly barometric pressure anomaly for 1999. (1999 temperatures – long term [1987-98] means).

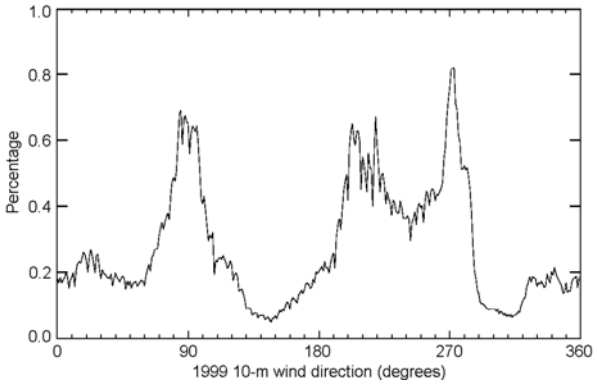

Figure 3. Frequency distribution of the 10-m wind for 1999.

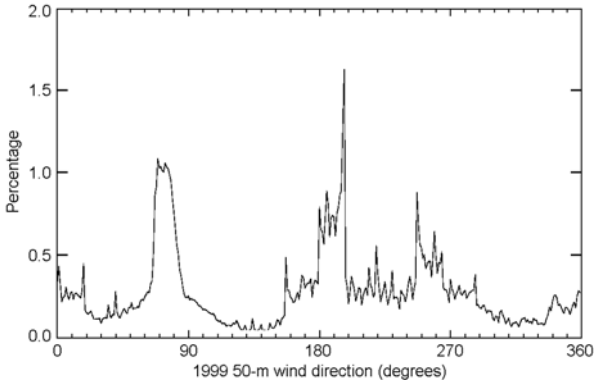

Figure 4. Frequency distribution of the 50-m wind for 1999.

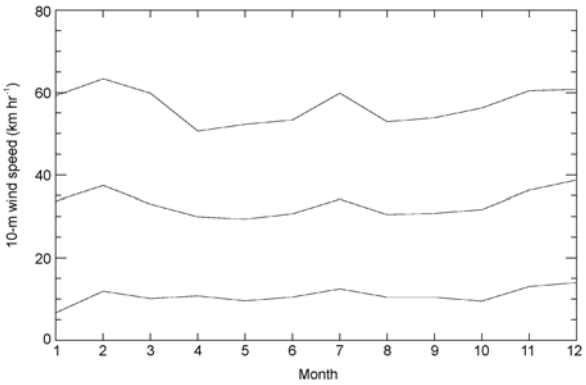

Figure 5. Monthly average wind speeds for 1999 at the 10-m level. Top line is mean maximum, middle is mean and bottom line is mean minimum.

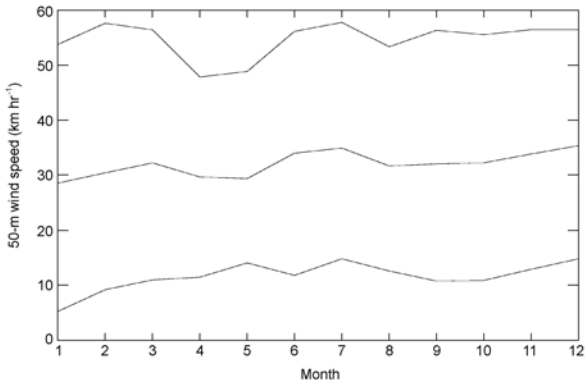

Figure 6. Monthly average wind speeds for 1999 at the 50-m level. Top line is mean maximum, middle is mean and bottom line is mean minimum.

Overview of 2000

In January 2000 well developed southerlies, caused by high pressure systems in the Bight and to the south of the State, led to lower than normal temperatures. In February, once again because of northerly and north-easterly flow, temperatures were elevated over most of the state though rainfall remained near normal. In March flow patterns returned to average with weak cold fronts embedded in a westerly flow leading to near normal temperatures. High pressure systems returned to dominate in April, bringing warmer days and cooler nights. On the 16 April there were severe storms on the north coast with some houses unroofed at Ulverstone (180 km or so to the east of Cape Grim). In May the state was under the influence of a westerly wind regime and there were gales at times over much of the state. In June, the warmer than average conditions returned with the state under the influence of persistent high pressure systems. On 12 and 16 July Tasmania experienced two powerful cold fronts that brought storm force winds and snow. On 26 July, snow falls cut many roads and several schools were closed. In August conditions returned to normal with the passage of cold fronts embedded in the westerlies and this continued in September where there were 15 cold front passages. October was wetter and warmer than normal though, under the influence of some very clear skies, there were some devastating frosts on the morning of the 17 October which cost the stone fruit industry many millions of dollars. There was an unseasonable shift southwards of the subtropical ridge in November. This reduced the incidence of westerly winds and meant temperatures were well above normal. Thirty sites with long-term (greater than 10 years) records had record high mean daily minimum temperatures and nearly half of those had also record high mean daily maximum temperatures. In December the state was buffeted with high winds in the week around Christmas and there was snow in the highlands.

Temperature: In January Marrawah had a record lowest daily maximum of 13.4°C. In February the hotter than usual conditions returned and Scottsdale reported both a record highest monthly mean (26.2°C) and highest mean minimum (13.3°C). Things remained fairly normal until 7 October when Marrawah recorded its lowest October temperature on record (1.5°C). In November temperatures returned to be above normal and many sites across Tasmania reported records. On the northwest coast these included Marrawah, with a record high mean maximum temperature for the month of 19.3°C and a highest mean minimum of 11.5°C. Scottsdale reported a highest mean minimum temperature of 11.4°C.

Humidity: Tables 13 and 14 show the mean relative and mean absolute humidity respectively in 2000. These show that the first 4 months were drier than normal, reverting near normal with a tendency for slightly drier than normal conditions in the second half of the year.

Pressure: Table 15 and Figure 8 show monthly average pressures during 2000 and show that pressures were near normal for most of the year with May and September having significant negative departures.
Rainfall: Table 17 shows rainfall at the station during 2000. The 712.2 mm recorded is higher than the values for the last three years but is still significantly lower than the 20-year average and it is the fourth year in a row with a substantial rainfall deficit.
Baseline time: Table 18 shows Baseline time during 2000. This peaked in winter but was, on average, below normal.
Wind regime: Tables 19 and 20 show the wind speed and direction at the 10-m level during 2000. Once again, they show a peak frequency in the winds from the south-westerly direction and a peak frequency of high speeds during December, though this time not as pronounced. As seen in 1999, there is also a smaller peak in the north-easterly to easterly quadrant. This can be seen in Figures 9 and 10, which show the frequency distribution at 10 and 50-m respectively for 2000. Figures 11 and 12 show the monthly means of daily maxima, means and minima one-minute wind speeds at both heights for 1999 and 2000.

Acknowledgement

The authors would like to thank Laurie Porter and Randall Wheaton and other Cape Grim staff for their dedicated efforts in maintaining instrumentation and records.

Table 12. Monthly mean dry bulb temperature (°C) for 2000.

Hour	*Jan*	*Feb*	*Mar*	*Apr*	*May*	*Jun*	*Jul*	*Aug*	*Sep*	*Oct*	*Nov*	*Dec*	*2000*
0000	14.4	16.4	14.9	13.4	12.3	11.0	10.1	9.8	10.6	10.7	13.7	13.9	12.6
0300	14.1	16.2	14.5	13.2	12.2	10.8	10.1	9.7	10.4	10.4	13.5	13.6	12.4
0600	14.6	16.4	14.6	13.2	12.1	10.7	9.9	9.5	10.4	10.7	14.3	14.3	12.5
0900	16.5	18.4	16.9	15.1	12.9	11.5	10.5	10.8	11.5	11.9	16.2	16.1	14.0
1200	17.2	19.8	18.5	16.2	13.7	12.3	11.5	12.0	12.3	12.7	21.0	17.0	15.3
1500	17.1	19.3	17.7	15.7	13.3	11.9	11.3	11.6	11.8	12.4	16.5	16.6	14.6
1800	15.7	17.6	16.0	14.2	12.5	11.2	10.6	10.2	11.2	11.2	15.1	15.0	13.4
2100	14.8	16.6	15.0	13.8	12.3	11.1	10.3	10.0	10.8	10.9	14.0	14.0	12.8
Mean	15.5	17.6	16.0	14.4	12.7	11.3	10.5	10.5	11.1	11.4	15.5	15.1	13.5

Table 13. Monthly mean relative humidity (%) for 2000.

Hour	*Jan*	*Feb*	*Mar*	*Apr*	*May*	*Jun*	*Jul*	*Aug*	*Sep*	*Oct*	*Nov*	*Dec*	*2000*
0000	79.1	78.7	75.3	76.3	77.1	82.0	82.0	81.0	77.7	81.3	86.1	75.1	79.3
0300	78.8	82.0	76.4	77.8	77.9	82.5	81.3	80.4	77.9	83.8	87.8	75.7	80.2
0600	77.7	81.6	76.6	79.4	77.6	82.3	81.2	81.3	78.0	83.4	84.5	73.9	79.8
0900	72.1	72.0	70.5	72.5	74.9	78.2	79.8	78.1	75.5	78.0	77.9	66.9	74.7
1200	69.1	64.8	63.9	67.4	71.7	76.3	76.7	74.2	73.4	73.8	75.6	63.7	70.9
1500	69.6	65.8	67.6	69.7	73.4	78.3	77.3	74.8	76.2	74.5	76.5	65.1	72.4
1800	74.9	73.1	73.9	75.0	77.2	81.4	80.6	81.0	78.2	78.9	81.3	69.7	77.1
2100	78.9	77.8	76.1	74.9	77.6	80.9	81.8	81.0	78.8	80.4	85.0	73.9	78.9
Mean	75.0	74.5	72.5	74.1	75.9	80.3	80.1	78.9	76.9	79.3	81.8	70.4	76.6

Table 14. Monthly mean absolute humidity (g m^{-3}) for 2000.

Hour	*Jan*	*Feb*	*Mar*	*Apr*	*May*	*Jun*	*Jul*	*Aug*	*Sep*	*Oct*	*Nov*	*Dec*	*2000*
0000	9.9	11.2	9.8	9.1	8.5	8.3	7.8	7.6	7.7	8.1	10.3	9.1	8.9
0300	9.7	11.5	9.7	9.1	8.5	8.2	7.8	7.5	7.6	8.2	10.3	9.1	8.9
0600	9.9	11.6	9.8	9.3	8.5	8.1	7.7	7.5	7.6	8.3	10.4	9.3	9.0
0900	10.2	11.5	10.3	9.5	8.6	8.1	7.8	7.8	7.9	8.4	10.8	9.4	9.2
1200	10.3	11.3	10.3	9.5	8.6	8.4	8.0	8.0	8.0	8.3	11.0	9.4	9.2
1500	10.2	11.1	10.3	9.5	8.6	8.4	7.9	7.9	8.0	8.2	10.9	9.3	9.2
1800	10.2	11.1	10.2	9.3	8.6	8.3	7.9	7.7	8.0	8.1	10.6	9.1	9.1
2100	10.2	11.2	9.9	9.0	8.6	8.2	7.9	7.7	7.8	8.1	10.3	9.1	9.0
Mean	10.1	11.3	10.0	9.3	8.6	8.2	7.9	7.7	7.8	8.2	10.6	9.2	9.1

Table 15. Monthly mean barometric pressure (hPa) for 2000.

Hour	*Jan*	*Feb*	*Mar*	*Apr*	*May*	*Jun*	*Jul*	*Aug*	*Sep*	*Oct*	*Nov*	*Dec*	*2000*
0000	1003.7	1005.7	1006.9	1009.5	1005.4	1008.4	1003.7	1002.9	998.8	1001.9	1005.4	1000.4	1004.4
0300	1002.9	1004.8	1006.3	1008.9	1004.9	1008.1	1003.2	1002.5	998.2	1000.9	1004.8	999.4	1003.7
0600	1003.7	1005.6	1006.9	1009.5	1005.3	1008.4	1003.5	1003.2	998.5	1001.3	1005.4	1000.3	1004.3
0900	1004.3	1006.6	1007.7	1010.3	1006.2	1009.3	1004.3	1003.9	999.0	1002.2	1005.9	1001.0	1005.1
1200	1004.0	1006.4	1007.2	1009.6	1005.4	1008.5	1003.8	1003.3	998.4	1001.9	1005.5	1000.9	1004.6
1500	1003.4	1005.7	1006.3	1008.8	1004.8	1007.7	1003.2	1002.5	997.8	1001.6	1004.8	1000.5	1003.9
1800	1003.5	1005.6	1006.6	1009.3	1005.3	1008.2	1003.6	1003.0	998.3	1002.3	1005.1	1000.9	1004.3
2100	1004.3	1006.3	1007.3	1009.8	1005.7	1008.7	1004.1	1002.9	998.9	1002.8	1005.9	1001.4	1004.8
Mean	1003.7	1005.8	1006.9	1009.5	1005.4	1008.4	1003.7	1003.0	998.5	1001.9	1005.4	1000.6	1004.4

Table 16. Monthly temperature data (°C) 2000.

	Jan	*Feb*	*Mar*	*Apr*	*May*	*Jun*	*Jul*	*Aug*	*Sep*	*Oct*	*Nov*	*Dec*
Extreme max	22.8	26.3	28.1	20.9	28.5	15.2	15.1	16.2	21.3	18.2	21.8	22.7
Mean daily max	18.4	21.3	19.9	17.4	15.3	13.3	12.6	13.1	13.6	13.9	18.1	18.2
Mean daily min	13.0	14.6	12.9	11.7	10.5	9.4	8.4	8.2	8.7	8.8	12.7	12.4
Extreme min	8.0	8.6	9.7	8.3	4.0	6.8	3.8	4.6	5.1	4.3	8.5	7.7

Table 17. Monthly rainfall (mm) 2000.

	Jan	*Feb*	*Mar*	*Apr*	*May*	*Jun*	*Jul*	*Aug*	*Sep*	*Oct*	*Nov*	*Dec*	*Total*
2000	37.2	47.2	32.0	57.4	81.0	71.8	124.8	77.2	69.8	58.0	27.2	28.6	712.2

Table 18. Monthly baseline time (%) 2000.

	Jan	*Feb*	*Mar*	*Apr*	*May*	*Jun*	*Jul*	*Aug*	*Sep*	*Oct*	*Nov*	*Dec*	*Mean*
2000	17.2	6.4	20.9	21.7	36.2	38.1	22.1	25.6	16.5	20.5	7.6	7.3	20.1

10-m vector wind summary for 2000 (%)

Table 19. Speed (km hr^{-1}), Range [a,b) meaning less than b and equal to or greater than a (%), 2000.

Range	*Jan*	*Feb*	*Mar*	*Apr*	*May*	*Jun*	*Jul*	*Aug*	*Sep*	*Oct*	*Nov*	*Dec*	*2000*
[0 - 10)	1.2	4.7	5.8	2.4	3.1	3.9	5.8	10.5	2.6	3.2	6.7	3.7	4.5
[10 - 20)	7.9	12.8	19.8	22.2	13.8	16.8	16.0	24.6	12.9	11.3	16.2	15.1	15.8
[20 - 30)	15.2	18.2	22.2	26.2	18.5	26.7	25.9	30.1	21.1	15.6	18.7	20.6	21.6
[30 - 40)	19.1	28.9	20.3	27.2	16.8	24.3	23.8	17.8	18.8	22.4	24.8	24.4	22.3
[40 - 50)	18.7	20.4	16.9	13.2	16.8	13.2	16.9	7.5	14.0	23.4	22.6	18.4	16.8
[50 - 60)	21.0	8.2	11.6	6.0	14.4	10.6	9.4	3.1	15.4	15.2	10.4	12.0	11.5
[60 - 70)	12.5	5.0	2.8	2.8	9.9	3.5	1.9	2.7	11.8	6.9	0.7	4.0	5.4
[70)	4.4	1.7	0.7	0.0	6.6	1.1	0.3	3.7	3.3	1.9	0.0	1.8	2.1

Table 20. Direction (°), Range [a,b) meaning less than b and equal to or greater than a (%), 2000.

Range	*Jan*	*Feb*	*Mar*	*Apr*	*May*	*Jun*	*Jul*	*Aug*	*Sep*	*Oct*	*Nov*	*Dec*	*2000*
[0 - 45)	0.5	2.2	3.2	11.5	6.6	15.1	9.9	9.4	9.6	6.9	2.5	3.3	6.7
[45 - 90)	19.5	28.4	17.3	15.3	2.8	2.8	13.2	16.7	3.5	6.2	20.5	7.5	12.8
[90 - 135)	21.4	23.3	17.1	6.9	4.0	1.0	7.4	12.7	12.8	13.1	33.3	4.0	13.0
[135 - 180)	5.6	4.6	8.1	8.2	3.2	4.3	9.3	7.6	1.2	1.0	3.9	2.0	4.9
[180 - 225)	35.8	23.3	14.9	19.3	17.3	19.3	18.1	7.9	1.9	17.6	27.7	17.1	18.4
[225 - 270)	10.8	12.6	26.1	18.2	25.9	23.1	13.0	25.4	16.4	28.4	7.5	42.8	20.9
[270 - 315)	5.5	4.5	11.8	15.1	29.3	20.7	13.6	11.7	45.1	20.6	3.3	20.7	16.9
[315 - 360)	0.9	1.1	1.5	5.4	10.8	13.8	15.5	8.6	9.4	6.2	1.3	2.6	6.4

50-m vector wind summary for 2000 (%)

Table 21. Speed (km hr^{-1}), Range [a,b) meaning less than b and equal to or greater than a (%), 2000.

Range	*Jan*	*Feb*	*Mar*	*Apr*	*May*	*Jun*	*Jul*	*Aug*	*Sep*	*Oct*	*Nov*	*Dec*	*2000*
[0 - 10)	2.2	6.0	9.1	2.8	2.8	4.2	8.5	10.1	2.5	3.5	7.7	2.9	5.2
[10 - 20)	13.2	20.4	19.2	16.2	9.9	12.3	12.9	25.2	10.3	16.0	28.3	15.0	16.5
[20 - 30)	18.8	22.6	24.1	30.6	17.3	24.5	17.1	24.1	17.4	16.5	24.1	24.4	21.8
[30 - 40)	23.8	24.7	21.6	22.2	15.6	21.8	22.5	19.3	19.6	19.1	22.2	24.6	21.4
[40 - 50)	18.0	18.0	14.7	17.1	17.3	18.0	19.8	10.8	13.5	17.0	13.6	18.6	16.4
[50 - 60)	12.5	6.5	7.8	8.2	18.0	14.4	12.8	4.4	18.8	18.3	3.9	8.8	11.2
[60 - 70)	8.6	1.7	3.2	2.5	13.7	4.0	5.7	3.8	11.7	9.0	0.3	3.8	5.7
[70)	3.0	0.0	0.3	0.4	5.2	0.8	0.8	2.3	6.1	0.7	0.0	1.9	1.8

Table 22. Direction (°), Range [a,b) meaning less than b and equal to or greater than a (%), 2000.

Range	*Jan*	*Feb*	*Mar*	*Apr*	*May*	*Jun*	*Jul*	*Aug*	*Sep*	*Oct*	*Nov*	*Dec*	*2000*
[0 - 45)	0.8	2.3	3.0	12.1	7.7	15.2	10.0	9.8	9.5	5.9	3.1	2.9	6.8
[45 - 90)	36.3	47.2	29.5	17.8	2.8	1.4	15.6	19.7	8.6	16.5	39.0	10.5	20.3
[90 - 135)	5.2	4.2	5.5	3.3	2.7	0.4	4.0	8.9	6.8	2.6	15.4	0.7	5.0
[135 - 180)	14.9	7.8	10.1	12.8	6.6	7.8	14.3	7.8	2.4	3.2	8.5	4.4	8.4
[180 - 225)	32.7	26.0	18.5	20.3	21.6	21.3	17.5	16.4	1.5	22.3	27.8	28.7	21.2
[225 - 270)	5.6	7.8	21.2	14.3	14.2	23.8	10.2	18.7	29.5	29.7	1.8	40.2	18.1
[270 - 315)	3.4	3.9	10.4	13.2	32.3	15.8	11.7	8.5	31.6	12.7	3.1	9.6	13.0
[315 - 360)	1.1	0.9	1.8	6.2	12.1	14.2	16.7	10.1	10.0	7.1	1.3	3.0	7.1

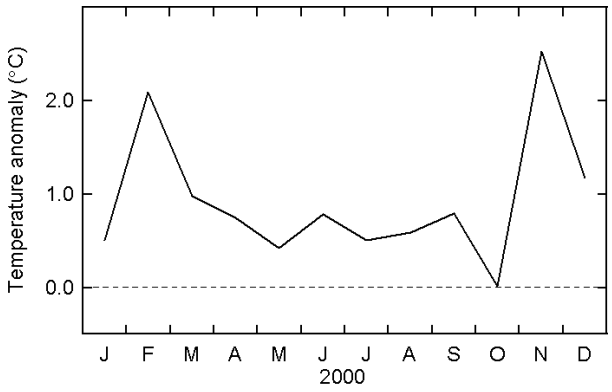

Figure 7. Monthly mean temperature anomaly during 2000 (2000 temperatures – long-term [1987-99] means).

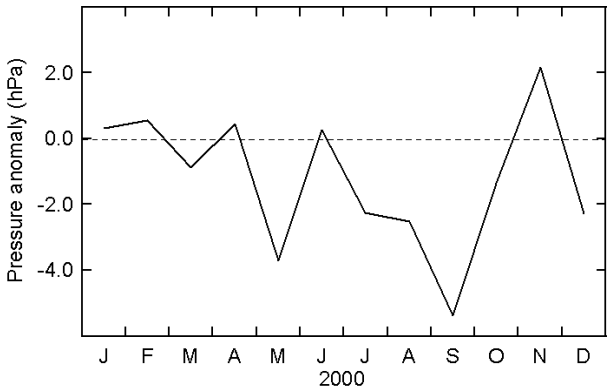

Figure 8. Mean monthly barometric pressure anomaly for 2000 (2000 temperatures – long-term [1987-99] means).

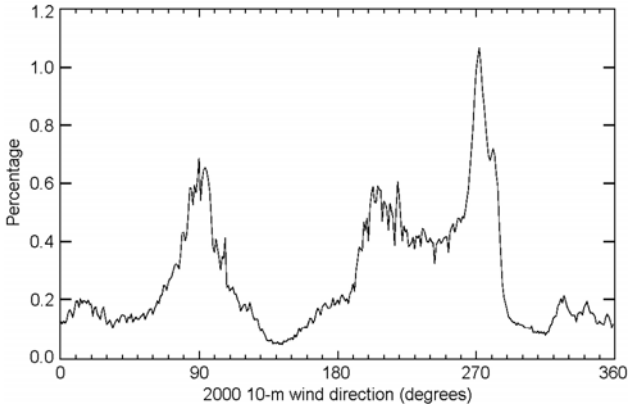

Figure 9. Frequency distribution of the 10-m wind for 2000.

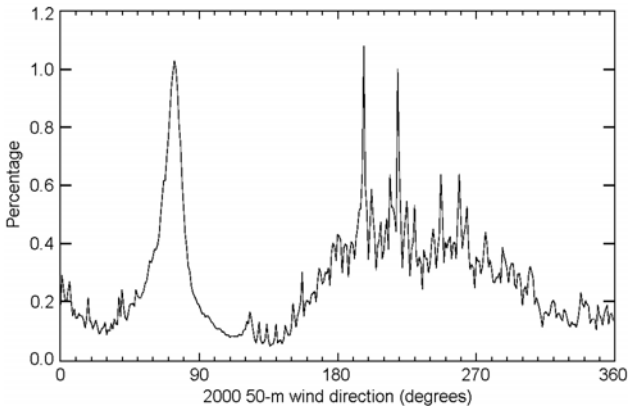

Figure 10. Frequency distribution of the 50-m wind for 2000.

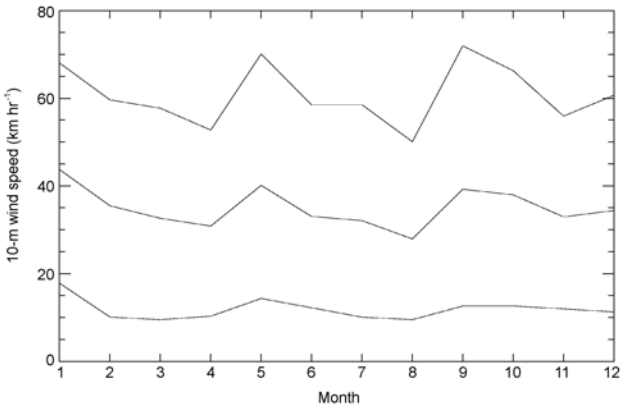

Figure 11. Monthly average wind speeds for 2000 at the 10-m level. Top line is mean maximum, middle is mean and bottom line is mean minimum.

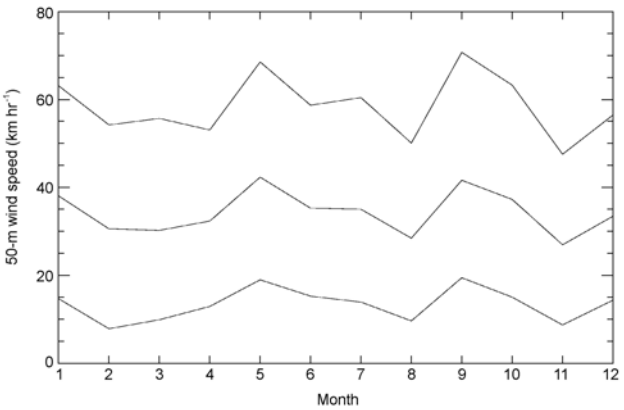

Figure 12. Monthly average wind speeds for 2000 at the 50-m level. Top line is mean maximum, middle is mean and bottom line is mean minimum.

4.5. $\delta^{13}C$ AND $\delta^{18}O$ OF CO_2 IN BASELINE CAPE GRIM AIR: 1999-2000

C E Allison, L N Cooper and R J Francey

CSIRO Atmospheric Research,
Aspendale, Victoria 3195, Australia

[Supported by CGBAPS research funds.]

CSIRO Atmospheric Research (CAR) operates two programs at Cape Grim to measure the isotopic composition of atmospheric carbon dioxide (CO_2). The *in situ* program (CIA), where CO_2 is extracted from baseline air at Cape Grim and sent to CAR for stable isotope (^{13}C and ^{18}O) analysis, has been operating since 1977 [Allison *et al.* 1994; Francey *et al.* 1995]. The flask sampling program (CGA), where samples of air are collected in 5.0 or 0.5 litre glass flasks and returned to CAR for analysis as part of the global flask network operated by CAR, has been in operation since 1991 (although collection of 5.0 litre flasks ceased in August 1998). Both programs sample air from the 70-m intake. Results from these two programs for 1999 and 2000 are summarised here and data from both programs is available through the Cape Grim data archive.

Baseline Selection

The criteria used to select baseline air have been in use since the beginning of the stable isotope sampling programs. These criteria are (1) that air originates from the marine sector, 190° to 280°, (2) that the '*in situ*' CO_2 concentration is steady, variation <0.2 ppm hr^{-1}, and (3) that the condensation nuclei (CN) count is less than 600 cm^{-3}. Our use of this fixed CN limit to indicate air of continental origin has persisted to maintain consistent records even though the marked seasonal cycle in CN, with median concentrations of around 100 cm^{-3} in winter and 700 cm^{-3} in summer [e.g. Gras 1995], as well as significant inter-annual variation, clearly indicates that using a fixed CN level is less than ideal. We have previously failed to detect a difference in $\delta^{13}C$ values in summer when criteria (1) and (2) are met but (3) is marginally exceeded. With the establishment at Cape Grim of a supplementary baseline criterion, and Baseline Switch, that is based on the previous five year's CN data for the current month selected for a 50-m level wind direction between 190º and 280º, we have revised the CN count requirement for the stable isotope program. The CN threshold, above which samples are considered to be non-baseline, is based on the 90th percentile of CN hourly medians for this period interpolated using cubic splines to give daily values. Collected samples that fail the new CN threshold test are retained but identified as high CN samples. This revised CN criteria will be used in the future for selecting baseline air. The application of the revised criteria to previously published data will be reported in a future publication.

In situ Program (CIA)

There were no serious disruptions to sampling recorded in the logbook.

Eighty-one samples were collected and analysed: CGIS (Cape Grim *in situ*) #899 through #979, with an average sampling interval of 10 ± 8 days. Nine of these samples were collected from a high-pressure cylinder of air (see below: Air Standard) and two samples were collected under non-baseline conditions (wind direction not in the sector between 190° and 280° [Francey and Goodman, 1985]) leaving 70 samples characteristic of marine air. Of these, two were collected under marginal baseline conditions. Four samples exceeded the CN rejection criteria based on the 90th percentile.

The *in situ* $\delta^{13}C$ record is presented in Figure 1 and a summary of the collection and storage details is presented in Table 1. The samples that failed the CN threshold test are plotted separately. Rejected, non-baseline, samples are not plotted.

The storage time for CIA samples, 34 ± 34 days, was longer than expected due to two failures on the inlet system on the MAT252 mass spectrometer at CAR in 1999. No CIA samples were analysed from January to May, and from August to November. This problem did not affect the CGA flask program.

Table1. Average collection details and storage times for the CIA and CGA samples.

	CIA	*CGA*
No. of retained samples	70	183
Average sampling frequency (days)	10 ± 8	8 ± 5
Average storage time prior to analysis	34 ± 34	41 ± 35
Average wind direction (°N)	249 ± 22	243 ± 34
Average wind speed (m s^{-1})	11 ± 4	12 ± 4
No. of samples with CN above 90th percentile	4	5

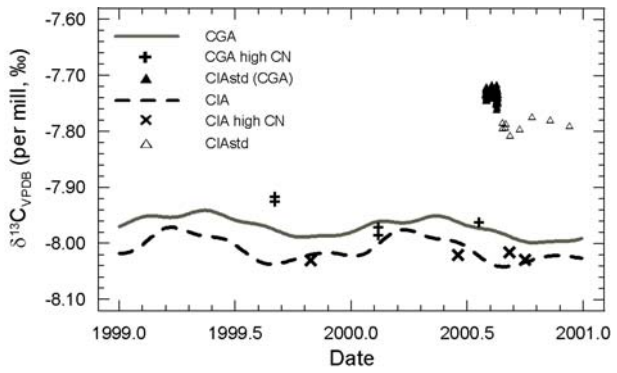

Figure 1. Smoothed fit to the 1999-2000 Cape Grim $\delta^{13}C$ records for CIA (dashed black line) and CGA (solid grey line). Samples collected when CN exceeded the 90th percentile threshold are indicated as ✕ for CIA and ✚ for CGA. The analyses of the air standard used at Cape Grim are represented by △ for the CO_2 extracted at Cape Grim and analysed at CSIRO GASLAB and by ▲ for CO_2 samples both extracted and analysed at GASLAB.

Flask Program (CGA)

Three hundred and fifty-four CGA samples were collected. Of these, one hundred and sixty-four were collected for use in other programs. Of the one hundred and ninety collected for the stable isotope program, five were not analysed and two were rejected due to poor analysis. The one hundred and eighty-three retained samples were collected at an average sampling interval of 8 ± 5 days. Of these, thirteen were collected un-

der marginal baseline conditions and four were collected under non-baseline conditions (wind direction). Of the one hundred and seventy-nine samples not rejected (marginal baseline samples were retained), five had CN counts greater than the 90th percentile threshold for the collection day. A smoothed curve has been fitted to the $\delta^{13}C$ of the 174 retained CGA samples using the fitting routines of Thoning et al. [1989]. This is presented in Figure 1. Samples collected under conditions of high CN are plotted separately. The four rejected non-baseline samples are not plotted. The collection and storage details for all CGA samples are presented in Table 1.

While not affected by the inlet system failure of the MAT252 mass spectrometer, the CGA flask storage time of 41 ± 35 days was longer than desired due to some CGA flasks being used for storage tests prior to analysis.

Comparison of the $\delta^{13}C$ records

A bias of about 0.1 ‰ between the two $\delta^{13}C$ records that was first observed in 1998 persists [Allison *et al.* 2001]. This is discussed below (CIA Air Standard).

$\delta^{18}O$ data

The $\delta^{18}O$ of the CO_2 is also measured for all samples collected in the CIA and CGA programs. The $\delta^{18}O$ results for the CIA and CGA samples have not been previously reported due to some problems in resolving calibration issues that have affected the $\delta^{18}O$ measurements but not the $\delta^{13}C$ measurements. These calibration issues have been largely resolved and the $\delta^{18}O$ results for samples collected during 1998-2000 are plotted in Figure 2. Data were selected using the same criteria as used for the $\delta^{13}C$. There is a small difference between the CIA and CGA records similar to that observed for $\delta^{13}C$. The complete Cape Grim $\delta^{18}O$ records will be presented in a future Research Report.

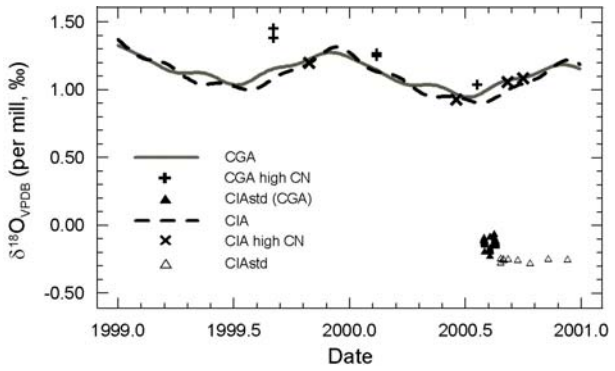

Figure 2. Smoothed fit to the 1999-2000 Cape Grim $\delta^{18}O$ records for CIA (dashed black line) and CGA (solid grey line). Samples collected when CN exceeded the 90th percentile threshold are indicated as ✕ for CIA and ✚ for CGA. The analyses of the air standard used at Cape Grim are represented by △ for the CO_2 extracted at Cape Grim and analysed at CSIRO GASLAB and by ▲ for CO_2 samples both extracted and analysed at GASLAB.

CIA Air Standard

In order to investigate the observed difference between the CIA and CGA records, a cylinder of air was prepared at CSIRO GASLAB. The CO_2 and N_2O concentration of air in this cylinder were measured, and the $\delta^{13}C$ and $\delta^{18}O$ of the CO_2 were measured with the Aspendale extraction line. In August 2000 the cylinder was sent to Cape Grim and connected to the *in situ* extraction line where CO_2 was extracted using the same protocols used to extract CIA samples (flow rate, trapping time, etc). Results for the analysis of this cylinder both at CSIRO GASLAB and through the Cape Grim *in situ* extraction line are presented in Figures 1 and 2.

The observed difference between the CIA and CGA records for both $\delta^{13}C$ and $\delta^{18}O$ is observed in the analyses of the air standard. The cause of this difference must be either the assignment of the isotopic composition of a reference gas or a bias introduced by the different extraction lines. Further analysis of the air standard at Cape Grim and at CSIRO GASLAB are required before conclusions can be made. Details of these analyses will be the subject of a future Research Report.

CO_2 and N_2O concentration

The concentrations (mixing ratios) of both CO_2 and nitrous oxide (N_2O) are used to correct for mass spectrometric interference from N_2O that is co-trapped with the CO_2 [Francey and Goodman 1988]. The CO_2 and N_2O concentrations of all CGA samples are measured at GASLAB [Langenfelds *et al.* 2003] while for CIA samples the average CO_2 concentration during the CO_2 trap is obtained from the *in situ* CO_2 program [Steele *et al*, 1999] and N_2O concentration is obtained using an interpolation procedure described previously [Allison *et al.* 2001]. If no CO_2 concentration data are available for either an *in situ* or flask sample, the CO_2 concentration is estimated by interpolation from a fitted equation (comprising a quadratic and four harmonic functions [Thoning *et al.* 1989]) to the 0.5 litre flask data over the period 1992 through 2000.

Acknowledgements

We would like to thank the Cape Grim staff for their expertise in maintaining both the CIA and CGA programs over many years. We specially thank Laurie Porter for his assistance in installing the air standard in August 2000. We also thank John Gras for helpful comments on the baseline selection criteria.

References

Allison, C. E., L. N. Cooper, and R. J. Francey, $\delta^{13}C$ of CO_2 in baseline Cape Grim air: 1997-98, *Baseline Atmospheric Program (Australia) 1996,* edited by N. W. Tindale, N. Derek, and R. J. Francey, Bureau of Meteorology and CSIRO Atmospheric Research, Melbourne, 67-69, 2001.

Allison, C. E., R. J. Francey, R. L. Langenfelds, and E. D. Welch, Comparison of high precision Cape Grim CO_2 isotope measurements using two mass spectrometers, in *Baseline Atmospheric Program (Australia) 1991,* edited by A. L. Dick and J. L. Gras, Bureau of Meteorology and CSIRO, Division of Atmospheric Research, Melbourne, 10-19, 1994.

Francey, R. J. and H. S. Goodman, Systematic error in, and selection of, *in situ* $\delta^{13}C$, in *Baseline Atmospheric Program (Australia) 1983-1984*, edited by R. J. Francey and B. W. Forgan, Bureau of Meteorology and CSIRO, Division of Atmospheric Research, Melbourne, Australia, 27-36, 1985.

Francey, R. J. and H. S. Goodman, The DAR stable isotope reference scale for CO_2, in *Baseline Atmospheric Program (Australia) 1986*, edited by B. W. Forgan and P. J. Fraser, Bureau of Meteorology and CSIRO, Division of Atmospheric Research, Melbourne, Australia, 40-46, 1988.

Francey, R. J., C. E. Allison and E. D. Welch, The 11-year high precision *in situ* CO_2 stable isotope record from Cape Grim, 1982-1992, in *Baseline Atmospheric Program (Australia) 1992*, edited by A. L. Dick and P. J. Fraser, Bureau of Meteorology and CSIRO, Division of Atmospheric Research, Melbourne, Australia, 16-25, 1995.

Gras, J. L. CN, CCN and particle size in Southern Ocean air at Cape Grim, *Atmos. Res*., 35, 233-251, 1995.

Langenfelds, R. L., L. P. Steele, L. N. Cooper, D. A. Spencer, P. B. Krummel and B. L. Dunse, Atmospheric methane, carbon dioxide, hydrogen, carbon monoxide and nitrous oxide from Cape Grim flask air samples analysed by gas chromatography, in *Baseline Atmospheric Program (Australia) 1999-2000*, edited by N. W. Tindale, N. Derek, and P. J. Fraser, Bureau of Meteorology and CSIRO Atmospheric Research, Melbourne, Australia, 76-77, 2003.

Steele, L. P., D. J. Beardsmore, G. A. Da Costa and G. I. Pearman, Baseline carbon dioxide monitoring, in *Baseline Atmospheric Program (Australia) 1996,* edited by J. L. Gras, N. Derek, N. W. Tindale and A. L. Dick, Bureau of Meteorology and CSIRO Atmospheric Research, Melbourne, 88-89, 1999.

Thoning, K. W., P. P. Tans and W. D. Komhyr, Atmospheric carbon dioxide at Mauna Loa observatory, 2, Analysis of the NOAA/GMCC data, 1974-1985, *J. Geophys. Res*., 94, 8549-8565, 1989.

4.6. FLASK SAMPLING FROM CAPE GRIM OVERFLIGHTS

R L Langenfelds[1], R J Francey[1], L P Steele[1], B L Dunse[1,2], T M Butler[3], D A Spencer[1], L M Kivlighon[1,4] and C P Meyer[1]

[1]CSIRO Atmospheric Research, Aspendale, Victoria 3195, Australia
[2]Chemistry Department, University of Wollongong, Wollongong, NSW 2522, Australia
[3]School of Earth Sciences, University of Melbourne, Parkville, Victoria 3052, Australia
[4]Chemistry Department, La Trobe University, Bundoora, Victoria 3086, Australia

[Supported by CGBAPS research funds.]

Since 1980, regular aircraft sampling flights over Bass Strait have measured vertical and horizontal variations in the long-lived trace gas composition of the troposphere [Pearman *et al.* 1983; Fraser *et al.* 1992; Langenfelds *et al.* 1996, 2001]. The 'climatological' variability of vertical gradients above Cape Grim has been analysed for the period 1992-1997 [Pak *et al.* 1996; 1999; Francey *et al*. 1999; Pak 2000]. CO data from two flights in 1994 were used for ground-truthing of space shuttle-based, remotely sensed CO measurements collected as part of the Measurement of Air Pollution from Satellites (MAPS) program [Reichle *et al*. 1999].

Updated data sets will soon be made available at the CAR website (http://www.dar.csiro.au). Details of analytical and data handling procedures are given by Francey *et al.* [1996] and Steele *et al.* [1996].

Logbook

Table 1 lists details of flights conducted in 1999 and 2000. Two profiles (30 January 1999 and 22 April 1999) were conducted about 50 km west of the usual sampling site in an attempt to avoid terrestrial influence on sampled air masses, due to winds at Cape Grim being either southerly and/or light and variable.

Two periods of intensive vertical profiling were coordinated with campaigns investigating the Southern Hemisphere atmosphere:

1. The Southern Ocean Atmospheric Photochemistry Experiment (SOAPEX-2) in January/February 1999 examined photochemical influences on the trace gas composition of background marine air above Cape Grim. Trace gases measured as part of CAR's aircraft sampling program included some species (e.g. CH_4, CO, H_2) that are potential tracers of photochemical processes via reaction with the hydroxyl radical. Sampling emphasis during this period was on the lower troposphere with one flight (8 February 1999) restricted to a maximum altitude of only 2.9 km. Preliminary analysis of the relative influence of photochemistry and long-range transport on the 0-7 km vertical profiles is given by Pak [2000]. Vertical profiles of selected species between 0 and 2 km are shown in Figure 1. Within the marine boundary layer (MBL), vertical profiles may be influenced by photochemistry, air-sea exchange and entrainment of air from above the MBL. However, any forcing of gradients by these processes is opposed by rapid convective mixing. The data in Figure 1 show few, if any, significant vertical gradients below 1 km. Larger variations begin to appear above 1 km, reflecting slower mixing above the MBL and influence of other processes such as long range transport [Pak 2000].
2. The Southern African Regional Science Initiative (SAFARI 2000) investigated trace gas emissions from African biomass burning during the dry season in August/September 2000. CAR's involvement in this campaign focused on detection of biomass burning plumes in the mid-troposphere above Cape Grim. Flights were scheduled with the aim of intercepting air masses enriched in biomass burning products. The outflow of such air masses from Africa out over the Indian Ocean was shown by satellite observations to occur in bursts of 1-2 days, approximately once a week. Model forecasts of the transport of these air masses between Africa and Australia suggested a transit time of about 7 days. Two of the vertical profiles during the SAFARI 2000 period (13 September 2000 and 28 September 2000) were conducted above Melbourne, rather than Cape Grim, in coordination with ground-based lidar measurements of aerosol backscatter above CAR in Aspendale. Results from the set of flights indicate large and variable vertical gradients in the mid to upper troposphere in multiple trace gases [Pak *et al.* 2003] and aerosol [Young *et al*. 2001], consistent with significant influence of biomass burning plumes.

Routine monthly flights were suspended at the end of 1999 for a range of reasons including a prolonged interruption due to the light aircraft fuel contamination crisis in late 1999 and early 2000, and growing constraints on time and availability of the CSIRO staff involved in this over-flight program.

Table 1. Cape Grim/Bass Strait aircraft overflights in 1999/2000. Sampling details are shown for the Bass Strait sampling site (39°08'S, 145°14'E), and for profiles collected either offshore from Cape Grim with co-ordinated ground-based flask sampling at the Cape Grim station or above Melbourne. Wind observations are hourly mean values at Cape Grim. Flights on 13 and 28 September 2000 included sampling above Bass Strait at multiple altitude levels.

		----Bass Strait Site----		----------Vertical Profile----------						-------Cape Grim Station-------		
Date	Flight #	Altitude (km)	No. of Samples	Latitude (°S)	Longitude (°E)	Max. Altitude (km)	Min. Altitude (km)	No. of Altitude Levels	No. of Samples	Wind Speed ($m\ s^{-1}$)	Wind Direction (°)	No. of Samples
Aircraft: Cessna C401A (VH-NAS)												
13 Jan 99	C248	4.9	1	40.5	144.3	7.1	0.15	21	32	10	228	2
19 Jan 99	C249	4.9	1	40.5	144.3	7.1	0.15	20	28	9	257	6
30 Jan 99	C250	4.9	1	40.5	143.7	7.1	0.15	22	44	13	197	0
7 Feb 99	C251	4.9	1	40.5	144.3	7.0	0.15	19	34	21	187	0
8 Feb 99	C252			40.5	144.3	2.9	0.15	14	26	9	196	2
16 Feb 99	C253	4.9	1	40.5	144.3	7.0	0.15	18	30	18	286	4
19 Feb 99	C254	5.0	1	40.5	144.3	7.0	0.15	19	34	10	270	2
5 Mar 99	C255	4.9	1	40.5	144.3	7.0	0.15	17	40	6	270	4
22 Apr 99	C256	4.9	1	40.5	143.7	7.0	0.15	18	34	3	194	0
Aircraft: Piper Chieftain (VH-PRJ)												
2 Jul 99	C257	4.9	1	40.5	144.3	5.5	0.15	12	30	8	249	4
2 Aug 99	C258	4.9	1	40.5	144.3	7.0	0.15	17	29	6	230	0
Aircraft: Cessna C401A (VH-NAS)												
1 Sep 99	C259	4.9	1	40.5	144.3	7.1	0.15	17	30	10	200	4
Aircraft: Piper Navajo (VH-EGK; later registered as VH-NAS)												
28Oct 99	C260	4.9	1	40.5	144.3	6.1	0.15	16	30	6	302	3
21 Dec 99	C261	4.9	1	40.5	144.3	6.1	0.15	16	30	12	190	0
30 Aug 00	C262	4.9	1	40.5	144.3	6.7	0.15	16	24	2	308	2
5 Sep 00	C263	4.9	1	40.5	144.3	6.7	0.15	16	17	19	258	4
13 Sep 00	C264			38.0	145.1	6.7	1.8	14	23			
18Sep 00	C265	4.9	1	40.5	144.3	6.7	0.15	20	24	14	281	4
28Sep 00	C266			38.0	145.0	6.7	1.8	19	30			

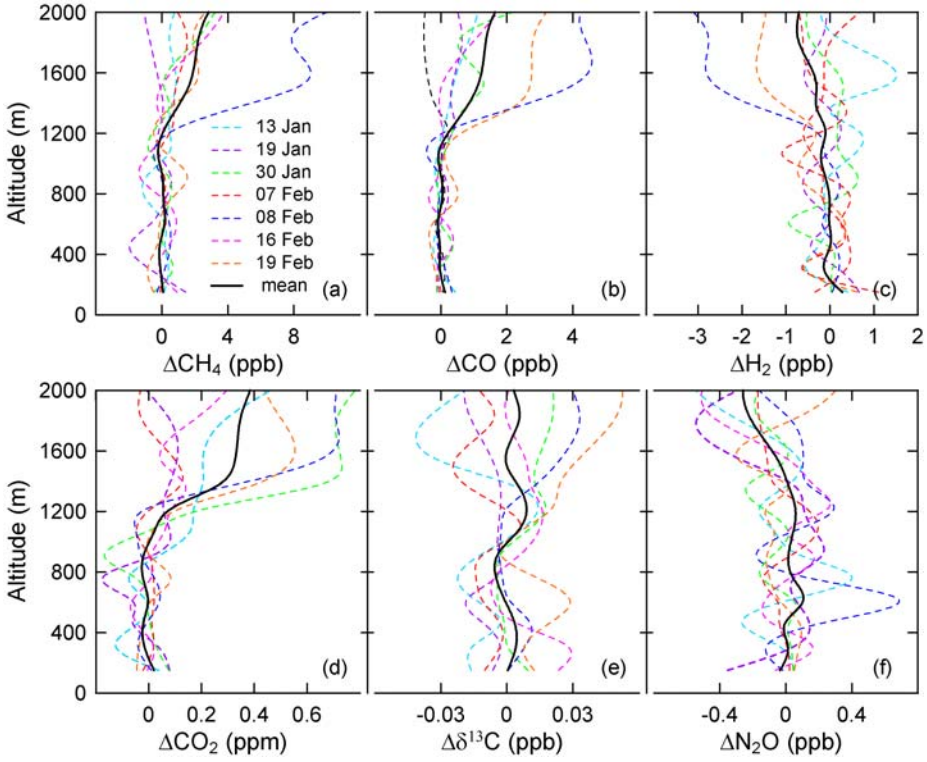

Figure 1. Vertical profiles of selected trace gas species measured at CAR GASLAB for the seven SOAPEX-2 flights. Data were calculated as residuals from mean values for the 0-1200 m range for each flight and were fitted by a spline with 50% attenuation at 500 m. Mean profiles were calculated by spline fitting residuals for all flights.

Aircraft / Air intakes

Three aircraft, each fitted with twin turbo-powered engines, were used during 1999/2000. The Cessna 401A (VH-NAS) employed since June 1998 was used through to April 1999 and again for an additional flight in September 1999, but was no longer available for charter after this time. Flights during the intervening period (July and August 1999) used a Piper Chieftain (VH-PRJ), with air sampled through the cabin ventilation ports. However, flow rates of air through the ventilation system were relatively low, causing samples to be contaminated with cabin air. No further sampling was attempted from this aircraft.

From October 1999, sampling flights employed a Piper Navajo (VH-EGK; later registered as VH-NAS). On the first flight in this aircraft (28 October 1999), air was also sampled through the cabin ventilation system. Thereafter, all sample air was drawn from a dedicated intake plate mounted on the side window of the aircraft. The plate is of stainless steel construction with separate ports (3/8" tube) available for up to four individual pump units or instruments. Each port is equipped with Swagelok fittings on the cabin side of the window plate, and a length of tubing protruding several centimetres from the external side of the window. Externally, each tube is right-angled such that the orifice faces the rear of the aircraft (opposite to the direction of travel), thus limiting accumulation of moisture inside the tube. The four tubes are positioned in separate horizontal planes to avoid the possibility of cross-contamination between ports during operation.

New instrumentation / measurements

Flights throughout 1999/2000 continued to provide vertical profiles of trace gas species measured at CAR GASLAB (CO_2 and its isotopes $\delta^{13}C$ and $\delta^{18}O$, CH_4, H_2, CO, N_2O, $\delta(O_2/N_2)$ etc.), University of Heidelberg (SF_6) and CGBAPS (halogenated compounds) [see Langenfelds *et al*. 2001 and references therein]. From January 1999, 4-6 additional samples spanning the full range of altitude were routinely collected in 6L, Silcosteel®-treated, stainless steel flasks (Restek Corporation, Bellefonte, PA, USA) for analysis of VOCs [Kivlighon et al. 2000; Kivlighon 2001]. These samples were collected undried, with a dedicated, stainless steel, metal bellows pump (MB-14 P/N 40043, Metal Bellows Div., Senior Flexonics Inc., Sharon, MA, USA). The flights of 30 August 2000, 13 September 2000 and 18 September 2000 included continuous measurement of O_3 using an instrument developed at CAR specifically for aircraft-based work. This instrument is a battery-powered, dual-beam photometer with a time resolution of 1 second and a precision of approximately 0.2 ppb.

References

Francey, R. J., L. P. Steele, R. L. Langenfelds, M. P. Lucarelli, C. E. Allison, D. J. Beardsmore, S. A. Coram, N. Derek, F. de Silva, D. M. Etheridge, P. J. Fraser, R. Henry, B. Turner, E. D. Welch, D. A. Spencer, and L. N. Cooper, Global Atmospheric Sampling Laboratory (GASLAB): supporting and extending the Cape Grim trace gas programs in *Baseline Atmospheric Program (Australia) 1993*, edited by R. J. Francey, A. L. Dick, and N. Derek, Bureau of Meteorology and CSIRO Division of Atmospheric Research, Melbourne, Australia, 8-29, 1996.

Francey, R. J., L. P. Steele, R. L. Langenfelds and B. C. Pak, High precision monitoring of radiatively active and related trace gases at surface sites and from aircraft in the Southern Hemisphere atmosphere, *J. Atmos. Sciences*, 56, 279-285, 1999.

Fraser, P., R. Francey, D. Beardsmore, S. Coram, H. Goodman, R. Langenfelds, and N. Richards, Cape Grim and Bass Strait aircraft overflights, 1989-1990 – CH_4, CO, CO_2 and CO_2 stable isotope data, in *Baseline Atmospheric Program (Australia) 1990*, edited by S. R. Wilson and J. L Gras, Bureau of Meteorology and CSIRO Division of Atmospheric Research, Melbourne, Australia, 49-53, 1992.

Kivlighon, L. M., I. E. Galbally and I. A. Weeks, *Proceedings of the 15th International Clean Air & Environment Conference*, Australia, 562-567, 2000.

Kivlighon, L. M., Tropospheric non-methane hydrocarbons at Cape Grim (41°S, 145°E), *MSc thesis*, La Trobe University, 2001.

Langenfelds, R. L., R. J. Francey, L. P. Steele, P. J. Fraser, S. A. Coram, M. R. Hayes, D. J. Beardsmore, M. P. Lucarelli, and F. R. de Silva, Improved vertical sampling of the trace gas composition of the troposphere above Cape Grim since 1991, in *Baseline Atmospheric Program (Australia) 1993*, edited by R. J. Francey, A. L. Dick, and N. Derek, Bureau of Meteorology and CSIRO Division of Atmospheric Research, Melbourne, Australia, 46-57, 1996.

Langenfelds, R. L., R. J. Francey, L .P. Steele, D. A. Spencer and B. L. Dunse, Flask sampling from Cape Grim overflights, in *Baseline Atmospheric Program (Australia), 1997-98*, edited by N. W. Tindale, Derek and R. J. Francey, Bureau of Meteorology and CSIRO Atmospheric Research, Melbourne, Australia, 74-84, 2001.

Pak, B. C., R. L. Langenfelds, R. J. Francey, L. P. Steele, and I. Simmonds, A climatology of trace gases from the Cape Grim Overflights, 1992-1995, in *Baseline Atmospheric Program (Australia), 1994-95*, edited by R. J. Francey, A. L. Dick, and N. Derek, Bureau of Meteorology and CSIRO Division of Atmospheric Research, Melbourne, Australia, 41-52, 1996.

Pak, B. C., M. Ramonet, P. Monfray, R. J. Francey, and I. Simmonds, Assessment of the spatial and temporal representativeness of the Cape Grim Overflight CO_2 data, in *Baseline Atmospheric Program (Australia), 1996*, edited by J. L. Gras, N. Derek, N. W. Tindale, and A. L. Dick, Bureau of Meteorology and CSIRO Atmospheric Research, Melbourne, Australia, 36-44, 1999.

Pak, B. C., Vertical structure of atmospheric trace gases over Southeast Australia, PhD Thesis, University of Melbourne, Australia, 273 pp. (available at the Australian Digital Theses Project via http://adt1.lib.unimelb.edu.au/adt-root/public/), 2000.

Pak, B. C., R. L. Langenfelds, S. A. Young, R. J. Francey, C. P. Meyer, L. M. Kivlighon, L. N. Cooper, B. L. Dunse, C. E. Allison, L. P. Steele, I. E. Galbally, and I. A. Weeks, Measurements of biomass burning influences in the troposphere over southeast Australia during the SAFARI 2000 dry season campaign, *J. Geophys. Res*., 108, 8480, doi:10.1029/2002JD002343, 2003.

Pearman, G. I., D. J. Beardsmore, and R. C. O'Brien, The CSIRO (Australia) atmospheric carbon dioxide monitoring program: Ten years of aircraft data, *CSIRO Division of Atmospheric Physics Technical Paper No. 45*, 113 p, 1983.

Reichle, H. G. Jr., B. E. Anderson, V. S. Connors, T. C. Denkins, D. A. Forbes, B. B. Gormsen, R. L. Langenfelds, D. O. Neil, S. R. Nolf, P. C. Novelli, N. S. Pougatchev, M. M. Roell and L. P. Steele, Space shuttle based global CO measurements during April and October 1994, MAPS instrument, data reduction, and data validation, *J. Geophys. Res*., 104, 21,443-21,454, 1999.

Steele, L. P., R. L, Langenfelds, M. P. Lucarelli, P. J. Fraser, L. N. Cooper, D. A. Spencer, S. Chea, and K. Broadhurst, Atmospheric methane, carbon dioxide, carbon monoxide, hydrogen and nitrous oxide from Cape Grim flask samples analysed by gas chromatography, in *Baseline Atmospheric Program (Australia), 1994-95*, edited by R. J. Francey, A. L. Dick, and N. Derek, Bureau of Meteorology and CSIRO Division of Atmospheric Research, Melbourne, Australia, 107-110, 1996.

Young, S. A., R. L. Langenfelds and J. M. Rosen, Observations over Australia of plumes from distant biomass burning sources using remote sensing and airborne techniques, Proceedings of the *International Geoscience and Remote Sensing Symposium*, 9-13 July 2001, Sydney, Australia, Institute of Electrical and Electronics Engineers, Piscataway, New Jersey, USA, 88-90, 2001.

4.7. ATMOSPHERIC METHANE, CARBON DIOXIDE, HYDROGEN, CARBON MONOXIDE AND NITROUS OXIDE FROM CAPE GRIM FLASK AIR SAMPLES ANALYSED BY GAS CHROMATOGRAPHY

R L Langenfelds[1], L P Steele[1], L N Cooper[1], D A Spencer[1], P B Krummel[1] and B L Dunse[1,2]

[1]CSIRO Atmospheric Research,
Aspendale, Victoria 3195, Australia
[2]Chemistry Department, University of Wollongong,
Wollongong, NSW 2522, Australia

[Supported by CGBAPS research funds.]

Air samples are regularly collected at Cape Grim in glass and stainless steel flasks, and returned to CSIRO Atmospheric Research's (CAR) Global Atmospheric Sampling Laboratory (GASLAB) for analysis of trace gas composition [Francey *et al*. 1996]. Gas chromatographic (GC) measurements of methane (CH_4), carbon dioxide (CO_2) and carbon monoxide (CO) commenced in 1980 [Fraser and Hyson 1986; Fraser *et al*. 1986, 1994]. Introduction of new and upgraded instrumentation in 1991/92 as part of the GASLAB development led to improved precision and calibration of previously measured species, and measurement of two additional species, hydrogen (H_2) and nitrous oxide (N_2O) [Francey *et al*. 1996; Steele *et al*. 1996; Cooper *et al*. 1999; Langenfelds *et al*. 2001a]. This report extends records of all species to the end of 2000.

Figure 1 shows time series and growth rates for CH_4 and CO. Figure 2 shows CO_2, H_2 and N_2O. Data are displayed for all flask samples with different symbols used to distinguish retained and rejected data. Causes of rejection are described by Steele *et al*. [1996] and Cooper *et al.* [1999]. Updated data sets will soon be made available at the CAR website (http://www.dar.csiro.au). The CO_2 and CH_4 data are contributed regularly to the 'Globalview' data sets generated by integration of measurements from participating international laboratories [*Globalview-CO_2* 2001; *Globalview-CH_4* 2001].

Recent publications using GASLAB GC data have addressed the prominent role that Cape Grim plays within CAR's trace gas measurement programs in the Southern Hemisphere [Francey *et al*. 1999a], trends in $\delta^{13}C$ of CO_2 [Francey *et al*. 1999b, 2001] and $\delta^{13}C$ of CH_4 [Francey *et al*. 1999c], inversion of CO_2 and $\delta^{13}C$ data to determine the global, spatiotemporal distribution of surface CO_2 fluxes since 1992 [Allison *et al*. 2001], correlations in interannual growth rate variability of multiple trace gas species during the 1990s [Langenfelds *et al.* 2001b, 2002] and results from the flask intercomparison program maintained by NOAA/CMDL and CSIRO since 1991 [Masarie *et al*. 2001].

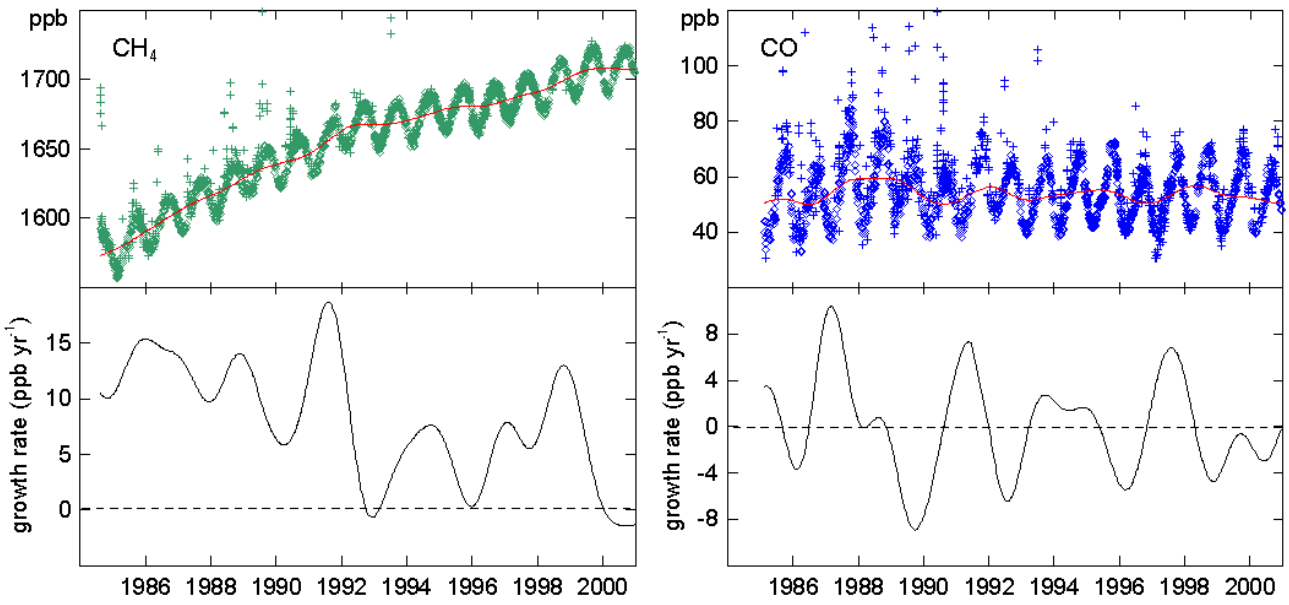

Figure 1. Top panels: Atmospheric CH_4 and CO in ppb (mole fraction in parts per 10^9 in dry air). CSIRO data are from individual Cape Grim flask air samples and are shown as retained (diamonds) or rejected (crosses), based on selection for baseline conditions and analytical quality assessment. The solid curves indicate long-term trends obtained from the curve fitting routine described by Thoning *et al*. [1989]. Bottom panels: Growth rate curves as given by the first derivative of the long-term trends.

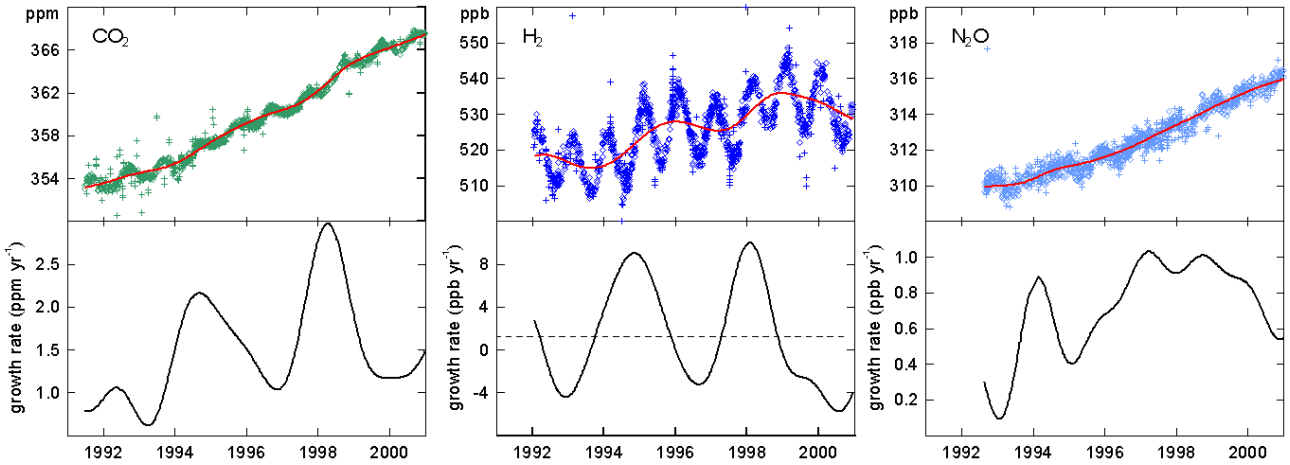

Figure 2. Top panels: Cape Grim records of CO_2, H_2 and N_2O. Results from all individual flask air samples are classified as retained (diamonds) or rejected (crosses). Solid curves indicate long-term trends. Bottom panels: Growth rate curves as given by the first derivative of the long-term trends.

References

Allison, C. E., R. J. Francey and P. J. Rayner, Stable isotopes of atmospheric carbon dioxide from the CSIRO global flask sampling network, *6th International CO_2 Conference: extended abstracts*, Sendai, Japan, 81-84, 2001.

Cooper, L. N., L. P. Steele, R. L. Langenfelds, D. A. Spencer and M. P. Lucarelli, Atmospheric methane, carbon dioxide, hydrogen, carbon monoxide and nitrous oxide from Cape Grim flask air samples analysed by gas chromatography, in *Baseline Atmospheric Program (Australia) 1996,* edited by J. L. Gras, N. Derek, N. W. Tindale and A. L. Dick, Bureau of Meteorology and CSIRO Atmospheric Research, Melbourne, Australia, 98-102,1999.

Francey, R. J., L. P. Steele, R. L. Langenfelds, M. P. Lucarelli, C. E. Allison, D. J. Beardsmore, S. A. Coram, N. Derek, F. R. de Silva, D. M. Etheridge, P. J. Fraser, R. J. Henry, B. Turner, E. D. Welch, D. A. Spencer and L. N. Cooper, Global Atmospheric Sampling Laboratory (GASLAB): supporting and extending the Cape Grim trace gas programs, *Baseline Atmospheric Program (Australia) 1993,* edited by R. J. Francey, A. L. Dick and N. Derek, Bureau of Meteorology and CSIRO Division of Atmospheric Research, Melbourne, Australia, 8-29, 1996.

Francey, R. J., L. P. Steele, R. L. Langenfelds and B. C. Pak, High precision monitoring of radiatively active and related trace gases at surface sites and from aircraft in the Southern Hemisphere atmosphere, *J. Atmos. Sciences*, 56, 279-285, 1999a.

Francey, R. J., C. E. Allison, D. M. Etheridge, C. M. Trudinger, I. G. Enting, M. Leuenberger, R. L. Langenfelds, E. Michel and L. P. Steele, A 1000-year high precision record of $\delta^{13}C$ in atmospheric CO_2, *Tellus*, 51B, 170-193, 1999b.

Francey, R. J., M. R. Manning, C. E. Allison, S. A. Coram, D. M. Etheridge, R. L. Langenfelds, D. C. Lowe and L. P. Steele, A history of $\delta^{13}C$ in atmospheric CH_4 from the Cape Grim Air Archive and Antarctic firn air, *J. Geophys. Res.*, 104, 23631-23643, 1999c.

Francey, R. J., C. E. Allison, C. M. Trudinger, P. J. Rayner, I. G. Enting and L. P. Steele, The interannual variation in global atmospheric $\delta^{13}C$ and its link to net terrestrial exchange, *6th International CO_2 Conference: extended abstracts*, Sendai, Japan, 43-46, 2001.

Fraser, P. and P.Hyson, Methane, carbon monoxide and methylchloroform in the Southern Hemisphere, *J. Atmos. Chem.*, 4, 3-42, 1986.

Fraser, P., P. Hyson, S. A. Coram, R. A. Rasmussen, A. J. Crawford, and M. A. K. Khalil, Carbon monoxide in the Southern Hemisphere, in *Proceedings of the Seventh World Clean Air Congress*, Sydney, edited by H. F. Hartmann, Sydney: Clean Air Society of Australia and New Zealand, 341-352, 1986.

Fraser, P., S. Coram and N. Derek, Atmospheric methane, carbon monoxide and carbon dioxide by gas chromatography, *Baseline Atmospheric Program (Australia) 1991*, edited by A. L. Dick and J. L. Gras, Bureau of Meteorology and CSIRO Division of Atmospheric Research, Melbourne, Australia, 60-64, 1994.

GLOBALVIEW-CH_4: Cooperative Atmospheric Data Integration Project - Methane. CD-ROM, NOAA CMDL, Boulder, Colorado [Also available on Internet via anonymous FTP to ftp.cmdl.noaa.gov, Path: ccg/ch4/GLOBALVIEW], 2001

GLOBALVIEW-CO_2: Cooperative Atmospheric Data Integration Project - Carbon Dioxide. CD-ROM, NOAA CMDL, Boulder, Colorado [Also available on Internet via anonymous FTP to ftp.cmdl.noaa.gov, Path: ccg/co2/GLOBALVIEW], 2001

Langenfelds, R. L., L. N. Cooper, L. P. Steele, D. A. Spencer, P. B. Krummel and P. J. Fraser, Atmospheric methane, carbon dioxide, hydrogen, carbon monoxide and nitrous oxide from Cape Grim flask air samples analysed by gas chromatography, in *Baseline Atmospheric Program (Australia) 1997-98,* edited by N. W. Tindale, N. Derek, and R. J. Francey, Bureau of Meteorology and CSIRO Atmospheric Research, Melbourne, Australia, 69-74, 2001a.

Langenfelds, R. L., R. J. Francey, B. C. Pak, L. P. Steele, J. Lloyd, C. M. Trudinger and C. E. Allison, The use of multi-species measurements for interpreting interannual variability in the carbon cycle, in *6th International CO_2 Conference: extended abstracts*, Sendai, Japan, 9-11, 2001b.

Langenfelds, R. L., R. J. Francey, B. C. Pak, L. P. Steele, J. Lloyd, C. M. Trudinger and C. E. Allison, Interannual growth rate variations of atmospheric CO_2 and its $\delta^{13}C$, H_2, CH_4 and CO between 1992 and 1999 linked to biomass burning, *Glob. Biogeochem. Cycles*, 16, 1048, doi:10.1029/2001GB001466, 2002.

Masarie, K. A., R. L. Langenfelds, C. E. Allison, T. J. Conway, E. J. Dlugokencky, R. J. Francey, P. C. Novelli, L. P. Steele, P. P. Tans, B. Vaughn and J. W. C. White, NOAA/CSIRO Flask Air Intercomparison Experiment: A strategy for directly assessing consistency among atmospheric measurements made by independent laboratories, *J. Geophys. Res.*, 106, 20,445-20,464, 2001.

Steele, L. P., R. L, Langenfelds, M. P. Lucarelli, P. J. Fraser, L. N. Cooper, D. A. Spencer, S. Chea and K. Broadhurst, Atmospheric methane, carbon dioxide, carbon monoxide, hydrogen and nitrous oxide from Cape Grim flask samples analysed by gas chromatography, in *Baseline Atmospheric Program (Australia), 1994-95*, edited by R. J. Francey, A. L. Dick and N. Derek, Bureau of Meteorology and CSIRO Division of Atmospheric Research, Melbourne, Australia, 107-110, 1996.

Thoning, K. W., P. P. Tans and W. D. Komhyr, Atmospheric carbon dioxide at Mauna Loa Observatory, Analysis of the NOAA/GMCC data, 1974 - 1985, *J. Geophys. Res.*, 94, 8549-8565, 1989.

4.8. ARCHIVING OF CAPE GRIM AIR

R L Langenfelds[1], P J Fraser[1], L P Steele[1] and L W Porter[2]

[1]CSIRO Atmospheric Research,
Aspendale, Victoria 3195, Australia
[2]Cape Grim Baseline Air Pollution Station, Bureau of Meteorology, Smithton, Tasmania 7330, Australia

[Supported by CGBAPS research funds.]

Regular collection of Cape Grim air in high-pressure metal cylinders for the purpose of maintaining an archive of atmospheric composition has continued since 1978. A history of sampling events, protocols, techniques and reconstruction of atmospheric trace gas records through 1995 has been given previously [Langenfelds *et al.* 1996 and references therein] and updated through 1998 [Langenfelds *et al*. 1999; 2001]. Recent publications using Cape Grim Air Archive data [Oram 1999; Fraser and Prather 1999; Prinn *et al.* 2000] have addressed long-term trends of several classes of halogenated trace gases (CFCs, HCFCs, HFCs, PFCs, halons, SF_6) implicated in stratospheric ozone depletion and/or the enhanced greenhouse effect.

Primary sampling

During 1999/2000, 14 cylinders were filled under baseline conditions and 2 under marginal baseline conditions (Table 1). Of these, 10 were filled specifically to be used as calibration standards at CGBAPS for measurement programs maintained by the Advanced Global Atmospheric Gases Experiment (AGAGE) and the University of East Anglia (UEA).

In January 1999, the intake line used to fill archive cylinders was modified to include a pressure relief valve. This device was introduced as an additional safety measure to protect against inadvertent cryotrapping of excess air. Immediately following the cryogenic collection of each sample, cylinders were removed from the liquid nitrogen bath and left to warm (and sample air to vapourise) with the cylinder valve left open to the pressure relief valve. For two samples (collected 21 July 1999 and 22 July 1999), some air was observed to vent through the pressure relief valve during this process. These samples were later found to be measurably fractionated as a result of the sample loss. This problem was overcome by slightly increasing the pressure relief setting and using a gas meter to routinely monitor the vent port during the warming phase, to ensure that any sample loss is detected and quantified. One affected cylinder earmarked for retention in the archive (S35L-C40), was refilled shortly afterwards (4 August 1999).

Table 1. Collection and status details for primary archive samples filled at Cape Grim. Samples are listed against UAN (a number unique to each sample, assigned at CAR), Tank ID (a label unique to each individual sample container) and Archive ID (a sample identifier commonly used before 1992). Wind data represent estimated averages over the period of collection. They are calculated either from collection records or from Cape Grim hourly average data.

[a]cryo immersion in liquid nitrogen
[b]wet no drying
[c]CAR managed and stored at CAR
[d]AGAGE used as a standard in the AGAGE program.
[e]UEA used as a standard in the measurement program maintained at CGBAPS by University of East Anglia.

UAN	Tank ID	Archive ID	Collection Date (GMT)	Sampling Method[a]	Drying Method[b]	Wind Speed ($m\ s^{-1}$)	Wind Direction (°)	Pressure Fill (kPa abs)	Pressure Current (kPa abs)	Current Status[c,d,e]
	S35L-C70	CG210199	21 Jan 99	cryo	wet	8	80	2900	0	exhausted
991060	S35L-C65	CG170299	17 Feb 99	cryo	wet	11	272	2900	2630	CAR
991061	S35L-C53	CG040399	4 Mar 99	cryo	wet	6	263	3380	0	exhausted
991062	S35L-C59	CG130499	13 Apr 99	cryo	wet	9	227	3300	2500	AGAGE
991063	S35L-C46	CG070699	7 Jun 99	cryo	wet	12	228		0	exhausted
991313	S35L-C40	CG210799	21 Jul 99	cryo	wet	17	272	3590	0	exhausted
991314	S35L-C53	CG220799	22 Jul 99	cryo	wet	12	225	3590	0	exhausted
991381	S35L-C40	CG040899	4 Aug 99	cryo	wet	10	227	2970	2700	CAR
	S35L-C46	CG181099	18 Oct 99	cryo	wet	14	225	4290	0	exhausted
992045	S35L-C38	CG161199	16 Nov 99	cryo	wet	14	210	3180	3180	CAR
	S35L-C53	CG190100	19 Jan 00	cryo	wet	9	221	4290	0	exhausted
	S35L-C39	CG010300	1 Mar 00	cryo	wet	8	74	4700	3460	UEA
992982	S35L-C46	CG140300	14 Mar 00	cryo	wet	14	229	3360	3250	CAR
	S35L-C70	CG190400	19 Apr 00	cryo	wet	4	253	4290	0	exhausted
	S35L-C53	CG060900	6 Sep 00	cryo	wet	15	256	4490	0	exhausted
993562	S35L-C55	CG290900	29 Sep 00	cryo	wet	21	273	3000	2460	CAR

Table 2. Preparation and status details for subsamples of primary archive samples. Current status entries denote the institute managing the sample.

UAN	Subsample Tank ID	Parent UAN	Archive Date	Subsample Preparation Date	Fill Pressure kPa abs	Current Pressure kPa abs	Current Status
991066	S320-204	991060	17 Feb 99	19 May 99	650		UEA
991067	S320-205	991061	4 Mar 99	19 May 99	650		UEA
991068	S320-206	991062	13 Apr 99	19 May 99	650		UEA

Subsampling

Table 2 lists collection details of 3 archive subsamples prepared during 1999/2000. All were prepared for University of East Anglia, UK (UEA) in 3.2 litre, stainless steel containers provided by them. This extends the air archive records of the halogenated trace gas species being measured by GC-MS techniques at UEA and is complemented by occasional, direct sampling of background Cape Grim air into similar containers.

Acknowledgements

We thank the CGBAPS and CAR personnel who have assisted in the collection, management and analysis of these samples.

References

Fraser, P. J. and M. J. Prather, Uncertain road to ozone recovery, *Nature*, 398, 663-664, 1999.

Langenfelds, R. L., P. J. Fraser, R. J. Francey, L. P. Steele, and L. W. Porter, The Cape Grim Air Archive: the first seventeen years, 1978 - 1995, in *Baseline Atmospheric Program (Australia), 1994-95*, edited by R. J. Francey, A. L. Dick and N. Derek, Bureau of Meteorology and CSIRO Division of Atmospheric Research, Melbourne, 53-70, 1996.

Langenfelds, R. L., P. J. Fraser, L. P. Steele, R. J. Francey, and L. W. Porter, Archiving of Cape Grim air, in *Baseline Atmospheric Program (Australia), 1996*, edited by J. L. Gras, N. Derek, N. W. Tindale, and A. L. Dick, Bureau of Meteorology and CSIRO Atmospheric Research, Melbourne, 94-95, 1999.

Langenfelds, R. L., P. J. Fraser, L. P. Steele and L. W. Porter, Archiving of Cape Grim air, in *Baseline Atmospheric Program (Australia), 1997-98*, edited by N. W. Tindale, N. Derek and R. J. Francey, Bureau of Meteorology and CSIRO Atmospheric Research, Melbourne, 84-86, 2001.

Oram, D. E., Trends of long-lived anthropogenic halocarbons in the Southern Hemisphere and model calculations of global emissions, PhD thesis, University of East Anglia, Norwich, UK, 1999.

Prinn, R. G., R. F. Weiss, P. J. Fraser, P. G. Simmonds, D. M. Cunnold, F. N. Alyea, S. O'Doherty, P. Salameh, B. R. Miller, J. Huang, R. H. J. Wang, D. E. Hartley, C. Harth, L. P. Steele, G. Sturrock, P. M. Midgley and A. McCulloch, A history of chemically and radiatively important gases in air deduced from ALE/GAGE/AGAGE, *J. Geophys. Res*., 105, 17,751-17,792, 2000.

4.9. SF_6 FROM FLASK SAMPLING

I Levin[1], R Heinz[1], R L Langenfelds[2], R J Francey[2], L P Steele[2] and D A Spencer[2]

[1]Institut für Umweltphysik, University of Heidelberg, D-69120 Heidelberg, Germany
[2]CSIRO Atmospheric Research, Aspendale, Victoria 3195, Australia

[Cooperative Research report.]

Sulfur hexafluoride (SF_6) is a man-made trace gas used predominantly in gas-insulated switchgear. Because of its well known, largely northern hemispheric source strength and distribution and its long lifetime of probably more than 1000 years, it is a useful tracer of atmospheric circulation and exchange between the atmosphere and linked reservoirs. It is also a strong greenhouse gas with radiative forcing 36000 times that of CO_2 on a per molecule basis.

A high precision record (Figure 1) of its accumulation in the atmosphere between 1978 and 1994 was reconstructed from measurements made at University of Heidelberg (UHEI-IUP) of the Cape Grim Air Archive. This record has been strengthened and extended by analysis of additional pre-1996 archived air and by regular, direct flask sampling of baseline Cape Grim air in 1.6 L stainless steel flasks since November 1995 [Maiss *et al.* 1996]. Measurement of SF_6 in Cape Grim surface air is complemented by sampling of the troposphere above Cape Grim as part of CSIRO's established aircraft sampling program [Levin et al. 2001]. Data are available on request, e-mail: Ingeborg.Levin@iup.uni-heidelberg.de

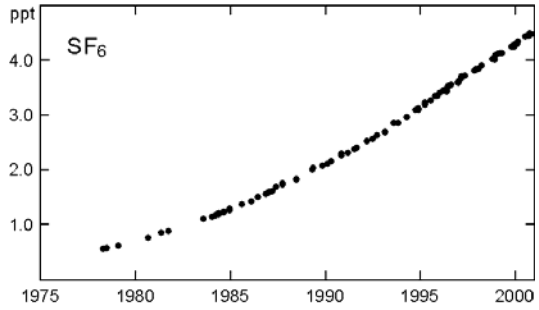

Figure 1. SF_6 at Cape Grim from measurements of the Cape Grim Air Archive and direct flask sampling since 1978.

References

Levin, I., R. Heinz, V. Walz, R. L. Langenfelds, R. J. Francey, L. P. Steele and D. A. Spencer, SF_6 from flask sampling, in *Baseline Atmospheric Program (Australia) 1997-98*, edited by N. W. Tindale, N. Derek, and R. J. Francey, Bureau of Meteorology and CSIRO Atmospheric Research, Melbourne, Australia, 87-88, 2001.

Maiss, M., L. P. Steele, R. J. Francey, P. J. Fraser, R. L. Langenfelds, N. B. A. Trivett and I. Levin, Sulfur hexafluoride - a powerful new atmospheric tracer, *Atmos. Environ.,* 30, 1621-1629, 1996.

4.10. BASELINE CARBON DIOXIDE MONITORING

L P Steele[1], P B Krummel[1], G A Da Costa[1], D A Spencer[1], L W Porter[2], S B Baly[2], R L Langenfelds[1], and L N Cooper[1]

[1]CSIRO Atmospheric Research, Aspendale, Victoria 3195, Australia

[2]Cape Grim Baseline Air Pollution Station, Bureau of Meteorology, Smithton, Tasmania 7330, Australia

[Supported by CGBAPS research funds]

The continuous monitoring of atmospheric carbon dioxide continued at Cape Grim during 1997-2000. Over this time several changes have been made, and these are described in this report.

BASGAM

During the four-year period of 1997 to 2000 inclusive, the continuous measurement of atmospheric carbon dioxide (CO_2) in air drawn from the 70-m intake continued with the Siemens ULTRAMAT 5E infrared gas analyser system known as BASGAM. On 26 May 1999, the ULTRAMAT 5E (serial number X07-389) was replaced with a similar analyser (serial number X08-397) due to the development of a fault (unstable chopper frequency) with the original analyser. Figure 1 shows the hourly CO_2 values for this period with corresponding baseline data and growth rate. Specifically, the top panel shows all instrumentally valid hourly values, with baseline data shown in red and non-baseline data shown in blue. This illustrates the large number of departures of CO_2 both above and below the baseline values. It is quite apparent that the largest negative departures from baseline levels occur predominantly in the winter months of each year, while the largest positive excursions occur in the summer months.

The second panel shows hourly baseline data only (see later for details of baseline selection technique). Also shown in this panel is the 80-day smooth curve (blue) and 650-day trend curve found using the filtering techniques of Thoning *et al*. [1989]. During the four year period, baseline CO_2 increased by approximately 7 ppm.

The last panel shows the instantaneous growth rate of CO_2 for the four-year period, derived by computing the derivative of the trend curve in panel 2. During this period the growth rate rose to a peak value of 2.9 ppm yr^{-1} in early 1998, making it the highest CO_2 growth rate ever recorded at Cape Grim. This finding at Cape Grim has also been reported by other investigators, showing that this unprecedented high growth rate of CO_2 was a global phenomenon [e.g. see Tans *et al*. 2002; Langenfelds *et al*. 2002a].

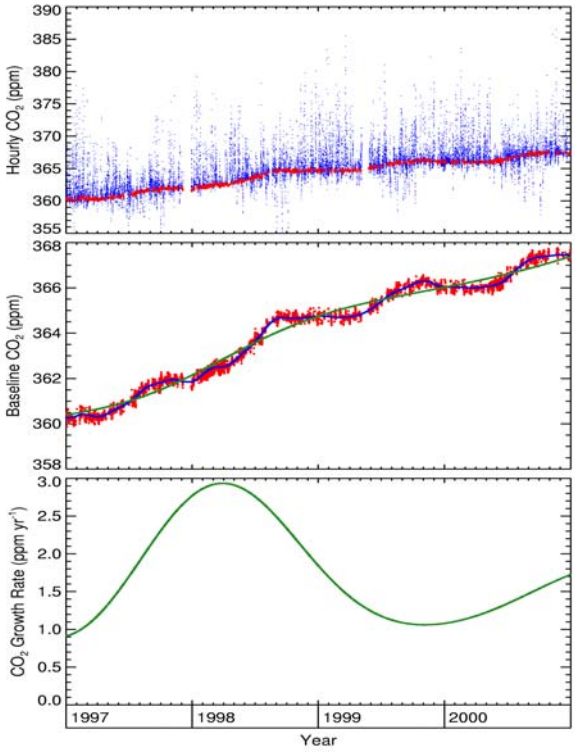

Figure 1. Cape Grim BASGAM *in situ* carbon dioxide (CO_2) record for 1997 to 2000 inclusive. First panel: all valid hourly CO_2 values, with baseline data shown in red and non-baseline shown in blue. Second panel: hourly baseline data only, with 80-day smooth curve (blue) and 650-day long-term trend curve (green). Third panel: Instantaneous CO_2 growth rate. See text for details.

A change to the BASGAM CO_2 monitoring program introduced from the beginning of 1997 was the use of high-span, low-span, and reference gases prepared in GASLAB from dry natural air. This development meant that it was no longer necessary to purchase CO_2-in-air calibration and reference gas mixtures that had been prepared commercially by The BOC Group (Preston, Victoria). Natural air was pumped into 29.5 L aluminium, high-pressure cylinders (manufactured by Luxfer, Riverside, California, and prepared by Scott-Marrin, Inc. of Riverside, California) with the use of a model SA-3 oil-less compressor (RIX Industries, Benicia, California). Drying of the air was carried out by the use of a chemical drying reagent (phosphorus pentoxide) on the outlet stream of the compressor. The CO_2 mixing ratios were adjusted to the desired values by either adding a known amount of high purity CO_2, or switching a tube filled with a CO_2-adsorbent material into the outlet stream of the compressor for a specified period of time. Cylinders were typically filled to a pressure of 2000 psig. After filling, the water vapour levels in each cylinder were measured with an Aquamatic+ analyser (Meeco, Inc., Warrington, Pennsylvania, USA) as part of the quality assurance procedure. Typically, water levels less than 0.2 ppm were achieved.

The details of the high-span, low-span, and reference gases used for BASGAM monitoring during 1997-2000 are given in Table 1. The dates and times specified are Australian Eastern Standard Time (AEST). The Universal Analysis Number (UAN) is a

unique identifier for each air sample measured in GASLAB that avoids possible confusion over the identity of any of the calibration gases, even when the same cylinder is re-filled several times, as has been the case here. All span and reference gases are measured for CO_2 (and other trace species) in GASLAB, prior to despatch to Cape Grim, and on return to Aspendale.

Table 1. Tank serial number, Universal Analysis Number (UAN), on/off dates and times (AEST) and carbon dioxide (CO_2) concentration (parts per million) of the high-span, low-span and reference gases used for BASGAM monitoring during 1997-2000.

Tank serial #	*UAN*	*Date On (AEST)*	*Hour*	*Date Off (AEST)*	*Hour*	*CO_2 (ppm)*
Hispan						
CA01687	960912	24 Dec 96	14	25 Mar 97	15	362.93
CA01696	970236	25 Mar 97	16	25 Jun 97	10	370.08
CA01697	970235	25 Jun 97	11	03 Sep 97	15	370.43
CA01696	970833	03 Sep 97	16	08 Dec 97	14	370.72
CA01697	971437	08 Dec 97	15	06 Mar 98	14	372.20
CA01696	980100	06 Mar 98	15	05 Jun 98	15	373.36
CA01607	980407	05 Jun 98	16	28 Aug 98	14	371.94
CA01697	980815	28 Aug 98	15	27 Nov 98	15	373.55
CA01696	981403	27 Nov 98	16	28 Jan 99	14	374.94
ALWA2681 (CA62)	970420	28 Jan 99	15	02 Feb 99	15	370.60
CA01675	971028	02 Feb 99	16	31 May 99	09	372.04
CA01607	990743	31 May 99	10	09 Sep 99	15	374.90
CA01697	990998	09 Sep 99	10	10 Dec 99	10	375.07
CA01607	991741	10 Dec 99	11	01 Mar 00	15	377.00
CA01696	992076	01 Mar 00	16	02 Jun 00	12	376.07
CA01653	992299	02 Jun 00	13	18 Aug 00	14	370.44
CA01607	992503	18 Aug 00	15	27 Nov 00	11	376.74
CA01696	993204	27 Nov 00	12	12 Feb 01	13	376.08
Lospan						
ALVF352 (CA95)	960968	02 Oct 96	11	28 Jan 97	15	355.74
CA01666	961264	28 Jan 97	16	23 Apr 97	16	358.62
CA01614	961265	23 Apr 97	17	24 Jul 97	10	358.70
CA01620	970651	24 Jul 97	11	20 Oct 97	13	353.84
CA01623	970834	20 Oct 97	14	09 Jan 98	16	357.09
CA01614	971486	09 Jan 98	17	15 Apr 98	16	355.98
CA01620	980101	15 Apr 98	17	20 Jul 98	12	357.71
CA01623	980408	20 Jul 98	13	19 Oct 98	13	355.17
CA01614	980814	19 Oct 98	14	18 Jan 99	11	360.27
CA01620	981614	18 Jan 99	12	26 Apr 99	13	359.11
CA01623	990598	26 Apr 99	14	16 Aug 99	11	363.70
CA01614	990996	16 Aug 99	12	05 Oct 99	15	359.52
CA01620	991293	05 Oct 99	16	10 Feb 00	13	361.95
CA01623	991879	10 Feb 00	14	11 May 00	16	361.96
CA01614	992077	11 May 00	17	08 Aug 00	12	360.50
CA01620	992504	08 Aug 00	13	14 Nov 00	09	358.08
CA01614	993205	14 Nov 00	10	01 Mar 01	11	361.00
Reference						
ALVP394 (DA07)	970570	12 Dec 96	13	29 Apr 97	15	328.54
CA01644	970405	29 Apr 97	16	08 Aug 97	10	335.15
CA01681	970406	08 Aug 97	11	17 Nov 97	14	329.09
CA01644	971394	17 Nov 97	14	26 Feb 98	14	328.96
CA01618	971487	26 Feb 98	15	05 Jun 98	15	333.92
CA01681	980406	05 Jun 98	16	18 Sep 98	15	337.08
CA01644	980816	18 Sep 98	16	30 Dec 98	15	335.00
CA01618	981615	30 Dec 98	16	01 Apr 99	14	338.67
CA01681	990591	01 Apr 99	15	12 Jul 99	12	338.43
CA01644	990933	12 Jul 99	13	25 Oct 99	14	335.98
CA01618	991292	25 Oct 99	15	10 Feb 00	13	340.79
CA01681	991900	10 Feb 00	14	26 May 00	12	339.18
CA01644	992078	26 May 00	13	11 Sep 00	09	339.82
CA01676	992542	11 Sep 00	10	21 Dec 00	13	342.60
CA01681	993159	21 Dec 00	13	06 Apr 01	16	342.42

The monthly average, and annual average baseline CO_2 values derived from the BASGAM system during 1997-2000 are tabulated in Table 2. Included in the Table are summaries of the number of CO_2 baseline hours, and the proportion of hours when instrumentally valid CO_2 data were obtained. In a departure from previous practice, the CO_2 values are reported to 3 digits after the decimal (rather than 2 digits after the decimal). While clearly not warranted at this stage, it is done here in anticipation of improvements in CO_2 measurements.

Another change that is explored here is in the method used to calculate the monthly average baseline CO_2 values shown in Table 2. There are several component parts of the overall method that are being evaluated, prior to a final acceptance. Firstly, the hourly average winds measured at the 50-m level on the tower are used here, rather than those at the 10-m level, since it is now clear that the 50-m winds are much less perturbed by local topographic influences [see Baines and Murray 2003]. Due to instrumentation problems, 50-m winds were not available for two significant periods, corresponding to 1400 hours, 14 January 1998 - 1100 hours, 19 February 1998, and 1300 hours, 11 May 1999 - 1000 hours, 04 June 1999. A few minor occurrences of missing 50-m wind data also occurred. For the purposes of this study, the 10-m wind data (where available) were used as a substitute for the missing 50-m wind data. The wind direction sector of 190°-280° was retained as the baseline sector. Two additional constraints were tried here: only those hourly periods with wind speeds ≥ 5 m s^{-1} were eligible for acceptance as baseline; and the hourly CN was required to be ≤ 600 cm^{-3}. The usual criterion for CO_2 stability was retained (i.e. for an hourly CO_2 value to be eligible for classification as baseline it must be part of a group of 5 consecutive hourly values during which time the CO_2 concentration varied by less than 0.3 ppm around the mean value).

After application of these criteria, an iterative filter based on smooth curve fitting techniques [Thoning *et al*. 1989] is then applied to the remaining data to clip outliers. First, a smooth curve is fitted to the hourly CO_2 values which meet all baseline criteria. Monthly averages are then calculated from daily values determined from the smooth curve. Hourly CO_2 values which lay greater than 0.4 ppm from their corresponding monthly average were flagged, and the curve fitting repeated. If necessary, this clipping was repeated until no hourly CO_2 values lay greater than 0.4 ppm from their corresponding monthly average. The daily values for baseline CO_2 are calculated from the final fitted smooth curve, and the monthly averages are calculated as the mean of all the daily values in each month. This approach has clear advantages in more reliably estimating monthly averages, especially during those times when there are relatively few periods of baseline conditions.

A full description of the evaluation of possible improvements to the definition of CO_2 baseline at Cape Grim will be provided elsewhere. After such evaluation and acceptance, any new definition will be then applied consistently to the full CO_2 record.

Table 2. Monthly mean baseline atmospheric carbon dioxide mixing ratios measured by the BASGAM *in situ* monitoring system at Cape Grim during 1997 to 2000 inclusive. The monthly mean values have been calculated from smooth curve fits to the hourly baseline data, see text for details. The mixing ratios are expressed in the WMO mole fraction calibration scale, as parts per million (ppm) of CO_2 in dry air. Also shown are the number of CO_2 baseline hours, the number of instrumentally valid CO_2 hours plus the total possible hours for each month.

	1997			*1998*			*1999*			*2000*		
Month	*CO_2 (ppm)*	*bl hrs*	*CO_2 hrs/ total hrs*	*CO_2 (ppm)*	*bl hrs*	*CO_2 hrs/ total hrs*	*CO_2 (ppm)*	*bl hrs*	*CO_2 hrs/ total hrs*	*CO_2 (ppm)*	*bl hrs*	*CO_2 hrs/ total hrs*
Jan	360.275	179	733/744	361.998	184	658/744	364.741	45	669/744	366.035	124	725/744
Feb	360.397	120	651/672	362.321	275	643/672	364.715	45	572/672	366.032	48	681/696
Mar	360.356	270	708/744	362.482	302	704/744	364.704	165	732/744	366.000	147	727/744
Apr	360.350	269	656/720	362.611	330	669/720	364.754	203	610/720	366.030	158	705/720
May	360.570	195	709/744	362.967	226	716/744	364.918	79	273/744	366.101	310	732/744
Jun	360.804	143	572/720	363.389	184	693/720	365.219	198	702/720	366.273	256	704/720
Jul	361.131	340	720/744	363.887	252	698/744	365.577	206	723/744	366.638	160	733/744
Aug	361.546	322	715/744	364.453	77	522/744	365.857	258	732/744	367.049	158	697/744
Sep	361.756	152	705/720	364.690	226	701/720	366.045	160	703/720	367.307	170	706/720
Oct	361.892	235	629/744	364.673	325	726/744	366.235	175	731/744	367.387	170	699/744
Nov	361.939	250	653/720	364.677	143	710/720	366.252	160	709/720	367.425	36	607/720
Dec	361.841	69	162/744	364.724	205	725/744	366.092	162	646/744	367.434	64	721/744
Year	361.071	2544	7613/8760	363.573	2729	8165/8760	365.426	1856	7802/8760	366.643	1801	8437/8784

LOFLO

In May 2000, a prototype LOFLO CO_2 analyser system was installed at Cape Grim, to operate in parallel with the BASGAM system, as one way of evaluating the operational performance of both systems. Both systems share the 70-m air intake line. The basic philosophy and architecture of the LOFLO has been described elsewhere [Da Costa and Steele 1997, 1999].

The LOFLO system is calibrated with a suite of 7 CO_2-in-dry (natural) air standards, prepared in 29.5 L high-pressure aluminium cylinders. The details of these standards are shown in Table 3. The CO_2 values were assigned to these standards in GASLAB, using the gas chromatographic technique described elsewhere [Francey *et al*. 1996]. Each standard was fitted with its own dedicated, pressure reducing regulator (high purity, single stage, stainless steel, 74-2400 series, available from Tescom Corporation, Elk River, Minnesota, USA). Each standard is effectively permanently connected to the LOFLO system. The reference gas is also CO_2-in-dry (natural) air contained in a similar high-pressure cylinder. Because of the considerably higher usage rate of the reference gas, these cylinders require to be changed every few months. The details of the first 3 reference gas tanks are also shown in Table 3. Initially, the reference tank was fitted with a pressure-reducing regulator of the same type as those used on the calibration standards. On 26 June 2000, a second such regulator was connected in series with the first, to provide better pressure regulation on the reference gas. This was found to be necessary because of the more demanding regular (hourly) switching between delivery flow rates of 15 ml min^{-1} and 30 ml min^{-1}.

The response function of the LOFLO system was determined 12 times during the time from its installation to the end of 2000. This entailed a classical 'calibration pyramid' approach, flowing gas from each calibration standard through the sample cell in turn. Multiple pyramids were run on each occasion. A 'zero' determination (reference gas passing through both cells simultaneously) was made each alternate sample, so that the measurement of each calibration sample was bracketed by the measurement of a 'zero'. The occasions of these response function determinations are given in Table 4. In this initial period of evaluating the operational performance of the LOFLO, more frequent (about double) calibrations have been run than is expected to be the case in routine operation. In each of these calibration experiments, the response function of the analyser system is determined (a shallow quadratic function), as well as the CO_2 value of the reference gas, relative to the suite of seven calibration standards. These are then deemed to define the response of the analyser during ambient air measurements, until the time of the next calibration experiment.

Instrumentally valid, minute-average CO_2 data from the LOFLO system through to the end of 2000 are shown in Figure 2. Most of the gaps in the record correspond to the times when calibration experiments were being run. The selection of instrumentally valid data is based primarily on the behaviour of the parameters such as differential pressure. Overall, the performance of the LOFLO over this period has been very encouraging.

Table 3. Details of the CO_2-in-air calibration suite used on the LOFLO CO_2 analyser system, as well as those of the first three CO_2-in-air reference gases. Consumption of gas in the first reference tank appears high, and was traced to the presence of a leaking fitting. The leak was identified and repaired on 16 May 2000.

ID	*Installation Date*	*Cyl. #*	*UAN*	*Starting Pressure (Psig)*	*GASLAB CO_2 (ppm)*
CAL1	20000510	CA01666	980773	1870	338.96
CAL2	20000510	CA01687	980772	1950	350.24
CAL3	20000510	CA01647	970830	1750	360.68
CAL4	20000510	CA01688	980771	1890	369.99
CAL5	20000510	CA01634	970337	1790	380.37
CAL6	20000510	CA01640	970338	1780	388.47
CAL7	20000510	CA01622	970339	1740	400.15
REF1	20000510	CA01686	991782	1400	367.39
REF2	20000607	CA01605	991071	1860	365.23
REF3	20001011	CA01698	992447	1880	366.59

Table 4. Basic details of the calibration experiments conducted on the LOFLO CO_2 analyser system, from the date of installation to the end of 2000. Dates (yyyymmdd) and times (hhmm) are in AEST. The reference gas is assigned a CO_2 value (last column) on the basis of each calibration experiment.

CAL #	*Start Date*	*Time*	*Finish Date*	*Time*	*REF CO_2 ppm*
REF1					
1	20000510	1840	20000516	1640	367.422
2	20000606	1351	20000607	1557	367.416
REF2					
3	20000607	1624	20000608	1756	365.251
4	20000628	1957	20000630	1614	365.256
5	20000717	1507	20000719	1230	365.258
6	20000804	1538	20000807	0935	365.255
7	20000825	1537	20000828	0903	365.260
8	20000915	1611	20000918	1024	365.267
9	20001009	1011	20001011	1246	365.273
REF3					
10	20001011	1312	20001013	0932	366.535
11	20001110	1609	20001113	1007	366.539
12	20001211	1424	20001214	1438	366.543

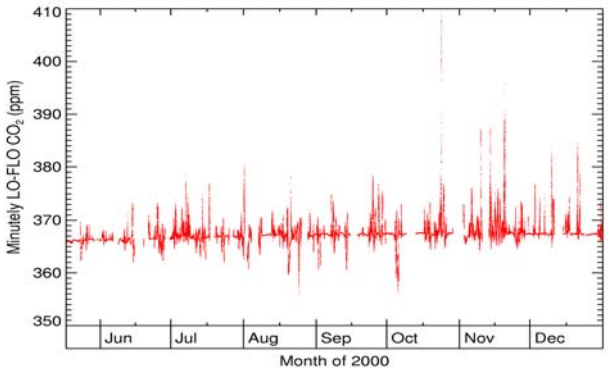

Figure 2. Cape Grim LOFLO *in situ* carbon dioxide (CO_2) record, all valid 1-minute average values for May to December 2000.

A revealing result has emerged over this period by comparing the ambient CO_2 data from BASGAM and LOFLO. This is shown in Figure 3, where only instrumentally valid hourly data from both systems are used. Systematic offsets are clearly present, at unexpected levels. Included in the figure are markers to indicate when calibration and reference tank changes occurred on BASGAM. The correlation between the timing of step changes in the CO_2 difference with changes in the working standards on BASGAM suggests strongly that these frequent changes of standards can inject a level of uncertainty into such records. It is difficult to imagine that this finding could be established without such an overlap experiment between these two analyser systems.

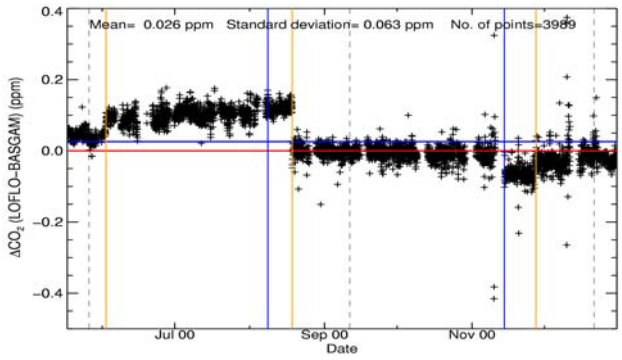

Figure 3. Difference between LOFLO and BASGAM hourly carbon dioxide (CO_2) data for all matching times during the overlap period May to December 2000 as a function of time. Vertical lines indicate calibration and reference tank changes on the BASGAM system: Dashed black - reference tanks; Orange - high-span tanks; Blue - low-span tanks.

Comparison between BASGAM and CO_2 flask data

Flask samples of air are collected at Cape Grim, and analysed in GASLAB for a range of trace species, including the CO_2 mixing ratio [see Langenfelds *et al*. 2003]. It is informative to compare the flask CO_2 data with the *in situ* measurements derived from the BASGAM system. The results of this comparison for the 4-year period 1997-2000 are shown in Figure 4. The flask air samples are typically collected during good baseline conditions, when the ambient CO_2 levels are very stable, and this helps to ensure a realistic comparison between the two methods. Only instrumentally valid data are included in the comparison, and an additional requirement is that the sampling times for both methods must match within 30 minutes. For the purpose of this type of comparison, the hourly average *in situ* data are assigned a sampling time corresponding to the middle of the hourly sampling period (e.g. data for 0800-0900 hours would be assigned a sampling time of 0830 hours). The match time of ±30 minutes then assures that a flask sample result is compared to the hourly *in situ* value measured for the hourly period within which the flask sample was taken.

The overall result of the comparison is encouraging. Through most of the 4-year period, the mean difference between the records is 0.1 ± 0.15 ppm, with the flask values being higher. The only clear exception was in early 1998 where the flask – *in situ* difference was as low as –0.2 ppm. A likely candidate for this feature is a spurious CO_2 assignment to one of the BASGAM standards, although this has not yet been verified.

The main factors responsible for the differences in the bottom panel of Figure 4 probably relate to gas handling procedures involving both flask samples and high pressure cylinders. The flask sample CO_2 values reflect any corrections applied for sample storage effects, which presently include an adjustment of +0.1 ppm to allow for an initial loss of CO_2 observed in test flasks filled from well-characterised standards in high-pressure cylinders [Masarie *et al*. 2001]. Recent evidence indicates that this initial loss of CO_2 includes a contribution due to mass-dependent fractionation of components of air during transfer of air from high-

pressure cylinders (via a pressure-reducing regulator) to flasks [Langenfelds 2002b], which should not be applied to Cape Grim flask data. The precise magnitude of this contribution is not well known at this stage, but it is certainly of the right sign to account for at least part of the mean difference observed in Figure 4. Further tests will be necessary to better quantify contributions from such fractionation effects.

It is also likely that there are fractionation effects present in the BASGAM CO_2 record shown here. As shown recently by Langenfelds [2002b] a mass-dependent fractionation of CO_2 can occur as dry, natural air is decanted from high-pressure cylinders. This effect is almost certainly occurring when the high-span and low-span CO_2-in-air calibration gases flow from the cylinder to the analyser, via their respective pressure-reducing regulators. It is expected that when corrections for these effects are better quantified and applied to the BASGAM data, a further part of the mean difference between flask CO_2 and *in situ* CO_2 will be accounted for.

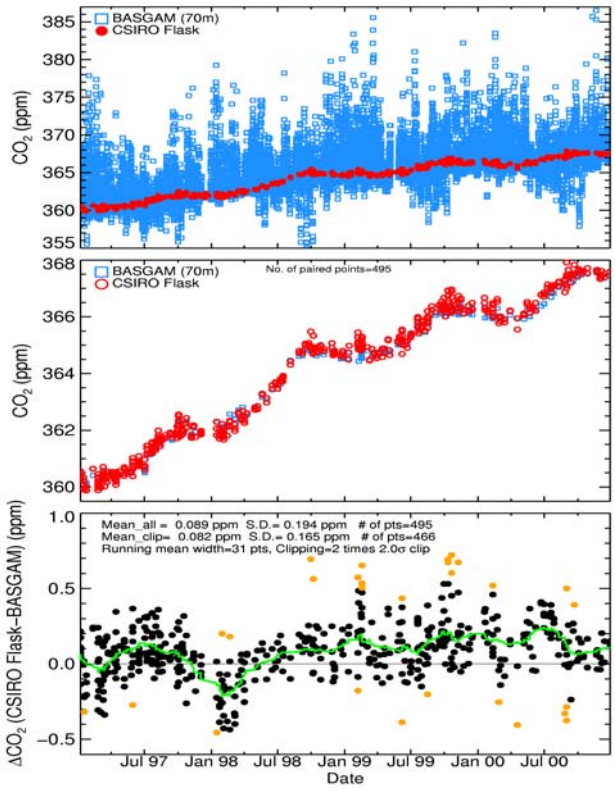

Figure 4. Comparison of CSIRO (GASLAB) flask CO_2 and hourly BASGAM *in situ* CO_2 records for Cape Grim for 1997 to 2000 inclusive. First panel: shows both of the full data sets as time series (Flask - red; *in situ* - blue). Second panel: shows only the matched data points as time series (match window is flask fill time ± 30 minutes). Third panel: shows the difference between the matched flask and *in situ* records as a function of time; orange dots indicate data that lie outside 2 standard deviations about a 31 point running mean (green line).

References

Baines, P. G., and D. L. Murray, Air flow over Cape Grim – a laboratory modelling study for optimum obervation sites, in *Baseline Atmospheric Program (Australia) 1999-2000*, edited by N. W. Tindale, N. Derek, and P. J. Fraser, Bureau of Meteorology and CSIRO Atmospheric Research, Melbourne, Australia, 13-17, 2003.

Da Costa, G. A., and L. P. Steele, A new analyser system for making measurements of atmospheric CO_2, in *Fifth International Carbon Dioxide Conference* [extended abstracts], 8-12 September 1997, Cairns, Queensland, CSIRO Atmospheric Research, Aspendale, Victoria, 43-44, 1997.

Da Costa, G. A., and L. P. Steele, A low-flow analyser system for making measurements of atmospheric CO_2, in *Report of the ninth WMO Meeting of Experts on Carbon Dioxide Concentration and Related Tracer Measurement Techniques*, Aspendale, Australia, edited by R. J. Francey, (Environmental Pollution Monitoring and Research Programme / Global Atmosphere Watch, 132; WMO/TD; no. 952), Secretariat of the World Meteorological Organization, Geneva, Austria, 16-20, 1999.

Francey, R.J., L. P. Steele, R. L. Langenfelds, M. P. Lucarelli, C. E. Allison, D. J. Beardsmore, S. A. Coram, N. Derek, F. R. de Silva, D. M. Etheridge, P. J. Fraser, R. J. Henry, B. Turner, E. D. Welch, D. A Spencer, and L. N. Cooper, Global atmospheric sampling laboratory (GASLAB): supporting and extending the Cape Grim trace gas programs, in *Baseline Atmospheric Program (Australia) 1993*, edited by R. J. Francey, A. L. Dick, and N. Derek, Bureau of Meteorology and CSIRO Division of Atmospheric Research, Melbourne, Australia, 8-29,1996.

Langenfelds, R. L., R. J. Francey, B. C. Pak, L. P. Steele, J. Lloyd, C. M. Trudinger and C. E. Allison, Interannual growth rate variations of atmospheric CO_2 and its $\delta^{13}C$, H_2, CH_4 and CO between 1992 and 1999 linked to biomass burning, *Glob. Biogeochem. Cycles*, 16, 1048, doi:10.1029/2001GB001466, 2002a.

Langenfelds, R.L., Studies of the global carbon cycle using atmospheric oxygen and associated tracers, *PhD Thesis*, University of Tasmania, Hobart, Tasmania, Australia, 2002b.

Langenfelds, R.L., L. P. Steele, L. N. Cooper, D. A. Spencer, P. B. Krummel and B. L. Dunse, Atmospheric methane, carbon dioxide, hydrogen, carbon monoxide and nitrous oxide from Cape Grim flask air samples analysed by gas chromatography, in in *Baseline Atmospheric Program (Australia) 1999-2000*, edited by N. W. Tindale, N. Derek, and P. J. Fraser, Bureau of Meteorology and CSIRO Atmospheric Research, Melbourne, Australia, 76-77, 2003.

Masarie, K.A., R.L. Langenfelds, C.E. Allison, T.J. Conway, E.J. Dlugokencky, R.J. Francey, P.C. Novelli, L.P. Steele, P.P. Tans, B. Vaughn, and J.W.C. White, NOAA/CSIRO Flask Air Intercomparison Experiment: A strategy for directly assessing consistency among atmospheric measurements made by independent laboratories, *J. Geophys. Res*., 106, 20445-20464, 2001.

Tans, P. P., P. S. Bakwin, L. Bruhwiler, T. J. Conway, E. J. Dlugokencky, D. W. Guenther, D. R. Kitzis, P. M. Lang, K. A. Masarie, J. B. Miller, P. C. Novelli, K. W. Thoning, B. H. Vaughn, J. W. C. White, and C. Zhao, Carbon Cycle, Chapter 2 in *Climate Monitoring and Diagnostics Laboratory Summary Report No. 26* 2000-2001, edited by D. B. King and R. C. Schnell, NOAA, Boulder, Colorado, USA, 28-50, 2002.

Thoning, K. W., P. P. Tans and W. D. Komhyr, Atmospheric carbon dioxide at Mauna Loa observatory, 2, Analysis of the NOAA/GMCC data, 1974-1985, *J. Geophys. Res*., 94, 8549-8565, 1989.

4.11. METHYL BROMIDE SATURATIONS IN SURFACE SEAWATER OFF CAPE GRIM

G A Sturrock[1], C R Parr[2,3], C E Reeves[1], S A Penkett[1], P J Fraser[2] and N W Tindale[3]

[1]School of Environmental Sciences, UEA, Norwich NR4 7TJ, U.K.
[2]CSIRO Atmospheric Research, Aspendale, Victoria 3195, Australia
[3]Cape Grim Baseline Air Pollution Station, Bureau of Meteorology, Smithton, Tasmania 7330, Australia

[Supported by DETR-UK /CGBAPS research funds.]

Introduction

The ocean is an important natural source of atmospheric CH_3Br. However there still remains considerable uncertainty in the global strength of this source, which could go some way to explaining the discrepancy between historical atmospheric concentrations derived from firn air data and those calculated from best estimates of source and sink strengths. Much of the uncertainty in the oceanic source strength comes from the large uncertainty in the spatial and temporal distribution of this source. Previously it was thought that open oceans were undersaturated and therefore a net sink of atmospheric CH_3Br, whilst coastal and upwelling waters were supersaturated and thus a net source. However, more recent studies have found supersaturations in open oceans, and coastal waters to sometimes be undersaturated.

This latter result came from a routine investigation of seasonal variations in CH_3Br saturation [Baker *et al.* 1999], the only such study undertaken. Supersaturation during the summer and undersaturation during the remainder of the year were found in the North Sea, a continental shelf sea off England. An analogous seawater measurement program on the coastal waters off NW Tasmania, was established in March 2000. This work is an extension of a preliminary study during SOAPEX2, which was carried out at Cape Grim (January - February 1999), in which CH_3Br was found to be supersaturated. The main purpose of the present study is to establish the temporal extent of this supersaturation and to see if a similar seasonal cycle exists and whether it is reproducible from year to year.

Furthermore, as CH_3Br is both produced and destroyed in the ocean, the role of the ocean in regulating the atmospheric burden of this gas is unresolved. The North/South interhemispheric concentration ratio varies from 1.35±0.04 (April) to 1.1±0.03 (September) [Wingenter *et al.* 1998]. An annual cycle, governed by reaction with seasonally varying hydroxyl (OH) radicals, is observed in atmospheric CH_3Br mixing ratios in the Northern Hemisphere [Wingenter *et al.* 1998] but there is not such a clearly discernable cycle in the Southern Hemisphere [Sturrock *et al.* 2001]. This implies the Southern Hemisphere must have one or more seasonal influences out of phase with OH removal.

Studies are focusing on how seasonal cycling of oceanic CH_3Br, caused by the combination of biological and chemical production/degradation, may contribute to obscuring the expected Southern Hemispheric atmospheric cycle. Knowledge of the magnitude and seasonality of all sources and sinks of CH_3Br are still required to help constrain modelling of the CH_3Br budget.

Seawater sampling

Saturation levels are determined from analysis of a seawater and an air sample which are collected simultaneously from sites alternating between 2 locations: Site 1 at Woolnorth Point and Site 2, situated ~3 miles offshore with a seawater depth of ~50 m. Sampling took place at each site on roughly a monthly basis although on a less regular basis by boat due to inclement weather conditions.

Saturation is calculated using the following equation:

$$\text{Saturation}(\%) = \left[C_w / \left[C_a / H\right]\right] \times 100$$

Where C_w and C_a indicate the concentration of a species in seawater and air respectively, and H is the Henry's law constant. Saturations exceeding 100% are referred to as supersaturations and imply a net flux from the seawater to the atmosphere.

GC-ECD measurements

CH_3Br and various other trace gases in both surface seawater and air samples were analysed with a purge and cryotrap system and GC-ECD, similar to that described in Baker *et al.,* [1999]. The work of Baker *et al.* [1999] included detailed investigations of purging efficiency, blank tests and detector linearity. Briefly, helium gas is used to purge gases from seawater samples (20 ml) contained in a glass purge tower. Water vapour is removed from the resultant gas stream by a glass spiral condenser immersed in an ice bath followed by a Nafion drier. The dried gas is cryofocused on a stainless steel loop prior to injection onto a capillary column by heating the cryotrap to 100°C and detection is achieved by electron capture. All seawater samples were analysed as soon as possible after collection. The same GC-ECD system was used for the analysis of air samples, however, a three-way valve was incorporated to isolate the spiral condenser and purge tower from the air flask sample flow.

A whole air sample (undried) collected at Cape Grim (filled March 2000) serves as a relative standard to ensure internally consistent results can be produced during the entire study. This standard was analysed along with each seawater and air sample to determine the concentration which is then used to calculate saturation levels. This reference standard has been calibrated against the AGAGE GC-MS 'gold' standard (L. Porter, personal communication.) for CH_3Br mixing ratio on the SIO98 scale.

Summary

Preliminary findings revealed CH_3Br to be highly supersaturated in the surface seawater in summer during SOAPEX2. The seawater has continued to be predominantly supersaturated, although there is evidence of a decrease with distance from the shore. The two

routine sampling sites are in coastal waters that are already known to be generally more saturated with respect to CH_3Br. Unresolved at present is how far these persistent CH_3Br supersaturations extend into open ocean areas at this latitude. By extending the measurements to the edge of the continental shelf, an attempt will be made to determine the spatial extent of the observed saturations.

Interannual variations in saturation levels, shown in Figure 1, indicate no reproducible or distinct cycle at the Tasmanian coastal sites, unlike the earlier systematic study in the North Sea [Baker *et al.,* 1999]. Furthermore, undersaturation is observed further offshore during the austral summer of 2000/2001 when the biological processes driving *in situ* CH_3Br production would be expected to contribute most substantially to production. The temperature range encountered during the study in Tasmanian waters is between 12 and 20^{o}C, while the North Sea study covered a larger temperature range (4°C - 18°C) although lower temperatures dominate apart from during the summer months of July - September.

Phytoplankton counts in the North Sea revealed that few species were present until May when the seawater temperature rises (>9°C). Baker *et al.* [1999] showed these coastal waters were predominately undersaturated until the summertime when an increase in water temperature and an associated phytoplankton bloom gave rise to a clear seasonal pattern in CH_3Br saturations. Studies on phytoplankton speciation for the more recent seawater samples collected off Cape Grim from Site 2 (from late November 2000 onwards) are ongoing in association with the University of Tasmania, Hobart to aid intepretation of the seawater data. Initial analysis of the biological data collected during this study is reported in a research paper in this *Baseline*.

Waters in the temperature range 12-20°C have been observed to show the greatest CH_3Br supersaturations [Groszko and Moore 1998; King *et al.* 2000] and likewise in this work, and although indicative of localised production, it is not necessarily extensive. The variation in coastal waters as a source of CH_3Br may potentially be influenced by a temperature regulation in combination with the variability in the biology rather than simply the time of year.

Other potential factors that could influence productivity and CH_3Br supersaturations include wind speed and depth of the ocean surface mixed layer, and nutrient concentrations and upwelling. The ongoing study will look at the relative importance of phytoplankton speciation, nutrients, water temperature, physical mixing and air-sea exchange on CH_3Br production and emission.

References

Baker, J. M., C. E. Reeves, P. D. Nightingale, S. A. Penkett, S. W. Gibb and A. D. Hatton, Biological Production of methyl bromide in the coastal waters of the North Sea and open ocean of the north-east Atlantic, *Mar.Chem,* 64, 267-285, 1999.

Grosko, W. and R. M. Moore, Ocean-atmosphere exchange of methyl bromide: NW Atlantic and Pacific Ocean studies, *J. Geophys. Res.,* 103, 16,737-16,741, 1998.

King, D. B, J. H. Butler, S. A. Montzka, S. A. Yvon-Lewis and J. W. Elkins, Methyl bromide supersaturations, *J. Geophys. Res.,*105, 19,763-19,769, 2000.

Sturrock, G.A, L.W. Porter and P.J. Fraser: In situ measurement of CFC replacement chemicals and halocarbons at Cape Grim: AGAGE GC-MS program, *Baseline Atmospheric Program (Australia) 1997-98,* edited by N. W. Tindale, N. Derek, and R. J. Francey, Bureau of Meteorology and CSIRO Atmospheric Research, Melbourne, Australia, 43-49, 2001.

Wingenter, O. W, C. J.-L. Wang, D. R. Blake and F. S. Rowland, Seasonal variation of tropospheric methyl bromide: Constraints on anthropogenic input, *Geophys. Res. Letts.,* 25, 2797-2800, 1998.

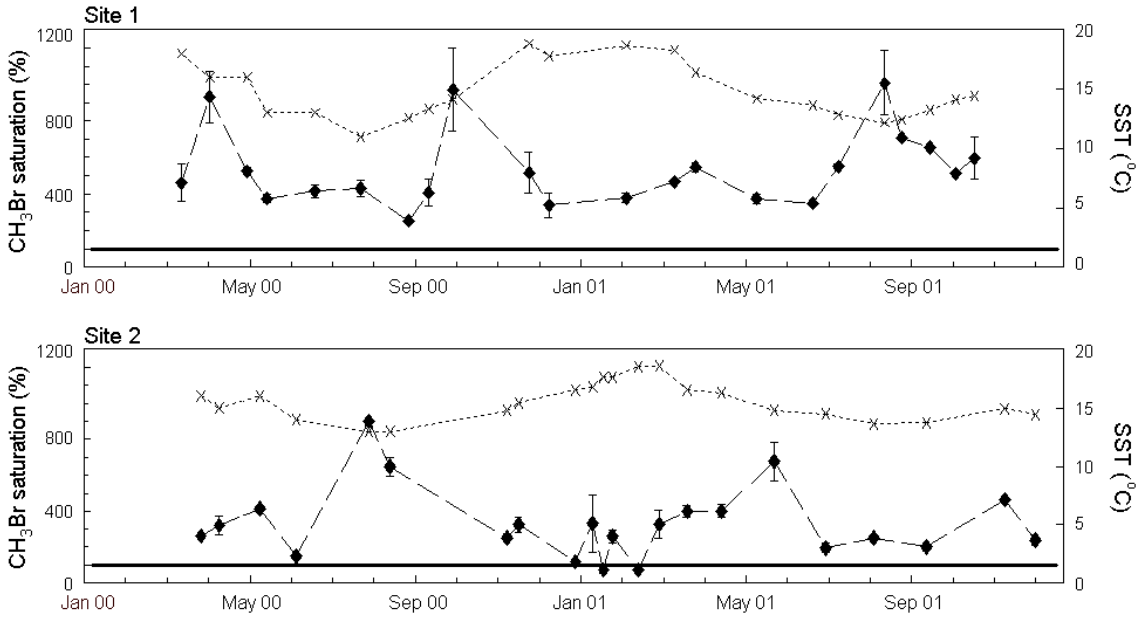

Figure 1. Preliminary data showing the interannual variation in CH_3Br saturations levels (") with associated seawater temperature (x) at the two sites sampled with the equilibrium level (100% saturation) marked as a solid line.

4.12. HALOCARBONS, NITROUS OXIDE, METHANE, CARBON MONOXIDE AND HYDROGEN – THE AGAGE PROGRAM, 1993–2000

P J Fraser[1], P B Krummel[1], L P Steele[1], N Derek[1] and L W Porter[2]

[1]CSIRO Atmospheric Research, Aspendale, Victoria 3195, Australia

[2]Cape Grim Baseline Air Pollution Station, Bureau of Meteorology, Smithton, Tasmania 7330, Australia

[Supported by CGBAPS research funds.]

Introduction

This report summarises *in situ* observations of ten trace gases at Cape Grim which are involved in stratospheric ozone depletion, climate change and tropospheric chemistry. Measurements of CFC-11 (CCl_3F), CFC-12 (CCl_2F_2), CFC-113 (CCl_2FCClF_2), chloroform ($CHCl_3$), methyl chloroform (CH_3CCl_3), carbon tetrachloride (CCl_4), nitrous oxide (N_2O), methane (CH_4), carbon monoxide (CO) and hydrogen (H_2) were made at Cape Grim during 1993-2000, using a composite instrument comprising a Hewlett Packard gas chromatograph (HP5890 GC) with two electron capture detectors (ECDs), a Carle Series 100 GC with a flame ionization detector (FID) and a Trace Analytical RGA2/RGD2 GC with a mercuric oxide reduction detector (MRD), as part of the Advanced Global Atmospheric Gases Experiment (AGAGE) program.

The instrument design and methodologies used to make these observations are discussed in *Baseline 94-95* and Prinn *et al.* [2000]. Data on all AGAGE species except CO have been published [Prinn *et al.* 2000 and references therein; Simmonds *et al*. 2000; O'Doherty *et al*. 2001; Cunnold *et al*. 2002]; all AGAGE data, including CO and H_2, are available from CDIAC (Carbon Dioxide Information Analysis Center, Oak Ridge National Laboratory, Oak Ridge, Tennessee, USA). The data can be accessed on the web at *http://cdiac.ornl.gov/ndps/alegage.html*. To access the Atmospheric Lifetime Experiment (ALE), Global Atmospheric Gases Experiment (GAGE) or AGAGE data, select the appropriate directory. The AGAGE data presented in this report (including CO and H_2) were updated by the Georgia Institute of Technology (GIT) on 17 December 2002.

Standard gases

The concentrations of all species are based on comparisons of ambient air to working standards (G- and J-series, Table 1). The concentrations of all trace gases (Table 2), except CH_4, CO and H_2, are reported in the SIO98 scale [Prinn *et al*. 2000]. The AGAGE CH_4 data are referenced to a gravimetrically prepared CH_4-in-air calibration scale developed by T. Nakazawa and coworkers at Tohoku University, Sendai, Japan, and maintained at CSIRO GASLAB [Cunnold *et al*. 2002]. The AGAGE CO data are referenced to a CSIRO scale closely linked to a CO gravimetric scale developed by NOAA-CMDL [Novelli *et al*. 1991]. The AGAGE H_2 data are referenced to a calibration scale developed by CSIRO GASLAB, boot-strapped from the CH_4 scale [Simmonds *et al*. 2000].

Table 1. Natural air standards used in the AGAGE program (updated by SIO, 26 September 2002) up to the end of 2000. Mole fractions of halocarbons and N_2O are listed in the SIO98 scale; mole fractions of CH_4, CO and H_2 are listed in scales maintained by CSIRO GASLAB.

Tank #	*On*	*CCl_3F (ppt)*	*CCl_2F_2 (ppt)*	*CCl_2FCClF_2 (ppt)*	*CH_3CCl_3 (ppt)*	*CCl_4 (ppt)*	*N_2O (ppb)*	*CH_4 (ppb)*	*$CHCl_3$ (ppt)*	*CO (ppb)*	*H_2 (ppb)*
G-016[a]	Aug 93	260.79	499.09	117.69	102.01	77.22	309.43	1683.37	11.34	60.40	492.20
G-023D[b]	Sep 93	262.86	506.71	112.89	95.16	79.41	309.40	1670.64	6.63	48.70	512.90
G-011D[b]	Feb 94	259.49	493.83	119.96	91.96	74.44	310.38	1670.60	7.02	69.20	513.90
G-025[b]	Mar 94	262.86	508.38	116.50	101.44	80.28	309.83	1682.43	8.89	59.10	508.50
G-029[b]	Jul 94	263.23	512.29	109.09	101.06	81.31	309.86	1654.92	6.07	42.30	518.40
G-031[b]	Nov 94	262.76	512.68	108.37	100.75	81.31	309.77	1662.68	5.77	43.50	518.90
G-035	Apr 95	264.11	517.78	105.49	100.39	81.94	310.75	1679.56	5.42	53.90	529.20
G-039	Sep 95	263.08	519.22	99.96	100.14	82.09	310.47	1670.13	12.03	47.10	523.10
J-005[c]	Apr 96	268.23	537.53	124.81	101.47	84.04	312.46	1787.55	12.12	176.20	531.60
J-011	Nov 96	267.79	536.23	102.13	101.56	83.91	312.22	1794.74	12.37	148.30	530.10
J-018	Aug 97	267.50	535.60	100.45	101.40	84.29	312.05	1782.63	12.88	156.40	502.20
J-023	May 98	265.94	542.73	72.49	99.55	83.53	314.13	1816.49	13.58	178.70	506.50
J-029	Jan 99	265.63	542.15	72.55	99.53	83.59	313.72	1819.16	12.92	165.40	512.90
J-036	Oct 99	265.65	542.10	72.64	98.95	83.42	313.92	1815.03	13.07	165.68	501.86
J-047	Jun 00	262.20	545.63	49.02	97.32	82.00	316.04	1825.91	10.93	153.00	542.20
G-085	Dec 00	257.95	539.20	44.07	94.68	81.97	315.20	1720.77	6.53	58.80	522.10

[a]G series standards are wet, baseline air, cryo-trapped (-196°C) at Cape Grim into evacuated, welded, electropolished 35 L stainless steel tanks; D indicates a cryogenically dried (-78°C) air standard.

[b]Standards used on GAGE and AGAGE simultaneously.

[c]J series standards are natural air from Trinidad Head, California, compressed (Rix pump) into evacuated, welded, electropolished 35 L stainless steel tanks and dried to 10 torr of water vapour.

Table 2. AGAGE monthly mean halocarbon, nitrous oxide, methane, carbon monoxide and hydrogen mixing ratios for 1993-2000, with pollution episodes removed statistically. Annual means are obtained from monthly means, monthly means from individual measurements. The halocarbon and N_2O data are in the SIO98 scale and the methane, carbon monoxide and hydrogen data are in calibration scales maintained by CSIRO GASLAB (see text). Data were updated by GIT on 17 December 2002.

month	*Jan*	*Feb*	*Mar*	*Apr*	*May*	*Jun*	*Jul*	*Aug*	*Sep*	*Oct*	*Nov*	*Dec*	*mean*
CFC-11; CCl_3F (ppt)													
1993								263.4	263.6	263.8	263.8	263.8	
1994	263.8	263.4	263.1	263.2	263.3	263.3	263.6	263.8	264.0	264.0	264.0	263.9	263.6
1995	263.9	263.7	264.1	262.8	262.8	263.0	263.1	263.2	263.3	263.4	263.4	263.4	263.3
1996	263.2	262.9	262.9	263.3	264.1	263.6	263.4	263.4	263.3	263.2	263.1	263.0	263.3
1997	262.9	262.6	262.5	262.6	262.5	262.6	262.6	262.7	262.6	262.4	262.3	262.0	262.5
1998	261.7	261.3	261.1	260.9	261.2	261.5	261.7	261.6	261.7	261.5	261.4	261.3	261.4
1999	261.1	260.8	260.4	260.2	260.2	260.0	260.0	260.1	260.0	259.7	259.6	259.5	260.1
2000	259.3	259.2	258.9	258.7	258.6	258.6	258.7	258.7	258.7	258.6	258.5	258.2	258.7
CFC-12; CCl_2F_2 (ppt)													
1993								509.3	509.7	510.3	510.8	511.2	
1994	511.6	512.7	512.8	513.6	514.1	514.7	515.3	516.0	516.9	517.6	518.2	518.7	515.2
1995	519.1	519.2	519.6	519.6	520.6	520.9	521.5	522.2	522.7	523.0	523.5	523.8	521.3
1996	524.1	524.1	524.8	524.8	526.2	526.1	526.5	527.0	527.5	528.1	528.4	528.7	526.4
1997	529.0	529.2	529.6	530.3	530.8	531.5	531.8	532.4	532.7	532.9	533.1	533.1	531.4
1998	533.0	532.9	533.0	533.2	533.5	533.7	534.6	535.0	535.5	535.6	535.9	536.2	534.3
1999	536.3	536.3	536.2	536.5	536.9	536.9	537.3	537.9	538.0	538.1	538.0	538.3	537.2
2000	538.3	538.5	538.4	538.6	538.9	539.2	539.3	539.7	539.7	540.0	540.2	540.0	539.2
CFC-113; CCl_2FCClF_2 (ppt)													
1993								80.9	80.5	80.3	80.4	80.4	
1994	80.4	80.6	81.0	81.1	81.2	81.3	81.6	81.8	82.0	82.0	82.1	82.0	81.4
1995	82.0	82.0	82.2	82.1	82.0	82.1	82.2	82.2	82.4	82.4	82.4	82.5	82.2
1996	82.4	82.4	82.4	82.6	82.7	82.7	82.8	82.8	82.8	82.9	82.9	82.8	82.7
1997	82.8	82.6	82.6	82.6	82.6	82.6	82.7	82.9	83.2	83.2	83.2	83.1	82.9
1998	83.1	83.0	82.9	82.8	82.7	82.7	82.8	82.8	82.8	82.8	82.8	82.8	82.8
1999	82.8	82.6	82.5	82.4	82.3	82.3	82.3	82.3	82.3	82.1	82.1	82.0	82.3
2000	81.9	81.8	81.8	81.8	81.8	81.8	81.5	81.6	81.6	81.6	81.6	81.6	81.7
Chloroform; $CHCl_3$ (ppt)													
1993											7.2		
1994	7.0	6.5	5.6	5.5	5.8	6.3	6.4	6.5	6.5	6.5	6.2	6.2	6.2
1995	6.0	5.4	5.6	5.4	5.6	6.0	6.1	6.4	6.5	7.1	6.8	5.8	6.1
1996	5.7	5.3	5.1	5.3	6.3	7.1	6.9	6.8	6.9	6.7	6.1	5.6	6.2
1997	5.3	5.0	5.0	5.3	5.7	6.1	6.4	6.7	6.9	6.6	6.1	5.7	5.9
1998	5.3	5.1	5.0	5.3	5.8	6.4	6.7	7.0	7.0	6.9	6.5	5.9	6.1
1999	5.6	5.2	5.1	5.2	5.8	6.4	6.7	6.8	6.9	6.5	6.7	5.7	6.0
2000	5.2	5.1	5.1	5.3	5.8	6.2	6.5	6.7	6.6	6.4	5.9	5.4	5.8
Methyl chloroform; CH_3CCl_3 (ppt)													
1993								115.4	115.1	115.3	114.8	114.1	
1994	112.9	111.5	109.8	109.2	109.2	109.1	108.3	107.9	107.5	106.5	105.5	103.9	108.4
1995	102.3	101.1	100.1	100.0	99.7	99.4	99.2	98.6	97.9	96.8	95.5	93.8	98.7
1996	92.0	90.9	89.6	89.3	88.7	88.5	87.8	86.9	86.2	85.1	83.7	82.5	87.6
1997	80.7	79.0	78.2	77.2	76.6	76.0	75.4	74.8	74.1	73.0	71.9	70.7	75.6
1998	69.3	68.2	66.5	65.9	65.2	64.6	64.1	63.5	62.7	61.9	60.8	59.5	64.3
1999	58.3	57.0	56.3	55.5	54.8	54.5	53.9	53.2	52.6	52.0	51.4	50.3	54.2
2000	49.1	48.1	47.6	46.8	46.2	45.7	45.3	44.9	44.5	43.7	42.8	42.2	45.6
Carbon tetrachloride; CCl_4 (ppt)													
1993								101.5	101.5	101.4	101.4	101.5	
1994	101.5	101.5	101.3	101.2	101.1	100.8	100.7	100.5	100.4	100.4	100.4	100.4	100.9
1995	100.4	100.3	100.2	100.0	100.1	99.9	99.8	99.7	99.6	99.6	99.6	99.7	99.9
1996	99.6	99.5	99.5	99.2	99.2	99.0	98.8	98.7	98.5	98.5	98.5	98.5	98.9
1997	98.6	98.5	98.5	98.4	98.4	98.3	98.2	98.1	98.1	98.0	97.9	97.9	98.2
1998	97.7	97.5	97.5	97.3	97.2	97.1	97.1	96.9	96.9	96.8	96.8	96.8	97.1
1999	96.8	96.7	96.6	96.4	96.3	96.1	96.0	96.0	95.8	95.7	95.6	95.7	96.1
2000	95.7	95.7	95.6	95.5	95.4	95.3	95.1	95.0	94.8	94.8	94.9	94.8	95.2
Nitrous oxide; N_2O (ppb)													
1993								309.8	309.9	310.0	310.1	310.1	
1994	310.2	310.0	310.1	310.2	310.2	310.2	310.2	310.2	310.5	310.6	310.7	310.9	310.3
1995	310.9	310.7	310.5	310.6	310.8	310.8	310.8	311.0	311.1	311.3	311.4	311.5	310.9
1996	311.5	311.5	311.5	311.3	311.4	311.5	311.7	311.8	311.9	312.0	312.1	312.3	311.7
1997	312.4	312.3	312.3	312.3	312.4	312.5	312.6	312.8	313.0	313.0	313.1	313.2	312.6
1998	313.2	313.1	312.9	312.8	312.9	313.0	313.3	313.5	313.7	313.8	313.9	314.1	313.4
1999	314.2	314.1	314.0	314.0	314.0	314.0	314.2	314.4	314.5	314.5	314.6	314.7	314.3
2000	314.8	314.8	314.7	314.7	314.7	314.8	315.0	315.2	315.3	315.5	315.6	315.6	315.0

Table 2. continued……..

month	*Jan*	*Feb*	*Mar*	*Apr*	*May*	*Jun*	*Jul*	*Aug*	*Sep*	*Oct*	*Nov*	*Dec*	*mean*
Methane; CH_4 (ppb)													
1993								1701.3	1701.8	1700.8	1696.1	1688.4	
1994	1680.7	1674.9	1675.7	1681.5	1687.9	1695.8	1701.8	1705.7	1708.3	1707.5	1703.9	1697.2	1693.4
1995	1691.3	1686.0	1685.5	1688.9	1696.7	1702.1	1706.1	1710.8	1714.2	1714.5	1711.4	1702.1	1700.8
1996	1692.2	1687.2	1686.9	1690.2	1698.5	1704.2	1709.1	1712.3	1713.8	1713.3	1709.4	1702.2	1701.6
1997	1695.0	1691.3	1692.8	1700.6	1709.4	1716.1	1720.9	1725.3	1727.2	1724.6	1720.7	1712.3	1711.3
1998	1704.1	1698.9	1698.6	1702.5	1711.1	1719.2	1726.5	1733.1	1734.8	1733.9	1730.1	1722.2	1717.9
1999	1715.2	1710.3	1711.2	1717.7	1724.7	1730.8	1736.3	1740.6	1742.8	1740.7	1736.4	1727.8	1727.9
2000	1718.6	1713.1	1713.9	1718.8	1726.3	1732.8	1738.9	1742.5	1742.6	1740.7	1735.5	1726.9	1729.2
Carbon monoxide; CO (ppb)													
1993								60.9	67.0	68.8	59.4	48.0	
1994	40.9	38.7	40.0	43.3	46.8	51.1	52.4	55.4	59.5	61.6	57.9	51.3	49.9
1995	45.6	41.5	40.0	40.7	45.0	47.9	53.0	58.4	67.4	76.2	70.5	55.5	53.5
1996	42.4	37.1	36.0	42.5	46.4	50.2	54.4	55.9	59.0	60.3	55.5	47.3	48.9
1997	40.4	36.7	37.5	41.7	47.2	51.9	56.5	60.0	64.2	65.0	61.5	55.0	51.5
1998	47.4	42.4	42.1	45.1	51.0	58.5	63.5	69.4	71.4	69.8	63.0	53.4	56.4
1999	45.4	41.5	41.1	44.6	47.2	52.0	56.7	60.4	66.7	70.4	63.3	51.1	53.4
2000	44.6	41.2	41.3	44.4	49.3	52.9	57.5	60.0	59.7	58.7	55.1	47.3	51.0
Hydrogen; H_2 (ppb)													
1993								502.9	506.7	513.1	516.4	518.6	
1994	521.7	520.4	520.3	517.5	513.6	508.4	507.9	508.6	511.2	517.8	522.3	526.9	516.4
1995	526.0	528.1	528.5	523.7	515.5	514.3	515.1	514.2	516.0	521.4	527.3	532.6	521.9
1996	533.4	533.9	530.4	526.5	521.7	515.0	512.4	514.4	515.0	520.2	523.4	526.9	522.8
1997	527.7	527.9	527.8	524.8	521.2	513.8	513.7	514.7	517.1	522.5	527.2	532.3	522.5
1998	536.7	539.1	538.6	535.7	531.5	527.9	525.6	523.4	527.6	532.4	533.8	540.0	532.7
1999	539.0	539.2	538.9	535.1	529.3	525.3	523.6	524.0	524.8	531.4	534.1	535.3	531.7
2000	537.3	533.9	533.8	530.7	528.3	522.1	519.9	520.1	522.8	524.3	527.9	531.5	527.7

Table 3. The average annual growth rates in CCl_3F, CCl_2F_2, CCl_2FCClF_2, CH_3CCl_3, CCl_4, N_2O, CH_4, $CHCl_3$, CO and H_2 observed at Cape Grim from the AGAGE program over the period 1993 to 2000. The uncertainties are one standard deviation.

Year	*CCl_3F (ppt yr^{-1}) (% yr^{-1})*	*CCl_2F_2 (ppt yr^{-1}) (% yr^{-1})*	*CCl_2FCClF_2 (ppt yr^{-1}) (% yr^{-1})*	*$CHCl_3$ (ppt yr^{-1}) (% yr^{-1})*	*CH_3CCl_3 (ppt yr^{-1}) (% yr^{-1})*	*CCl_4 (ppt yr^{-1}) (% yr^{-1})*	*N_2O (ppb yr^{-1}) (% yr^{-1})*	*CH_4 (ppb yr^{-1}) (% yr^{-1})*	*CO (ppb yr^{-1}) (% yr^{-1})*	*H_2 (ppb yr^{-1}) (% yr^{-1})*
1993	0.32±0.03	7.51±0.002	1.41±0.09	-0.43±0.04	-10.14±0.41	-0.87±0.05	0.69±0.03	7.14±0.10	-2.09±0.92	5.03±0.28
	0.12±0.01	1.47±0.003	1.75±0.11	-6.24±0.52	-8.83±0.27	-0.85±0.05	0.22±0.01	0.42±0.01	-3.99±1.77	0.98±0.06
1994	0.04±0.31	7.03±0.404	1.37±0.30	-0.68±0.16	-9.23±0.16	-1.07±0.07	0.58±0.03	8.20±0.57	-1.15±2.90	5.47±0.64
	0.01±0.12	1.37±0.083	1.68±0.37	-10.45±2.35	-8.53±0.31	-1.07±0.06	0.19±0.01	0.48±0.03	-2.23±5.69	1.06±0.12
1995	-0.36±0.26	5.24±0.448	0.39±0.10	0.20±0.19	-10.23±0.42	-0.83±0.08	0.73±0.04	3.11±3.17	2.90±3.45	4.34±2.03
	-0.14±0.10	1.00±0.089	0.48±0.13	3.20±3.03	-10.38±0.74	-0.83±0.08	0.23±0.01	0.18±0.19	5.54±6.54	0.83±0.39
1996	-0.20±0.36	5.17±0.256	0.36±0.11	-0.18±0.24	-11.85±0.35	-0.95±0.14	0.90±0.09	4.43±4.36	-5.06±2.66	-3.23±1.32
	-0.08±0.14	0.98±0.046	0.44±0.13	-2.88±3.74	-13.55±0.91	-0.96±0.14	0.29±0.03	0.26±0.26	-9.87±5.15	-0.62±0.25
1997	-1.13±0.09	4.02±0.858	0.14±0.04	-0.14±0.27	-11.74±0.26	-0.81±0.17	0.83±0.12	8.66±2.51	6.92±2.01	7.41±4.10
	-0.43±0.04	0.76±0.163	0.17±0.05	-2.27±4.48	-15.53±0.35	-0.83±0.17	0.27±0.04	0.51±0.15	13.27±3.65	1.42±0.78
1998	-0.95±0.15	2.87±0.172	-0.25±0.16	0.34±0.15	-10.94±0.30	-1.01±0.06	0.86±0.09	9.91±2.74	0.10±3.26	4.01±4.17
	-0.37±0.06	0.54±0.031	-0.31±0.19	5.45±2.43	-17.03±0.40	-1.04±0.06	0.27±0.03	0.58±0.16	0.17±5.79	0.76±0.79
1999	-1.56±0.09	2.41±0.379	-0.67±0.06	-0.24±0.08	-9.26±0.55	-1.49±0.16	0.75±0.08	5.44±4.18	-2.40±0.58	-2.02±0.30
	-0.60±0.03	0.45±0.071	-0.82±0.07	-3.81±1.31	-17.09±0.18	-1.55±0.17	0.24±0.03	0.32±0.24	-4.39±1.03	-0.38±0.06
2000	-1.53±0.12	1.44±0.196	-0.62±0.03	-0.32±0.02	-8.15±0.22	-0.45±0.37	0.77±0.03	-0.94±0.15	-1.57±2.28	-4.22±0.47
	-0.59±0.05	0.27±0.036	-0.76±0.03	-5.35±0.43	-17.90±0.46	-0.47±0.39	0.24±0.01	-0.05±0.01	-2.98±4.37	-0.80±0.09

Instrument maintenance/modifications

1999

In March the palladium cell in the hydrogen purifier for the GC-FID was bypassed (it had ruptured) with no apparent effect on the methane data. The palladium catalyst was regenerated in November. In May the Trace Analytical UV lamp was replaced (GC-MRD). During June, July, October and November problems were experienced with contaminated carrier gas (argon/methane) for the GC-ECD. In August, the Aadco zero air generator was serviced (GC-FID) – the purification reactor, solenoid, check valves and timer were replaced. In September an electronic timer was installed in the Aadco zero air generator, replacing the electro-mechanical unit. A Supelco catalytic carrier gas purifier was installed in the argon/methane (GC-ECD) supply line in October, later switched off in December when no longer required. The hydrogen generator (GC-FID) was serviced (sticky non-return valve) in December.

2000

The hydrogen generator (GC-FID) was serviced in January and March (sticky non-return valve). Sample pump contamination (CFC-11) was detected in March and pump modifications were made in May (installed an isolating coil to reduce 'dead' volume problems) and November (isolation coil and pressure relief valve replaced by back-pressure regulator). The Aadco zero air generator was serviced (GC-FID) in April and October

(failed solenoid valve). The GC-MRD oven temperature controller failed and was replaced in July. In July and August new regulators (Veriflo model 959 Magnum) were installed on the SIO working standard tank and high carbon monoxide standard tank. Blank tests in August showed no contamination from the new Veriflo regulators. Argon/methane carrier gas (GC-ECD) was changed from 10% to 5% in August. During September problems were experienced with contaminated carrier gas (argon/methane) for the GC-ECD. The Supelco catalytic purifier (argon/methane) was switched on in September and charcoal traps were also installed, initially upstream of the SIO clean-up trap, later (October) downstream. In November a molecular sieve trap was installed between the SIO trap and the charcoal trap (argon/methane – GC-ECD).

AGAGE data

Identification of pollution

The identification of pollution in the AGAGE data is achieved using an objective, automated algorithm [Prinn *et al*. 2000]. The algorithm considers a 4-month period centred on each observation. After removal of a second-order polynomial fit to the data in this period, the algorithm seeks to identify a statistically normal distribution of unpolluted (baseline) mole fractions over this period. This is achieved by iteratively removing (and labelling as pollution) those mole fractions which exceed the median plus 2.5 standard deviations. Simultaneously, the algorithm fits a normal distribution to these baseline values to produce a mean and standard deviation of the distribution. Further checks using standard synoptic analyses and back trajectory calculations ensure that the pollution events so identified are meteorologically reasonable.

The data

The AGAGE monthly mean halocarbon, N_2O, CH_4, CO and H_2 baseline data (pollution episodes removed) for 1993-2000 are presented in Table 2. Figures 1-4 show AGAGE total (baseline monthly means and non-baseline) data where available. The average annual growth rates in CCl_3F, CCl_2F_2, CCl_2FCClF_2, $CHCl_3$, CH_3CCl_3, CCl_4, N_2O, CH_4, CO and H_2 observed at Cape Grim from the AGAGE program over the period 1993 to 2000 are listed in Table 3 and shown in Figure 5. The growth rates are calculated using the curve fitting techniques of Thoning *et al*. [1989], by finding a long-term trend curve with 650-day smoothing and seasonal cycles removed. The derivative of the long-term trend curve is then taken to give an instantaneous growth rate curve. The annual averages are then found from this curve.

Chlorofluorocarbons

CFC-11 (CCl_3F)

The annual average CCl_3F mixing ratios in 1999 and 2000 were 260.1 and 258.7 ppt respectively. The 1998-99 and 1999-2000 changes were -1.3 and -1.4 ppt respectively. These are the largest decreases (0.5% yr^{-1}) in CCl_3F observed at Cape Grim, but larger decreases are expected in the future, up to 2% per year when global emissions are near zero.

A distinct feature of the pre-1995 data was the occurrence of CCl_3F (Figure 1a) pollution episodes, particularly in winter. These are largely found in air masses at Cape Grim that had previously passed over Melbourne. The data suggest that the emissions of CCl_3F into the Melbourne atmosphere have declined significantly since 1994, in line with the Montreal Protocol total phase-out of the consumption of CFCs from the beginning of 1996. Melbourne emissions of CCl_3F in 1999-2000 averaged about 30-40 tonnes yr^{-1} [Dunse *et al*. 2001, 2002].

CFC-12 (CCl_2F_2)

The annual average CCl_2F_2 mixing ratios in 1999 and 2000 were 537.2 and 539.2 ppt respectively and the 1998-99 and 1999-2000 increases were 2.9 and 2.0 ppt respectively. These are the smallest increases in CCl_2F_2 observed at Cape Grim and continue a slowdown in growth of CCl_2F_2 first observed in 1988-89. The data indicate that CCl_2F_2 levels should stop growing in 2-3 years. The intensities of CCl_2F_2 pollution episodes at Cape Grim have declined, but not disappeared, compared to the mid-1980s (Figure 1b). There are remaining emissions of CCl_2F_2 in Melbourne, presumably from old refrigeration and auto-air conditioning systems. Melbourne emissions of CCl_2F_2 in 1999-2000 averaged about 90-120 tonnes yr^{-1} [Dunse *et al*. 2001, 2002].

CFC-113 (CCl_2FCClF_2)

The annual average CCl_2FCClF_2 mixing ratios in 1999 and 2000 were 82.3 and 81.7 ppt respectively and the 1998-99 and 1999-2000 changes were -0.5 and -0.6 ppt respectively. The data suggest that the levels of CCl_2FCClF_2 in the atmosphere have started to decline, the second CFC, along with CCl_3F, to do so. Significant emissions of CCl_2FCClF_2 in Melbourne appear to be small (less than 10 tonnes yr^{-1}) after 1995, based on the CCl_2FCClF_2 pollution episode data observed at Cape Grim (Figure 1c) [Dunse *et al*. 2001, 2002].

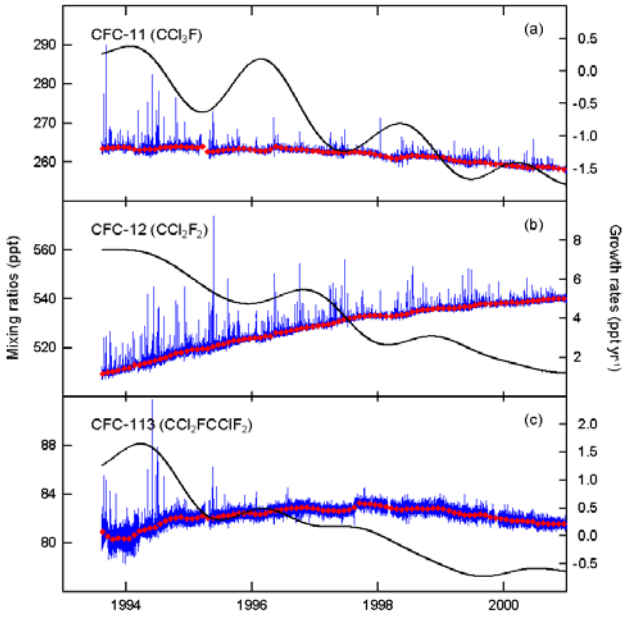

Figure 1. Total (blue) and baseline monthly mean (♦) *in situ* observations of CFCs (ppt) made at Cape Grim on the AGAGE HP5890 gas chromatograph over the period 1993-2000. (a) CFC-11 (CCl_3F, silicone column); (b) CFC-12 (CCl_2F_2, Porasil C column) and (c) CFC-113 (CCl_2FCClF_2, silicone column). The black line represents growth rates (ppt yr^{-1}).

Chlorocarbons

Chloroform ($CHCl_3$)

The annual average $CHCl_3$ mixing ratios in 1999 and 2000 were 6.0 and 5.8 ppt respectively and the 1998-99 and 1999-2000 changes were 0.0 and -0.2 ppt respectively. The AGAGE background $CHCl_3$ data (1993-2000) do not show a long-term trend (Figure 2a). The non-baseline data at Cape Grim show frequent episodes of elevated mixing ratio from local and mainland sources, both natural and anthropogenic. The baseline and non-baseline data show seasonality of different phases, reflecting the roles of background seasonal destruction by hydroxyl radicals and seasonally-dependent local sources [Cox *et al*. 2003; O'Doherty *et al*. 2001]. Melbourne appears to be a significant source of $CHCl_3$, approximately 600 tonnes yr^{-1} [Dunse *et al*. 2001, 2002].

Methyl chloroform (CH_3CCl_3)

The annual average CH_3CCl_3 mixing ratios in 1999 and 2000 were 54.2 and 45.6 ppt respectively and the 1998-99 and 1999-2000 decreases were -10.2 and -8.6 ppt respectively. The magnitude of the decreases, in ppt, over the past four years have declined (-11.9, 1996-1997; -8.5, 1999-2000) but the percentage decline has been stable at 17% for 1998-1999 and 1999-2000, close to the expected maximum decrease of about 20% per year, indicating that global emissions are close to zero. Significant emissions of CH_3CCl_3 in Melbourne appeared to stop after 1997, based on the CH_3CCl_3 pollution episode data observed at Cape Grim (Figure 2b) [Dunse *et al*. 2001, 2002]. The current Melbourne CH_3CCl_3 source appears to be small, less than 20 tonnes yr^{-1}.

Carbon tetrachloride (CCl_4)

The annual average CCl_4 mixing ratios in 1999 and 2000 were 96.0 and 94.9 ppt respectively and the 1998-99 and 1999-2000 decreases were -1.1 ppt for both. The decreases over the six-year period (1994-2000) have stabilised at 1.0 ppt, currently 1% yr^{-1}. The maximum decrease possible is about 2% per year if global emissions were close to zero. CCl_4 emissions (Figure 2c) for Melbourne have not been detected since 1996 [Dunse *et al*. 2001]; they are probably less than 10 tonnes yr^{-1}.

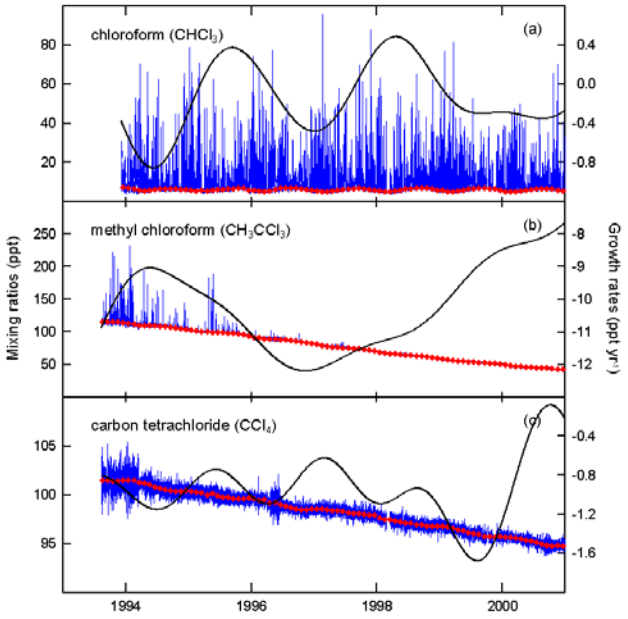

Figure 2. Total (blue) and baseline monthly mean (♦) *in situ* observations of chlorocarbons (ppt) made at Cape Grim on the silicone column of the AGAGE HP5890 gas chromatograph over the period 1993-2000. (a) chloroform ($CHCl_3$), (b) methyl chloroform (CH_3CCl_3) and (c) carbon tetrachloride (CCl_4). The black line represents growth rates (ppt yr^{-1}).

Nitrous oxide (N_2O)

The annual average N_2O mixing ratios in 1999 and 2000 were 314.3 and 315.0 ppb respectively and the 1998-99 and 1999-2000 increases were 0.9 and 0.8 ppb respectively. The increases over the six year period (1994-2000) have averaged 0.8 ppt yr^{-1}, currently 0.25±0.04 % per year. The 22 year (1978-2000) average increase is 0.7±0.5 ppb yr^{-1}. The pollution data (Figure 3a) indicate that there is a poorly understood source of N_2O in the Melbourne/Port Phillip region of about 10-15 ktonnes yr^{-1} [Dunse *et al*. 2001, 2002].

Methane (CH_4)

The annual average CH_4 mixing ratios in 1999 and 2000 were 1728.0 and 1729.2 ppb respectively and the 1998-99 and 1999-2000 increases were 10.1 and 1.2 ppb respectively. The 1999-2000 growth rate of 1.2 ppb is the lowest since 1995-1996 (0.9 ppb) and 1992-1993 (-0.9 ppb). There are significant CH_4 pollution

events observed at Cape Grim (Figure 3b), largely in air influenced by Melbourne CH_4 sources (natural gas, land-fills, sewerage treatment etc). The average intensity of the pollution events up to 1997 appears to be approximately constant in time. In 1998 the average pollution episodes appear to be less intense than in previous years. Emissions from Melbourne appear to be increasing (around 150 ktonnes yr^{-1} in 1995-1996) to 250 ktonnes in 1999-2000 [Dunse *et al*. 2001, 2002].

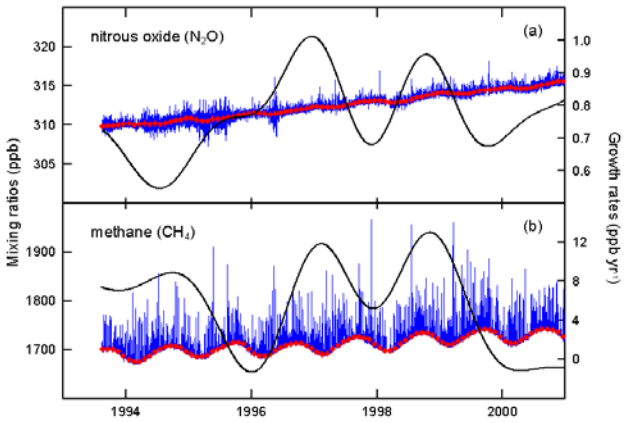

Figure 3. Total (blue) and baseline monthly mean (♦) *in situ* observations of (a) nitrous oxide (N_2O; ppb) measured on the Porasil C column of the HP5890 gas chromatograph and (b) methane (CH_4; ppb) measured on the molecular sieve 5A column of the Carle gas chromatograph at Cape Grim over the period 1993-2000. The black line represents growth rates (ppb yr^{-1}).

Carbon monoxide (CO)

The annual average CO mixing ratio was 53.3 ppb in 1999 and 51.0 in 2000. The general features of the data (Figure 4a) are: (i) a distinct seasonality with a minimum concentration in late summer, reflecting enhanced destruction by hydroxyl radical and (ii) the regular observation of CO pollution episodes at Cape Grim, usually associated with air that had previously passed over Melbourne. The average intensity of the pollution events appears to be approximately constant in time.

Hydrogen (H_2)

The annual average H_2 mixing ratio was 531.6 ppb in 1999 and 527.7 ppb in 2000. The general features of the data (Figure 4b) are: (i) a distinct seasonality with a minimum concentration in winter and a maximum in late summer, reflecting the major photochemical H_2 source in the atmosphere [Simmonds *et al*. 2000], (ii) the regular observation of elevated, with respect to baseline, H_2 levels at Cape Grim, usually associated with air that had previously passed over Melbourne (unidentified source, 5-15 ktonnes yr^{-1}) [Dunse *et al*. 2001, 2002] and (iii) the regular observation of reduced, with respect to baseline, H_2 levels at Cape Grim, usually associated with air that had previously passed over the rural mainland (soil H_2 sink).

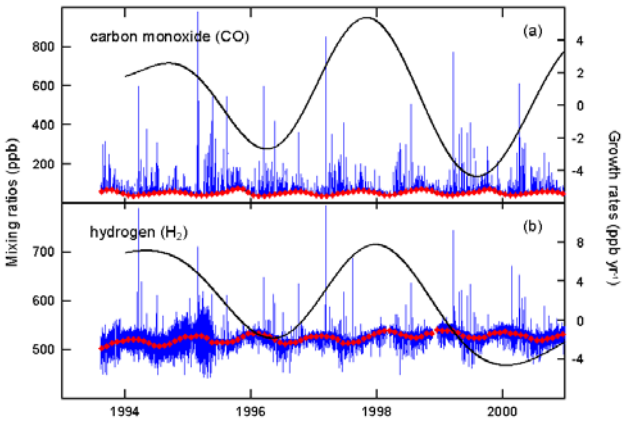

Figure 4. Total (black) and baseline monthly mean (♦) *in situ* observations of (a) carbon monoxide (CO; ppb) and (b) hydrogen (H_2; ppb) measured on the molecular sieve 5A column of the Trace Analytical gas chromatograph at Cape Grim over the period 1993-2000. The black line represents growth rates (ppb yr^{-1}).

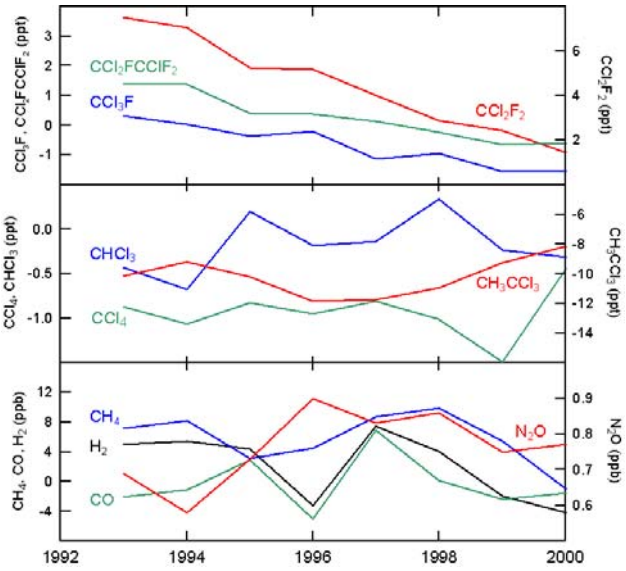

Figure 5. The average annual growth rates observed at Cape Grim from the AGAGE program over the period 1993 to 2000. (a) CCl_3F (—), CCl_2F_2 (—), CCl_2FCClF_2 (—); (b) CH_3CCl_3 (—), CCl_4 (—), $CHCl_3$ (—); (c) N_2O (—), CH_4 (—), CO (—)) and H_2 (—).

References

Cox, M. L., G. A. Sturrock, P. J. Fraser, S. Siems, P. Krummel, and S. O'Doherty, Regional Sources of Methyl Chloride, Chloroform and Dichloromethane Identified from AGAGE Observations at Cape Grim, Tasmania, 1998-2000, *J. Atmos. Chem*., in press, 2003.

Cunnold, D. M., L. P. Steele, P. J. Fraser, P. G. Simmonds, R. G. Prinn, R. F. Weiss, L. W. Porter, S. O'Doherty, R. L. Langenfelds, P. B. Krummel, H. J. Wang, L. Emmons. X. X. Tie, and E. J. Dlugokencky, *In situ* measurements of atmospheric methane at GAGE/AGAGE sites during 1985–2000 and resulting source inferences, *J. Geophys. Res.*, 107, doi:10.1029/2001JD001226, 2002.

Dunse, B. L., L. P. Steele, P. J. Fraser and S. R. Wilson, An analysis of Melbourne pollution episodes observed at Cape Grim from 1995-1998, in *Baseline Atmospheric Program (Australia) 1997-98*, edited by N. W. Tindale, N. Derek and R. J. Francey, Bureau of Meteorology and CSIRO Atmospheric Research, Melbourne, Australia, 34-42, 2001.

Dunse, B. L., Investigation of urban emissions of trace gases by use of atmospheric measurements and a high-resolution atmospheric transport model, *Ph.D. Thesis*, University of Wollongong, Wollongong, Australia, 298 p., 2002.

Novelli, P. C., J. W. Elkins, and L. P. Steele, The development and evaluation of a gravimetric reference scale for measurements of atmospheric carbon monoxide, *J. Geophys. Res*., 96, 13,109-13,121, 1991.

O'Doherty, S., P. G. Simmonds, D. M. Cunnold, H. J. Wang, G. A. Sturrock, P. J. Fraser, D. Ryall, R. G. Derwent, R. F. Weiss, P. Salameh, B. R. Miller, and R. G. Prinn, In situ chloroform measurements at Advanced Global Atmospheric Gases Experiment atmospheric research stations from 1994 to 1998, *J. Geophys. Res.*, 106, 20,429-20,444, 2001.

Prinn, R. G., R. F. Weiss, P. J. Fraser**,** P. G. Simmonds, D. M. Cunnold, F. N. Alyea, S. O'Doherty, P. Salameh, B. R. Miller, J. Huang, R. H. J. Wang, D. E. Hartley, C. Harth, L. P. Steele, G. Sturrock, P. M. Midgley, and A. McCulloch, A history of chemically and radiatively important gases in air deduced from ALE/GAGE/AGAGE, *J. Geophys. Res.*, 105, 17,751-17,792, 2000.

Simmonds, P. G., R. G. Derwent, S. O'Doherty, D. B. Ryall, L. P. Steele, R. L. Langenfelds, P. Salameh, H. J. Wang, C. H. Dimmer, and L. E. Hudson, Continuous high-frequency observations of hydrogen at the Mace Head baseline atmospheric monitoring station over the 1994-1998 period. *J. Geophys. Res*., 105, 12,105-12,121, 2000.

Thoning, K. W., P. P. Tans and W. D. Komhyr, Atmospheric carbon dioxide at Mauna Loa Observatory, 2, Analysis of the NOAA/GMCC data, 1974 - 1985, *J. Geophys. Res.,* 94, 8549-8565, 1989.

4.13. HCFCS, HFCS, HALONS, MINOR CFCS AND HALOMETHANES – THE AGAGE *IN SITU* GC-MS PROGRAM AT CAPE GRIM, 1998-2000

P J Fraser[1], L W Porter[2], P B Krummel[1], B Dunse[1], N Derek[1] and G A Sturrock[3]

[1]CSIRO Atmospheric Research, Aspendale, Victoria 3195, Australia

[2]Cape Grim Baseline Air Pollution Station, Bureau of Meteorology, Smithton, Tasmania 7330, Australia

[3]School of Environmental Science, University of East Anglia, Norwich, UK

[Supported by CGBAPS research funds.]

Introduction

Gas chromatography-mass spectrometry (GC-MS) instruments were installed at Mace Head, Ireland, and Cape Grim, Tasmania, in late-1997 as part of the AGAGE global GC-MS program for the measurement of chlorofluorocarbon (CFC) replacements – hydrochlorofluorocarbons (HCFCs) and hydrofluorocarbons (HFCs) – as well as halons, minor CFCs and halomethanes. The Cape Grim instrument, its installation and operation, are discussed in detail in Sturrock *et al*. [2001a,b], along with initial observations of these halocarbon species. A summary of the AGAGE GC-MS program has been published in Prinn *et al*. [2000]. The AGAGE halomethane data (methyl chloride, CH_3Cl; methyl iodide, CH_3I; dichloromethane, CH_2Cl_2; chloroform, $CHCl_3$) have been published or accepted for publication [Cox 2001; O'Doherty *et al*. 2001; Cohan *et al*. 2003; Cox *et al*. 2003a, b].

This report summarises the major instrumental problems encountered in the AGAGE GC-MS program at Cape Grim during 1999-2000 and presents and discusses the HCFC, HFC, halon, minor CFCs and halomethane data for 1998-2000.

Instrument maintenance/modifications

1999

The MS filament was switched to the alternate in February; this filament burnt out in March and the MS operation was continued by switching to the alternate. New GC-MS data processing software was installed in March. The GC-MS turbo-molecular vacuum pump failed in April and was replaced in May. ADS microtrap heating problems were experienced in May and repaired. In June the MS ion source was cleaned, the MS filaments replaced and the operating system upgraded. In August the zero-air supply was changed from an Aadco generator to a Linde cylinder. The fore-line vacuum failed in December and was replaced by the spare pump during the same month. In December the MS was cleaned, the filaments replaced and the vacuum pump oil was changed.

2000

The original fore-line vacuum pump was repaired and re-installed in January. A new GC-MS operating system was installed in March. In May the ADS Peltier cooling units were replaced. In June the GC capillary column broke and was repaired. Also in June, the MS was cleaned, the filaments replaced and the vacuum pump oil was changed. The fore-line vacuum pump failed in July and was replaced with the spare pump. The repaired vacuum pump was re-instated in August. In October the working standard regulator (Veriflo) was changed and returned to the manufacturer after showing signs of methyl chloroform contamination.

Standard gases

AGAGE GC-MS data are reported in a number of standard scales (Table 1). SIO98 is the long-term AGAGE standard scale and UB00 is an interim AGAGE standard scale. The origin and propagation of these scales are described in Prinn *et al*. 2000 and Sturrock *et al*. 2001a,b. At present AGAGE has adopted the NOAA-CMDL standard scale for HCFC-123 and the UEA standard scale for CH_3I. The concentrations of all species are based on comparisons of ambient air to working standards (G- series, Table 2).

The data

The monthly and annual mean baseline data for HCFCs, HFCs, halons, minor CFCs and halomethanes from 1998 to 2000 are listed in Table 3.

Figure 1 shows the HCFCs: (a) HCFC-22, $CHClF_2$; (b) HCFC-123, $CHCl_2CF_3$; (c) HCFC-124, $CHClFCF_3$; (d) HCFC-141b, CH_3CCl_2F; (e) HCFC-142b, CH_3CClF_2; Figure 2 shows the HFCs: (a) HFC-125, CHF_2CF_3; (b) HFC-134a, CH_2FCF_3; (c) HFC-152a, CH_3CHF_2); Figure 3 shows minor CFCs: (a) CFC-114, CCl_2FCF_3 and $CClF_2CClF_2$; (b) CFC-115, $CClF_2CF_3$; Figure 4 shows the halons: (a) H-1211, $CBrClF_2$; (b) H-1301, $CBrF_3$ and Figure 5 shows the halomethanes: (a) methyl chloride, CH_3Cl; (b) methyl bromide, CH_3Br; (c) methyl iodide, CH_3I; (d) chloroform, $CHCl_3$; (e) dichloromethane, CH_2Cl_2.

Temporal trends and annual cycles

The annual mean trends in ppt yr^{-1} and % $yr^{-1}$are listed in Table 4. Several of the AGAGE GC-MS species show clear evidence of annual cycles at Cape Grim.

Regional pollution

The AGAGE *in situ* data show clear evidence of local urban sources (largely Melbourne) of HCFC-22 (refrigeration/air conditioning), HCFC-141b (foams), HFCs-125, -134a and -152a (refrigeration) and H-1211.

Table 1. The standard scales used in reporting AGAGE GC-MS data.

HCFCs		*HFCs*		*minor CFCs*		*halons*		*halomethanes*	
HCFC-22	UB00	HFC-125	UB00	CFC-114	UB00	H-1211	UB00	CH_3Br	SIO98
HCFC-123	NOAA/CMDL	HFC-134a	UB00	CFC-115	UB00	H-1301	UB00	CH_3Cl	SIO98
HCFC-124	UB00	HFC-152a	UB00					CH_3I	UEA
HCFC-141b	UB00							$CHCl_3$	SIO98
HCFC-142b	UB00							CH_2Cl_2	UB00

Table 2. The working standards employed at Cape Grim from 1998 to 2000 (updated by SIO, 21 November 2002).

Tank	*On*	*HCFC-22*	*HCFC-123*	*HCFC-124*	*HCFC-141b*	*HCFC-142b*	*HFC-125*	*HFC-134a*	*HFC-152a*
		ppt	*ppt*	*ppt*	*ppt*	*ppt*	*ppt*	*ppt*	*ppt*
G-064	Jan 98	121.15	0.05	0.90	6.45	8.47	0.43	4.46	0.67
G-051	Mar 98	116.19	0.06	0.69	4.44	7.29	0.29	2.48	0.62
G-064	Mar 98	121.15	0.05	0.90	6.45	8.47	0.43	4.46	0.67
ALM64447	Mar 98	137.42	0.09	1.33	8.94	12.80	0.83	6.87	1.84
G-065	Mar 98	121.04	0.05	0.92	6.66	8.58	0.49	4.79	0.65
ALM64447	May 98	137.42	0.09	1.33	8.94	12.80	0.83	6.87	1.84
G-051	May 98	116.19	0.06	0.69	4.44	7.29	0.29	2.48	0.62
G-067	May 98	122.82	0.05	1.00	7.27	8.92	0.58	5.52	0.73
G-069	Sep 98	124.58	0.05	1.03	7.71	9.20	0.63	6.06	0.79
G-071	Dec 98	125.41	0.04	1.08	8.14	9.41	0.92	6.85	0.80
G-073	Mar 99	127.43	0.05	1.11	8.72	9.78	0.77	7.78	0.76
G-075	Jun 99	128.56	0.05	1.17	9.13	10.01	0.80	8.27	0.86
G-077	Sep 99	124.87	0.05	1.13	9.02	9.78	0.79	8.32	0.87
G-079	Nov 99	131.11	0.06	1.24	9.78	10.41	0.84	9.36	0.95
G-081	Feb 00	132.06	0.05	1.27	10.22	10.70	0.95	10.35	0.87
G-083	Jun 00	132.94	0.05	1.32	10.54	10.91	1.03	10.91	0.90
G-084	Sep 00	135.74	0.05	1.38	11.31	11.40	1.14	12.24	1.04

Tank	*On*	*CFC-114*	*CFC-115*	*H-1211*	*H-1301*	*CH_3Br*	*CH_3Cl*	*CH_3I*	*CH_2Cl_2*	*$CHCl_3$*
		ppt	*ppt*	*ppt*	*ppt*	*ppt*	*ppt*	*ppt*	*ppt*	*ppt*
G-064	Jan 98	17.12	7.64	3.59	2.67	8.10	530.90	1.13	7.79	5.40
G-051	Mar 98	17.10	7.38	3.41	2.58	8.10	532.48	1.20	9.09	6.99
G-064	Mar 98	17.12	7.64	3.59	2.67	8.10	530.90	1.13	7.79	5.40
ALM64447	Mar 98	17.33	7.84	3.85	2.77	0.00	633.56	0.87	40.05	10.29
G-065	Mar 98	17.07	7.60	3.58	2.67	8.15	520.92	1.15	6.71	4.96
ALM64447	May 98	17.33	7.84	3.85	2.77	0.00	633.56	0.87	40.05	10.29
G-051	May 98	17.10	7.38	3.41	2.58	8.10	532.48	1.20	9.09	6.99
G-067	May 98	17.08	7.69	3.66	2.70	8.57	560.85	1.41	8.43	6.52
G-069	Sep 98	17.12	7.74	3.70	2.75	7.89	567.00	1.06	9.68	6.88
G-071	Dec 98	16.94	7.72	3.70	2.77	8.00	534.11	1.05	7.21	5.49
G-073	Mar 99	17.18	7.80	3.77	2.80	8.57	562.90	1.27	7.37	6.94
G-075	Jun 99	17.10	7.81	3.79	2.83	8.05	551.00	1.28	8.46	6.09
G-077	Sep 99	17.05	7.81	3.69	2.83	7.94	536.37	1.03	8.92	6.35
G-079	Nov 99	17.15	7.88	3.86	2.86	8.77	554.88	0.78	9.43	6.43
G-081	Feb 00	17.14	7.95	3.89	2.85	8.83	544.32	2.19	7.14	5.96
G-083	Jun 00	17.15	8.00	3.91	2.84	8.62	525.03	1.13	7.50	5.08
G-084	Sep 00	17.14	8.03	3.98	2.93	7.65	555.97	0.83	9.95	7.11

Table 3. AGAGE monthly mean HCFC, HFC, minor CFC and halomethane mixing ratios for 1998-2000, with pollution episodes removed statistically. Annual means are obtained from monthly means, monthly means from individual measurements. The data were updated by GIT on 17 Dec 2002.

month	*Jan*	*Feb*	*Mar*	*Apr*	*May*	*Jun*	*Jul*	*Aug*	*Sep*	*Oct*	*Nov*	*Dec*	*mean*
HCFC-22; $CHClF_2$ (ppt)													
1998			122.1	122.5	123.1	123.5	124.4	125.1	125.7	126.1	126.1	126.3	124.5
1999	126.7	127.0	127.5	128.4	129.2	129.8	130.7	131.6	131.6	131.8	132.1	131.9	129.9
2000	132.0	132.3	132.8	133.4	134.3	135.0	135.6	136.4	136.2	136.5	137.3	137.0	134.9
HCFC-123; $CHCl_2CF_3$ (ppt)													
1998			0.046	0.046	0.048	0.048	0.052	0.051	0.051	0.051	0.051	0.048	0.049
1999	0.042	0.041	0.044	0.042	0.045	0.048	0.055	0.057	0.056	0.057	0.052	0.050	0.049
2000	0.047	0.046	0.047	0.049	0.053	0.051	0.051	0.054	0.054	0.054	0.050	0.049	0.050

Table 3. continued……..

month	Jan	Feb	Mar	Apr	May	Jun	Jul	Aug	Sep	Oct	Nov	Dec	mean
HCFC-124; $CHClFCF_3$ (ppt)													
1998			0.952	0.982	1.000	1.025	1.063	1.079	1.101	1.086	1.104	1.118	1.1
1999	1.120	1.145	1.128	1.146	1.212	1.233	1.258	1.271	1.253	1.250	1.244	1.287	1.2
2000	1.293	1.301	1.318	1.334	1.350	1.398	1.438	1.444	1.392	1.381	1.387	1.405	1.4
HCFC-141b; CH_3CCl_2F (ppt)													
1998			6.9	7.1	7.3	7.4	7.7	7.8	8.0	8.1	8.2	8.3	7.7
1999	8.4	8.6	8.7	8.9	9.2	9.3	9.5	9.7	9.8	9.8	10.0	10.0	9.3
2000	10.1	10.2	10.4	10.6	10.8	11.0	11.2	11.3	11.4	11.5	11.7	11.7	11.0
HCFC-142b; CH_3CClF_2 (ppt)													
1998			8.8	8.8	8.9	9.0	9.1	9.2	9.4	9.4	9.5	9.5	9.2
1999	9.6	9.7	9.8	9.9	10.0	10.1	10.2	10.4	10.4	10.5	10.5	10.6	10.1
2000	10.6	10.7	10.8	10.9	11.1	11.1	11.3	11.4	11.4	11.4	11.5	11.6	11.1
HFC-125; CHF_2CF_3 (ppt)													
1998			0.5	0.6	0.6	0.6	0.7	0.7	0.7	0.7	0.7	0.8	0.7
1999	0.8	0.8	0.8	0.8	0.9	0.9	0.9	0.9	0.9	0.9	0.9	0.9	0.9
2000	1.0	1.0	1.0	1.1	1.1	1.1	1.2	1.2	1.2	1.2	1.3	1.3	1.1
HFC-134a; CH_2FCF_3 (ppt)													
1998			5.1	5.4	5.6	5.8	6.0	6.3	6.6	6.7	6.9	7.2	6.2
1999	7.4	7.6	7.9	8.2	8.6	8.8	9.0	9.3	9.4	9.7	9.9	10.1	8.8
2000	10.4	10.6	10.9	11.2	11.6	11.8	12.1	12.3	12.4	12.7	13.1	13.2	11.9
HFC-152a; CH_3CHF_2 (ppt)													
1998			0.7	0.7	0.8	0.8	0.8	0.9	0.9	0.9	0.8	0.8	0.8
1999	0.8	0.8	0.8	0.8	0.9	0.9	1.0	1.0	1.0	1.0	1.0	0.9	0.9
2000	0.9	0.9	0.9	0.9	1.0	1.0	1.0	1.1	1.1	1.1	1.1	1.1	1.0
CFC-114; $CClF_2CCl\,F_2$ (ppt)													
1998			17.1	17.1	17.1	17.1	17.1	17.1	17.2	17.1	17.1	17.1	17.1
1999	17.1	17.2	17.2	17.2	17.2	17.2	17.2	17.2	17.1	17.2	17.2	17.1	17.2
2000	17.2	17.2	17.2	17.2	17.2	17.1	17.2	17.2	17.1	17.0	17.0	17.1	17.1
CFC-115; $CClF_2CF_3$ (ppt)													
1998			7.7	7.6	7.7	7.7	7.7	7.7	7.8	7.8	7.8	7.8	7.7
1999	7.8	7.8	7.8	7.9	7.8	7.8	7.9	7.9	7.8	7.8	7.8	7.9	7.8
2000	7.9	7.9	8.0	8.0	8.0	8.0	8.0	8.1	8.1	8.1	8.1	8.1	8.0
H-1211; $CBrClF_2$ (ppt)													
1998			3.6	3.6	3.7	3.7	3.7	3.7	3.7	3.7	3.8	3.8	3.7
1999	3.8	3.8	3.8	3.8	3.8	3.8	3.9	3.9	3.9	3.9	3.9	3.9	3.8
2000	3.9	3.9	3.9	3.9	3.9	4.0	4.0	4.0	4.0	4.0	4.0	4.0	4.0
H-1301; $CBrF_3$ (ppt)													
1998			2.7	2.7	2.7	2.7	2.7	2.7	2.8	2.8	2.8	2.8	2.7
1999	2.8	2.8	2.8	2.8	2.8	2.8	2.9	2.9	2.9	2.9	2.9	2.9	2.8
2000	2.9	2.9	2.9	2.9	2.9	2.9	2.9	2.9	2.9	2.9	2.9	3.0	2.9
methyl chloride; CH_3Cl (ppt)													
1998		530.2	534.1	540.7	549.6	565.0	570.9	574.4	568.0	564.1	553.7	544.7	554.1
1999	539.6	532.0	529.9	539.7	555.7	569.4	570.5	571.2	564.2	556.9	553.7	536.1	551.6
2000	521.7	513.6	514.4	522.6	541.0	553.3	563.6	562.8	546.7	539.8	533.0	528.1	536.7
methyl bromide; CH_3Br (ppt)													
1998			8.2	8.4	8.4	8.4	8.6	8.7	8.1	7.9	8.0	8.0	8.3
1999	8.4	8.4	8.3	8.2	8.2	8.2	7.9	7.9	8.1	8.1	8.2	8.0	8.2
2000	8.0	7.9	7.9	8.0	8.1	8.2	8.2	8.3	8.0	7.8	8.0	7.8	8.0
methyl iodide; CH_3I (ppt)													
1998			1.50	1.69	1.75	1.79	1.65	1.69	1.51	1.45	1.68	1.97	1.7
1999	2.11	2.05	1.71	1.75	1.79	1.72	1.52	1.29	1.29	1.29	1.25	1.41	1.6
2000	1.59	1.66	1.59	1.52	1.54	1.48	1.46	1.31	1.32	1.18	1.62	1.56	1.5
chloroform; $CHCl_3$ (ppt)													
1998			5.2	5.4	5.8	6.6	6.9	7.2	7.5	7.3	6.9	6.3	6.5
1999	5.6	5.3	5.2	5.3	5.8	6.4	6.8	6.9	7.0	6.8	6.4	5.8	6.1
2000	5.3	5.2	5.2	5.4	5.9	6.1	6.5	6.7	6.9	6.8	6.0	5.7	6.0
dichloromethane; CH_2Cl_2 (ppt)													
1998		7.0	7.2	7.5	8.2	8.9	9.6	10.2	10.1	9.7	9.0	8.2	8.7
1999	7.5	7.3	7.3	7.5	8.5	9.0	9.6	10.0	10.1	9.7	9.0	8.0	8.6
2000	7.4	7.1	7.1	7.6	8.4	8.9	9.5	9.9	10.0	9.5	8.9	8.0	8.5

Table 4. The annual mean trends for HCFCs, HFCs, minor CFCs, halons and halomethanes

Species	*Formula*	*Trend (ppt yr^{-1})*			*Trend (% yr^{-1})*		
		1998	*1999*	*2000*	*1998*	*1999*	*2000*
HCFC-22	$CHClF_2$	5.96 ±0.15	5.63 ±0.416	4.76 ±0.07	4.79 ±0.06	4.34± 0.37	3.53± 0.05
HCFC-123	$CHCl_2CF_3$	-0.002 ±0.001	0.003 ±0.001	-0.000 ±0.002	-3.95 ±1.68	6.78± 2.87	-0.49± 3.74
HCFC-124	$CHClFCF_3$	0.22 ±0.01	0.18 ±0.01	0.09 ±0.04	20.74 ±1.60	14.35± 1.60	6.68± 2.95
HCFC-141b	CH_3CCl_2F	1.89 ±0.03	1.73 ±0.05	1.63 ±0.03	24.72 ±1.83	18.62± 1.58	14.82± 0.92
HCFC-142b	CH_3CClF_2	1.11 ±0.01	1.03 ±0.04	1.04 ±0.04	12.15 ±0.44	10.19± 0.70	9.33± 0.14
HFC-125	CHF_2CF_3	0.27 ±0.02	0.21 ±0.02	0.32 ±0.029	41.23 ±3.20	23.83± 3.43	27.82± 1.48
HFC-134a	CH_2FCF_3	2.88 ±0.10	2.95 ±0.03	3.16 ±0.09	47.24 ±3.82	33.57± 3.47	26.67± 1.31
HFC-152a	CH_3CHF_2	0.11 ±0.03	0.11 ±0.03	0.12 ±0.027	12.91 ±2.86	11.53± 3.07	11.38± 2.28
CFC-114	$CHClF_2$	0.12 ±0.01	-0.01 ±0.05	0.01 ±0.05	0.73 ±0.06	-0.03± 0.32	0.07± 0.30
CFC-115	$CHClF_2$	0.17 ±0.04	0.12 ±0.05	0.21 ±0.07	2.24 ±0.49	1.49± 0.62	2.57± 0.89
H-1211	$CHClF_2$	0.15 ±0.01	0.13 ±0.001	0.11 ±0.016	4.05 ±0.29	3.46± 0.04	2.87± 0.42
H-1301	$CHClF_2$	0.12 ±0.004	0.08 ±0.03	0.11 ±0.04	4.46 ±0.18	2.84± 0.95	3.78± 1.33
methyl chloride	CH_3Cl	2.09 ±2.48	-10.10 ±6.62	-10.06 ±4.43	0.38 ±0.45	-1.83± 1.21	-1.86± 0.81
methyl bromide	CH_3Br	-0.15 ±0.07	-0.13 ±0.10	-0.18 ±0.18	-1.75 ±0.85	-1.61± 1.24	-2.25± 2.24
methyl iodide	CH_3I	0.17 ±0.09	-0.33 ±0.11	0.16 ±0.12	9.58 ±5.08	-20.39± 6.96	10.18± 7.92
chloroform	$CHCl_3$	0.10 ±0.16	-0.32 ±0.07	-0.11 ±0.04	1.56 ±2.50	-5.10± 1.03	-1.86± 0.61
dichloromethane	CH_2Cl_2	0.18 ±0.03	-0.07 ±0.08	-0.09 ±0.05	2.12 ±0.38	-0.81± 0.91	-1.09± 0.52

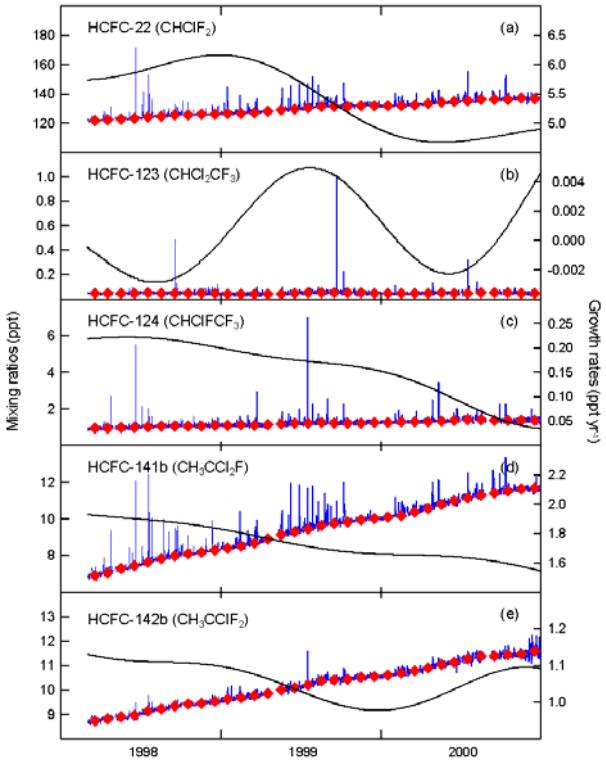

Figure 1. Total (blue) and baseline monthly mean (♦) *in situ* observations of HCFCs (ppt) made at Cape Grim on the AGAGE GC-MS over the period 1998-2000. The black line represents growth rates (ppt yr^{-1}). (a) HCFC-22 ($CHClF_2$); (b) HCFC-123 ($CHCl_2CF_3$); (c) HCFC-124 ($CHClFCF_3$); (d) HCFC-141b (CH_3CCl_2F); (e) HCFC-142b (CH_3CClF_2).

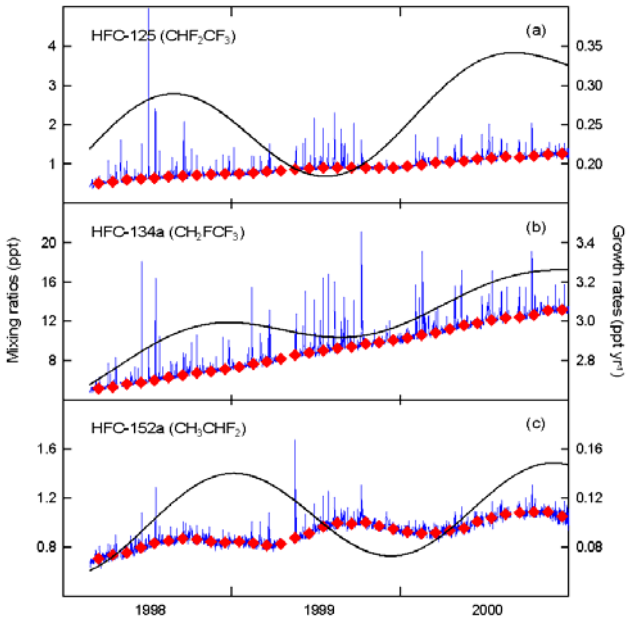

Figure 2. Total (blue) and baseline monthly mean (♦) *in situ* observations of HFCs (ppt) made at Cape Grim on the AGAGE GC-MS over the period 1998-2000. The black line represents growth rates (ppt yr^{-1}). (a) HFC-125 (CHF_2CF_3); (b) HFC-134a (CH_2FCF_3,); (c) HFC-152a (CH_3CHF_2).

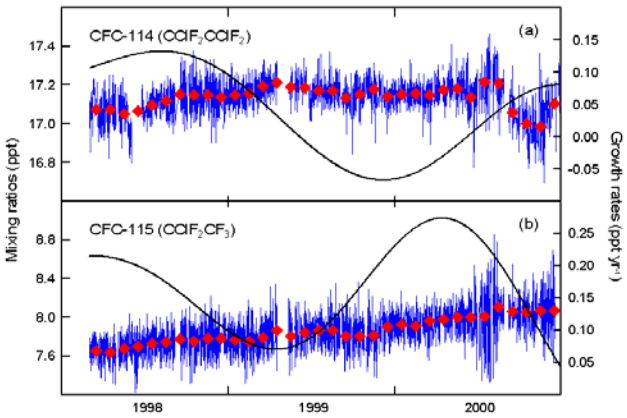

Figure 3. Total (blue) and baseline monthly mean (♦) *in situ* observations of minor CFCs (ppt) made at Cape Grim on the AGAGE GC-MS over the period 1998-2000. The black line represents growth rates (ppt yr^{-1}). (a) CFC-114 ($CClF_2CClF_2$); (b) CFC-115 ($CClF_2CF_3$).

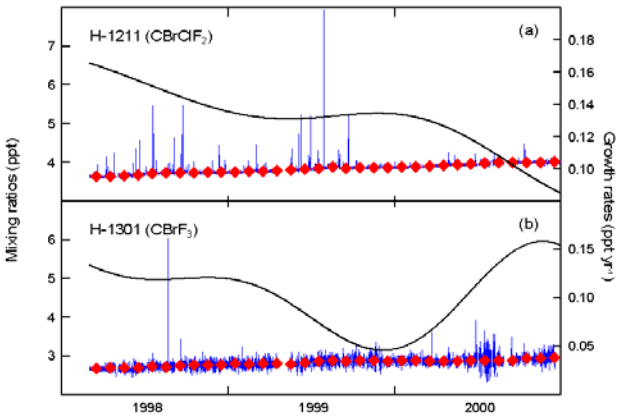

Figure 4. Total (blue) and baseline monthly mean (♦) *in situ* observations of halons (ppt) made at Cape Grim on the AGAGE GC-MS over the period 1998-2000. The black line represents growth rates (ppt yr^{-1}). (a) H-1211 ($CBrClF_2$); (b) H-1301 ($CBrF_3$).

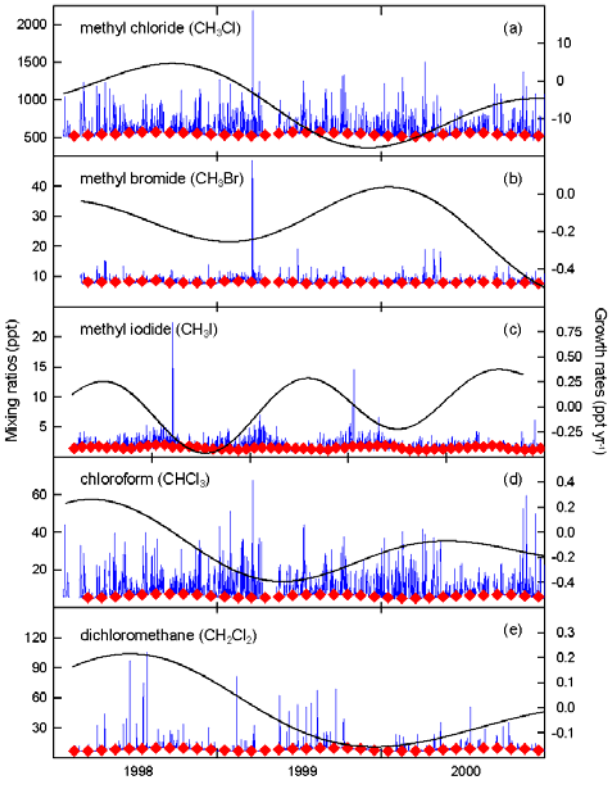

Figure 5. Total (blue) and baseline monthly mean (♦) *in situ* observations of the halomethanes (ppt) made at Cape Grim on the AGAGE GC-MS over the period 1998-2000. The black line represents growth rates (ppt yr^{-1}). (a) Methyl chloride (CH_3Cl); (b) methyl bromide (CH_3Br); (c) methyl iodide (CH_3I); (d) chloroform ($CHCl_3$); (e) dichloromethane (CH_2Cl_2).

References

Cohan, D. S., G. A. Sturrock, A. P. Biazar, and P. J. Fraser, Atmospheric methyl iodide at Cape Grim, Tasmania, from AGAGE observations, *J. Atmos. Chem.*, 44, 131-150, 2003.

Cox, M. L., A regional study of the natural and anthropogenic sources and sinks of the major halomethanes, *PhD Thesis*, Monash University, Clayton, Australia, 188 p., 2001.

Cox, M. L., G. A. Sturrock, P. J. Fraser, S. Siems, P. Krummel, and S. O'Doherty, Regional sources of methyl chloride, chloroform and dichloromethane identified from AGAGE observations at Cape Grim, Tasmania, 1998-2000, *J. Atmos. Chem.*, in press, 2003a.

Cox, M., S. Siems, P. Fraser, P. Hurley, and G. Sturrock, TAPM modelling studies of AGAGE dichloromethane observations at Cape Grim, in *Baseline Atmospheric Program (Australia) 1999-2000*, edited by N. W. Tindale, N. Derek and P. J. Fraser, Bureau of Meteorology and CSIRO Atmospheric Research, Melbourne, Australia, 25-30, 2003b.

O'Doherty, S., P. G. Simmonds, D. M. Cunnold, H. J. Wang, G. A. Sturrock, P. J. Fraser, D. Ryall, R. G. Derwent, R. F. Weiss, P. Salameh, B. R. Miller, and R. G. Prinn, In situ chloroform measurements at Advanced Global Atmospheric Gases Experiment atmospheric research stations from 1994 to 1998, *J. Geophys. Res.*, 106, 20,429-20,444, 2001.

Prinn, R. G., R. F. Weiss, P. J. Fraser, P. G. Simmonds, D. M. Cunnold, F. N. Alyea, S. O'Doherty, P. Salameh, B. R. Miller, J. Huang, R. H. J. Wang, D. E. Hartley, C. Harth, L. P. Steele, G. Sturrock, P. M. Midgley, and A. McCulloch, A history of chemically and radiatively important gases in air deduced from ALE/GAGE/AGAGE, *J. Geophys. Res.*, *105*, 17,751-17,792, 2000.

Sturrock, G. A., L. W. Porter, and P. J. Fraser, *In situ* measurement of CFC replacement chemicals and other halocarbons at Cape Grim: The AGAGE GC-MS program, in *Baseline Atmospheric Program (Australia) 1997-98*, edited by N. W. Tindale, N. Derek, and R. J. Francey, Bureau of Meteorology and CSIRO Atmospheric Research, Melbourne, Australia, 43-49, 2001a.

Sturrock, G. A., L. W. Porter, P. J. Fraser, N. Derek and P. B. Krummel, HCFCs, HFCs, minor CFCs and halomethanes – The AGAGE *in situ* GC-MS pogram, 1997-1998, and related measurements on flask air samples collected at Cape Grim, in *Baseline Atmospheric Program (Australia) 1997-98*, edited by N. W. Tindale, N. Derek, and R. J. Francey, Bureau of Meteorology and CSIRO Atmospheric Research, Melbourne, Australia, 97-100, 2001b.

4.14. PARTICLES

J L Gras
CSIRO Atmospheric Research,
Aspendale, Victoria 3195, Australia
[supported by CGBAPS research funds.]

Introduction: Program and instrumentation

During 1999-2000 the Cape Grim particles program included measurements of atmospheric condensation nucleus (CN) concentration, cloud condensation nucleus (CCN) concentration, the size distribution of CN and aerosol optical absorption (interpreted as elemental carbon). The instrumentation used is listed in Table 1. As shown in Table 1, the instrumentation included a TSI 3025 UCPC ultrafine particle condensation particle counter that was introduced into the program in January 1999 during the SOAPEX-2 experiment. A wide range of additional particle measurements was also made as part of the SOAPEX-2 study. In August 2000 the Cape Grim automated CCN counter was a part of the international CCN workshop at Albany New York, a study comparing the performance of a number of traditional and new CCN counter designs.

Data summary

In keeping with previous *Baseline* 'Particles' reports, data presented here should be considered provisional and may be subject to further editing and revision. Only 'baseline' data obtained when the wind at 10 m is in the 190°-280° 'baseline sector' are reported. No other criteria have been applied for baseline data selection.

CN concentration - Auto Nolan-Pollak Counter

Values of CN concentration for 1999-2000 are given in Table 2. Values presented are monthly medians of the hourly medians of Baseline CN, as determined using the auto Nolan-Pollak counter. The hourly medians are derived from 15 direct CN readings per hour on counter #1. All concentrations are referenced to the local manual counter Nolan-Pollak #2 using three monthly data blocks. Data presented here, were derived using the 1993 calibration of Nolan-Pollak #2 to the 'standard' Nolan-Pollak #3. Figure 1 shows baseline median CN concentrations, corrected to counter #3 (as above) for 1977-2000. As shown in previous *Baseline* reports, CN data show a pronounced annual cycle with a summer concentration maximum and winter minimum. Inter-annual modulation of particle number concentration, with a long-term cyclic nature is also evident in Figure 1 and this has also been reported previously. As clearly shown in Figure 1 the longer-term modulations for the summer and winter concentrations do not have a consistent phase relationship.

CCN concentration

Concentration data for CCN that are active at 1.2%, 0.96%, 0.71%, 0.47% and 0.23% supersaturation are given in Table 2. These are monthly median concentrations for 1999-2000 Baseline conditions only determined using the manual CCN counter. Criteria used for selecting Baseline are the same as those for CN concentration. Daily mean spectra are calculated from a minimum of three daily spectra, and the monthly medians are determined from the daily means. The number of Baseline spectra for each month is also included in Table 2.
For some months the number of baseline spectra is small; a factor that should be taken into account when using these data. Usually the cause for few spectra is a combination of the manual operation of the CCN counter and a low baseline frequency. CCN concentrations for all five supersaturations are plotted in Figure 2 for the period covering 1980 to 2000. As with CN concentration, the CCN concentrations follow a clear annual cycle but with emerging evidence of longer-period cyclic inter-annual modulation.

Table 1. Instrumentation for Particles program, 1999-2000.

CN counters	Manual Nolan-Pollak, CSIRO #2, operated daily. Automated Nolan-Pollak, CSIRO #1, quasi-continuous (3 diffusion battery cycles per hour, includes 15 direct CN samples per hour). TSI 3020, continuous TSI 3025, continuous TSI 3760, continuous
CCN - 1	Static thermal gradient counter, 5 supersaturations, nominal values 0.25%, 0.5%, 0.7%, 1% and 1.2%. Operated manually, 3 spectra daily
ASCCN	Automated static thermal gradient counter. Operated continuously September 1999 – July 2000, 0.5% supersaturation
Particle size	Diffusion battery, CSIRO #8. Operated automatically, 3 cycles per hour in conjunction with Nolan-Pollak CSIRO #1.
Aerosol optical absorption	B_{ap} - aethalometer, Magee scientific. Continuous, 30 minute measurement cycle.

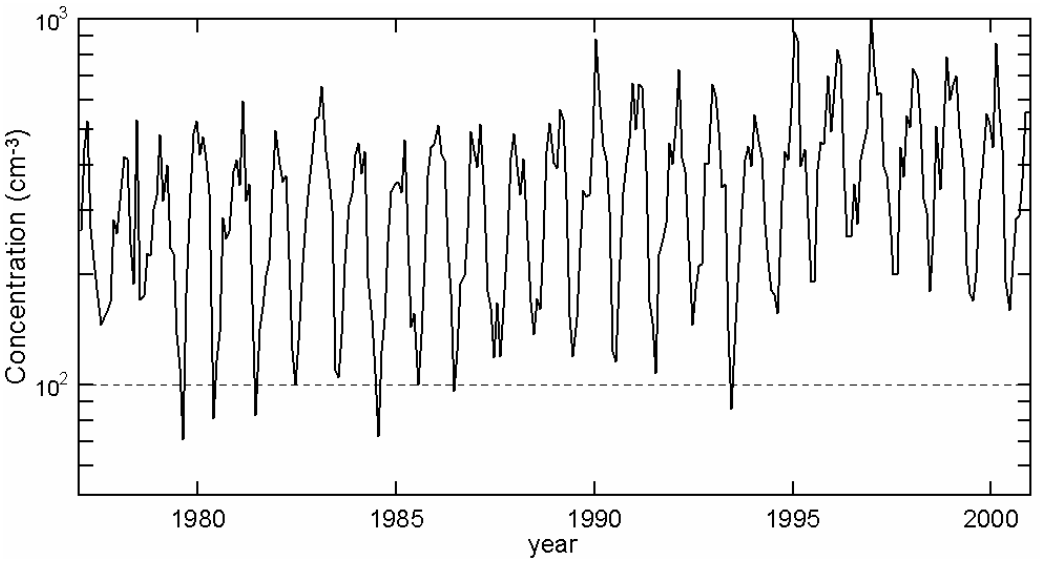

Figure 1. Baseline median CN concentrations from 1976 to 2000. CN are referenced to the standard Nolan-Pollak counter #3.

Table 2. Baseline monthly median CCN and CN concentrations (cm^{-3}) for 1999 and 2000. CCN concentrations are given for nuclei active at the indicated supersaturation. N is the number of baseline CCN spectra determined for the indicated month. CN monthly median (of hourly medians) baseline concentrations are converted to an equivalent Nolan-Pollak #3 (reference counter) value.

Month	*Supersaturation*						*Supersaturation*						
	N	*1.25%*	*1.00%*	*0.75%*	*0.50%*	*0.23%*	*CN*	*N*	*1.25%*	*1.00%*	*0.75%*	*0.50%*	*0.23%*	*CN*
				1999							*2000*			
Jan	1	201.0	190.0	160.0	134.0	162.0	661	6	239.0	228.5	223.0	201.0	162.0	447
Feb	2	160.0	136.5	108.0	79.0	65.0	702	3	1054.0	790.0	596.0	386.0	238.0	857
Mar	6	194.0	160.0	157.5	146.0	101.5	504	6	120.5	118.5	109.5	101.0	98.5	570
Apr	2	91.5	93.0	74.5	95.0	50.5	395	7	261.0	134.0	131.0	166.0	148.0	440
May	0						212	10	128.5	105.0	89.0	123.5	78.5	191
Jun	4	65.5	52.5	56.0	40.5	36.5	178	9	37.0	41.0	36.0	50.0	36.0	159
Jul	1	18.0	35.0	54.0	31.0	21.0	169	5	43.0	35.0	34.0	40.0	44.0	218
Aug	8	56.0	46.5	41.5	33.5	33.5	201	7	53.0	51.0	44.0	46.0	33.0	284
Sep	7	146.0	132.0	97.0	93.0	73.0	321	4	172.5	135.0	154.5	124.5	112.0	290
Oct	10	85.0	87.0	83.5	79.5	78.0	391	8	138.0	136.0	133.0	115.0	76.5	365
Nov	9	198.0	167.0	151.0	104.0	82.0	553	2	500.0	384.0	374.0	207.0	158.5	556
Dec	9	172.0	131.0	118.0	95.0	71.0	516	13	231.0	202.0	207.0	168.0	132.0	560

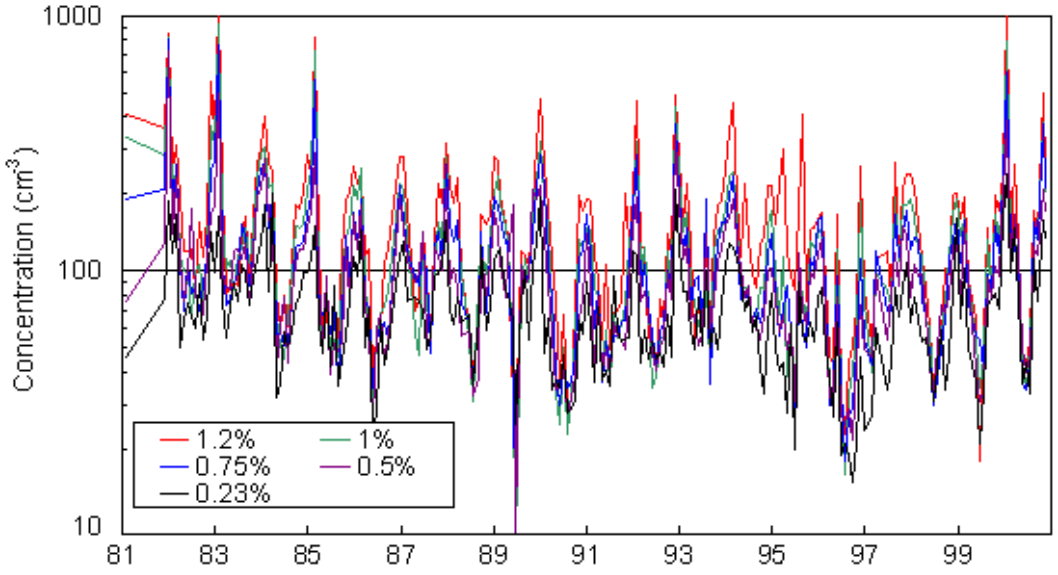

Figure 2. Median concentrations for CCN active at 0.23%, 0.47% and 1.2% supersaturations for baseline conditions 1981-2000.

Aethalometer

Equivalent elemental carbon loadings are determined at Cape Grim by light absorption, using a Magee Scientific Aethalometer. Values of elemental carbon mass loading, derived using the aethalometer, are plotted in Figure 3 for Baseline sector winds (190°-280°). No other Baseline selection criteria have been applied. Values plotted are determined from hourly absorption measurements, interpreted as aerosol optical absorption per cubic metre of air that has passed through the filter, converted to equivalent elemental carbon (EC) concentration using a mass absorption coefficient of 19 $m^2 g^{-1}$. Data are recorded as 30-minute integrals and a three point running average has been applied before the hourly average was taken. Values plotted in Figure 3 are daily means determined from hourly absorption/carbon values. All hourly values of absorption/carbon concentration are included irrespective of the sign (positive or negative).
Sample air for the aethalometer is taken from the main 10 m inlet stack. An impactor with a greased collector is used to remove coarse particles, particularly wind-eroded sand from the nearby cliff-face. The impactor has a 50% collection efficiency (cut) at 3.6 μm diameter (for a particle density of 1 g cm^{-3}) and a flow rate of 15 litres min^{-1}.

The median of the baseline equivalent elemental carbon loadings for 1999 was 8.1 ng m^{-3} and for 2000 it was 8.7ng m^{-3}.

Logbook summary (1999-2000)

Few significant problems were encountered in the operation of aerosol sampling equipment during 1999-2000. For the SOAPEX-2 experiment, in January-February 1999, additional aerosol instruments were housed in a CSIRO van that was located near the main gate. These included an additional UCPC, the automated static CCN counter, DMA sizing system, ASASP-X size spectrometer, TSI aerodynamic particle sizer and two Radiance nephelometers, one operating at low humidity, the other at high humidity. The new TSI 3025 UCPC for Cape Grim was also commissioned during the SOAPEX-2 study. Minor equipment problems during 1999 included aethalometer lamp connections, air leaks in the auto Pollak and some problems with the driving PC. Frequent trimming of the TSI 3020 photometer zero was necessary. In June 1999 the chamber end plate on the TSI 3025 was replaced with a new plate constructed at CSIRO, and an automated control system installed to allow for automatic flushing of the butanol saturation chamber. The automated CCN counter (ASCCN) was installed in September 1999. Calibrations during 1999 included Pollak #2 in May, TSI 3025 flow calibrations in June, and November and the ASCCN in September.

During 2000 problems that were identified included low reference volts on the ASCCN (in June) later found to be due to an intermittent signal plug connection. In September the TSI 3760 sample nozzle required cleaning and in October an air leak in the auto Pollak was fixed. The ASCCN was returned to Aspendale in July in preparation for the International CCN workshop in Albany New York in August. Calibrations in 2000 included TSI 3025 flow calibration and Pollak #2 count calibration in June. The ASCCN was recalibrated in Aspendale for the CCN workshop.

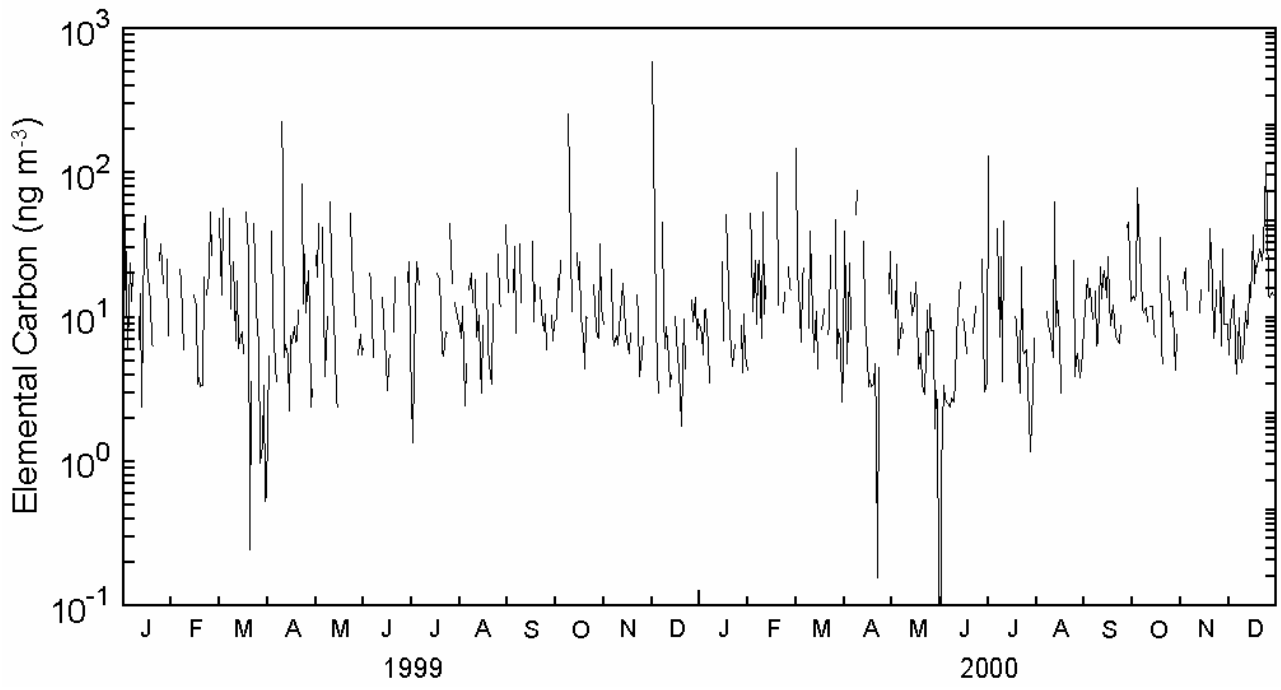

Figure 3. Aethalometer output for baseline sector winds (190°-280°) for 1999-2000. Inferred elemental carbon (EC) concentrations assume a mass absorption coefficient of 19 $m^2 g^{-1}$.

4.15. FINE PARTICLE SAMPLING AT CAPE GRIM

D D Cohen, D Garton and E Stelcer

Australian Nuclear Science Technology Organisation, Menai, NSW 2234, Australia.

[Cooperative Research Report.]

Fine particles (PM2.5) are being sampled at Cape Grim using a cyclone sampler with a 50% cut-off point for a flow rate 22 L min^{-1}. Samples are collected on 220 $\mu g\ m^{-2}$ stretched-Teflon filters of 25 mm diameter. Two, 24-hour (midnight-midnight) samples per week are obtained.

These stretched-Teflon filters are ideal for multi-elemental analysis using the accelerator based ion beam analysis IBA techniques at Australian Nuclear Science Technology Organisation (ANSTO). Currently the following elements can be detected at levels around or below 10 ng m^{-3} of air sampled; H, C, N, O, F, Na, Al, Si, P, S, Cl, K, Ca, Ti, Cr, Mn, Fe, Co, Cu, Ni, Zn, Br, and Pb. Measured average annual concentrations for many of these species for two twelve month periods covering January to December 1998 and 1999 are given in Table 1. A time series plot of the fine mass, as PM2.5, for 1997 and 1998 is given in Figure 1.

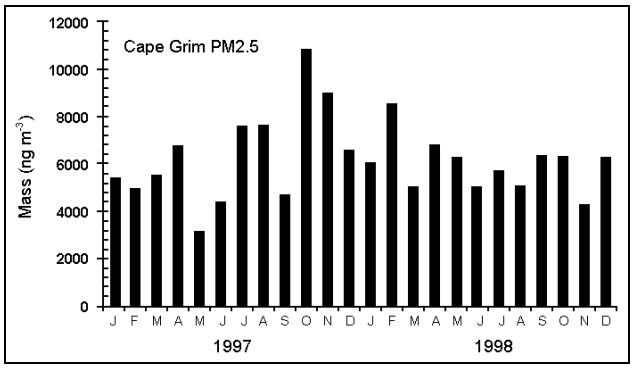

Figure 1. Average monthly mass for PM2.5 fine particles at Cape Grim 1997-1998.

The annual averages are calculated from all the 24-hour samples and contain components from the baseline sector as well as all other sectors (continental and Tasmanian sectors).

The non sea-salt sulfur (nss-S) was calculated assuming the S/Na for sea-salt was 0.084 and the non sea-salt potassium (nss-K) assumes K/Na = 0.036 for sea-salt.

If all the elemental sulfur measured on the filter was assumed to occur as fully neutralised ammonium sulphate then this would correspond to an annual average of (0.94±0.5) $\mu g\ m^{-3}$ or about 16% of the total fine mass. From the sodium and chlorine values we estimate that sea-salt was about 58% of the total measured fine mass during 1998. Soil was estimated from the oxides of Al, Si, Ti, Ca and Fe and represents about 2.0% of the total fine mass at Cape Grim.

Elemental carbon estimates were obtained by standard laser integrating plate methods, pre- and post- filter exposure assuming a mass absorption coefficient of $7 m^2 g^{-1}$ and show that at Cape Grim elemental carbon is only about 5% of the total average annual fine mass.

Organic matter was estimated from the hydrogen not associated with ammonium ions and assumed the average organic particle was composed of 9% H, 20% O and 71% C. It corresponds to about 7% of the annual average fine particle mass.

Table 1. 1998 and 1999 annual average concentrations (ng m^{-3}, except where indicated by * ($\mu g\ m^{-3}$)) of selected species and some derived parameters in the sub 2.5 µm size fraction at Cape Grim, based on 2 day per week, 24-hour average, non-sectored sampling.

Species	*1998*			*1999*		
(ng m^{-3})	*Annual average*	*Min*	*Max*	*Annual average*	*Min*	*Max*
Mass*	5.9±3	1.4	17	5.3±2	1.4	13
Hydrogen	94±101	16	955	76±55	5	271
Sodium*	1.1±1.0	0	5.0	0.96±0.7	0.1	3.1
Aluminium	6±5	0	37	4±5	0	38
Silicon	12±12	1	99	15±20	3	163
Phosphorous	2±2	0	8	2±2	0	19
Sulfur	228±127	42	602	247±171	58	961
Chlorine*	1.7±1	0.04	5.6	1.2±0.7	0.04	3.4
Potassium	40±22	10	110	36±18	9	112
Calcium	39±25	7	117	35±29	8	229
Titanium	0.6±0.4	0	2	0.8±0.6	0	5
Vanadium	0.5±0.8	0	6	1±1.5	0	8
Chrome	0.1±0.2	0	2	0.1±0.2	0	1
Manganese	0.8±2	0	12	0.6±1	0	7
Iron	4±5	0	28	5±7	0	54
Cobalt	0.1±0.2	0	1	0.2±0.2	0	1
Nickel	0.2±0.3	0	2	0.2±0.2	0	1
Copper	0.2±0.2	0	2	0.25±0.6	0	6
Zinc	0.5±0.8	0	6	0.6±0.8	0	4
Bromine	3±2	0	10	2±2	0	11
Lead	0.8±1.3	0	9	0.9±1.3	0	8
nnsS	133±110	0	493	166±182	0	946
nss-K	3±20	0	44	2±21	0	84
Seasalt*	3.4±2.4	0.45	13	2.5±1.6	0.32	8.0
Soil	116±65	31	495	117±112	36	1003
Organics	409±1070	0	9630	151±402	0	1788
Elemental Carbon	298±161	72	859	308±158	96	933
Reconstructed mass (%)	73±28			77±20		

4.16. PRECIPITATION CHEMISTRY

R W Gillett, G P Ayers, M D Keywood and P W Selleck

CSIRO Atmospheric Research, Aspendale, Victoria 3195, Australia

[supported by CGBAPS research funds.]

Table 1 shows the results of the chemical analysis of rainwater collected at Cape Grim under baseline conditions. Samples are collected in an ERNI wet only sampler as described by Ayers and Ivey [1990]. The sampler opens after activation from the baseline event switch (BEVS) when the wind direction is between 190° and 280° and the condensation nucleus (CN) concentration is <600 cm^{-3}.

Samples were collected on a weekly basis. As suggested by Gillett and Ayers [1991], and further quantified by Ayers *et. al*. [1998], thymol was added to

the collection bottle before sampling, to inhibit biological degradation of ions such as organic acids and ammonia.

After collection samples were sent to CSIRO atmospheric Research (CAR) where the chemical analysis was carried out. Anion and cation concentrations were measured by supressed ion chromatography (IC) using a Dionex DX500 gradient ion chromatograph. Anions were determined using a Dionex AS11 column, a Dionex ARSUltra supressor and a gradient eluent of sodium hydroxide. Cations were determined using a Dionex CS12 column and a Dionex CRSUltra supressor with a 20 millimolar methanesulfonic acid eluent. Conductivity was measured in a flow system using a Waters auto-sampler to inject samples into a Milli-Q water stream; detection was done using a Dionex conductivity detector. pH measurements were carried out using an Orion Ross pH electrode calibrated with Orion low ionic strength buffers.

The data set presented here is raw and has not been subjected to more than preliminary quality checks. The cation anion balance is a useful quality control check since the total number of cation equivalents should equal the total number of anion equivalents because electroneutrality is assumed.

References

Ayers G. P., and J. P. Ivey, Methanesulfonate in rainwater at Cape Grim, Tasmania, *Tellus*, 428, 217-222, 1990.

Gillett, R. W., and G. P. Ayers, The use of thymol as a bacteriocide in rain water samples, Atmos. Environ., 25a, 2677-2681, 1991.

Ayers G. P., N. Fukuzaki, R. W. Gillett, P. W. Selleck, J. C. Powell , and H. Hara, Thymol as a biocide in Japanese rainwater, *J. Amos. Chem*., 30, 301-310, 1998.

Table 1. Baseline rainfall, cation and anion concentrations and pH and conductivity in precipitation collected at Cape Grim.

Sample	Date On	Time GMT	Date Off	Time GMT	rainfall (mm)	H^+ [	Na^+	NH_4^+	K^+	Mg^{2+}	Ca^{2+}	Total Cations $\mu eq\ l^{-1}$	Conductivity Meas. [$\mu s\ cm^{-1}$	Calc.]
									$\mu mol\ l^{-1}$					
575	13/01/99	1100	09/02/99	1030	2.8		2140.0	8.2	39.7	192.4	63.6	2700.0		
576	09/02/99	1030	23/02/99	0950	3.3		1172.5	4.1	20.6	90.7	39.9	1458.4		
577	23/02/99	0950	09/03/99	0930	0.7		2070.6	23.7	54.9	196.3	77.5	2696.7		
578	09/03/99	0930	16/03/99	1255	11.9		338.4	3.6	8.7	40.5	13.0	457.6		
579	16/03/99	1255	30/03/99	1120	1.2		4037.7	11.1	65.4	387.1	128.3	5145.0		
580	30/03/99	1120	06/04/99	1030	1.1		1355.9	7.7	27.0	133.3	50.4	1757.9		
581	06/04/99	1100	20/04/99	1053	1.6		1888.4	7.2	35.4	187.3	58.3	2422.2		
582	20/04/99	1035	27/04/99	1120	1.1		1099.4	9.9	25.4	96.2	33.5	1394.1		
583	27/04/99	1120	11/05/99	1110	2.1		4252.9	13.5	73.0	441.9	126.5	5476.2		
584	11/05/99	1110	18/05/99	1115	4.0	3.1	1631.6	8.8	34.7	140.1	38.4	2035.3	253.6	256.3
585	18/05/99	1115	01/06/99	1000	5.9	2.9	1841.7	9.6	39.9	176.5	45.1	2337.3	288.3	294.0
586	01/06/99	1000	08/06/99	1055	1.5	1.8	975.3	6.7	20.0	88.2	26.5	1233.3	157.3	154.8
587	08/06/99	1055	15/06/99	1045	2.8	3.3	1618.6	17.4	36.2	166.6	43.4	2095.4	246.2	262.8
588	15/06/99	1045	22/06/99	1120	4.7	2.6	1180.6	15.1	31.2	105.8	26.6	1494.1	173.2	186.9
589	22/06/99	1120	06/07/99	1035	7.2	3.4	994.5	6.6	21.7	86.1	21.2	1240.7	155.9	156.1
590	06/07/99	1035	13/07/99	1110	2.3	2.1	1366.5	27.5	43.0	138.8	38.5	1793.9		225.7
591	13/07/99	1110	21/07/99	1045	8.4	2.3	1372.5	6.1	28.6	125.5	28.8	1718.2	205.2	214.3
592	21/07/99	1045	28/07/99	1600	3.4	1.0	3019.1	15.0	59.8	295.7	76.9	3840.0	443.5	485.1
593	28/07/99	1600	03/08/99	1117	7.4	2.6	427.9	3.0	10.5	29.7	7.2	517.8	62.4	65.6
594	03/08/99	1117	10/08/99	1115	8.0	3.0	244.5	5.5	7.7	17.9	4.6	305.7		38.7
595	10/08/99	1115	17/08/99	1045	4.8	3.9	535.0	4.2	11.7	41.8	10.3	658.9		83.4
596	17/08/99	1045	24/08/99	1100	5.4	2.9	1089.3	5.7	21.8	96.5	24.4	1361.6		169.9
597	24/08/99	1100	07/09/99	1050	0.8	5.2	693.6	9.6	15.7	54.7	15.3	864.1		108.6
598	07/09/99	1050	21/09/99	1200	5.1	0.8	1612.2	8.7	32.6	119.0	37.0	1966.2		244.0
599	21/09/99	1200	12/10/99	0950	0.3	0.3	3658.6	34.8	76.2	412.1	130.4	4854.8		
600	12/10/99	0950	26/10/99	1145	5.7	1.5	904.0	5.5	19.0	79.9	26.4	1142.6	142.1	142.2
601	26/10/99	1145	02/11/99	1035	2.5	0.4	3083.3	15.8	57.4	233.5	83.7	3791.3	445.1	
602	02/11/99	1035	16/11/99	1020	4.3	0.5	1700.9	8.6	37.0	129.7	42.0	2090.3	255.8	257.1
603	16/11/99	1020	23/11/99	1000	1.1	4.6	804.8	8.0	18.7	65.0	22.3	1010.8	127.5	126.4
604	23/11/99	1000	07/12/99	1030	0.6	3.5	4357.1	54.9	101.3	459.2	167.3	5769.7	649.0	738.6
605	07/12/99	1030	14/12/99	1015	1.4	0.8	2129.3	14.2	44.8	168.2	57.7	2640.8	316.3	328.4
606	14/12/99	1015	21/12/99	1015	8.7	1.6	849.9	4.7	19.5	69.1	21.2	1056.4	134.9	132.0
607	21/12/99	1015	04/01/00	0954	1.9	2.1	294.9	8.0	9.9	18.3	7.6	366.8	51.9	45.6
608	04/01/00	0954	25/01/00	1027	1.8	0.4	3564.3	17.3	68.3	318.3	110.3	4507.3	533.0	
609	25/01/00	1027	15/02/00	1530	8.2	0.9	727.9	5.5	17.3	61.3	21.0	916.3	117.8	113.8
610	15/02/00	1530	14/03/00	1200	0.3	1.8	4149.0	30.9	75.7	386.7	144.2	5319.1	621.4	
611	14/03/00	1200	21/03/00	1045	0.6	2.6	1445.0	14.0	29.5	128.9	47.2	1843.4	227.3	229.4
612	21/03/00	1045	28/03/00	1200	2.7	0.1	1967.1	11.4	22.9	8.5	3.9	2026.3	247.0	245.1
613	28/03/00	1200	04/04/00	1100	2.7	0.2	1843.7	10.1	35.0	58.3	20.9	2047.6	248.1	250.4
614	04/04/00	1100	18/04/00	0000	1.3	0.3	1496.8	5.2	33.7	127.9	45.5	1882.8	214.8	241.7
615	18/04/00	0000	26/04/00	0000	5.1	0.4	1341.8	1.9	27.5	103.5	34.5	1647.6	199.0	213.3
616	26/04/00	0000	02/05/00	0000	1.0	0.5	1920.6	11.2	39.8	181.0	63.5	2461.0	280.1	321.0
617	02/05/00	0000	09/05/00	0000	2.2	2.1	4016.8	4.4	75.5	435.9	107.8	5186.2	569.0	689.2
618	09/05/00	0000	16/05/00	0000	4.3	2.0	1781.9	2.7	39.3	168.2	43.6	2249.6	259.1	294.8
619	16/05/00	0000	23/05/00	0000	10.2	0.6	1608.2	1.3	33.9	156.3	48.7	2053.8	234.8	270.6
620	23/05/00	0000	30/05/00	0000	17.9	0.6	1553.5	0.8	32.0	143.7	38.7	1951.7	224.6	257.8
621	30/05/00	0000	06/06/00	0000	7.0	0.6	1127.0	1.4	24.1	109.3	27.4	1426.5	169.2	187.3
622	06/06/00	0000	13/06/00	0000	9.0	0.5	589.3	1.2	12.7	59.1	13.4	748.8	93.6	98.7

Table 1. continued….

623	13/06/00	0000	20/06/00	0000	2.9	0.9	1533.4	2.9	33.4	146.3	37.7	1938.7	219.6	257.1
624	20/06/00	0000	27/06/00	0000	3.5	1.5	661.0	3.2	15.5	64.5	16.0	842.2	102.6	112.2
625	27/06/00	0000	04/07/00	0000	0.4	1.6	3562.6	6.9	59.0	487.4	122.5	4849.8	523.0	648.5
626	04/07/00	0000	11/07/00	0000	2.0	2.2	809.2	5.7	19.4	76.0	19.0	1026.6	124.4	136.1
627	11/07/00	0000	18/07/00	0000	0.8	2.3	1170.0	9.6	26.0	115.7	30.7	1500.7	173.4	199.7
628	18/07/00	0000	25/07/00	0000	9.4	0.6	2434.2	1.5	50.3	238.7	62.4	3088.6	344.9	414.7
629	25/07/00	0000	01/08/00	0000	6.8	0.5	1453.9	1.5	33.1	143.7	33.6	1843.6	212.6	246.7
630	01/08/00	0000	15/08/00	0000	9.6	0.4	2318.3	1.4	47.2	238.1	60.0	2963.5	338.0	399.8
631	15/08/00	0000	29/08/00	0000	1.8	0.6	745.5	3.0	22.1	66.6	18.8	942.1	112.2	125.2
632	29/08/00	0000	05/09/00	0000	7.0	0.6	1620.8	1.6	33.1	151.2	40.3	2039.0	230.6	274.5
633	05/09/00	0000	12/09/00	0000	4.3	0.4	3489.3	1.2	70.4	348.3	91.2	4440.3	487.3	603.0

Sample	*Date On*	*Time GMT*	*Date Off*	*Time GMT*	*pH*	*Cl^-*	*Br^-*	*NO_3^-*	*SO_4^{2-}*	*$C_2O_4^{2-}$*	*F^-*	*CH_3COO^-*	*$HCOO^-$*	*$CH_3SO_3^-$*	*Total Anions*
						[				*µmol l^{-1}*				*]*	*µeq l^{-1}*
575	13/01/99	1100	09/02/99	1030		2317.9	3.2	4.5	125.4	5.0					2583.1
576	09/02/99	1030	23/02/99	0950		1208.2	1.6	1.6	62.6	4.1					1343.2
577	23/02/99	0950	09/03/99	0930		2156.8	3.2	18.9	135.6	14.2					2475.3
578	09/03/99	0930	16/03/99	1255		359.6	0.5	2.1	20.7	1.9					407.0
579	16/03/99	1255	30/03/99	1120		4614.2	7.1	7.3	243.6	7.3					5123.3
580	30/03/99	1120	06/04/99	1030		1495.9	3.2	2.4	76.9	4.1					1660.2
581	06/04/99	1100	20/04/99	1053		2095.6	3.2	8.9	107.9	5.4					2330.9
582	20/04/99	1035	27/04/99	1120		1161.9	1.9	2.6	61.8	3.6					1295.3
583	27/04/99	1120	11/05/99	1110		4947.2	7.6	7.2	257.4	5.8					5480.9
584	11/05/99	1110	18/05/99	1115	5.51	1780.7	2.1	1.1	88.5	1.8	0.52	2.9	7.7		1973.1
585	18/05/99	1115	01/06/99	1000	5.53	2042.9	2.3	4.2	101.6	1.8	0.28	1.6	5.1	0.26	2261.0
586	01/06/99	1000	08/06/99	1055	5.75	1070.6	1.1	1.2	52.0	1.8	0.23	2.1	6.9		1188.4
587	08/06/99	1055	15/06/99	1045	5.48	1789.1	2.1	13.4	97.3	2.0	0.68	3.1	7.2		2011.4
588	15/06/99	1045	22/06/99	1120	5.59	1274.7	1.5	1.0	68.6	2.0	0.32	2.6	6.3		1425.8
589	22/06/99	1120	06/07/99	1035	5.47	1078.0	1.1	1.6	52.8	1.0	0.39	2.2	6.3		1195.7
590	06/07/99	1035	13/07/99	1110	5.68	1488.7	1.4	35.7	89.5	2.1	1.02	6.6	13.6		1727.6
591	13/07/99	1110	21/07/99	1045	5.63	1488.2	1.7	1.1	72.1	0.8	0.35	1.2	2.8		1639.0
592	21/07/99	1045	28/07/99	1600	6.00	3387.6	4.4	0.7	178.4	1.1	0.68	1.6	4.5	0.20	3753.6
593	28/07/99	1600	03/08/99	1117	5.59	451.8	0.3	0.8	20.8	0.6	0.13	1.8	4.0		501.2
594	03/08/99	1117	10/08/99	1115	5.52	258.3	2.3		11.8	0.6	0.61	2.2	4.8		290.0
595	10/08/99	1115	17/08/99	1045	5.41	576.8	0.4	0.6	24.6	0.6	0.28	1.8	4.5		634.0
596	17/08/99	1045	24/08/99	1100	5.54	1180.6	1.3	0.7	53.9	0.8	0.46	2.3	4.1		1296.9
597	24/08/99	1100	07/09/99	1050	5.29	736.2	0.6	3.4	32.7	2.4	0.15	3.5	8.7		822.0
598	07/09/99	1050	21/09/99	1200	6.11	1675.0	1.9	1.4	91.3	1.9	0.63	1.1	1.9		1866.0
599	21/09/99	1200	12/10/99	0950	6.49	4156.3	6.1	18.9	234.9	16.1	0.48		21.8		
600	12/10/99	0950	26/10/99	1145	5.84	981.1	0.9	1.4	47.5	1.8	1.37	2.3	2.2		1085.5
601	26/10/99	1145	02/11/99	1035	6.36	3298.9	4.3	1.5	184.7	2.3	0.46		12.7		
602	02/11/99	1035	16/11/99	1020	6.27	1750.0	1.9	2.2	97.2	1.6	0.74	1.1	2.5		1953.3
603	16/11/99	1020	23/11/99	1000	5.34	844.6	0.7	3.1	44.4	2.0	0.70	6.1	11.4		958.0
604	23/11/99	1000	07/12/99	1030	5.46	4978.9	5.7	70.4	306.8	11.3	22.99	0.2	57.6		5743.3
605	07/12/99	1030	14/12/99	1015	6.12	2240.2	2.6	2.8	123.1	3.0	1.21	7.0	15.7		2518.0
606	14/12/99	1015	21/12/99	1015	5.80	910.8	0.8	0.7	45.3	1.0	0.56	2.0	3.4		1009.4
607	21/12/99	1015	04/01/00	0954	5.67	282.2	2.6		19.2	0.9	1.40	8.3	15.7		346.3
608	04/01/00	0954	25/01/00	1027	6.44	3936.7	5.2	1.1	222.3	5.8	0.77		11.9		
609	25/01/00	1027	15/02/00	1530	6.03	783.3	0.6	3.4	38.9		0.24	1.7	1.2		867.4
610	15/02/00	1530	14/03/00	1200	5.74	4641.1	4.1	22.0	259.5	13.6	1.31		40.4		
611	14/03/00	1200	21/03/00	1045	5.58	1553.3	1.2	5.5	83.1	4.9	1.49	4.3	8.8		1747.8
612	21/03/00	1045	28/03/00	1200	6.87	1662.3	1.8	5.8	86.3	3.2	2.62	8.1	15.1		1870.3
613	28/03/00	1200	04/04/00	1100	6.69	1701.8	2.0	3.1	90.0	4.6	0.11	5.6	10.8		1910.4
614	04/04/00	1100	18/04/00	0000	6.53	1665.1	2.3	5.2	91.3	5.5	1.75	5.7	30.7	0.59	1900.6
615	18/04/00	0000	26/04/00	0000	6.43	1497.8	2.5	1.2	84.1	2.8	0.84	3.0	6.7	0.37	1682.8
616	26/04/00	0000	02/05/00	0000	6.35	2249.0	3.6	12.9	125.0	3.7	1.79	5.4	15.1	0.41	2540.0
617	02/05/00	0000	09/05/00	0000	5.68	4970.3	7.4	5.8	260.5	2.9	0.65	2.4	9.9		5515.1
618	09/05/00	0000	16/05/00	0000	5.69	2094.1	3.0	2.7	112.9	2.4	2.45	1.6	4.1		2333.0
619	16/05/00	0000	23/05/00	0000	6.24	1909.4	3.0	0.6	117.4	1.3	0.96	1.6	2.8		2151.8
620	23/05/00	0000	30/05/00	0000	6.24	1840.6	2.7	0.4	105.3	0.6	0.95	1.0	2.0		2055.8
621	30/05/00	0000	06/06/00	0000	6.20	1338.3	2.3	0.2	71.1	0.8	0.83	1.7	4.0	0.18	1488.1
622	06/06/00	0000	13/06/00	0000	6.29	705.1	1.0	0.5	36.2	0.8	0.78	2.2	4.7		786.3
623	13/06/00	0000	20/06/00	0000	6.06	1834.6	2.9	1.7	103.6	1.5	0.87	2.4	5.6		2054.4
624	20/06/00	0000	27/06/00	0000	5.84	797.4	1.6	1.9	42.5	1.2	0.75	2.9	7.6		897.2
625	27/06/00	0000	04/07/00	0000	5.80	4703.2	7.4	2.1	230.8	3.4	13.84	4.5	32.1		5210.2
626	04/07/00	0000	11/07/00	0000	5.66	950.3	1.7	5.0	56.0	2.1	0.92	2.2	7.5	0.19	1081.4
627	11/07/00	0000	18/07/00	0000	5.64	1418.2	2.3	4.6	77.2	1.7	0.69	3.8	8.7		1593.1
628	18/07/00	0000	25/07/00	0000	6.26	3021.7	4.3	1.1	156.9	1.2	0.57	0.5	2.1		3341.7
629	25/07/00	0000	01/08/00	0000	6.30	1782.3	2.7	0.4	97.6	0.8	1.23	1.0	2.4		1982.9
630	01/08/00	0000	15/08/00	0000	6.35	2899.8	4.4	2.3	161.7	1.2	0.63	0.8	1.9		3230.8
631	15/08/00	0000	29/08/00	0000	6.20	886.1	2.3	2.2	49.2	2.8	2.11	2.1	6.7		1001.0
632	29/08/00	0000	05/09/00	0000	6.23	1991.1	3.4	1.2	106.9	1.4	0.79	2.0	5.9		2216.9
633	05/09/00	0000	12/09/00	0000	6.44	4409.6	6.8	0.6	237.2	1.4	0.55	1.3	7.4		4895.9

4.17. SPECTRAL SOLAR RADIATION

S R Wilson[1] and B W Forgan[2]

[1]University of Wollongong,
Wollongong, NSW 2522, Australia
[2]66 Haversham Avenue,
Wheelers Hill, Victoria 3150, Australia

[Supported by CGBAPS research funds.]

Reported here are the data from the Spectral Radiation program, which includes measurements of spectral irradiance and turbidity.

Optical depth

The operation of this system was relatively trouble free for the two years. The tracker controlling for the sunphotometer failed on 25 January 1999, but the sunphotometer was returned to service on 27 January 1999.

On 2 June 2000 it was found that the sunphotometer was partially shaded by the global irradiance system. An unused arm was removed to solve the problem.

Spectral irradiance

This section reports on measurements from two instruments; a spectral radiometer (SRAD) (Optronics Laboratories OL-752), and a broad band UV-B detector (Solar Light model 501 UV-Biometer). Included in this section are changes of note that occurred during the two years.

Computer problems occurred sporadically. Te controlling computer 'del' stopped for a variety of reasons on 10 January 1999, 15 – 18 January 1999 (server problems), 5 February 1999, 12 February 1999, 1 April, 30 April, 6 May – 4 June (UPS power problems). On July 20 1999 a software patch was applied to the operating system to remove the 49.7 day crash problem. The system stopped again on 17 September 1999.

On 23 October 1999 SRAD failed, a fault that was eventually traced to a faulty capacitor, and the system returned to service on 9 November 1999.

On 28 October a major system service was undertaken, as the diffuser and lightguide was now unserviceable, due to corrosion. This was replaced with a Lumatec 300 lightguide and a Bo series 3 diffuser. The new diffuser provided a 100-fold increase in signal throughput, at least partially due to the steady decay of the optical train of the older system. The front panel display of SRAD was found to have failed totally.

A major upgrade of the software was also undertaken, and installed on 10 December 1999, with testing completed on 21 December 1999.

On 9-10 April 2000 the controlling computer was upgraded to a system running Windows NT. Minor problems occurred on a number of days following this installation until the problems were sorted out.

The Biometer system ran reliably through this entire period, with the data collected by the main Grimco data collection system.

4.18. PASSIVE SOLAR RADIATION

S R Wilson

University of Wollongong,
Wollongong, NSW 2522, Australia

[Supported by CGBAPS research funds.]

The Passive Solar Radiation monitoring program continued throughout 1999-2000 The Regional Instrument Centre the Bureau of Meteorology is responsible for the maintenance and calibration of the instruments and data processing of all irradiance quantities apart from UV.

Continuous measurements of global, direct, diffuse, and terrestrial measurements continued in 1999-2000.

Data processing is largely automated. Daily exposure and irradiance data were edited to exclude those days when instrument failures or data acquisition errors were evident from system logs or trace examination. Daily data are excluded from the monthly averages when quality control and assurance tests reject more than 2 minutes in a day. Tables 1 and 2 provide monthly statistics of the processed quantities.

Table 1. Monthly mean daily terrestrial (long wave) irradiance for 1999-2000. The sample estimate of the standard deviation and number of days included in the average is given in brackets for each month.

Month	Terrestrial Irradiance ($W\ m^{-2}$)	s.d.	days	Terrestrial Irradiance ($W\ m^{-2}$)	s.d.	days
1999				2000		
Jan	350.37	21.9	28	339.85	24.79	28
Feb	364.7	25.67	28	349.94	24.08	26
Mar	351.5	23.95	31	348.15	22.39	30
Apr	326.87	26.04	26	329.58	20.52	30
May	345.17	20.71	30	338.79	16.26	31
Jun	322.8	20.84	28	323.89	13.01	28
Jul	327.11	23.32	31	324.04	20.6	31
Aug	326.34	20.13	31	316.48	19.28	31
Sep	323.61	22.94	30	329.11	18.71	30
Oct	324.22	25.68	31	327.09	23.95	31
Nov	318.23	25.23	30	338.82	25.04	30
Dec	332.7	28.91	31	327.2	18.97	31

Table 2. Monthly mean daily solar exposure and sunshine hours for 1999-2000

		Exposure									Sunshine		
		Direct (MJ m^{-2})	s.d	# days /month	Global (MJ m^{-2})	s.d	# days /month	Diffuse (MJ m^{-2})	s.d	# days /month	#hours per day	s.d	# days /month
Jan	99	18.25	12.25	28	24.39	6.98	28	10.58	3.63	28	7.18	4.27	28
Feb	99	13.65	10.32	28	18.91	7.82	28	9.49	3.44	28	5.93	3.96	28
Mar	99	10.96	8.86	31	14.94	5.71	31	8.08	2.36	31	4.93	3.43	31
Apr	99	14.13	8.49	25	12.18	3.28	25	5.31	1.73	25	6.06	3.17	25
May	99	5.69	6.39	30	6.18	3.09	30	3.72	1.19	30	2.79	2.6	30
Jun	99	6.48	5.43	29	5.67	1.94	29	3.34	0.88	29	3.47	2.54	29
Jul	99	6.11	6.97	31	5.66	2.05	29	3.61	0.97	31	3.05	2.88	31
Aug	99	8.93	6.86	31	8.83	3.34	31	4.6	1.56	31	4.18	2.8	31
Sep	99	11.57	9.62	30	13.45	5.37	30	6.82	2.56	30	5.2	3.72	30
Oct	99	17.73	11.92	31	19.47	7.5	31	7.49	3.2	31	7.2	4.19	31
Nov	99	24.05	14.25	30	25.8	8.15	30	8.21	3.82	30	8.88	4.47	30
Dec	99	22.25	13.08	29	27.34	8.01	31	9.81	3.35	29	8.9	4.43	29
Jan	00	18.99	12.78	29	23.85	8.56	28	9.84	3.18	27	7.49	4.38	29
Feb	00	20.66	10.84	29	22.93	5.57	29	8.3	3.03	29	8.11	3.64	29
Mar	00	11.91	9.4	28	16.05	5.3	31	8.24	2.37	28	5.26	3.66	28
Apr	00	13.64	8.72	25	12.29	3.19	29	5.54	1.66	25	5.97	3.17	25
May	00	5.18	4.54	27	6.95	2.39	31	4.48	0.85	27	2.77	2.08	27
Jun	00	6.51	4.81	30	5.72	1.67	30	3.45	0.69	30	3.37	2.21	30
Jul	00	6.41	6.57	31	5.73	2.23	29	3.5	0.98	31	3.13	2.81	31
Aug	00	10.64	7.39	29	9.69	3.62	31	4.46	1.27	29	4.66	2.9	29
Sep	00	7.68	6.85	30	11.87	4.25	30	7.34	1.98	30	3.89	2.87	30
Oct	00	12.22	8.24	29	17.84	5.56	31	9.57	2.8	29	5.71	3.25	29
Nov	00	17.92	12.43	29	23.63	7.45	30	10.53	3.66	29	7.15	4.17	29
Dec	00	24.6	10.65	26	28.32	5.22	31	9.78	3.17	26	9.58	3.33	26

APPENDICES

Appendix A - PUBLICATIONS

(Peer-reviewed research papers in international journals are listed first with 'project leader' names in bold. Conference presentations and proceedings are listed next, followed by other significant publications).

International Journal Papers

Andreae, M. O., W. Elbert, Y. Cai, T. W. Andreae, and J. L. **Gras**, Non-sea-salt sulfate, methanesulfonate, and nitrate aerosol concentrations and size distributions at Cape Grim, Tasmania. *J. Geophys. Res.*, 104(D17), 21,695-21,706, 1999.

Ayers, **G. P.**, R. W., Gillett, J. M., Cainey, and A. L. Dick, Chloride and bromide loss from sea-salt particles in southern ocean air, *J. Atmos. Chem*., 33(3), 299-319, 1999.

Ayers, **G. P.**, and R. W. Gillett, DMS and its oxidation products in the remote marine atmosphere: implications for climate and atmospheric chemistry, *J. Sea Res*., 43(3-4), 275-286, 2000.

Esler, M. B., D. W. T. Griffith, S. R. **Wilson**, and L. P. **Steele**, Precision trace gas analysis by FT-IR spectroscopy. 1. Simultaneous analysis of CO_2, CH_4, N_2O, and CO in air, *Anal. Chem*., 72(1), 206-215, 2000.

Esler, M. B., D. W. T. Griffith, S. R. **Wilson**, and L. P. **Steele**, Precision trace gas analysis by FT-IR spectroscopy. 2. The $^{13}C/^{12}C$ isotope ratio of CO_2, *Anal. Chem*., 72(1), 216-221, 2000.

Francey, R. J., C. E. Allison, D. M. Etheridge, C. M. Trudinger, I. G. Enting, M. L. Leuenberger, R. L. Langenfelds, E. Michel, and L. P. **Steele**, A 1000-year high precision record of $\delta^{13}C$ in atmospheric CO_2, *Tellus*, 51B(2), 170-193, 1999.

Francey, R. J., M. R. Manning, C. E. Allison, S. A. Coram, D. M. Etheridge, R. L. Langenfelds, D. C. Lowe, and L. P. **Steele**, A history of $\delta^{13}C$ in atmospheric CH_4 from the Cape Grim Air Archive and Antarctic firn air, *J. Geophys. Res*., 104(D19), 23,631-23,634, 1999.

Francey, R. J., L. P. **Steele**, R. L. Langenfelds, and B. C. Pak, High precision long-term monitoring of radiatively active and related trace gases at surface sites and from aircraft in the Southern Hemisphere atmosphere, *J. Atmos. Sci.*, 56(2), 279-285, 1999.

Gillett, R. W., T. D. van Ommen, A. V. Jackson, and **G. P. Ayers**, Formaldehyde and peroxide concentrations in Law Dome (Antarctica) firn and ice cores, *J. Glac.*, 46(152), 15-19, 2000.

Langenfelds, R. L., R. J. **Francey**, L. P. **Steele**, M. Battle, R. F. Keeling, and W. F. Budd, Partitioning of the global fossil CO_2 sink using a 19-year trend in atmospheric O_2, *Geophys. Res. Letts*., 26(13), 1897-1900, 1999.

Monks, P. S., G. Salisbury, G. Holland, S. A. Penkett, and **G. P. Ayers**, A seasonal comparison of ozone photochemistry in the remote marine boundary layer, *Atmos. Environ*., 34(16), 2547-2561, 2000.

Prinn, R. G., R. F. Weiss, P. J. **Fraser**, P. G. Simmonds, D. M. Cunnold, F. N. Alyea, S. O'Doherty, P. Salameh, B. R. Miller, J. Huang, R. H. J. Wang, D. E. Hartley, C. Harth, L. P. **Steele**, G. A. Sturrock, P. M. Midgley, and A. McCulloch, A history of chemically and radiatively important gases in air deduced from ALE/GAGE/AGAGE, *J. Geophys. Res*., 105(D14), 17,751-17,792, 2000.

Reichle, H. G., B. E. Anderson, V. S. Connors, T. C. Denkins, D. A. Forbes, B. B. Gormsen, R. L. Langenfelds, D. O. Neil, S. R. Nolf, P. C. Novelli, N. S. Pougatchev, M. M. Roell, and L. P. **Steele**, Space shuttle based global CO measurements during April and October 1994, MAPS instrument, data reduction, and data validation, *J. Geophys. Res*., 104(D17), 21,443-21,454, 1999.

Simmonds, P. G., R. G. Derwent, S. O'Doherty, D. B. Ryall, L. P. **Steele**, R. L. Langenfelds, P. Salameh, H. J. Wang, C. H. Dimmer, and L. E. Hudson, Continuous high-frequency observations of hydrogen at the Mace Head baseline atmospheric monitoring station over the 1994-1998 period, *J. Geophys. Res*., 105(D10), 12,105-12,121, 2000.

Conferences

Climate Monitoring and Diagnostics Laboratory Annual Meeting [abstracts], 12-13 May 1999, Boulder, Colorado, National Oceanic and Atmospheric Administration, Boulder, Colorado, USA, 1999

Steele, L. P., R. J. **Francey**, G. A. Da Costa, C. E., Allison, and R. L. Langenfelds, Intercalibration of greenhouse gas measurements, 11.

IUGG 99 [abstracts], 19-30 July 1999, Birmingham, U.K., International Union of Geodesy and Geophysics, Birmingham, U.K., 1999.

Cunnold, D. M., L. P. **Steele**, P. J. **Fraser**, R. G. Prinn, P. G. Simmonds, R. Weiss, and L. Emmons, On interpreting the seasonal cycle in AGAGE methane observations and variations in the methane cycle, [abstract JSP21/E/04-A5], 112.

Iinuma, Y., G. P. Box, J. L. **Gras**, M. D. Keywood, and G. P. **Ayers**, Prediction of aerosol optical properties from physical and chemical measurements in Canberra, Australia [abstract MI01/W/19-A2], 208-209.

Cape Grim Baseline Air Pollution Station Annual Scientific Meeting 1999 [abstracts], 3-4 November 1999, Aspendale, Victoria, edited by N. Tindale and N. Derek, CSIRO Atmospheric Research, Aspendale, Victoria, 1999.

Allison, C., and R. **Francey**, Instrumental effects on stable isotope measurements of atmospheric CO_2, 38.

Boers, R., S. Young, and B. Forgan, Clouds and radiation at Cape Grim, 6.

Brunke, E., S. **Whittlestone**, and W. Zahorowski, Air mass characterisation at Cape Point, 12.

Cooper, L., R. **Francey**, P. **Steele**, R. Langenfelds, D. Spencer, C. Alison, P. Krummel, and K. Masarie, Comapring trace gas measurements from flasks collected at Cape Grim and analysed at different laboratories, 11.

Cox, M., P.**Fraser**, G. Sturrock, and S. Siems, Regional and background measurements of halomethanes at Cape Grim, Tasmania, 42.

Fraser, P., G. Sturrock, N. Derek, P. Krummel, M. Cox, D. Etheridge, and L. Porter, review of Montreal Protocol trace gas measurements at Cape Grim, Tasmania, 40.

Fraser, P., G. Sturrock, N. Derek, P. Krummel, D. Etheridge, and L. Porter, review of Kyoto Protocol synthetics measurements at Cape Grim, Tasmania, 41.

Garton, D., D. Cohen, B. Weymouth, and J. **Gras**, Ion beam methods for fine particle characterisation, 5.

Granek, H., G. **Ayers**, R. Gillett, and R. Johns, Cape Grim photochemical boundary layer Box Model: Recent developments, 16.

Gras, J. L., Cape Grim particle program review 1999, 50.

Keywood, M. D., and G. P. **Ayers**, DMS, marine aerosol, and climate: what can we learn from MSA? 39.

Griffith, D., F. Turatti, S. **Wilson**, M. Esler, and G. Toon, Positionally- dependent fractionation of ^{15}N in sources and sinks of atmospheric N_2O, 43.

Cooper, L. N., R. J. **Francey**, L. P. **Steele**, R. L. Langenfelds, D. A. Spencer, C. E. Allison, P. B. Krummel, and K. A. Masarie, Comparing trace gas measurements from flasks collected at Cape Grim and analysed at different laboratories, 11.

Da Costa, G., P. **Steele**, and D. Spencer, Cape Grim's new low flow CO_2 analyser: results of operational trials at Aspendale, 19.

Downey, A., Air mass origin: a climatology, [Poster], 33.

Dunse, B., P., **Steele**, P., **Fraser**, P., Hurley, and S. **Wilson**, Investigation of urban and regional emissions of trace gases, 9.

Etheridge, D. M., C. Trudinger, L. **Steele**, A. Smith, D. Lowe, and V. Levchenko, Methane isotopic record extended into the pre-nuclear era, 45.

Francey, R., L. **Steele**, C. Allison, P. Tans, and K. Masarie, A new global quality control for long-lived trace gas measurements, 7.

Galbally, I., M. Meyer, W. Zahorowski, and S. **Whittlestone**, Comparison of the regionally averaged surface exchange rates of ozone and radon made through atmospheric concentration observations, 36.

Gras, J., Particle Program Review 1999, 50.

Kivlighon, L., I. **Galbally**, and I. Weeks, Non-methane hydrocarbon measurements at Cape Grim, [Poster], 34.

Krummel, P. B., L. P. **Steele**, and B. Weymouth, The vital role of data management in studies of atmospheric trace species, 8.

Meier, A., D. Griffith, C. Bernado, S. **Wilson**, I. Jamie, F. Turatti, and F. Phillips, Total column amounts, isotopic ratios, and information on trace gas profile variations retrieved from solar infrared spectroscopy, 15.

Meyer, C. P., I. **Galbally**, and S. Bentley, Auditing instrument and system performance and data quality in surface ozone monitoring systems, 17.

Porter, L., G. Sturrock, P. **Fraser**, S. O'Doherty, and P. Simmonds, Methodology of the Cape Grim GC-MS, 39.

Spencer, D., G. Da Costa, and L. **Steele**, Atmospheric air dryer system for Cape Grim's new low flow CO_2 analyser, 18.

Sturges, W., D. Oram, S. Penkett, P. **Fraser**, and A. Engel, Long-lived haogenated compounds in the stratosphere, [Poster], 30.

Tindale, N., and A. **Downey**, Identification and transport of air masses at Cape Grim during SOAPEX2 field campaign, [Poster], 32.

Turatti, F., D. Griffith, S. **Wilson**, M. Esler, and P. **Steele**, Isotopic analysis of atmospheric N_2O by FTIR spectroscopy ^{15}N, ^{18}O and positional dependence, 44.

Wilson, S., and D. Griffith, Teaching atmospheric chemistry, [Poster], 25.

Wilson, S., and B. Forgan, Aerosol optical depth at Cape Grim (1985-1999), 37.

AMOS 2000: the use and application of meteorological and oceanographic information: Seventh National Australian Meteorological and Oceanographic Society Conference [abstracts], 7-9 February 2000, Melbourne, Victoria (AMOS Publication, 16), AMOS Conference Committee, Melbourne, Victoria, 2000.

Dunse, B. L., L. P. **Steele**, P. J. **Fraser**, P. J. Hurley, and S. R. Wilson, Investigation of urban and regional emissions of trace gases, p. 29.

Jimi, S. I., S. T. Siems, and J. L. **Gras**, Ultrafine particles in the marine environment. p. 59-60.

Geophysical Research Abstracts: 25th General Assembly, 25-29 April 2000, Nice, France, European Geophysical Society, Katlenburg-Lindau, Germany, 2000.

Etheridge, D. M., L. P. **Steele**, A. M. Smith, C. M. Trudinger, R. L. Langenfelds, D. C. Lowe, V. A. Levchenko, G. A. Sturrock, R. J. **Francey**, P. J. **Fraser**, V. I. Morgan, I. Levin, and J.-M. Barnola, Records of atmospheric trace gases and some isotopic ratios from Law Dome firn air, p. OA41.

Climate Monitoring and Diagnostics Laboratory Annual Meeting [abstracts], 3-4 May 2000, Boulder, Colorado, National Oceanic and Atmospheric Administration. Boulder, Colorado, USA, 2000.

Tindale, N. W. and A. **Downey**, The non-baseline summer of 1998-1999 at Cape Grim, p. 3.

Tindale, N. W., J. Seymour, P. P. Pease and S. **Whittlestone**, Aerosol levels and chemistry at Macquarie Island, [Poster].

Nucleation and Atmospheric Aerosols 2000, 15th International Conference [AIP Conference Proceedings, 534], 6-11 August 2000, Rolla, Missouri, edited by B. N. Hale and M. Kulmala, Melville, NewYork, USA, American Institute of Physics, 2000.

Gras, J. L., Maritime CCN measurement and delayed droplet growth, p. 869-872.

Cape Grim Baseline Air Pollution Station Annual Scientific Meeting 2000 [abstracts], 7-8 December 2000, Aspendale, Victoria, edited by N. Tindale and N. Derek, CSIRO Atmospheric Research, Aspendale, Victoria, 2000.

Allison, C., Development of a consistent calibration scale for CO_2 stable isotope measurements (*forming part of the review of the Cape Grim carbon dioxide program*), 35.

Dunse, B., P. **Steele**, P. **Fraser**, P., Krummel, P., Hurley, and S. Wilson, Investigating the emission and transport of trace gases using The Air Pollution Model (TAPM), 11.

Jimi, S., J. **Gras**, and S. Siems, Characterisation of post-frontal flow using ultrafine particles and trace gases measured during SOAPEX-2, 38.

Francey, R., Current status and future requirements of observations of the global carbon cycle, illustrated with a study of interannual variability in the 20-year Cape Grim CO_2 and $\delta^{13}C$ records (*forming part of the review of the Cape Grim carbon dioxide program*), 33.

Fraser, P.,M. Cox, B. Dunse, N. Derek, and P. Krummel, CFC, HCFC and HFC refrigerants: Port Phillip regional emissions derived from AGAGE GC-MS data, 40.

Galbally, I., and W. Kirstine, The global cycle of methanol, 44.

Keywood, M., and G. **Ayers**, DMS, marine aerosol, and climate: What can we learn from MSA?, 39.

Kivlighon, L., I. **Galbally**, and I. Weeks, Measurements of C_2 and C_3 hydrocarbons in marine air at Cape Grim (41°S, 145°E), 10.

Kowalczyk, E., S. **Whittlestone**, and J. McGregor, Global scale soil moisture estimation from radon concentrations, 42.

Langenfelds, R., R. **Francey**, P. **Steele**, C. Allison, B. Pak, and J. Lloyd, A multiple trace gas diagnoses of the interannual variability in the global carbon cycle, 1992-2000 (*forming part of the review of the Cape Grim carbon dioxide program*), 36.

Meier, A., D. Griffith, S. **Wilson**, and C. Rinsland, Biomass burning plumes above Wollongong - measurements by solar FTIR remote sensing, 4.

Meyer, M., J. Easson, and I. **Galbally**, Ozone profiles in the troposphere over south-eastern Australia during August and September 2000, 43.

Spencer, D., G. Da Costa, P. **Steele**, P. Krummel, and S. Baly, The prototype (MARK I) LOFLO CO_2 analyser performance and its comparison with the existing BASGAM system (*forming part of the review of the Cape Grim carbon dioxide program*), 34.

Steele, P., Addressing the carbon cycle measurement challenge: initiatives in measurement technology and global intercalibration (*forming part of the review of the Cape Grim carbon dioxide program*), 33.

Sturrock, G., C. Reeves, S. Penkett, R. Parr, L.Porter, and N. **Tindale**, Measurement of methyl bromide and other trace gas saturations in surface seawater off Cape Grim, [Poster], 20.

Tindale, N., Progress report on establishing a regional Surface Ocean-Lower Atmosphere Study (ANZ-SOLAS), 16.

Trudinger, C., D. Etheridge, G. Sturrock, P. Rayner, P. **Fraser**, I. Enting, P. **Steele**, D. Lowe, and Smith, Reconstructing atmospheric records from firn and ice core measurements, 37.

Wilson, S., D. Griffith, F. Turatti, and J. Menegazzo, Characterisation of agricultural N_2O emission sources using isotopic labelling studies, 6.

2000 Fall Meeting [abstracts], 15-19 December 2000, San Francisco, California, (Supplement to EOS: Transactions of the American Geophysical Union, 81(48)), American Geophysical Union, Washington, D.C., USA, 2000

Cunnold, D. M., L. P. **Steele**, P. J. **Fraser**, P. G. Simmonds, R. G. Prinn, R. F. Weiss, L. W. Porter, R. L. Langenfelds, and H. R. Wang, Source information from GAGE/AGAGE measurements of methane at 5 sites from 1985 to 1999, [Poster], A62A-21.

Tindale, N. W., J. Seymour, P. P. Pease, S. **Whittlestone** and J. Harris, Aerosol micronutrients at Macquarie Island and input to the Southern Ocean, [Poster], A21D-03.

Other Significant Publications

Cox, M., P. J. Hurley, P. J. **Fraser**, and W. L. Physick, Investigation of Melbourne region pollution events using Cape Grim data, a regional transport model (TAPM) and the EPA Victoria carbon monoxide inventory, *Clean Air*, 34(1), 35-40, 2000.

Da Costa, G. A., and L. P. **Steele**, A low-flow analyser system for making measurements of atmospheric CO_2, in *Report of the Ninth WMO Meeting of Experts on Carbon Dioxide Concentration and Related Tracer Measurement Techniques*, Aspendale, Victoria, edited by R. J. Francey, (Environmental Pollution Monitoring and Research Programme/Global Atmosphere Watch, 132; WMO/TD; no. 952), Secretariat of the World Meteorological Organization, Geneva, Switzerland, 16-20, 1999.

Francey, R. J., L. P. **Steele**, R. L. Langenfelds, L. N. Cooper, C. E. Allison, N. B. A. Trivett, and V. Hudec, CSIRO trace gas measurements from Canadian sites, in *Canadian Baseline Program: summary of progress to 1998*, Atmospheric Environment Service, Environment Canada, Toronto, Ontario, Canada, 5.35-5.41, 1999.

Kurylo, M. J., J. M. Rodriguez, M. O. Andreae, E. L. Atlas, D. R. Blake, J. H. Butler, S. Lal, D. J. Lary, P. M. Midgley, S. A. Montzka, P. C. Novelli, C. E. Reeves, P. G. Simmonds, L. P. **Steele**, W. T. Sturges, R. F. Weiss, and Y. Yokouchi, Short-lived ozone-related compounds, in *Scientific assessment of ozone depletion: 1998*, WMO Global Ozone Research and Monitoring Project – Report No. 44, NOAA/NASA/UNEP/WMO/EC, Geneva, Switzerland, 2.1-2.56, 1999.

Langenfelds, R. L., Francey, R. J., **Steele**, L. P., and Budd, W. F. (1999?). The CSIRO atmospheric O_2/N_2 measuring program, in *Report of the Ninth WMO Meeting of Experts on Carbon Dioxide Concentration and Related Tracer Measurement Techniques*, Aspendale, Victoria, edited by R. J. Francey, (Environmental Pollution Monitoring and Research Programme/Global Atmosphere Watch, 132; WMO/TD; no. 952), Secretariat of the World Meteorological Organization, Geneva, Switzerland, 26-30, 1999.

Masarie, K. A., T. Conway, E. J. Dlugokencky, P. C. Novelli, P. P. Tans, B. Vaughn, J. White, M. Trolier, R. J. **Francey**, R. L. Langenfelds, L. P. **Steele**, and C. E. Allison, An update on the ongoing flask-air intercomparison program between the NOAA CMDL Carbon Cycle Group and the CSIRO DAR Global Atmospheric Sampling Laboratory, in *Report of the Ninth WMO Meeting of Experts on Carbon Dioxide Concentration and Related Tracer Measurement Techniques*, Aspendale, Victoria, edited by R. J. Francey, (Environmental Pollution Monitoring and Research Programme/Global Atmosphere Watch, 132; WMO/TD; no. 952), Secretariat of the World Meteorological Organization, Geneva, Switzerland, 40-44, 1999.

Appendix B - PERSONNEL

Station Staff

Officer-in-Charge	Neil Tindale
Computing systems officers	Brian Weymouth, Alan Gough (left March 1999), Randall Wheaton (arrived August 1999)
Technical officers	Laurie Porter, Stuart Baly
Administrative services officer	Jan Britton
Temporary staff	Ellen Porter, Daniel Evenhuis, Craig McCulloch, Bob Parr
Post Doctral Fellow	Georgina Sturrock (Left Cape Grim for CSIRO-AR in March 1999)

Lead Scientists

Greg Ayers	Multiphase Atmospheric Chemistry	CAR
Reinout Boers	Remote Sensing of Clouds	CAR
Arthur Downey	Meteorology/Climatology	BoM
John Gras	Particles	CAR
Roger Francey	Carbon isotopes and air archives	CAR
Paul Fraser	Halocarbons, nitrous oxide and air archives	CAR
Ian Galbally	Ozone/NO_x and air archives	CAR
(No Lead Scientist)	Precipitation chemistry/High Volume aerosol	
Paul Steele	Carbon dioxide	CAR
Paul Steele	Methane, carbon monoxide, hydrogen	CAR
Stewart Whittlestone	Radon	ANSTO
Stephen Wilson	Radiation (spectral)	UoW

CGBAPS Funded Research Personnel

Lisa Cooper	Technical officer	CAR
Grant Da Costa	Research engineer	CAR
Nada Derek	Technical officer	CAR
Paul Krummel	Research scientist	CAR
Paul Selleck	Technical officer	CAR

Management Group

Doug Gauntlett	Deputy Director (Research and Systems)	BoM
Graeme Pearman	Chief, CSIRO	CAR

List of Working Group Attendees

Colin Allison	CAR	John Gras	CAR
Greg Ayers	CAR	Mick Meyer	CAR
Stuart Baly	CAR	Stuart Penkett	UEA
John Bennett	CAR	Laurie Porter	CGBAPS
Simon Bentley	CAR	Peter Price	BoM
Reinout Boers	CAR	Brian Sawford	CAR
Willem Bouma	CAR	George Scott	CAR
Jan Britton	CGBAPS	Paul Steele	CAR
Arthur Downey	BoM	Neil Tindale	CGBAPS
Roger Francey	CAR	Randall Wheaton	CGBAPS
Paul Fraser	CAR	Stewart Whittlestone	ANSTO
Ian Galbally	CAR	Stephen Wilson	UoW
Rob Gillett	CAR	Wlodek Zahorowski	ANSTO

Appendix C - DEFINITIONS

(Most frequently used acronyms and symbols in this issue)

AGAGE	Advanced Global Atmospheric Gases Experiment
AGAL	Australian Government Analytical Laboratories, Hobart, Tasmania
ANSTO	Australian Nuclear Science and Technology Organisation, Menai, NSW
BoM	Bureau of Meteorology
CGBAPS	Cape Grim Baseline Air Pollution Station
CMDL	Climate Monitoring and Diagnostics Laboratory, NOAA, Boulder, USA
CSIRO	Commonwealth Scientific and Industrial Research Organisation
CAR	CSIRO Atmospheric Research, Aspendale, Victoria
GASLAB	Global Atmospheric Sampling Laboratory, CSIRO-AR
NIES	National Institute for Environmental Studies, Tsukuba, Japan
NIST	National Institute of Standards and Technology
NOAA	National Oceanic and Atmospheric Administration, USA
PU	Princeton University, Princeton, New Jersey, USA
SIO	Scripps Institution of Oceanography, La Jolla, California, USA
UEA	University of East Anglia, Norwich, England, U.K.
UoW	University of Wollongong, Wollongong, NSW
WMO	World Meteorological Organization

AEST	Australian Eastern Standard Time
BEVS	Baseline Events Switch
CCN	cloud CN
CN	condensation nuclei
$\delta^{13}C$	relative isotopic ratio $^{13}C/^{12}C$
GC	gas chromatograph
GRIMCO	CGBAPS computing system
HP	Hewlett Packard
NDIR	Non-Dispersive InfraRed
UV	ultraviolet

ppm	parts per 10^6
ppb	parts per 10^9
ppt	parts per 10^{12}
‰	per mil, parts per 10^3
V-PDB	international scale for expressing C and O isotopic composition relative to PDB carbonate